

SKB

**TECHNICAL
REPORT**

91-24**Hydrogeological conditions in the
Finnsjön area.
Compilation of data and conceptual
model**

Jan-Erik Andersson, Rune Nordqvist, Göran Nyberg,
John Smelliie, Sven Tirén

February 1991

SVENSK KÄRNBRÄNSLEHANTERING AB

SWEDISH NUCLEAR FUEL AND WASTE MANAGEMENT CO

BOX 5864 S-102 48 STOCKHOLM

TEL 08-665 28 00 TELEX 13108 SKB S

TELEFAX 08-661 57 19

HYDROGEOLOGICAL CONDITIONS IN THE FINNSJÖN AREA.
COMPILATION OF DATA AND CONCEPTUAL MODEL

Jan-Erik Andersson, Rune Nordqvist, Göran Nyberg,
John Smellie, Sven Tirén

February 1991

This report concerns a study which was conducted for SKB. The conclusions and viewpoints presented in the report are those of the author(s) and do not necessarily coincide with those of the client.

Information on SKB technical reports from 1977-1978 (TR 121), 1979 (TR 79-28), 1980 (TR 80-26), 1981 (TR 81-17), 1982 (TR 82-28), 1983 (TR 83-77), 1984 (TR 85-01), 1985 (TR 85-20), 1986 (TR 86-31), 1987 (TR 87-33), 1988 (TR 88-32) and 1989 (TR 89-40) is available through SKB.

SWEDISH GEOLOGICAL CO
Engineering Geology
Client: SKB

REPORT
ID-no: IRAP 91204
Date: 1991-02-25

**HYDROGEOLOGICAL CONDITIONS IN
THE FINNSJÖN AREA**
Compilation of data and
conceptual model

Jan-Erik Andersson
Rune Nordqvist
Göran Nyberg
John Smellie
Sven Tirén

Uppsala
February 1991

FOREWORD

In the present report all available data gathered from the Finnsjön area of potential use for numerical modelling are compiled and discussed. The data have been collected during different phases during the period 1977-1989. This inevitable means that the quality of the measured and interpreted data varies in accordance with the continuous developments of improved equipments and interpretation techniques.

Several people within SGAB have been involved in the preparation of this report. Jan-Erik Andersson was the lead author and the editor of the report with assistance of Tapsa Tammela. The contour maps of the groundwater level were prepared by Göran Nyberg and Tapsa Tammela. The statistical analysis of the hydraulic conductivity distributions in the rock mass was performed by Rune Nordqvist (final version) and Leif Stenberg (first version). John Smellie prepared the hydrochemical data compilation. Finally, the comprehensive compilation of geological data of lineaments and fractures on different scales was carried out by Sven Tirén. The CAD-model of the Finnsjön Rock Block together with the calculation of the intersection coordinates and equations of the fracture zones was established by Tomas Stark.

The present report is an updated version of the SKB Progress Report 89-24 with the same title and authors, see Introduction.

CONTENTS

	Page
1. INTRODUCTION	1
2. SURFACE HYDROLOGY AND GROUNDWATER RECHARGE	5
2.1 Water courses	5
2.2 Water-logged grounds	5
2.3 Lakes	5
2.4 Water balance and groundwater recharge	5
3. GROUNDWATER HEAD CONDITIONS	7
3.1 Groundwater table	7
3.2 Piezometric borehole conditions	7
3.2.1 Long-term piezometric measurements	7
3.2.2 Pressure measurements from injection tests	9
4. HYDRAULIC CONDUCTIVITY DISTRIBUTIONS	11
4.1 Methods used	11
4.1.1 Single-hole tests	11
4.1.2 Interference tests	11
4.2 Hydraulic units	13
4.3 Hydraulic properties of fracture zones	16
4.3.1 Fracture zones outside Zone 2	16
4.3.2 Fracture Zone 2	18
4.4 Hydraulic properties of the rock mass	25
4.5 Geostatistical analysis	29
5. OTHER HYDRAULIC PARAMETERS	32
5.1 Preliminary tracer test	32
5.1.1 Hydraulic fracture conductivity and aperture	32
5.1.2 Flow porosity	32
5.1.3 Dispersivity	33
5.1.4 Heterogeneity and anisotropy of Zone 2	35
5.2 Radially converging tracer test	35
5.2.1 Hydraulic fracture conductivity and aperture	36
5.2.2 Flow porosity	36
5.2.3 Dispersivity	37
5.2.4 Hydraulic interconnection within Zone 2	37
5.3 Other tracer tests	38
5.4 Tracer dilution tests	39
5.4.1 Natural groundwater flow rates through boreholes	40
5.4.2 Estimated natural groundwater flow through Zone 2	43
5.5 Estimation of conductive fracture frequency	44
6. HYDROCHEMICAL CONDITIONS	48
6.1 Hydrochemical features of the studies performed	48
6.1.1 Chemical and isotopic character of the groundwaters	49
6.1.2 Redox character of the groundwaters	50
6.1.3 Groundwater flow	51
6.1.4 Equilibrium modelling of the groundwaters	52
6.2 Changes of water conductivity during hydraulic interference tests	53

7.	LINEAMENTS AND FRACTURES	54
7.1	Introduction	54
7.2	Definition of terms and description of methods	54
7.2.1	Lineament maps	54
7.2.2	Lineaments of different orders	54
7.2.3	Location, length and orientation of lineaments	56
7.2.4	Fractures	56
7.3	Lineaments of northeastern Uppland	56
7.3.1	Lineament pattern	56
7.3.2	Lineament characteristics	57
7.4	Lineaments of the Gåvastbo area	61
7.5	Lineaments of the Finnsjön site	66
7.6	Fracture mapping in the Finnsjön site	71
7.7	Detailed fracture mapping in a excavated trench	71
8.	PREVIOUS NUMERICAL MODELLING OF THE FINNSJÖN AREA	75
8.1	Preliminary regional and local groundwater flow models	75
8.2	Local modelling of the Brändan area (Zone 2)	76
8.3	Modelling of the hydraulic interference tests	77
8.3.1	Predictive modelling	77
8.3.2	Model calibration after interference tests	78
8.4	Modelling of radially converging tracer test	83
8.4.1	Predictive modelling	83
8.4.2	Comparison between predicted and observed results	83
9.	CONCEPTUAL MODEL OF THE FINNSJÖN AREA	86
9.1	General	86
9.2	Modelling strategy	86
9.3	Semi-regional model	89
9.4	Local and detailed model	91
9.5	Hydraulic properties of Zone 1	94
9.6	Modelling of Zone 2	95
9.7	Tentative model of groundwater circulation at Finnsjön	96
9.8	Available data for model calibration and validation	97
10.	DATA SUMMARY	99
10.1	Groundwater head conditions	99
10.2	Hydraulic parameters	99
10.3	Parameters from tracer tests	100
10.4	Hydrochemical parameters	100
10.5	Geological and geometric data of fracture zones	100
10.6	Borehole data	100
11.	REFERENCES	101
	APPENDICES	105

LIST OF APPENDICES

	Page
Appendix 1 Drainage basins and larger lakes in Northern Uppland	A1
Appendix 2 Contour maps of the groundwater table	
2:1 Semi-regional model area	A2
2:2 Local model area	A3
Appendix 3 Groundwater head conditions	
3:1 Piezometric measurements in multiple-borehole sections	A4
3:2 Pressure differences in 2 m borehole sections	A8
3:3 " " 20 m "	A10
Appendix 4 Hydraulic conductivity distributions along the boreholes from single-hole tests	A11
Appendix 5 CAD-model and geometric data of the Finnsjön Rock Block	
5:1 CAD-pictures from different views	A17
5:2 Geometric data of fracture zones	A22
Appendix 6 Statistical analysis of the hydraulic conductivity distributions of the rock mass	
6:1 Mean of log(K) + standard deviation in 100 m intervals displayed in a Box Plot	A26
6:2 Regression analysis of rock mass data	A29
6:3 Plots showing the 95% confidence interval	A31
Appendix 7 Geostatistical analysis of hydraulic conductivity data	A33
Appendix 8 Groundwater chemical parameters	
8:1 Major chemical parameters	A44
8:2 Isotope analyses	A47
8:3 Chemical parameters from KFI09 and BFI01	A49
8:4 Saturation index with respect to calcite	A51
8:5 Changes of electric conductivity of discharged water during the hydraulic interference tests	A52
Appendix 9 Data on lineaments/fracture zones and fractures in the Finnsjön site and surroundings	
9:1 Lineament/fracture zone data	A55
9:2 Fracture data	A64

1. INTRODUCTION

The objective of this report is to give a detailed description of the hydrogeological conditions of the Finnsjön area. The intention is that the report should provide sufficient input data needed for a variety of model campaigns planned for the safety assessment (SKB-91) of a generic repository located at the Finnsjön site. Thus, in the report all available data of potential use for different kinds of groundwater flow and transport models and hydrochemical models are included together with an assessment of the quality of the data and a brief description of the actual sampling and analysis methods used. In addition, all previously modelling efforts within the Finnsjön area are briefly summarized. The report mainly constitutes an updating and extension of the previous report by Carlsson and Gidlund (1983) concerning the hydrogeological conditions in the Finnsjön area.

The present report is an updated version of the report by Andersson et al. (1989b) with the same title and issued as SKB Progress Report 89-24. The updated parts mainly concern Section 4.2 (Hydraulic units) in which slight modifications of the hydraulically conductive fracture zone intervals in some of the boreholes have been made according to the updated geological interpretation by Ahlbom and Tirén (1991) and consequences hereof on the conceptual model in Sections 9.1-4. Furthermore, additional fracture mapping data for fracture network modelling have been described in Section 7.6 and listed in Appendix 9:2.

In the present report the same definitions of regional, semi-regional and local areas are used as in the geological overview report by Ahlbom and Tirén (1989, 1991). In addition, a semi-regional and local area for the hydrogeological modelling is proposed. A subdivision of hydraulic conductivity data in hydraulic units according to the geological interpretation has been made together with an identification of possible model boundaries, e.g major fracture zones.

As a background to the following chapters a location map of the Finnsjön area showing borehole locations and some of the fracture zones is presented in Figure 1.1. The regional and semi-regional areas, defined by Ahlbom and Tirén (1989, 1991) are shown in Figures 1.2 and 1.3, respectively. The semi-regional area includes the Finnsjön Rock Block in its central part.

Chapter 2 summarizes the hydrology and water balance of northern Uppland and the Finnsjön area. Chapter 3 describes the groundwater head conditions, Chapter 4 presents all available hydraulic parameters calculated from single-hole tests and interference tests and a subdivision of data in hydraulic units together with a geostatistical analysis of hydraulic conductivity data. Chapter 5 presents the results of tracer tests, dilution tests and an estimation of the natural groundwater flow within Zone 2 and the conductive fracture frequency in selected boreholes. Chapter 6 summarizes the hydrochemical data of groundwater from the Finnsjön area. Chapter 7 provides statistical data of lineaments and fractures on different scales. Chapter 8 summarizes the previous modelling of the Finnsjön area. In Chapter 9 conceptual models of the hydrogeological conditions on semi-regional and local scales are presented. Finally, a data summary including the accessibility of the data is presented in Chapter 10.

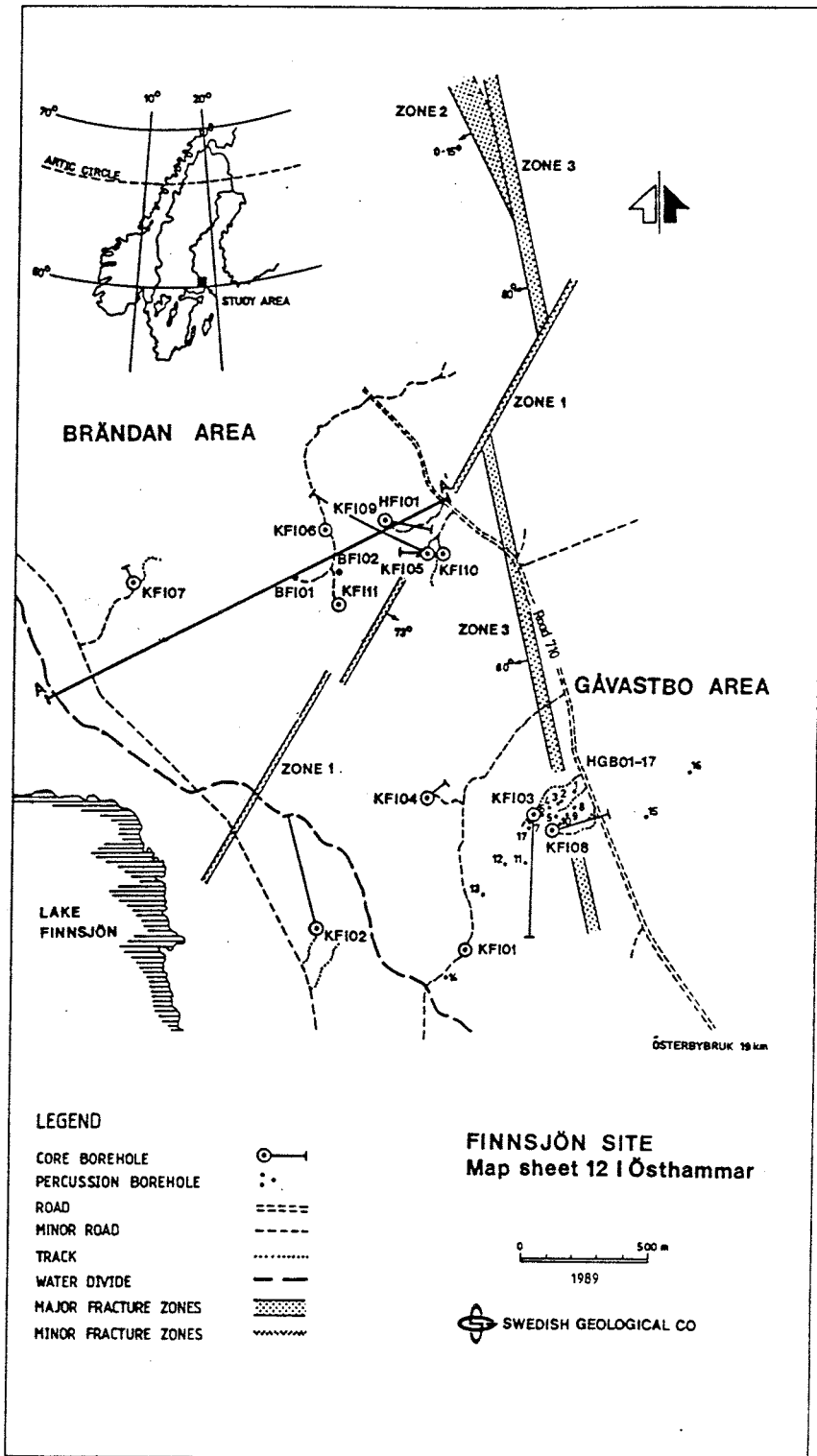
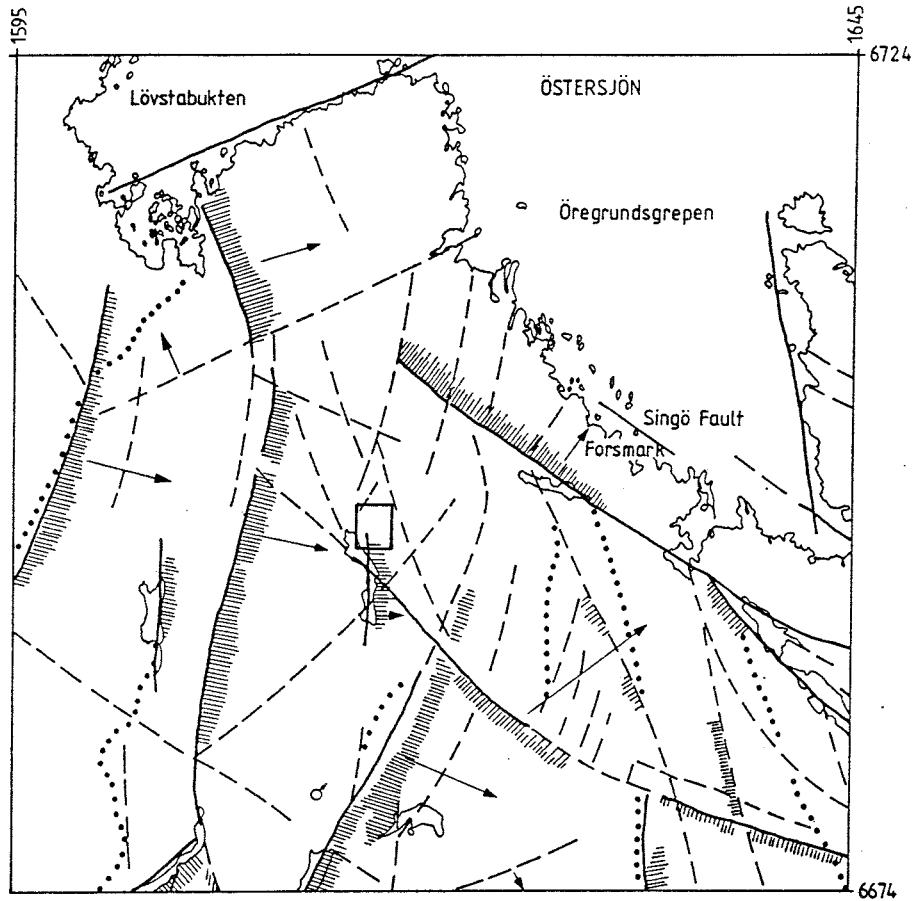


Figure 1.1 Location map of the Finnsjön area (including the Brändan and Gåvastbo areas).



LINEAMENT MAP, NORTHEASTERN UPPLAND

REGIONAL AREA

- Lineament, well expressed
- - - Lineament, less well expressed
- ▨ The elevated side of the structure is marked with a line screen
- Dip direction of the ground surface
- Glaciafluvial deposits, eskers
- ♁ Dannemora mine
- Finnsjön site

The glacial striation is north-south

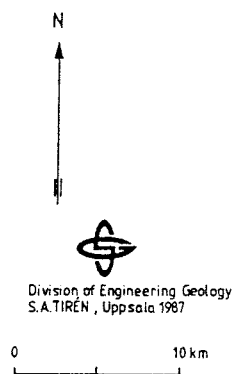


Figure 1.2 Lineament map of the regional area. From Ahlbom and Tirén (1989, 1991).

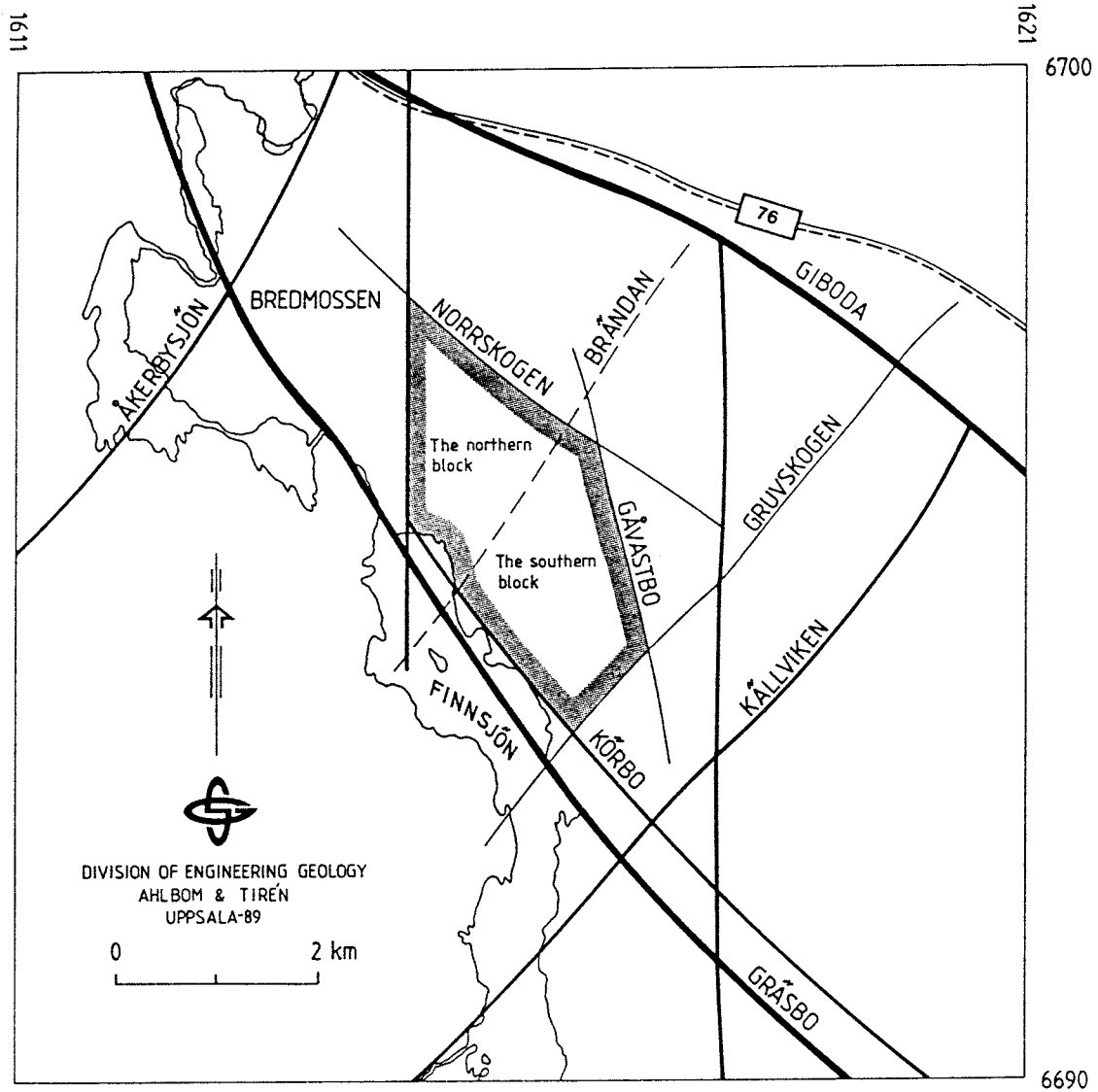


Figure 1.3 The Finnsjön Rock Block (rastered area) and surrounding lineaments in the semi-regional area. From Ahlbom and Tirén (1991).

2. SURFACE HYDROLOGY AND GROUNDWATER RECHARGE

The hydrologic and hydrometeorological conditions within northern Uppland with emphasis on the Finnsjön area have previously been described by Carlsson and Gidlund (1983). In the current report the main results of this report are summarized.

2.1 Water courses

Northern Uppland with surrounding areas is drained into the Bottenhavet, part of the Baltic Sea, primarily by the rivers Dalälven, Tämnarån, Forsmarksån and Olandsån. Towards the south the area is drained into the lake Mälaren system via the rivers Örsundaån and Fyrisån, see Appendix 1.

The Finnsjön area is drained via two separate surface water-course systems. The major system drains the central and southern parts of the area whereas the north-western part is drained by another system. The two systems merge together in the north-eastern part of the area (Jacobsson and Larsson, 1980).

2.2 Water-logged grounds

Northern Uppland belongs, with regard to soil types, to a till area characterized in its northwestern part by about 25% mire and 45% till. The proportion of mires decreases towards the south and east. To the west of Lake Finnsjön, there is the mire complex Flororna of an approx. 50 km² acreage.

Within the Finnsjön study area, about 20% is mires (5 km²). Of this approx. 3 km² is swamp and 2 km² bog. In the northern and western parts there are mainly bogs whereas the swamps are most prevalent in the southern and eastern parts. Bogs are primarily found in recharge areas whereas the swamps mostly are located in low-lying parts of the area where more nutritious groundwater is discharged.

2.3 Lakes

The major lakes in the northern part of Uppland are listed in Table 2.1. The location of the lakes is shown in Appendix 1. Within the Finnsjön study area there is a (nowadays) drained lake, Tannsjön. Its area is, as a free water surface, 0,01 km². Lake Finnsjön belongs to the run-off area of the river Forsmarksån. The size of the catchment area of lake Finnsjön is 93 km² at the inlet and 117 km² at the outlet. Lake Finnsjön is long and narrow with a north-south extension with a length 6.5 km and a width of 1 km. The maximum depth is 4.1 meter.

2.4 Water balance and groundwater recharge

An estimate of the overall water balance for northern Uppland was made by Carlsson and Gidlund (1983). The areal proportion of groundwater discharge areas in the region was estimated to about 30% and recharge areas to 70%. In the discharge areas no

groundwater recharge was assumed and the potential evapotranspiration was used in the water balance calculations whereas in the recharge areas the actual evapotranspiration was used (Table 2.2).

Table 2.1 Major lakes in the northern part of Uppland. From Carlsson and Gidlund (1983).

Lake	Lake surface area (km ²)
Tämnarån + Storsjön	39.4
Erken	24.9
Vällan	10.9
Vendelsjön	5.6
Giningen	6.1
Närdingen	5.6
Strömaren	4.8
Finnsjön	4.3

The potential groundwater recharge to the soil layers was estimated by Carlsson and Gidlund (1983) using observed groundwater level variations in the Quaternary deposits. The effective porosity of these deposits was estimated at 0.04 which corresponds to an average groundwater recharge of about 180 mm/year to the soil layers (Table 2.2). This figure should be compared with the estimated groundwater recharge in the Forsmark area, ranging from 112-max.168 mm/year (Andersson and Olsson, 1978). A reasonable estimate of the groundwater recharge in the uppermost part of the groundwater system in the Forsmark area would be 100-125 mm/year (Carlsson et al., 1987).

As pointed out by Axelsson (1986) the actual recharge to the bedrock is much smaller than those values presented above. The average groundwater recharge to the bedrock in the Forsmark area can be estimated to 10-20 mm/year (Carlsson et al., 1987).

Table 2.2 Estimated water balance and groundwater recharge in northern Uppland, expressed in mm/year (long-term). From Carlsson and Gidlund (1983).

Precipitation	P	670
Run-off	R	240
In discharge areas (30%)		
Evaporation	E _D	540
Groundwater recharge		-
Groundwater discharge	G _p	420
Available run-off precipitation	R _p	130
In recharge areas (70%)		
Evaporation	E _R	380
Groundwater recharge	G _R	180
Groundwater discharge		-
Snowmelting run-off water	R _S	105

3. GROUNDWATER HEAD CONDITIONS

3.1 Groundwater table

Contour maps of the groundwater table have been prepared for the semi-regional and local model areas. These areas are defined in Chapter 9. The equipotentials used are 2 m and 1 m, respectively. The maps, which are shown in Appendix 2, characterize the contours of the groundwater table schematically only but are considered detailed enough to serve as input data for numerical models in the actual scales. The semi-regional map shows that the regional, shallow groundwater flow is mainly directed from southwest to northeast. In the local area the shallow groundwater flow pattern is more complex.

The following background material was used for the preparation of the groundwater table maps:

Semi-regional map: the altitude of the water table at surface water courses and wetlands is assumed to coincide with the shallow groundwater table and was therefore read directly from topographical maps. The groundwater table elsewhere in the terrain was determined according to the following principles:

- at nearby surface water courses and in low-lying areas the groundwater table is assumed to be located successively 0-2 m below the ground level.
- at hill slopes and on the hills the groundwater table is assumed to be located successively 1-3 m below the ground level.

Local map: the groundwater table was determined as for the semi-regional map but as background material a detailed topographical map of the Finnsjön site, contoured every 1 m, was used.

The corresponding data files of the groundwater table within the semi-regional and local model areas are also prepared on diskette with the actual x, y and z-coordinates in the RAK-system in digitalized form.

It should be observed that the groundwater table contours at the boundaries of the local area do not coincide exactly in the semi-regional and local maps due to the different scales of interpolation used.

3.2 Piezometric borehole conditions

3.2.1 Long-term piezometric measurements

In conjunction with the drilling of borehole BF101 piezometric measurements were made in isolated observation borehole sections (Ahlbom et al., 1988). In general, pressure measurements were carried out in 3-5 isolated sections of the cored boreholes in the Brändan area (Fig 1.1) and in three sections of borehole HF101. Outside the Brändan area observations were

made in three sections of borehole KFI08. Undisturbed measurements of the piezometric pressure in the borehole sections were obtained before the pumping and after the recovery periods of the drilling. To calculate the groundwater potentials, the pressures were corrected for the varying salinity along the boreholes (Ahlbom et al., 1988).

The relative groundwater potentials along the boreholes, measured at a specific time, are shown in Appendix 3:1. The difference in potential, expressed in metres, in the borehole sections relative to the potential of the uppermost section (groundwater table) is presented. This difference constitutes a potential gradient along the boreholes. Besides the groundwater potential also the salinity logs along the open boreholes (Ahlbom et al., 1986) are presented.

The potential gradients in Appendix 3:1 indicate that in boreholes where Zone 2 is located deep below the ground surface (e.g. KFI07 and KFI11), infiltration of shallow nonsaline groundwater, and to a certain extent also deep saline groundwater, occurs to the zone (Ahlbom et al., 1988).

In boreholes where Zone 2 is located closer to the ground surface (e.g. KFI05 and KFI10), the gradient is reversed thus implying that saline groundwater is discharged from Zone 2. The groundwater potentials indicate that the gradient is mainly directed upward. The potential gradient thus causes saline water to rise into the upper fresh water zone in the boreholes KFI05, KFI09, KFI10 and HFI01 when the boreholes are left open. This is also reflected in the salinity logs which in these boreholes are more subdued because of mixing. However, under natural groundwater flow conditions the high transmissivity of the uppermost part of Zone 2 in the lateral direction will prevent saline water to rise to the surface. Instead, the groundwater is assumed to be discharged laterally to Zone 1 (Gustafsson and Andersson, 1989).

The absolute groundwater potentials represent the hydraulic head. The distribution of hydraulic head in the lateral direction in the upper part of Zone 2 within the Brändan area, estimated from the piezometric measurements, is shown in Figure 3.1. The contour map of the hydraulic head presented is considered as schematic due to the few observation points. Figure 3.1 indicates that the main direction of groundwater flow in the upper part of Zone 2 is towards ENE with a small gradient (0.2%) in the western part of the area. In the eastern part the groundwater flow is more directed towards ESE to Zone 1 with a gradient of 0.3% (Gustafsson and Andersson, 1989).

As pointed out by Ahlbom et al. (1988) there are considerable uncertainties in the interpretation of the piezometric measurements due to the varying salinities along the boreholes and the registration methods adopted. Nevertheless, the measurements are assumed to represent the general pattern of the groundwater potentials in the vertical and lateral directions. In summary, Zone 2 is assumed to be recharged at deeper parts in the western part of the Brändan area and dis-

charged to Zone 1 in more surficial locations in the eastern part.

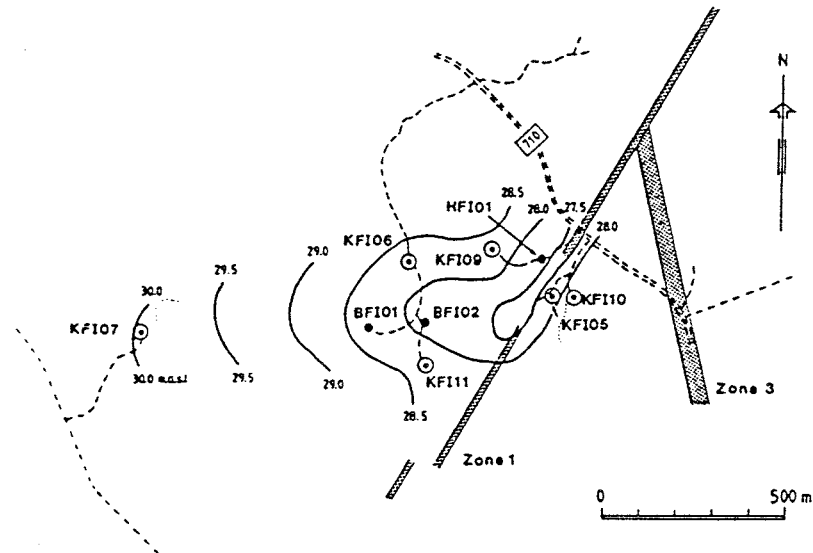


Figure 3.1 Estimated distribution of hydraulic head (m.a.s.l.) in the upper part of Zone 2 within the Brändan area. From Ahlbom et al.(1988).

3.2.2 Pressure measurements from injection tests

Prior to a single-hole injection test in an isolated borehole section, the integrated borehole pressure or hydrostatic pressure (P_i) is measured in the open borehole before packer sealing at the actual depth. After packer sealing, a certain time is allowed for the pressure in the isolated test section to approximately stabilize (P_o) before start of injection. The pressure difference ($P_o - P_i$) before and after packer sealing is a rough measure of the natural pressure conditions in the tested section, i.e. underpressure or overpressure in relation to the hydrostatic pressure, provided that the section pressure has (approximately) stabilized. This is normally the case in high-conductive sections but not in low-conductive sections.

The estimated pressure differences ($P_o - P_i$) from steady-state injection tests in 2 m-sections in boreholes within the Brändan area (Andersson et al., 1988) are presented in Appendix 3:2. These tests are generally restricted to borehole intervals within Zone 2, see Section 4.1. In very low-conductivity sections the pressure after packer sealing is normally disturbed due to the expansion of the packers. Therefore, only sections with a hydraulic conductivity greater than about $1E-8$ m/s are included in the graphs in Appendix 3:2. The pressure differences measured along the boreholes are rather small, normally ranging between -2 and 2 kPa. The most extreme values

are considered as very uncertain and probably caused by instrumental malfunctions. These data represent the only estimates available on the natural pressure in short sections along boreholes in the Finnsjön area.

Since the 2 m-tests in general only covered borehole intervals within Zone 2, the natural pressure has also been estimated from transient injection tests in 20 m-sections in boreholes where such tests are performed over the entire length (KFI09, KFI10, KFI11 and BFI01), see Table 4.1. In these boreholes (except KFI09) the pressure differences ($P_s - P_i$), representing the natural pressure in the sections, were calculated. P_s is the estimated natural pressure in the section determined during the recovery period after injection. In borehole KFI09 the pressure difference ($P_o - P_i$) was calculated. The estimated pressure differences along the boreholes from the 20 m-tests are shown in Appendix 3:3. Only sections with a hydraulic conductivity higher than about $1E-10$ m/s are included.

Since the estimated pressure differences generally are rather small, also in the borehole intervals above and below Zone 2, any conclusions based on the results presented must be regarded as uncertain. The potential error in the pressure differences is estimated to about ± 1 kPa (0.1 m) regarding the accuracy of the actual pressure transducers. Furthermore, potential errors may also derive from insufficient time allowed for the section pressure to stabilize and from pressure fluctuations. Nevertheless, bearing the above potential sources of error in mind, the pressure differences seem to support some of the results from the piezometric measurements, i.e. the presence of a small pressure gradient directed upward below Zone 2 and recharge conditions above the zone in borehole KFI11. The small pressure differences estimated in borehole KFI10 are generally considered as within the potential error band of the measurements.

To conclude, both the piezometric measurements and the pressure differences estimated from the injection tests indicate that only small pressure gradients exist within Zone 2 both in the vertical and lateral directions and also above and below the zone, i.e. the pressures in the boreholes are near the hydrostatic pressure.

The pressure differences estimated from the injection tests in 2 m and 20 m sections are stored in the GEOTAB database. The data from the piezometric measurements are available on protocols at SGAB, Uppsala, see Chapter 10.

4. HYDRAULIC CONDUCTIVITY CONDITIONS

4.1 Methods used

4.1.1 Single-hole tests

Single-hole water injection tests have been carried out during different phases since 1977 at the Finnsjön study site. Table 4.1 compiles information on the boreholes tested, actual packer spacing, intervals measured, lower measurement limits and year of testing for all single-hole tests carried out at the Finnsjön area. As can be seen from the table the oldest tests in boreholes KFI01-08 normally were performed in 3m-sections, covering almost the entire boreholes. These tests, which were carried out as short-time steady-state tests, are reported by Hult et al. (1978) and Carlsson et al. (1980). In the deepest parts of boreholes KFI02 and KFI03 no hydraulic tests were performed due to intense fracturing.

The Fracture Zone project was initiated 1984. The tests in this project were generally performed in 2m-sections and covered mainly fracture Zone 2 and its immediate surroundings. Tests in 20m-sections were generally performed above Zone 2 and in some cases along the entire boreholes. In the bottom part of the boreholes, single-packer tests were generally carried out. The 2m-tests were performed as short steady-state tests whereas the 20m-tests were transient tests of 2 hours injection followed by 2 hours of pressure recovery. Finally, very detailed tests in 0.11m-sections were carried out in segments of borehole BFI02.

Single-hole test results from the Fracture Zone Project have been reported by Ahlbom et al. (1986, 1988), Andersson et al. (1988) and Ekman et al. (1988). The prime objective of the testing in this project was to investigate the hydraulic properties of Zone 2 in detail. The performance and interpretation of the single-hole tests are described in Almén et al. (1986). A comparison of results from old 3m-tests and new 2m-tests in boreholes KFI05-07 was performed by Andersson et al. (1988). The hydraulic conductivity distributions along the boreholes determined from single-hole tests are shown in Appendix 4. All calculated hydraulic conductivity values from the single-hole tests are stored in the GEOTAB database, see Chapter 10.

4.1.2 Interference tests

During the drilling of borehole BFI01 the groundwater head was registered in isolated sections of the other boreholes within the Brändan area. Since water was flushed out of borehole BFI01 by compressed air at a fairly constant rate during the drilling periods, these periods could be regarded as (preliminary) drawdown tests. Between the drilling periods the groundwater head in the boreholes was allowed to recover. The recorded head changes in the observation sections were analyzed preliminary to determine the hydraulic properties of Zone 2 and adjacent bedrock. These tests are reported in Ahlbom et al. (1988).

Subsequently, more sophisticated hydraulic interference tests were carried out by pumping from different parts of Zone 2 in borehole BFI02 and monitoring the head changes in isolated multiple-borehole sections within Zone 2 and in a few boreholes outside the zone. The detailed interference tests were analysed both qualitatively and quantitatively by Andersson et al. (1989). The results are summarized in Section 4.3.2.

Table 4.1 Compilation of data from hydraulic single-hole tests in the Finnsjön site.

Borehole	Inclination	Borehole length (m)	Section length (m)	Interval measured (m)	Lower measurement limit K (m/s)	Year of testing
KFI01	90°	500	2	14-494	2.4 E-9	1977
KFI02	50°	698	3	16-673	2.0 E-9	1977
KFI03	50°	730	3	8-677	3.3 E-10	1977
KFI04	80°	602	3	50-596	1.9 E-10	1979
KFI05	50°	750	3 2	50-743 141-320	1.9 E-10 7.5 E-10	1979 1986
KFI06	90°	691	3 2	58-679 192-293	1.9 E-10 7.5 E-10	1979 1987
KFI07	85°	552	3 2	18-543 263-364	1.9 E-10 7.5 E-10	1979 1987
KFI08	60°	464	3	40-460	1.6 E-10	1980
KFI09	60°	375	20 2	10-350 109-263	1.0 E-11 1.0 E-10	1985 1986
KFI10	50°	255	20* 5* 5* 2	10-230 75-105 205-235 60-224	1.0 E-11 4.0 E-11 " 1.0 E-10	1985 " " 1986
KFI11	90°	389	20 2	6-386 210-360	1.0 E-11 1.0 E-10	1986 1986/87
HFI01	90°	129	10 2 2	4-124 34-44 104-114	1.0 E-10 2.0 E-9 2.0 E-9	1985 1985 1985
BFI01	90°	460	20 2	30-450 220-450	1.0 E-11 1.0 E-10	1987 1987
BFI02	90°	289	20 2 0.11 " "	10-200 200-284 201.89-206.07 211.89-214.09 257.89-262.18	1.0 E-11 1.0 E-10 5.0 E-9 " "	1987 1987 1988 " "

* The tests were repeated at three different occasions before and after gas-lift pumping.

4.2 Hydraulic units

To establish a conceptual hydraulic model of the Finnsjön area and its surroundings the hydraulic conductivity data have been subdivided into different hydraulic units based on the geological interpretation of fracture zones. The hydraulic units defined are 1) the rock mass excluding fracture zones and 2) fracture zones of different orders. These units are regarded as statistically homogeneous regarding the hydraulic properties. A preliminary interpretation of fracture zones was made by Ahlbom and Tirén (1989) and Tirén and Stark (1989). The latter reference constitutes a tentative model of hydraulically conductive fracture zones in the Finnsjön site.

Subsequently, the geological interpretation of fracture zones was updated by Ahlbom and Tirén (1991). In this interpretation slight modifications of the dip and orientation of some of the fracture zones (mainly Zone 11) have been made. The subdivision of data in hydraulic units is mainly based on the updated interpretation.

A generalized map of fracture zones within the Finnsjön Rock Block is shown in Figure 4.1. The positions of interpreted fracture zones in the boreholes and their strike and dip together with a characterization of the zones, according to Ahlbom and Tirén (1991) and Tirén and Stark (1989) are presented in Table 4.2. For Zone 9 an alternative interpretation was discussed by Ahlbom et al. (1986) and Tirén and Stark (1989). According to that interpretation Zone 9 is steep to vertical and displaces Zone 2. It should be noted that Zones 3 and 11 intersect in borehole KFI08. Notable is also that the lower boundary of Zone 2 coincides with the upper boundary of Zone 5 in borehole KFI09. The inclination of Zone 5 is somewhat uncertain. It may be more steeply inclined (c.80 degrees) than suggested in Table 4.2. From the regional fracture zones (4, 12, 13 and 14), delimiting the Finnsjön Rock Block in Figure 4.1, no borehole information is available.

A three-dimensional CAD-model of the Finnsjön Rock Block, viewed from 40 degrees above from different directions showing the fracture zones and the boreholes is presented in Appendix 5. In this Appendix also the equations in the RAK-system of the fracture zones (according to the updated geological interpretation) together with the coordinates of their intersections with the delimiting fracture zones of the Finnsjön Rock Block are given.

Based on the updated geological interpretation a subdivision of the hydraulic conductivity data from the single-hole tests was made. By this process, emphasis was made to define the hydraulically most important (gross) fracture zone intervals in the boreholes. Therefore, slight differences of the interpreted hydraulically conductive borehole intervals compared to the geological interpretation may occur. Besides the measured hydraulic conductivity distributions along the boreholes, the interpretation of the hydraulically conductive fracture zone intervals is also based on core logs and geophysical logs (Olkiewicz et al. 1979, Ahlbom et al. 1986).

The estimated hydraulically conductive fracture zone intervals in the boreholes used by the subdivision of the hydraulic conductivity data in hydraulic units are shown in Table 4.3. The borehole intervals of the subhorizontal Zone 2 are mainly based on information in Ahlbom et al. (1988) and Ekman et al. (1988).

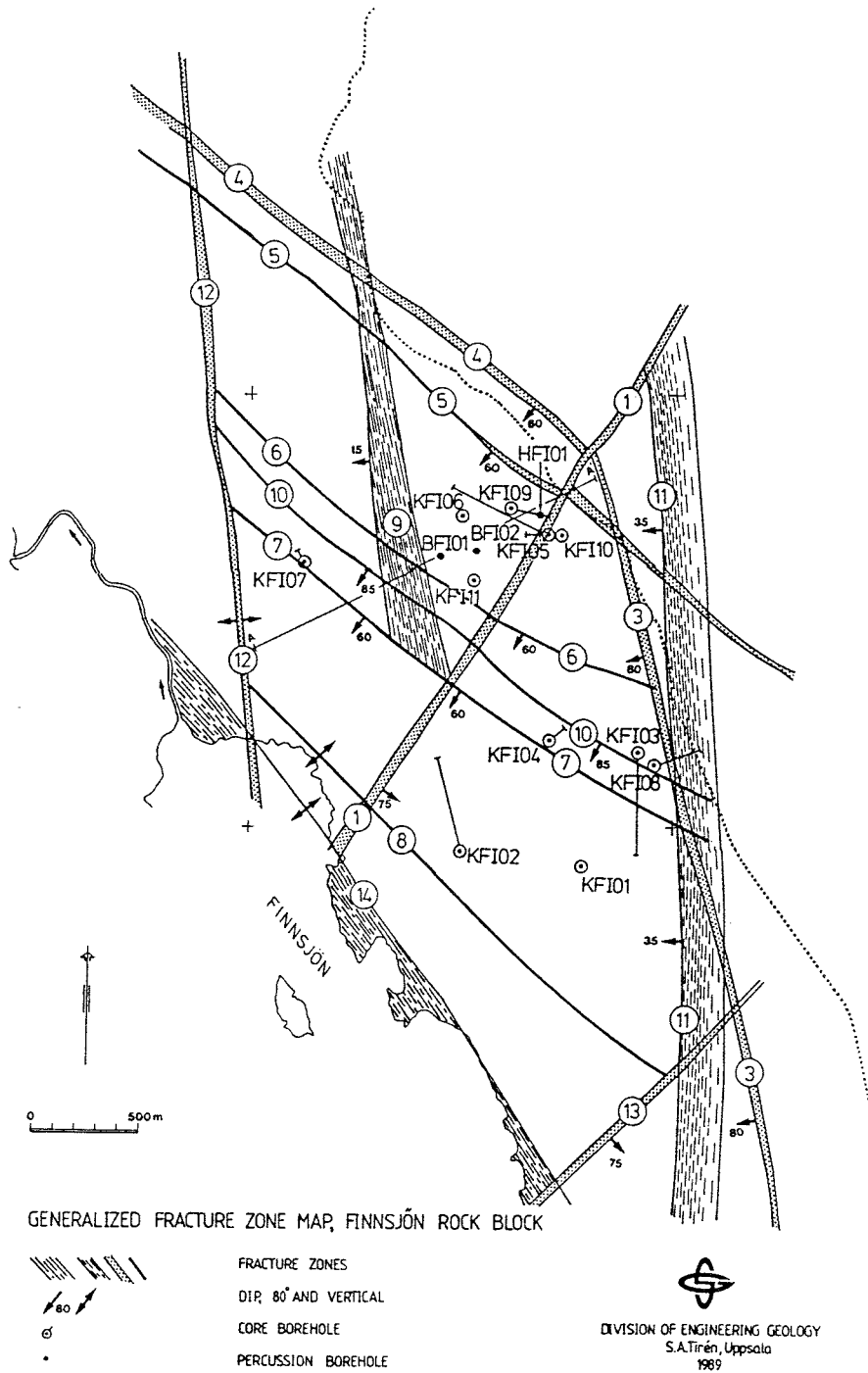


Figure 4.1 Generalized map of fracture zones in the Finnsjön Rock Block. From Ahlbom and Tirén (1991).

Table 4.2 Interpreted fracture zone intervals in the boreholes together with the orientation and width of the zones in the Finnsjön Rock Block. From Ahlbom and Tirén (1991) and Tirén and Stark (1989).

Fracture zone	Borehole	Borehole length(m)	Orientation strike	dip	Width (m)	Character
1	KFI05 KFI10	10-48 75-105	N30E	75SE	20	Local
2	KFI05 KFI06 KFI07 KFI09 KFI10 KFI11 BFI01 BFI02 HFI01	166-305 201-305 295-380 130-212 152-256+ 221-338 240-365 204-289+ 105-125+	N28W	16SW	100	Local?
3	KFI08	20-150	N15W	80SW	50	Regional
4	no boreholes		N50W	60SW	10	Regional
5	KFI05 KFI06 KFI09	485-498 554-557 212-216	N50W	60SW	5	Local
6	KFI07	530-537	N55-65W	60SW	5	Local
7	no boreholes		N55W	60SW	5	Local
8	no boreholes		N50W	90	5	Local
9	KFI07	109-154	N10W	15SW	50	Local
10	KFI03	57-62	NW	85SW	5	Local
11	KFI01 KFI03 KFI04 KFI08	332-436 107-245 368-440 20-125	N 5W	35W	100	Local?
12	no boreholes		N-S	90	25	Regional
13	"		N30E	75SE	20	Regional
14	"		NW	90	100	Regional

+ zone not fully penetrated

Table 4.3 Estimated gross hydraulically conductive fracture zone intervals in the boreholes in the Finnsjön site.

Fracture zone	Borehole	Interval (m.b.g.l.)	Vertical depth (m.b.g.l.)	Character
1	KFI10	77-104	58-78	Local
2	KFI05	166-304	128-234	Local?
	KFI06	213-272	213-272	
	KFI07	294-338	293-337	
	KFI09	130-212	112-183	
	KFI10	140-210	106-159	
	KFI11	222-338	222-336	
	HFI01	108-125+	108-124+	
	BFI01	242-356	239-350	
	BFI02	200-280	198-275	
3	KFI08	40-150	33-129	Regional
5	KFI05	455-497	347-379	Local
	KFI06	556-559	556-559	
	KFI09	213-217	243-247	
6	KFI07	531-537	528-534	Local
9	KFI07	109-162	108-161	Local
10	KFI03	57-62	45-48	Local
11	KFI01	364-436	364-436	Local?
	KFI03	107-275	82-307	
	KFI04	368-398	364-394	
	KFI08	20-140	16-120	

m.b.g.l.= metres below ground level

4.3 Hydraulic properties of the fracture zones

4.3.1 Fracture zones outside Zone 2

Hydraulic single-hole tests have been performed in some of the fracture zones outside Zone 2. The total transmissivity (T) and the average hydraulic conductivity (K_{ave}) of the conductive fracture zone intervals in Table 4.3, calculated from single-hole tests with different section lengths (L), together with the number of tests (N) are presented in Table 4.4. The average hydraulic conductivity is calculated by dividing the total transmissivity of the zone with the estimated fracture zone interval. In addition, the maximal transmissivity (T_{max}) of the most permeable test section within the zone and the ratio of T_{max}/T are calculated.

This ratio gives some information about the transmissivity distribution within the zones. For example, a ratio close to one indicates that the total transmissivity of the actual zone is dominated by only one test section. On the other hand, a low ratio indicates a more evenly distributed transmissivity within the zone. Obviously, the ratio also depends strongly on the number of test sections in the zone. For example, the intervals in boreholes KFI06 and KFI09 (intersecting Zone 5) only include one or two test sections resulting in a high ratio. On the other hand, rather high ratios were calculated for fracture Zone 9 and Zone 11 (borehole KFI04) despite the rather long zone intervals. This indicates that in the latter zone intervals only one or a few test sections dominate the total transmissivity. In Zone 1 about 50% of the total transmissivity is concentrated to only one short test section. For Zone 3, Zone 5 (borehole KFI05) and Zone 11 (boreholes KFI01 and KFI08) relatively low ratios were calculated, indicating a more even transmissivity distribution in these zones.

The updated geological interpretation by Ahlbom and Tirén (1991) mainly concerns the dip of fracture zones 10 and 11. Hydraulically, this implies that the transmissivity of Zone 10 in Table 4.4 is significantly decreased (about four orders of magnitude) while the transmissivity of Zone 11 is increased about 15 times, c.f. Table 4.4 in Andersson et al., 1989b.

Table 4.4 Estimated transmissivity and average hydraulic conductivity together with the apparent transmissivity distributions within the fracture zones outside Zone 2 in the Finnsjön Rock Block.

Fracture Zone	Bore-hole	L (m)	N	T (m ² /s)	K _{ave} (m/s)	T _{max} (m ² /s)	T _{max} /T
1	KFI10	20	2	2.6E-4	8.7E-6	1.4E-4	0.55
	KFI10	2	14	2.1E-4	7.0E-6	9.8E-5	0.47
3	KFI08	3	37	1.0E-4	9.4E-7	2.6E-5	0.26
5	KFI05	3	14	1.6E-5	3.7E-7	2.8E-6	0.18
	KFI06	3	1	1.4E-6	4.6E-7	1.4E-6	1.00
	KFI09	2	2	2.9E-5	7.2E-6	2.8E-5	0.97
	KFI09	20	1	1.2E-4	3.1E-5	1.2E-4	1.00
6	KFI07	3	2	2.9E-8	4.1E-9	2.0E-8	0.70
9	KFI07	3	18	2.5E-6	4.8E-8	5.1E-6	0.68
10	KFI03	3	2	2.8E-8	5.7E-9	6.1E-9	0.64
11	KFI01	2	28	5.9E-7	1.0E-8	1.8E-7	0.31
	KFI03	3	56	6.6E-4	3.9E-6	2.8E-4	0.42
	KFI04	3	10	1.7E-4	5.7E-6	1.5E-4	0.88
	KFI08	3	33	1.1E-4	9.0E-7	2.6E-5	0.24

Due to the limited number of data from fracture zones outside Zone 2 and the uncertainties in the geological interpretation of the zones, it is difficult to draw any firm conclusions about the variation of hydraulic conductivity of the fracture zones with depth. No borehole data are available from Zones 7 and 8 and the lineaments delimiting the Finnsjön Rock Block (Zones 4, 12, 13 and 14). Zone 14 has the same strike as the Singö fault (Fig. 1.2) and is assumed to be related genetically to the latter zone, see Section 9.3.

A few data exist from single-hole tests in boreholes penetrating the Singö fault at the SFR-area near Forsmark. The average hydraulic conductivity of the Singö Zone in the SFR-area was estimated at $7E-7$ m/s from hydraulic tests (Carlsson et al. 1986). This corresponds to a transmissivity of about $1E-5$ m^2/s . According to Tirén and Stark (1989), Zone 4 (and also Zone 14) is part of a major geological structure to which also the Singö Line is likely to be related. The assumed orientation of Zone 4 is shown in Table 4.2. No subsurface information is available from Zone 4 and 14.

4.3.2 Fracture Zone 2

In the local scale, Zone 2 constitutes a dominating hydraulic structure. The total thickness of Zone 2 is estimated to about 100 m. Zone 2 has been extensively investigated by several boreholes. A large number of single-hole tests with different packer spacings (frequently 2 m) have been performed in Zone 2 (Table 4.1 and 4.7). In addition, a series of hydraulic interference tests with multiple-section observation boreholes and tracer tests have been conducted in Zone 2 (Andersson et al., 1989).

The single-hole tests demonstrated the existence of about 2-5 narrow subzones with very high hydraulic conductivity in the boreholes. Very detailed tests in 0.11 m sections indicated a width of approximately 0.5 m of the subzones (Ekman et al. 1988). The single-hole tests also indicated that the uppermost subzone consistently appeared close to the upper boundary of Zone 2 in the boreholes. Frequently, the lowermost subzone was located near the lower boundary of Zone 2. Finally, the single-hole tests demonstrated a high hydraulic conductivity contrast between Zone 2 and the overlying rock (Ahlbom et al. 1988).

The hydraulic interference tests were performed by pumping from different isolated parts of Zone 2, i.e. lower part (test 1), upper part (test 2) and finally, the entire zone (tests 3A and 3B) in borehole BFI02. The configuration in the pumping borehole during the different tests is shown in Figure 4.2. In this borehole the drawdown and flow rate and also the changes of downhole groundwater temperature, atmospheric pressure and the electric conductivity of the discharged water were registered. The changes of water conductivity, which provided useful information about the flow pattern within Zone 2 during the tests, are discussed in Section 6.2 and presented in Appendix 8:5.

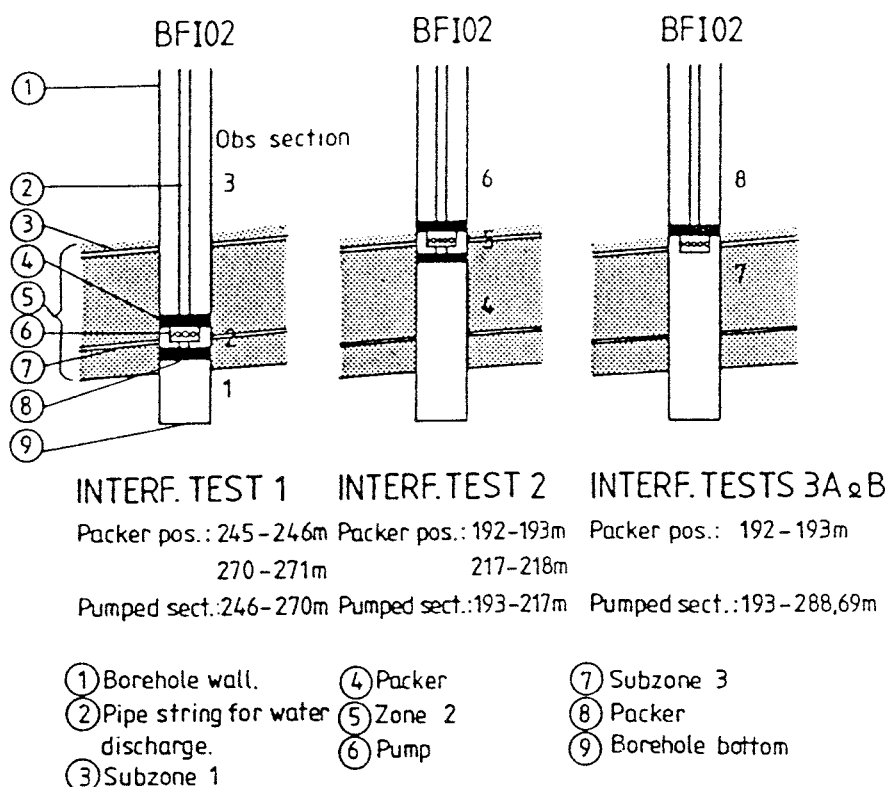


Figure 4.2 Schematic illustration of the configurations in the pumping borehole during the hydraulic interference tests together with the numbering of the monitored sections. (From Andersson et al., 1989).

The drawdown was normally measured in five isolated observation sections in each borehole, i.e. in the lower, middle and upper part of Zone 2 and just above and below the zone in the adjacent rock. The observation borehole sections within Zone 2 are listed in Table 4.7. In addition, the groundwater level in the upper parts of the boreholes was registered. Drawdown observations were also performed in a few peripheral, open boreholes (KFI01, KFI02, KFI04, KFI07, KFI08 and HGB02) in the southern part of the Finnsjön Rock Block between Zone 1 and 3, see Figure 1.1.

The interference tests demonstrated that different drawdown response patterns were generated in the nearest and more distant observation boreholes from the pumping borehole. Examples of typical near-region and distant region borehole responses during interference test 2 are shown in logarithmic graphs in Figures 4.3a and b, respectively. The graphs show the multiple-section response curves in different parts of Zone 2

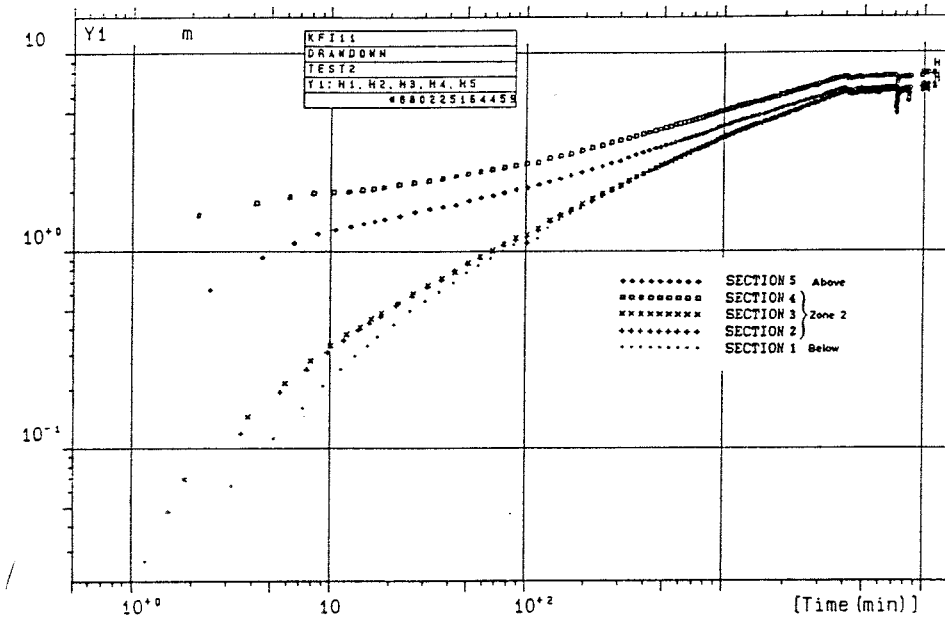
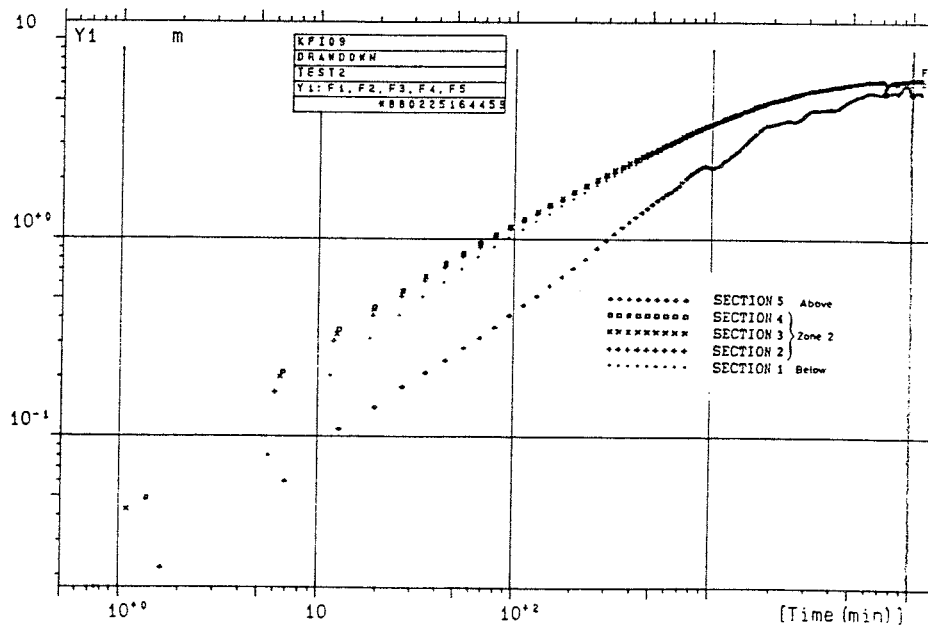


Figure 4.3 Drawdown responses in multiple-sections of two observation boreholes during interference test 2 (upper part of Zone 2) in logarithmic graphs. (From Andersson et al., 1989).
 a) borehole KFI11 (Near-region)



b) borehole KFI09 (Distant-region)

and above and below the zone as indicated by the legend. In the near-region borehole KFI11 (Fig 4.3a) the primary response (uppermost curve) occurred very rapidly in the upper part of Zone 2 (section 4) after start of pumping. The (secondary) response in the lower part of the zone (section 2) was much more delayed, i.e. the response curves were markedly separated from each other.

In the distant-region borehole KFI09 (Fig. 4.3b) all response curves in the zone almost coincide. These curves are very similar to the secondary response curves in the near-region. The responses in the rock above and below Zone 2 were generally much more delayed compared to those in the zone, provided that sufficient hydraulic isolation between these sections and the zone was achieved. This is questionable in some cases.

The uppermost, highly conductive subzone of Zone 2 was proved to be hydraulically interconnected in the boreholes over several hundred of metres. The interference tests also showed that hydraulic interaction occurred in the vertical direction of the zone although a certain anisotropy of the vertical hydraulic conductivity within the zone was indicated (Fig. 4.3a). A certain anisotropy of the hydraulic properties along the zone was also observed. This feature was most accentuated in the near-region observation boreholes and mainly concerned the calculated storativity values rather than the transmissivity values (Andersson et al., 1989).

Furthermore, the interference tests showed that Zone 2 is delimited by outer hydraulic boundaries, probably constituted by steeply dipping fracture zones (Fig 4.1). One of the observation sections in borehole KFI10 (76-134 m) is located in Zone 1, see Table 4.7. A significant drawdown (similar to that in Zone 2) was observed in this section during all interference tests. It was also demonstrated that Zone 2 was recharged by the end of the tests, possibly via other fracture zones or by natural groundwater flow along Zone 2. Finally, in some of the peripheral observation boreholes in the southern block (e.g. KFI04) a significant response to the interference tests occurred. This indicates a hydraulic interaction between the northern and southern part of the Finnsjön Rock Block, see Section 9.4.

The results of the time-drawdown analysis of the interference tests within Zone 2 are summarized in Table 4.5. The transmissivity (T), storativity (S), hydraulic diffusivity (T/S) in different parts of Zone 2 together with the leakage coefficient (K'/b') were calculated. Test no 1 and 2 in Table 4.5 refer to the pumping of the lower and upper parts of Zone 2, respectively and test no 3B to the pumping of the entire zone (Andersson et al., 1989).

In Table 4.5 the part of Zone 2 in which the actual primary responses in the observation boreholes occurred during the tests are also listed. Boreholes KFI05, KFI06, KFI11 and BFI01 are assumed to represent the hydraulic properties of the near-region around the pumping borehole, BFI02. This means that the hydraulic parameters calculated from these boreholes should

represent that part of Zone 2 where the primary response occurred. The distant-region boreholes KFI09, KFI10 and HFI01 are assumed to represent the average hydraulic properties of the entire Zone 2.

Table 4.5 reveals that the transmissivities calculated for the upper and lower parts of Zone 2 from the near-region boreholes are rather uniform at about $1\text{-}2\text{E-}3$ m^2/s . The transmissivity of the entire Zone 2, calculated from the distant-region boreholes is also rather uniform, ranging between $2\text{-}4\text{E-}3$ m^2/s . The latter values are also confirmed from the distance-drawdown analysis of the interference tests (Table 4.6). The almost coinciding drawdown responses in the distant-region observation boreholes indicate that Zone 2 responded as a porous medium with averaged hydraulic properties beyond a certain distance from the pumping borehole. In contrast, the near-region responses were much more influenced by local heterogeneities (Andersson et al., 1989).

Table 4.5 Summary of results of the hydraulic interference tests within Zone 2. Time-drawdown analysis.
(From Andersson et al., 1989)

Observation borehole	T (m^2/s)	S (-)	T/S (m^2/s)	K'/b' (s^{-1})	Part of Zone 2	Test no
KFI05	1.6 E-3	1.0 E-5	160	4.1 E-8	lower	1
"-	1.7 E-3	1.3 E-5	131	6.9 E-8	lower	3B
KFI06	1.6 E-3	7.1 E-6	225	4.8 E-8	lower	1
"-	1.4 E-3	2.4 E-6	583	4.5 E-8	upper	2
"-	1.4 E-3	3.8 E-6	368	4.1 E-8	upper	3B
KFI09*	2.4 E-3	2.0 E-5	120	1.3 E-8	whole	1
"-	2.5 E-3	9.9 E-6	253	1.5 E-8	whole	2
"-	3.5 E-3	1.7 E-5	206	1.0 E-8	whole	3B
KFI10*	2.0 E-3	2.2 E-5	91	7.1 E-8	whole	1
"-	2.5 E-3	1.0 E-5	250	9.3 E-8	whole	2
"-	2.4 E-3	1.8 E-5	133	8.7 E-8	whole	3B
KFI11	1.3 E-3	3.7 E-6	351	1.7 E-8	lower	1
"-	1.4 E-3	5.7 E-7	2460	2.9 E-8	upper	2
"-	1.3 E-3	2.6 E-6	500	1.1 E-7	upper	3B
BFI01	2.4 E-3	5.7 E-5	42	4.2 E-8	upper	1
"-	1.4 E-3	9.4 E-6	149	1.6 E-8	upper	2
"-	2.0 E-3	2.0 E-5	100	1.3 E-8	upper	3B
HFI01*	3.9 E-3	2.3 E-5	170	1.4 E-9	(upper)	1
"-	2.4 E-3	1.5 E-5	160	1.3 E-9	(upper)	2
"-	3.5 E-3	1.9 E-5	184	1.4 E-9	(upper)	3B

* Distant-region observation borehole

Table 4.5 also reveals that the storativity values calculated from the near-region boreholes (KFI05, KFI06, KFI11 and BFI01) differ in the upper and lower parts of Zone 2. Low storativity values were generally calculated for the upper part of the zone, c.f. KFI11. These values represent the narrow, highly conductive subzone close to the upper boundary of Zone 2. Consequently, the hydraulic diffusivity (T/S) is very high in this subzone. On the other hand, the storativity calculated from the distant-region boreholes, representative of the entire Zone 2, is rather uniform and generally ranges between 1-2 E-5 in all tests, c.f. Table 4.6.

The leakage coefficient (K'/b') represents the hydraulic conductivity in the vertical direction of Zone 2. The analytical model used for interpretation of the interference tests corresponds to a leaky two-aquifer system (upper and lower parts of Zone 2) separated by a semi-permeable layer. This layer is considered as an equivalent porous medium of uniform thickness. The calculated leakage coefficients, which are determined from the separation between the response curves in the upper and lower parts of Zone 2, generally range between 2-5 E-8 s⁻¹ (except in HFI01). This borehole is considered as non-representative of the properties within Zone 2 since it only penetrates the upper part of the zone. Assuming an average thickness of the semi-permeable layer of about 50 m, the above values correspond to an average hydraulic conductivity of 1-2.5 E-6 m/s in the vertical direction of Zone 2. However, due to the fractured nature of Zone 2, higher values can be expected locally.

Table 4.6 Results of the hydraulic interference tests within Zone 2. Distance-drawdown analysis.

Test	T (m ² /s)	S (-)	Part of Zone 2
1	2.7 E-3	1.7 E-5	whole
2	2.7 E-3	1.2 E-5	whole
3A, B	2.7 E-3	1.7 E-5	whole

For comparison, the corresponding transmissivities of the observation borehole sections within Zone 2 used during the interference tests, calculated from single-hole tests in 2 m sections are presented in Table 4.7. As seen from this table the agreement between transmissivities calculated from single-hole and interference tests is reasonable. Since the two types of tests investigate different size of rock volumes they cannot be directly comparable and a perfect agreement cannot be expected. The transmissivities calculated from the single-hole tests are in general somewhat lower compared to those from the

interference tests. It should be pointed out that the single-hole test results in the most high-conductive parts of the observation borehole sections are above the (practical) upper measurement of the test equipments used and thus considered as very uncertain. Furthermore, in borehole KFI06 a potentially high-conductive section was not tested due to intense fracturing (Andersson et al., 1988).

All calculated data from the hydraulic interference tests are stored in the GEOTAB database. In addition, data files have been prepared on discette with time-drawdown data from interference test 3B in Zone 2, see Chapter 10.

Table 4.7 Comparison of total transmissivities of the observation borehole sections within Zone 2 calculated from single-hole tests (T_s) in 2 m-sections and transmissivities calculated from the interference tests (T_i).

Borehole	Observation section, no	Interval (m)	T_s (m^2/s)	Part of Zone 2	T_i (m^2/s)
KFI05	4	163-189	1.2 E-3	upper	-
	3	227-240	4.2 E-3	middle	-
	2	241-296	2.6 E-4	lower	1.6-1.7E-3
KFI06	4	202-227	5.6 E-4	upper	1.4E-3
	3	250-259	4.0 E-4	lower	
	2	260-279	2.7 E-4*	lower	1.6E-3
KFI09	4	119-151	1.0 E-3	upper	
	3	152-188	5.8 E-4	middle	2.4-3.5E-3
	2	189-230	1.2 E-4	lower	
KFI10	4	76-134	2.7 E-4	Zone 1	
	3	139-158	1.2 E-4	upper	
	2	159-193	7.6 E-5	middle	2.0-2.5E-3
	1	194-225	2.2 E-4	lower	
KFI11	4	217-240	3.7 E-4	upper	1.3-1.4E-3
	3	285-304	1.8 E-6	lower	
	2	327-340	1.5 E-5	lower	1.3E-3
BFI01	4	239-250	1.3 E-3	upper	
	3	261-270	2.5 E-6	upper	1.4-2.4E-3
	2	345-364	1.1 E-4	lower	-
HFI01	1	82-129	4.6 E-4	(upper)	2.4-3.9E-3
BFI02	pumped	193-217	1.7 E-3	upper	Test 2
	"	246-270	8.3 E-4	lower	Test 1
	"	193-288	2.6 E-3	whole	Tests 3A, 3B

* Section 270.35-272.40 m not tested

4.4 Hydraulic properties of the rock mass

The remainder of the hydraulic conductivity data, excluding all data from regional and local fracture zones, are assumed to represent the hydraulic properties of the rock mass. In large statistically homogeneous formations (hydraulic units) the distribution of hydraulic conductivity may be described by a lognormal distribution. Hydraulic conductivity values from single-hole tests in 2 m and 3 m sections are generally assumed to be lognormally distributed within specific depth intervals. To test this assumption selected populations of conductivity data from the rock mass at Finnsjön (excluding data from the fracture zones) were divided into 100 m (vertical) depth intervals. For each interval the median value, the geometric and arithmetic mean were calculated. For a lognormally distributed parameter the geometric mean and the median value should be equal.

To test if there are any significant differences between the statistical distributions of hydraulic conductivity of the rock mass in the southern and northern parts of the Finnsjön Rock Block (Fig. 4.1), separate analyses were performed of data from these two regions. Data from the 3 m-tests were used in these analyses. Due to the relatively high (lower) measurement limit of the 3 m-tests from boreholes KFI01 and KFI02 (Table 4.1) data from these boreholes were excluded. Otherwise, the results may be biased due to the different measurement limits, particularly at depth where a large number of values at the measurement limit occur. Thus, data from the rock mass from boreholes KFI03, KFI04 and KFI08 were used to analyse the conductivity distribution of the rock mass in the southern block. In the northern block, data from boreholes KFI05, KFI06 and KFI07 were used. The median value, the geometric and arithmetic mean in each interval for each region are presented in Table 4.8.

The statistical analyses of the hydraulic properties of the rock mass presented in this section are based on the subdivision in hydraulic units according to the preliminary geological interpretation of fracture zones (Table 4.3 in Andersson et al.1989b). Since only slight modifications of the geological interpretation of some of the fracture zones were made by Ahlbom and Tirén (1991) these changes should not significantly alter the analyses and conclusions drawn regarding the hydraulic properties of the rock mass.

Table 4.8 shows that the geometric mean and median value are very close for all depth intervals both in the southern and northern region. This indicates lognormal hydraulic conductivity distributions of the rock mass. Furthermore, the mean values of hydraulic conductivity of the rock mass in the southern block are generally lower than in the northern block, particularly at greater depths. In Appendix 6:1 statistical data from each 100m-interval for the two regions are listed and displayed graphically, in a Box Plot. The graphs show the median value (50 %) and the 75, 25, 90 and 10% percentiles together with outliers (NCSS, 1987). In addition, Appendix 6:1 contains a listing of the means of $\log(K)$ and the standard

deviation for each 100 m interval. Apparently, the standard deviation of $\log(K)$ decreases with depth.

The significance of the differences in means of $\log(K)$ between the two blocks at different depths were tested by employing two-sample t-tests, using NCSS. This test assumes that data is normally distributed and that samples from both populations are random. Although it can be argued whether $\log(K)$ really is normally distributed within each depth interval, t-tests are nevertheless used here as an indication. It can be mentioned

Table 4.8 Median value (K_{50}), geometric mean (K_g) and arithmetic mean (K_a) of the hydraulic conductivity distribution of the rock mass in 100 m depth intervals for the southern and northern parts of the Finnsjön Rock Block, calculated from single-hole tests in 3m-sections. (n = number of data).

Region/ boreholes	Interval (m.b.g.l)	K_{50} (m/s)	K_g (m/s)	K_a (m/s)	n
Southern/ KFI03,04, 08	0-100	1.6 E-8	1.7 E-8	7.5 E-6	52
	100-200	8.9 E-9	1.2 E-8	4.1 E-7	53
	200-300	1.3 E-9	1.7 E-9	7.5 E-8	85
	300-400	1.0 E-9	1.0 E-9	4.8 E-9	105
	400-500	3.4 E-9	2.4 E-9	3.7 E-9	45
	500-600	9.5 E-10	8.6 E-10	1.2 E-9	30
Northern/ KFI05,06, 07	0-100	3.2 E-7	1.2 E-7	8.1 E-7	68
	100-200	9.0 E-9	1.0 E-8	6.8 E-8	61
	200-300	6.5 E-9	5.6 E-9	5.6 E-8	76
	300-400	3.1 E-9	5.0 E-9	5.4 E-8	85
	400-500	2.7 E-9	2.6 E-9	1.1 E-8	114
	500-600	6.8 E-9	4.4 E-9	8.3 E-9	69
	600-700	1.0 E-8	7.9 E-9	1.4 E-8	26

that non-parametric tests (Mann-Whitney test) also were performed (but not presented here), yielding very similar results as the t-tests. The results of the t-tests (two-tailed) are presented as significance levels in Table 4.9. The significance level is defined as the probability that the test variable \hat{t} is exceeded. These levels should be interpreted as follows. If you are testing at a certain significance level, (e.g. 0.05), the hypothesis that the means are equal must be rejected if the actual level falls below this value. For example, in Table 4.9, the hypothesis that the mean of $\log(K)$ is equal must be rejected for all intervals except 100-200 m and 400-500 m at a significance level of 0.05.

As a preliminary conclusion based on Table 4.9, one may suggest that the mean of $\log(K)$ in the two blocks are not significantly different in the 100-200 and the 400 - 500 m interval, while the opposite would be the case for the other intervals.

The largest differences in hydraulic conductivity between the two regions occur in the depth intervals 300-400 m and 500-600 m although the lower measurement limits are similar for all boreholes used in the analyses. Data from borehole KFI06 dominate the latter depth interval (and also the interval 600-700 m) in the northern region. One explanation to the high K-values in this interval could be that Zone 5, which is assumed to penetrate borehole KFI06 in this depth interval, may possibly be wider than assumed by the subdivision of data in hydraulic units (Table 4.3). As pointed out by Ahlbom and Tirén (1989) and Tirén and Stark (1989) the geological/structural

Table 4.9 Significance levels for difference in means of $\log(K)$ in the northern and southern block at different depth intervals.

Depth interval (m)	Significance level
0 - 100	0.0005
100 - 200	0.8
200 - 300	0.0002
300 - 400	0.0
400 - 500	0.8
500 - 600	0.0

interpretation of the deeper part of borehole KFI06 is uncertain. Zero-flow test sections have been assigned the actual value of the lower measurement limit in the statistical analyses (Table 4.1).

Preliminary regression analyses of the hydraulic conductivity distribution in the rock mass with depth have been made for the southern and northern parts of the Finnsjön Rock Block. In the analyses, all data from the rock mass in 3 m-sections, according to the previous division of boreholes in the southern and northern part have been used. The regression analysis is based on a power function:

$$K = az^{-b} \quad (4.1)$$

where z is vertical depth and a, b are constants.

In the southern part the hydraulic conductivity of the rock mass versus depth may be expressed as:

$$K = 1.04 \times 10^{-6} z^{-1.10} \quad (\text{m/s}) \quad (4.2)$$

In the northern part the hydraulic conductivity of the rock mass may be expressed as:

$$K = 3.90 \times 10^{-5} z^{-1.53} \quad (\text{m/s}) \quad (4.3)$$

The regression curves, together with smoothed curves of the hydraulic conductivity data of the rock mass in the southern and northern part of the Finnsjön Rock Block, are shown in Appendix 6:2. The same data is also presented in an alternative way in Appendix 6:3, where the assumed linear relationship between $\log(K)$ and $\log(z)$, as obtained from eqn. (4.1), is shown. The least square regression line is shown along with 95 % confidence bands for individual $\log(K)$ values, as calculated by NCSS.

As an indication of whether the decreasing trend of $\log(K)$ with $\log(z)$ is significant, 95 % confidence intervals for b (in eqn. 4.1) were obtained from NCSS. Those were:

Southern block : $-1.37 < b < -0.82$

Northern block : $-1.76 < b < -1.29$

As a further elaboration on investigating the above trend, a regression analysis were performed from 200 m vertical depth and below. The 95 % confidence intervals in this case were:

Southern block: $-1.00 < b < 0.31$

Northern block: $-1.03 < b < 0.17$

The latter analysis could then be an argument that there may not necessarily be a significant trend, when ignoring the uppermost part of the rock. Therefore, some statistical analysis were performed using the entire interval below a depth of 200 m, and is presented in Table 4.10.

Table 4.10 Median value (K_{50}), geometric mean (K_g) and arithmetic mean (K_a) of the hydraulic conductivity distribution of the rock mass below a depth of 200 m for the southern and northern parts of the Finnsjön Rock Block. (n = number of data).

Region	Interval (m.b.g.l)	K_{50} (m/s)	K_g (m/s)	K_a (m/s)	n
Southern	200 - 600	1.3 E-9	1.4 E-9	5.1 E-9	265
Northern	200 - 700	5.0 E-9	4.2 E-9	3.0 E-8	370

As before, a t-test was carried out in order to test the difference of the means of $\log(K)$ between blocks resulting in a significance level of 0.0, suggesting that the two blocks are not hydraulically similiar.

As a final step in the statistical analysis, the southern and northern block were broken down to individual boreholes and analysed for the entire interval of 200 m depth and below. This

is presented in Table 4.11, where mean of $\log(K)$ along with the standard deviation of $\log(K)$ is presented.

Further, t-tests were performed to test the difference in means of $\log(K)$ between individual boreholes, and are presented in Table 4.12.

Thus, Tables 4.11 and 4.12 may suggest that means of $\log(K)$ in most boreholes are different. A conclusion might be that it is difficult to determine with certainty that the two blocks are hydraulically different, with available data from only three boreholes in each of the blocks.

Table 4.11 Mean and standard deviation of $\log(K)$ in individual boreholes in interval 200 m and below for the southern and northern parts of the Finnsjön Rock Block. (n = number of data).

Region	Borehole	Mean of $\log(K)$	St.dev.	n
Southern	KFI03	-8.6	0.6	98
	KFI04	-8.9	0.5	104
	KFI08	-9.3	0.7	63
Northern	KFI05	-8.4	0.6	133
	KFI06	-7.9	0.7	140
	KFI07	-9.1	0.6	97

Table 4.12 Significance levels of difference in means of $\log(K)$ between individual boreholes in interval 200 m and below for the southern and northern parts of the Finnsjön Rock Block.

Borehole	S o u t h e r n			N o r t h e r n			
	KFI03	04	08	05	06	07	
Southern	KFI03	.	0.01	0.0	0.007	0.0	0.0
	KFI04	.	.	0.0	0.0	0.0	0.057
	KFI08
Northern	KFI05	.	.	0.0	.	0.0	0.0
	KFI06	.	.	0.0	.	.	0.0
	KFI07	.	.	0.036	.	.	.

4.5 Geostatistical analysis

Geostatistical analysis of hydraulic conductivity data from single-hole injection tests with different packer spacings (Table 4.1) has been carried out by Cvetkovic and Kung (1989).

This analysis constitutes an introductory study of the proposal by Neuman (1988) which implies that the fractured rock in the Finnsjön area may be treated as a continuum on a certain scale.

The objective of the present study was mainly to construct semivariograms of the data and estimate statistical parameters and the correlation properties of the rock. Furthermore, two special items were to be studied, firstly, the influence of different packer spacings on the semivariograms constructed and secondly, the influence of the borehole inclination on the variograms.

By the geostatistical analysis the whole population of the hydraulic conductivity data in the measured borehole intervals was used, i.e. no subdivision of data in hydraulic units was made. Hydraulic conductivities below the lower measurement limit were assigned the actual value of this limit (Table 4.1). Before the analysis, the trend in the hydraulic conductivity values versus depth was eliminated. Semivariograms were constructed for data sampled in 2 m, 3 m and 20 m borehole sections. The variograms are presented in Appendix 7.

The constructed variograms for the 2 m and 3 m data have been fitted to an analytical variogram in the form of the negative exponential using the least square method. The exponential variogram has the form

$$\gamma(h) = w - a \exp(-bh) \quad (4.4)$$

where h is the separation distance, a is the sill, or the true variance of the data uncorrupted by noise, the inverse of b is the correlation scale and $(w-a)$ is the nugget effect. In Appendix 7, the full line illustrates the constructed data variogram while the broken line illustrates the analytical approximation of the variogram. The statistical parameters calculated are shown in Table 4.13. No attempt was made to fit the variograms for the 20 m data to analytical models.

Table 4.1 shows that only in three boreholes (KFI05, KFI06 and KFI07) sufficiently long intervals are measured with both 2 m and 3 m packer spacing to make a comparison of the influence of different packer spacings possible. Table 4.13 shows that the variances calculated for the 3 m straddle intervals in these boreholes are consistently lower compared to the 2 m intervals. Both the nugget value and the variances are relatively large for the 2 m data, particularly for boreholes KFI05 and KFI06. The correlation scale for the 3 m data is about 20 m and for the 2 m data between 5 to 10 m. It should be observed that the 2 m data are mainly restricted to Zone 2 whereas the 3 m data cover almost the entire borehole lengths. Furthermore, the 2 m data generally include a large number of values below the measurement limit, resulting in a high variance.

The variograms for the boreholes KFI09, KFI10, KFI11, BFI01 and BFI02 do not indicate a consistency regarding the influence of the borehole inclination. Both the variance and nugget are large for KFI09 which is inclined 60 degrees. However, for borehole KFI10, which is inclined 50 degrees, the variance and

nugget are similar to those for boreholes KFI11 and BFI02 which are vertical (Table 4.13).

To conclude, well defined variograms were obtained for the 2 m and 3 m borehole data. Since the 20 m data are relatively sparse, rather poor variograms were obtained for these data. The maximal variance of the natural logarithm of the hydraulic conductivity is approximately 9 while the average correlation scale for the constructed variograms is approximately 10 m. The sill of the variograms is well defined for all 2 m and 3 m data, except the 3 m data from borehole KFI05. No consistency in variograms for borehole data with different inclinations was observed. This may indicate that the rock can be treated as an isotropic porous medium on a certain scale (Cvetkovic and Kung, 1989).

Table 4.13 Statistical parameters calculated from geostatistical analysis of hydraulic conductivity data from single-hole tests ($1/b$ =correlation scale, a =sill, $w-a$ =nugget effect). From Cvetkovic and Kung, (1989).

Borehole	Inclination (degrees)	Packer spacing(m)	$1/b$ (m)	a	$w-a$
KFI01	90	2	8.70	0.27	0.77
KFI02	50	3	12.50	2.25	1.52
KFI03	50	3	12.05	2.25	1.76
KFI04	80	3	9.17	3.87	2.07
KFI08	60	3	15.87	2.98	3.81
KFI05	50	2	10.87	8.32	9.20
"	"	3	63.30	5.54	3.15
KFI06	90	2	4.42	8.85	6.70
"	"	3	17.54	2.96	1.91
KFI07	85	2	4.93	7.49	3.00
"	"	3	20.00	2.73	3.31
KFI09	60	2	7.52	9.68	7.52
KFI10	50	2	15.00	6.45	5.29
KFI11	90	2	5.71	7.76	3.22
BFI01	90	2	12.20	3.54	3.33
BFI02	90	2	11.11	4.80	7.10

5. OTHER HYDRAULIC PARAMETERS

In this Chapter, additional parameters which might be used in the modelling of the Finnsjön area are described. These include parameters determined from the preliminary and radially converging tracer tests, such as hydraulic fracture conductivity, flow (kinematic) porosity and dispersivity and from dilution tests (natural flow). Finally, estimations of the conductive fracture frequency (CFF) from boreholes at Finnsjön are described.

5.1 Preliminary tracer test

Several parameters were determined from the preliminary tracer tests in the upper part of Zone 2 by injecting tracers in boreholes KFI06, KFI11 and BFI01 and monitoring the breakthrough of tracers in the pumping borehole BFI02 during interference test 2 (Andersson et al. 1989, Chapter 7).

5.1.1 Hydraulic fracture conductivity and aperture

The hydraulic fracture conductivity was determined, assuming flow in a single fracture, in two different ways, i.e. on the basis of the fracture geometry and discharge rate (K_{esf}^q) and the residence time (K_{esf}^t). The subscript 'esf' denotes 'equivalent single fracture'. The corresponding (equivalent) fracture apertures (e_{esf}^q and e_{esf}^t) were also calculated. In addition, an equivalent fracture aperture based on the mass balance in the fracture (volume divided by area), e_{esf}^m , was calculated. From the fracture conductivity and the fracture aperture, the corresponding values of transmissivity were calculated according to the different methods. The transmissivity value, based on mass balance, T^m , was calculated as the product of K_{esf}^t and e_{esf}^m . The results, which represent the properties of the (uppermost subzone) of Zone 2, are presented in Table 5.1.

The fracture conductivities calculated are notably high ($K_{esf}^q = 1.3 - 1.7$ and $K_{esf}^t = 1.6E-1 - 9.7E-1$ m/s), but are only a factor 5-10 higher than the average hydraulic conductivity, K_{ss} , determined by hydraulic single-hole tests in 0.11 m sections of borehole BFI02 (Ekman et al., 1988). The results in Table 5.1 can also be compared with the results of the hydraulic interference tests in the upper part of Zone 2 (Section 4.3.2). The transmissivity values based on flow-rate, T^q , should be directly comparable with the corresponding transmissivity values calculated from interference test 2 (Table 4.5). As can be seen from Tables 5.1 and 4.5 these transmissivity values are in good agreement.

5.1.2 Flow porosity

In analogy with the hydraulic fracture conductivity and aperture, the flow porosity (ϕ_k) was calculated in three different ways. By calculating the flow porosities, flow is assumed to be concentrated to a one metre thick subzone, i.e. the uppermost part of Zone 2. The values of flow porosity

presented in Table 5.1, or better, the flow porosity times the fracture aperture, may be compared, in a relative way, with the corresponding values on the storativity calculated from the hydraulic interference tests in the upper part of Zone 2 presented in Table 4.5. For radial flow, the storativity is directly related to the flow porosity (but also to the compressibility of the aquifer and water) and to the thickness of the aquifer. The flow porosity values in Table 5.1 show the same pattern as the corresponding storativity values from interference test 2 in Table 4.5. However, the differences between boreholes are more accentuated by the calculated storativity values.

The differences in calculated flow porosity and storativity between the boreholes are likely to reflect the nature of flow in the different directions. By regression analysis of the breakthrough curves it was concluded that several flow paths including a relatively large number of fractures, or alternatively, some kind of flow restriction (e.g. a fault) are likely to be involved in the solute transport between boreholes BFI01 and BFI02, see Figure 5.1 and Table 5.2. On the other hand, rather few fractures are assumed to be involved in the transport between boreholes KFI11 and BFI02 in the upper part of Zone 2 (Andersson et al., 1989).

Table 5.1 Summary of parameters determined from the preliminary tracer test in the uppermost subzone of Zone 2 at Finnsjön. (From Andersson et al. 1989).

Route	BFI01 - BFI02	KFI06 - BFI02	KFI11 - BFI02
Tracer	Uranine	Iodide	Amino G Acid
Distance (m)	168	189	155
t (hours)	20	8	5
t ₀ (hours)*	35	16	8
Recovery (%)	68	81	70
K ^q _{esf} (m/s)	1.3	1.5	1.7
K ^t _{esf} (m/s)	1.6E-1	6.1E-1	9.7E-1
e ^q _{esf} (m)	1.4E-3	1.5E-3	1.6E-3
e ^t _{esf} (m)	5.1E-4	9.9E-4	1.2E-3
e ^m (m)	1.2E-2	4.3E-3	3.2E-3
T ^q (m ² /s)	1.8E-3	2.3E-3	2.7E-3
T ^t (m ² /s)	8.2E-5	6.0E-4	1.2E-3
T ^m (m ² /s)	1.9E-3	2.6E-3	3.1E-3
∅ _k ^q (1 m sect.)	1.1E-3	9.4E-4	8.2E-4
∅ _k ^t (1 m sect.)	8.8E-3	2.3E-3	1.4E-3
∅ _k ^m (1 m sect.)	1.2E-2	4.3E-3	3.2E-3
A (m)**	2.4	3.9	1.3
Pe	70	49	118

* t₀ = time at peak concentration

** assuming flow in a single fracture

5.1.3 Dispersivity

The calculated dispersivities (A) and Peclet numbers (Pe) are presented in Tables 5.1 and 5.2. In all three directions

towards the observation boreholes the dispersivity is low for the primary flow paths, 1.3 - 7.2 m, and for most of the secondary flow paths. This implies that the solute transport in the groundwater flow paths studied, and at the distances involved, is dominated by advection whereas dispersion is of minor importance. No perceptible effect of sorption or matrix diffusion was observed of the non-sorbing tracers used.

Table 5.2 Regression estimates of dispersivity (A) and residence time (t_0) from preliminary tracer test in the upper part of Zone 2 at Finnsjön. (From Andersson et al., 1989).

Route and Tracer	Flow paths	t_0 (hours)	A (m)	Pe
BFI01 - BFI02 Uranine	One, 1A	47.0	10.9	15
	Three, 3A	31.0	2.4	70
	3B	48.6	6.8	25
	3C	99.3	14.8	11
KFI06 - BFI02 Iodide	One, 1A	21.1	13.7	14
	Two, 2A	17.5	7.2	26
	2B	40.7	31.3	6
KFI11 - BFI02 Amino G Acid	One, 1A	11.0	8.5	18
	Two, 2A	8.8	2.7	57
	2B	14.8	11.4	14

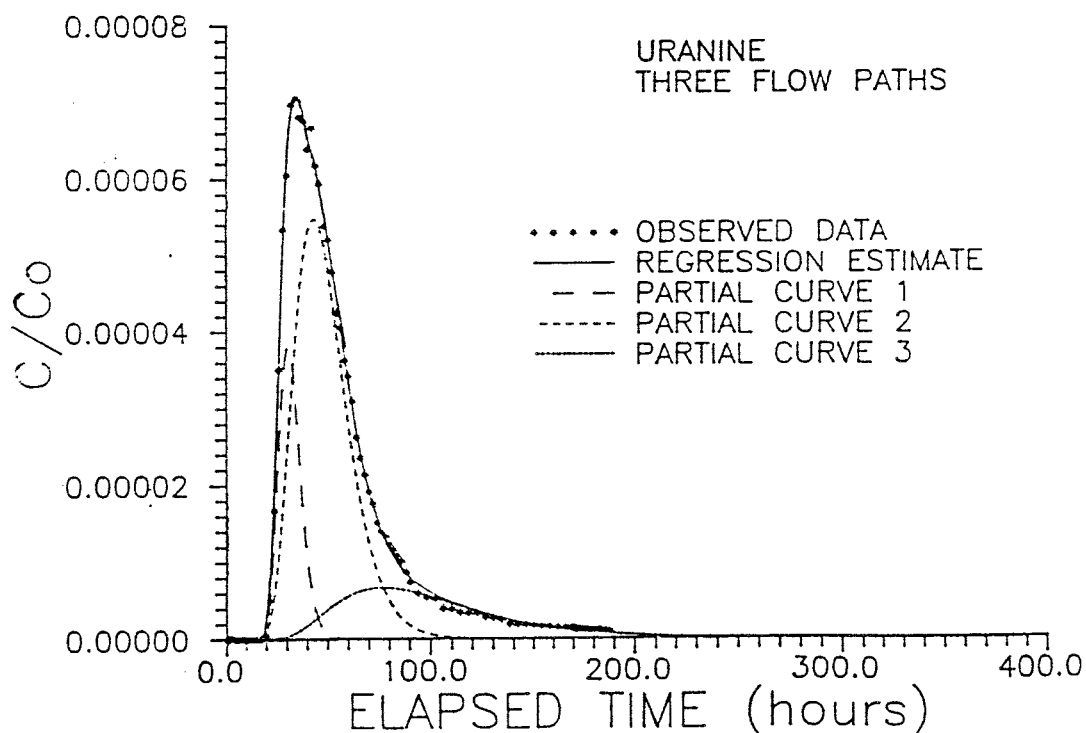


Figure 5.1 Regression analysis with three flow paths to the break-through curve from borehole BFI01. (From Andersson et al., 1989).

5.1.4 Heterogeneity and anisotropy of Zone 2

Heterogeneity of Zone 2 is evident from directional comparisons between the parameters governing the solute transport (Table 5.1). Within the radius of the present tracer test the upper highly conductive part of Zone 2 is fairly homogeneous regarding transmissivity, but the other parameters essential to solute transport show directional variations indicating anisotropic conditions. In the direction of the dip of Zone 2, i.e. towards borehole BFI01, the calculated aperture and hydraulic conductivity of the single fractures (e_{esf}^t and K_{esf}^t) or flow paths contributing to solute transport are lower than in the direction of the strike, i.e. towards boreholes KFI06 and KFI11. The apparent number of fractures or flow paths contributing to solute transport is on the other hand likely to be larger in the direction towards BFI01, resulting in a higher calculated porosity in this direction, c.f. Andersson et al. (1989 p. 144). The results also indicate that the ratio of the apparent wetted surface area per volume of water is larger in the direction towards BFI01 than towards KFI06 and KFI11. If parallel-plate fractures are assumed the ratios are about $1.8E3$ and $3.9E3 \text{ m}^{-1}$, respectively (Andersson et al., 1989).

5.2 Radially converging tracer test

This section is mainly after Gustafsson et al., 1989. The objective of the radially converging tracer test was primarily to determine the transport parameters of fracture Zone 2 and to utilize the experimental results for validation and verification of radionuclide transport. In a radial geometry of a central pumping borehole (BFI02) and three peripheral injection boreholes (KFI06, KFI11 and BFI01), tracers were injected in three packed-off intervals in each borehole in totally nine injection points at distances of c. 150 m from the pumping borehole (Table 5.3).

The central borehole was pumped from a packed-off interval enclosing the entire Zone 2. Totally eleven (11) different tracers were injected, eight (8) of them continuously for 5-7 weeks and three (3) were injected as pulses.

Tracer breakthrough was registered from all nine injection intervals, with first arrivals ranging between 24 - 3500 hours. An analytical evaluation of transport parameters was made including hydraulic conductivity, fracture aperture, flow porosity and dispersivity. Possible interconnections between highly conductive intervals were also studied by detailed sampling in the pumping borehole. In addition, a comparison between predictions of the tracer breakthroughs, based on a numerical model calibrated by the hydraulic interference tests, and the experimental results was performed, see Section 8.4. The radially converging tracer tests are reported by Gustafsson et al., (1989).

Table 5.3 Injection intervals selected for the radially converging tracer experiment at Finnsjön. (After Gustafsson et al., 1989).

Borehole	Injection interval Zone 2	Interval (m)	Length (m)	Transmiss.* (m ² /s)	Type of injection
BFI01	Upper	241.5-246.5	5.0	1.3 E-3	continuous
	Middle	263.5-266.5	3.0	1.5 E-6	"
	Lower	351.5-356.5	5.0	1.0 E-4	"
KFI06	Upper	212.0-217.0	5.0	5.6 E-4	pulse
	Middle	236.5-239.5	3.0	4.2 E-6	continuous
	Lower	252.5-271.5	19.0	6.7 E-4	"
KFI11	Upper	221.5-226.5	5.0	3.7 E-4	cont.+pulse
	Middle	287.5-294.5	7.0	1.6 E-6	continuous
	Lower	329.5-338.5	9.0	1.5 E-5	"

* determined from hydraulic single-hole tests in 2 m-sections

5.2.1 Hydraulic fracture conductivity and aperture

The hydraulic conductivity of an equivalent single fracture, K_{esf} , was calculated for ten different tracer breakthroughs, see Table 5.4. Both the tracer residence time and the flow rate was used as input data. The fracture conductivity based on the flow rate, Q , was determined in two different ways, which in the case of a homogeneous and isotropic media, should give the same result. Both the pumping rate and the flow through the injection interval were used and are here denoted K_{esf}^Q and K_{esf}^q , respectively. The two values given for section KFI11:U in Table 5.4 correspond to continuous and pulse injection, respectively.

Comparing the values presented in Table 5.4, the values of K_{esf}^t (based on the residence time) are lower than the other two estimated values of fracture conductivity in all cases. There are also differences up to a factor 10 between the two different ways of calculating K_{esf}^Q , indicating heterogeneity of the zone. The measured flow rates through the intervals seems to be larger than what would be expected in a homogeneous and isotropic medium, i.e. K_{esf}^q is larger than K_{esf}^Q (Gustafsson et al., 1989).

The aperture of a single equivalent fracture was also calculated using the values of K_{esf} in Table 5.3. The e_{esf} values are denoted according to the input parameter used respectively. In addition, the fracture aperture based on mass balance, e_{esf}^m , was calculated. The calculated apertures are shown in Table 5.4.

5.2.2 Flow porosity

The flow porosity, ϕ_k , was determined using K_{esf}^t as input parameter. The flow porosity is dependent on the length of the interval over which K was measured, i.e. in this case the packer spacing. However, since very detailed hydraulic tests in 0.11 m intervals (Ekman et al. 1988) have shown that the highly conductive subzones of Zone 2 are only 0.5-1 m thick, the flow porosity was calculated over a thickness of 1 m. The calculations, presented in Table 5.5, were only made for the flow paths with a simple flow geometry, i.e. in borehole sections in which the tracers injected in the upper part of Zone 2 also were detected at the upper part of the zone in borehole BFI02.

Table 5.4 Hydraulic fracture conductivity, K_{esf} , and fracture aperture, e_{esf} , calculated from the radially converging tracer test at Finnsjön (After Gustafsson et al., 1989).

Section of Zone 2	K_{esf}^Q (m/s)	e_{esf}^Q (m)	K_{esf}^q (m/s)	e_{esf}^q (m)	K_{esf}^t (m/s)	e_{esf}^t (m)	e^m (m)
<u>Upper</u>							
BFI01:U	1.1	4.3E-3	11.4	1.3E-3	0.13	4.1E-4	1.1E-2
KFI06:U	1.7	2.4E-3	3.5	1.6E-3	0.30	6.9E-4	9.3E-3
KFI11:U	1.4	4.8E-3	14.7	1.5E-3	0.62	1.0E-3	3.2E-3
	2.1	1.4E-3	1.2	1.8E-3	0.80	1.1E-3	4.8E-3
<u>Middle</u>							
BFI01:M	0.06	1.3E-3	0.99	3.1E-4	0.01	1.0E-4	1.4E-3
KFI06:M	2.1	1.0E-3	0.68	1.8E-3	0.04	2.2E-4	1.3E-1
KFI11:M	1.9	8.5E-4	0.46	1.7E-3	0.03	2.1E-4	1.2E-1
<u>Lower</u>							
BFI01:L	0.95	9.2E-4	0.53	1.2E-3	0.01	1.4E-4	9.8E-2
KFI06:L	1.0	3.6E-3	8.0	1.3E-3	0.23	6.1E-4	5.7E-3
KFI11:L	1.4	1.7E-3	1.7	1.5E-3	0.01	1.4E-4	1.7E-1

5.2.3 Dispersivity

The dispersivity was calculated according to the theories by Gelhar (1987). The corresponding Peclet numbers (Pe) are also shown in Table 5.5. Only the breakthrough curves reaching steady state or, in the case of BFI01:M, being possible to extrapolate to steady state concentration, were evaluated regarding dispersivity.

5.2.4 Hydraulic interconnection within Zone 2

It is obvious from the hydraulic testing that the flow within Zone 2 is concentrated to a few highly conductive parts. The

results of the radially converging tracer experiment show that these highly conductive parts are hydraulically interconnected. Tracers injected in the upper part of Zone 2 were found in the lower part and conversely. This is also indicated by the hydraulic interference tests (Andersson et al., 1989).

Table 5.5 Flow porosity, \emptyset_k , calculated over a thickness of 1 m, dispersivities (A) and Peclet numbers (Pe) calculated from radially converging tracer tests at Finnsjön. (After Gustafsson et al., 1989).

Section of Zone 2	\emptyset_k (1 m) (-)	A (m)	Pe (-)
<u>Upper</u>			
BFI01:U	1.2 E-2	5.0	33
KFI06:U	3.8 E-3	5.5	35
KFI11:U	1.7 E-3	10.0	15
	1.3 E-3	7.9	20
<u>Middle</u>			
BFI01:M	1.4 E-3	28.2	6
<u>Lower</u>			
KFI06:L	3.2 E-3	8.1	23

5.3 Other tracer tests

During drilling of borehole KFI11 the flushing water was recovered from borehole HFI01 located at a distance of about 440 m from KFI11. The flushing water was labelled with a tracer at the surface before it was pumped down in borehole KFI11. By the penetration of the top of Zone 2 during drilling, a total loss of flushing water occurred to the formation (Gustafsson and Andersson, 1989). The tracer content of the water recovered from borehole HFI01 was recorded continuously. The first breakthrough of tracer (Uranine) from borehole KFI11 was recorded in borehole HFI01 about one month after start of drilling.

The hydraulic fracture conductivity was estimated, firstly based on the assumption of radial flow in a single fracture between boreholes KFI11 and HFI01 and secondly, assuming linear flow in the fracture between the boreholes. In addition, the flow porosity was estimated for a 1 metre thick zone. The results are shown in Table 5.6. The same parameters were then recalculated including the effect of the radius of influence (r_e) and finally, including the combined effects of both radius

of influence and enhanced transport velocity in the vicinity of the pumping borehole.

Table 5.6 Hydraulic fracture conductivity (K_{esf}^t) and flow porosity (θ_k^t) calculated from tracer break-through in borehole HFI01 from KFI11. (After Gustafsson and Andersson, 1989).

Route	Flow regime	K_{esf}^t (m/s)	θ_k^t	Remarks
KFI11-HFI01	Radial	1.5 E-1	6.7 E-3	
	Linear	3.4 E-2	2.9 E-2	
"-"	Radial	1.3 E-1	7.7 E-3	Effects of r_e included
	Linear	2.9 E-2	3.4 E-2	
"-"	Radial	7.2 E-2	1.4 E-2	Effects of enh. transp. velocity
	Linear	1.7 E-2	5.9 E-2	

Tracer tests have also been conducted in a minor fracture zone at Gåvastbo between boreholes KFI01 and KFI02, see Figure 1.1 (Gustafsson and Klockars, 1981). The equivalent hydraulic fracture conductivity and flow porosity were calculated. To be comparable to other calculated values within Zone 2, the flow porosity has also been calculated for a 1 m thick zone. The results are presented in Table 5.7.

Table 5.7 Hydraulic fracture conductivity (K_{esf}^t) and flow porosity (θ_k^t) calculated from tracer tests at Gåvastbo. (From Gustafsson and Andersson, 1989).

Route	K_{esf}^q (m/s)	K_{esf}^t (m/s)	θ_k^t (-)	$(\theta_k^t)_{1m}$ (-)	T (m ² /s)
KFI01-KFI02	1.4 E-2	2.7 E-3	8.4 E-4	1.6 E-3	4.4 E-6

5.4 Tracer dilution tests

This section is mainly after Gustafsson and Andersson, (1989). Tracer dilution tests were performed in boreholes BFI01 and HFI01 to determine the natural groundwater flow rate in Zone 2, and secondly to establish the flow rate in the rock and fracture zones adjacent to Zone 2. The percussion borehole BFI01, 165 mm in diameter, penetrated the entire Zone 2, whereas the percussion borehole HFI01, 110 mm in diameter, only

penetrates the upper part of Zone 2. The borehole sections selected for measurement are presented in Table 5.8.

Table 5.8 Borehole sections selected for tracer dilution tests. (From Gustafsson and Andersson, 1989).

Borehole	Section	K (m/s)	Hydraulic units
BFI01	9- 50	8 E-6	Highly conductive shallow rock
"	50-230	3.1 E-8	Low conductive part between shallow rock and Zone 2
"	242-244	3.0 E-4	Upper part of Zone 2
"	244-246	3.4 E-4	"
"	264-266	1.1 E-6	Within Zone 2
"	352-354	1.7 E-5	Lower part of Zone 2
"	354-356	3.5 E-5	"
HFI01	38- 40	7.2 E-5	Fracture zone in the shallow rock
"	108-110	3.8 E-5	Upper part of Zone 2
"	112-114	1.9 E-4	"
"	104-124	2.3 E-5	"
"	84-129	1.3 E-5	Upper part of Zone 2 and affected country rock above

The dilution measurements were successful in 10 of the 12 selected borehole sections. In the borehole section 264-266 m in BFI01 no measurements could be made due to chemical precipitation. In test section 84-129 m (borehole HFI01) problems with dissolved gases in the water made it impossible to conduct any dilution measurements with the surface sampling equipment used (Gustafsson and Andersson, 1989).

5.4.1 Natural groundwater flow rates through boreholes

From the dilution measurements, the natural groundwater flow rate through the borehole sections, Q_w , the volumetric flux density, Q_f , and the specific groundwater flow rate, v_f , have been calculated under different assumptions (Gustafsson and Andersson, 1989). The results from the dilution measurements in borehole BFI01 are presented in Table 5.9 and Figure 5.2.

The results show that the natural groundwater flow in Zone 2 is concentrated to the upper, highly conductive part (242-246 m). In the lower, highly conductive part (352-356 m) of the zone the groundwater flow was found to be below the measurement limit and thus only at the rate of molecular diffusion, which in this case is estimated to less than $3E-11$ m/s. This confirms that the driving force, i.e. the hydraulic gradient, is minimal in the lower part of Zone 2 (Gustafsson and Andersson, 1989). Above Zone 2, a high groundwater flow rate was measured in the shallow, fractured and high-conductive rock (the 9 - 50 m test

section). Below this rock interval there is almost 200 m of medium- to low-conductive rock, in which the measured groundwater flow was low.

Table 5.9 Results of point dilution measurements in borehole BFI01. (From Gustafsson and Andersson, 1989).

Section (m)	K (m/s)	Q _w (ml/min)	Q _f (m ³ /m ² ·yr)	v _f ^d (m/s) (m/d)	v _f ^{g*} (m/s)
9- 50	8 E-6	381.2	14.2	4.5 E-7 0.039	0.4 E-7
50-230	3.1 E-8	7.9	0.07	2.2 E-9 0.0002	8.9 E-11
242-244	3.0 E-4	169.4	131.7	4.2 E-6 0.361	0.8 E-6
244-246	3.4 E-4	61.9	48.3	1.5 E-6 0.132	0.9 E-6
352-354	1.7 E-5	no measurable flow		<3 E-11	0.5 E-7
354-356	3.5 E-5	"		<3 E-11	0.9 E-7

* calculated with a hydraulic gradient $i=1/200$ in the uppermost section and $1/350$ in the other sections.

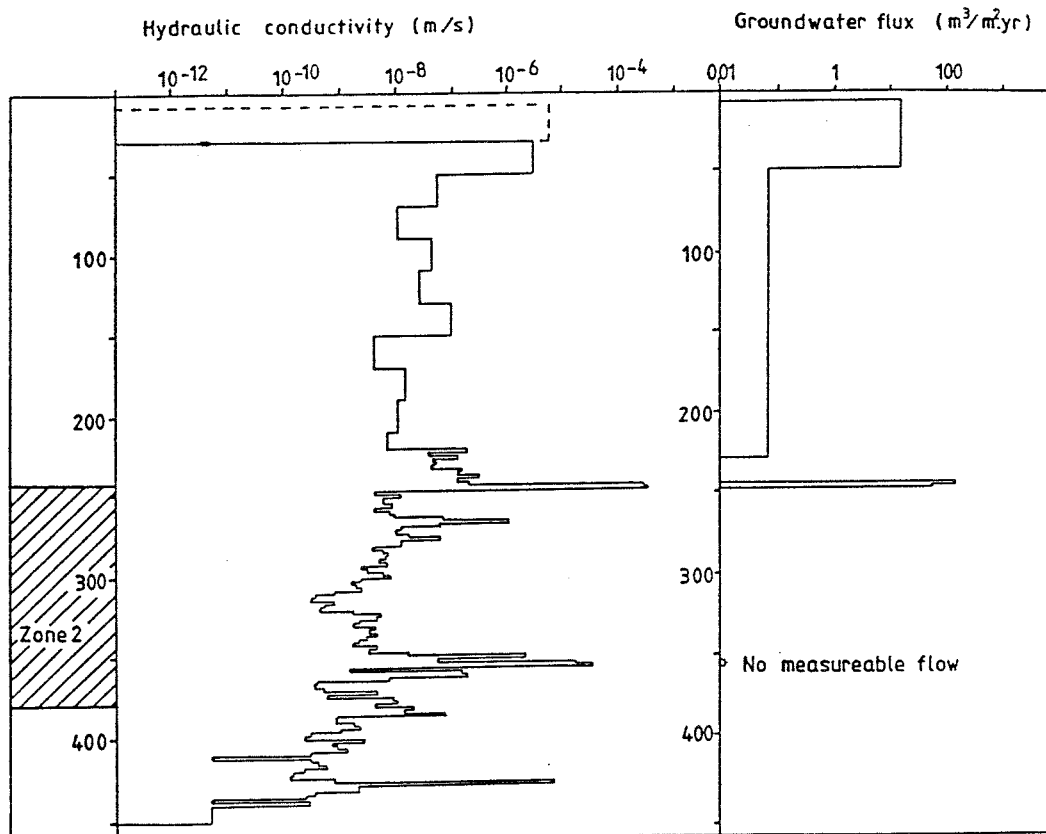


Figure 5.2 Hydraulic conductivity profile and estimated natural groundwater flow through borehole BFI01. (From Gustafsson and Andersson, (1989)

In Table 5.9 also the specific groundwater discharge, calculated from the groundwater flow rate determined from the point dilution method, v_f^d are presented together with the corresponding values calculated from the hydraulic conductivities and gradients v_f^g , determined from hydraulic tests and piezometric measurements. The v_f^d and v_f^g values are in reasonable agreement in the upper part of Zone 2 as well as in the above-lying country rock. However, in the lower part of Zone 2 (sections 352-354 m and 354-356 m) the specific discharge calculated from hydraulic conductivities and gradients, v_f^g , was overestimated by about three orders of magnitude compared to those determined from the dilution measurements (Andersson and Gustafsson, 1989).

The results of the dilution measurements in borehole HFI01 are presented in Table 5.10. A relatively high groundwater flow rate was measured in the highly conductive, shallow section at 38-40 m. This indicates, in similarity to borehole BFI01, a high groundwater circulation in the shallow, fractured rock. The calculated groundwater volumetric flux density, Q_f , in the minor fracture zone at 38-40 m depth in HFI01 is also well in accordance with the flux determined in the highly conductive shallow rock in borehole BFI01, i.e. 12 and 14 $m^3/m^2 \cdot yr$, respectively (Gustafsson and Andersson, 1989).

The point dilution measurement in the 20 m-section 104-124 m clearly shows that the upper part of Zone 2 also at borehole HFI01 exhibits a high groundwater flow rate. Assuming that the groundwater flow rate measured in the actual 20 m-section is concentrated to the two straddled high-conductive 2 m-sections (108-110 m and 112-114 m), the groundwater flux in the upper part of Zone 2 (4 m width) becomes 67 $m^3/m^2 \cdot yr$ at borehole HFI01, which is in good agreement with the corresponding average flux measured in borehole BFI01, 90 $m^3/m^2 \cdot yr$ (Gustafsson and Andersson, 1989).

Table 5.10 Results of point dilution measurements in borehole HFI01 (From Andersson and Gustafsson, 1989).

Section (m)	K (m/s)	Q_w (ml/min)	Q_f ($m^3/m^2 \cdot yr$)	v_f^d (m/s) (m/d)	$v_f^g^*$ (m/s)
38- 40	7.2 E-5	10.4	11.7	3.7 E-7 0.0320	4.8 E-7
108-110	3.8 E-5	0.2	0.3	9.6 E-9 0.0008	2.5 E-7
112-114	1.9 E-4	1.3	1.6	5.0 E-8 0.0043	1.3 E-6
104-124	2.3 E-5	106.4	13.3	4.2 E-7 0.0365	3.1 E-7

* calculated with a hydraulic gradient $i=1/150$

5.4.2 Estimated natural groundwater flow through Zone 2

The natural groundwater flow determined in situ by the point dilution method in packed off borehole sections indicates that nearly stagnant flow conditions prevail in the lower part of Zone 2. A significant groundwater flow rate only takes place in the upper, highly conductive part of Zone 2. The natural groundwater flow rate through a 1000 m wide vertical section of Zone 2, calculated by extrapolation of the results from the dilution measurements, is in the order of 150 000 - 370 000 m³/year (4.7-11.7 l/s).

This estimate of the flow rate can be compared with 150 000 - 315 000 m³/year (4.7-10 l/s) calculated from the results of the hydraulic interference tests and hydraulic head measurements. The higher figure is based on a total transmissivity of 3E-3 m²/s of the zone and an average hydraulic gradient of 0.0035. The lower figure assumes that all groundwater flow is concentrated to the upper part of the zone with a transmissivity of 1.5E-3 m²/s and the same hydraulic gradient. The flow rate calculated by these two independent methods are in good agreement (Gustafsson and Andersson, 1989).

The piezometric measurements indicated that Zone 2 is recharged in areas where the zone is located relatively deep (e.g. boreholes KFI07 and KFI11). The vertical hydraulic head gradient above Zone 2 directed towards the zone is estimated to be in the range of 0.3-3E-3. This corresponds to an infiltration rate of 0.5-5 mm/year. Assuming an average hydraulic conductivity of the rock above the zone of 5E-8 m/s, the rate of infiltration to the zone from the overlying rock can thus be estimated to only about 500 - 5000 m³/year over an area of 1 km², which is approximately the size of the Brändan area. It seems thus most reasonable to assume that regional groundwater flow to a large extent contributes to the groundwater flow in Zone 2 in the Brändan area, although minor sub-vertical fracture zones, which may increase the infiltration rate locally, were not included in the estimation of the infiltration rate (Gustafsson and Andersson, 1989).

Contribution of regional groundwater flow to Zone 2 is further indicated by the estimation of the total groundwater recharge at the Finnsjön site based on data from Carlsson and Gidlund (1983). From these data the recharge over an area of 1 km² has been calculated to a maximum of 150 000 m³/year, of which the most part is recharged to the soil layers and the shallow, fractured and highly conductive rock, as is also shown by the dilution measurements. Hence, approximately 60 - 80 % of the groundwater flow in Zone 2 is likely to be regionally recharged (Gustafsson and Andersson, 1989).

Knowing the natural groundwater flow rate through a 1000 m wide vertical section of Zone 2 and the hydraulic gradient (0.0035), the required aperture of an equivalent single fracture (with parallel planar plates representing the fracture surfaces) to discharge the assumed flow rate can be estimated. The calculated equivalent aperture is in the range 1.3-1.7E-3 m. If the same flow rate is divided into five or ten parallel-

plate fractures the equivalent aperture of the fractures are approx. $0.8E-3$ m and $0.7E-3$ m, respectively. This makes up a total aperture of Zone 2 of $4.0E-3$ m and $7.0E-3$ m respectively. The aperture of Zone 2 calculated for one single equivalent fracture is to be compared with that calculated from the pulse injection of tracers (section 5.2) in the central part of the highly conductive upper part of Zone 2, ranging between $5.1E-4$ - $1.3E-3$ m (Gustafsson and Andersson, 1989).

5.5 Estimation of conductive fracture frequency

The conductive fracture frequency (CFF) implies the hydraulically conductive portion of the total number of (coated) fractures mapped over a given length in a borehole or an underground opening. This entity has previously been estimated employing statistical techniques (Carlsson et al., 1984; Osnes et al., 1988), using information on mapped fracture properties (Winberg and Carlsson, 1987) and finally by multivariate analysis of integrated borehole data (Andersson and Lindqvist, 1989). Based on results from single-hole hydraulic tests in detailed sections (2 and 3 m) in the cored boreholes within the Brändan area (Table 4.1), the conductive fracture frequency within Zone 2 and of the adjacent rock was calculated using statistical methods (Andersson et al., 1988).

The statistical techniques, utilizing information from hydraulic tests and core logs, yield an estimate of the probability that one fracture is conductive. A borehole section with a hydraulic conductivity equal to the lower measurement limit is in this context regarded as non-conductive. Combined with the average frequency of coated fractures in the studied domain an estimate of CFF can be obtained. Statistical homogeneity of the rock volume studied and independence of fractures are assumed. The details of the analysis are presented in Andersson et al. (1988).

The CFF was calculated for the entire Zone 2, the adjacent rock mass above (denoted B1), and below (B2) the zone. Three subparts of the zone were defined; an upper (A1) and a lower (A3) more conductive part and the remainder of the zone (A2). The former two correspond respectively to the more fractured and more conductive portions of the zone consistently observed in the detailed hydraulic testing along its upper and lower boundary.

Data from recent hydraulic testing in boreholes KFI05, KFI06, KFI07, KFI09, KFI10 and KFI11 (2 m sections) were used in the analysis (data set 1). Since hydraulic single-hole tests in 3 m sections were performed previously (Table 4.1), and corresponding old core mapping is available for boreholes KFI05, KFI06 and KFI07, a unique opportunity existed to make a comparison between calculated values of CFF based on new (data set 1) and old data (data set 2) for these boreholes. The results of the calculations are compiled in Tables 5.11-12 and Figure 5.3.

The results show that Zone 2 has an average CFF of around 1 fracture/m which is of the same order as the calculated CFF of

the surficial rock mass above the zone and twice that of the bedrock below the zone. The estimated CFF for Zone 2 should be compared with an average frequency of coated fractures in the zone of 5.2 fractures/m. The lack of entries for subparts A1 and B2 in the case of boreholes KFI05-07 (data set 1) are due to a lack of convergence in the calculations and lack of data, respectively. The two extreme values calculated for data set 2, subparts A1 and B1, are due to a total lack of no-flow sections and influences of very surficial data, respectively.

A comparison between the analyses of the old and new data sets reveals that the calculated CFF, based on data set 2, is 1.2-1.4 times higher when discounting the above mentioned extreme values. This is in agreement with that expected from the lower measurement limits of the two data sets, i.e. 2×10^{-10} m/s (except KFI05, 2×10^{-9} m/s) and 7.5×10^{-10} m/s (KFI09-KFI11, 1×10^{-10} m/s) for the old and new data sets, respectively. A lower measurement limit may be conceptualized by adding more minor conductive fractures to the measured quantity, i.e. the hydraulic conductivity, which in turn would entail an increase in the portion of conductive fractures.

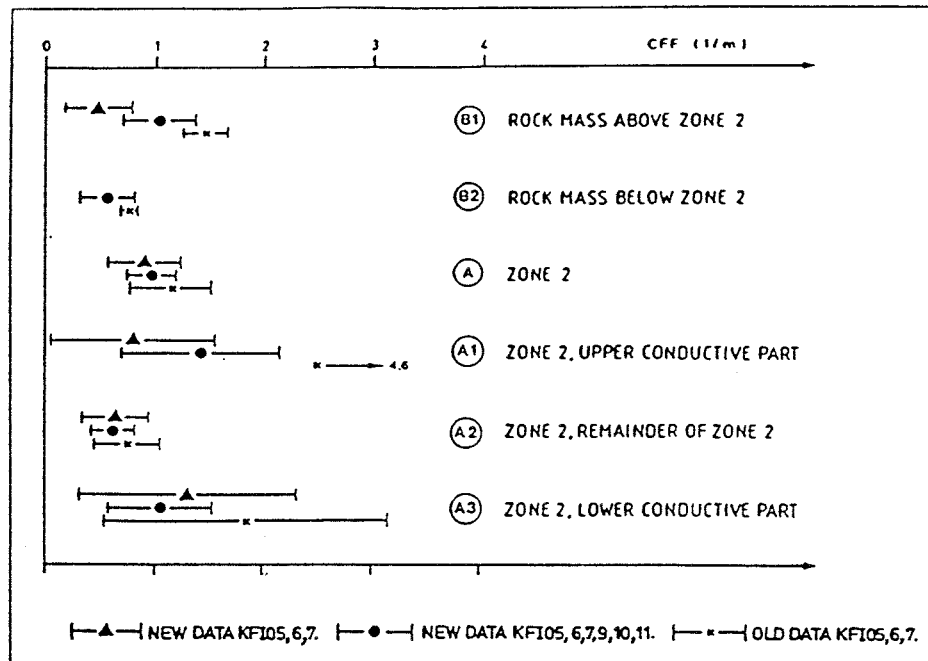


Figure 5.3. Estimated CFF of different rock units at the Finnsjön area. From Andersson et al.(1988).

Table 5.11 Probability 1-P (one fracture is conductive) and the total number of data (M) used in the analysis of the two data sets from fracture Zone 2 and adjacent rock mass in the Brändan area, Finnsjön. From Andersson et al. (1988).

Bedrock unit	Data Set 1				Data Set 2	
	1-P	All M	1-P	KFI05-07 M	1-P	KFI05-07 M
A	0.19	263	0.14	127	0.30	113
A1	0.25	50	-	28	1.00	20
A2	0.18	122	0.15	57	0.27	54
A3	0.15	91	0.15	42	0.38	39
B1	0.29	79	0.13	33	0.80	177
B2	0.21	34	-	-	0.32	322

Table 5.12 Conductive fracture frequency (CFF) and confidence limit (δ) based on the two data sets from fracture Zone 2 and adjacent rock mass in the Brändan area. From Andersson et al. (1988).

Bedrock unit	Data Set 1				Data Set 2	
	CFF	All $\pm \delta$	CFF	KFI05-07 $\pm \delta$	CFF	KFI05-07 $\pm \delta$
A	0.98	0.22	0.90	0.46	1.15	0.38
A1	1.43	0.72	-	-	4.60	-
A2	0.62	0.19	0.65	0.31	0.75	0.30
A3	1.06	0.47	1.29	1.01	1.85	1.29
B1	1.02	0.33	0.47	0.31	1.44	0.20
B2	0.56	0.25	-	-	0.76	0.12

Possible leakage around packers, particularly in the case of the old tests performed in KFI05, KFI06, KFI07 (data set 2), tends to overestimate the difference between the two data sets. This fact is moderated by a contemporaneous underestimation of the average fracture frequency in the case of data set 2 (c.f. Tables 5.11-12). The respective sizes of the confidence limits reflect the variance in the estimator. The greater the amount of data (n_m), the higher the values of P and N ($m=1, \dots, N$) used, the smaller the variance and the narrower the confidence limit obtained.

The calculated values of the conductive fracture frequency (CFF) are compatible with the overall results of the single-hole hydraulic testing. The results indicate that only 10-40 % of the coated fractures mapped are hydraulically active, the actual figure being closely related to the lower measurement limit of the hydraulic testing equipment used.

6. HYDROCHEMICAL CONDITIONS.

6.1 Hydrochemical features of the studies performed.

Since site characterisation studies commenced in the Finnsjön region in 1977, a total of 11 rotary cored water-flushed boreholes, and 1 booster air-flush borehole, have been drilled and specifically sampled for hydrochemical studies. These results are presented by Hultberg et al. (1981), Laurent (1982), Ahlbom et al. (1986), Smellie et al. (1989) and Smellie and Wikberg (1989). The chemical parameters have been discussed by Allard et al. (1983), Ahlbom et al. (op. cit.), Smellie et al. (op. cit.) and Smellie and Wikberg (op. cit.), and the geochemical association between the groundwater and the fracture minerals by Tullborg and Larson (1982). The groundwater chemical parameters are presented in Appendices 8:1 to 8:5.

Although not all data are available for the earlier investigations (1981/82), for example, no oxidation potential measurements are presented, the results distinguish two major types of groundwater: saline and non-saline, with the former usually increasing in extent with depth. The groundwater chemistries (Appendix 8:1) show the following characteristics:

- saline groundwaters are emphasised from boreholes KFI05, KFI06 and KFI08 whereupon chloride concentrations range from 2500-5900 mg/l. Low tritium contents (<3-7 TU) and old relative C-14 ages (ca. 5500-10 000 years) also typify these waters thus establishing them as representative and free from major contamination (i.e. from near-surface fresh water or flushing water).
- groundwaters from boreholes KFI04 and KFI07 exhibit higher tritium (3-14 TU) and younger relative C-14 ages (ca. 4000-6000 years) which, together with smaller concentrations of chloride (approx. 30-650 mg/l), indicate varying degrees of contamination from other sources.
- the two boreholes which would appear to represent only non-saline water (KFI01 and KFI02) are characterised by high to very high tritium (38-50 TU) and correspondingly low relative C-14 ages (ca. 2000-4000 years). These waters are thus highly contaminated by surface to near-surface derived water and not representative for the measured holes.

The major features of the groundwaters resulting from recent studies (1985-1987) are summarised in Appendices 8:2 and 8:3. Boreholes KFI09 and BFI01 show the transition of non-saline to saline groundwater with depth, the boundary between the two being the low angle fracture zone (Zone 2). These non-saline and saline groundwaters are considered representative, i.e. low chloride (<100 mg/l), high tritium (up to 36 TU) and high percentage modern carbon (up to 85%) for the non-saline type, compared to high chloride (5000-5500 mg/l), low tritium (<3 TU) and low percentage modern carbon (<30%) in the saline type.

In summary, boreholes KFI05, KFI06, KFI08, KFI09 and BFI01 can be regarded as relatively free of contamination during

groundwater sampling procedures, and are therefore representative for the borehole section length isolated and sampled. In contrast, boreholes KFI04 and KFI07 show varying degrees of contamination from other sources during sampling, and should be regarded with some caution. Finally, boreholes KFI01 and KFI02 are contaminated by near-surface and/or flushing water during sampling, and should not be considered for any quantitative interpretation.

6.1.1 Chemical and isotopic character of the groundwaters

Surface recharge waters for the Finnsjön area are moderately acidic (e.g. pH 5.9), of low conductivity (e.g. 4.12 mSm), and contain only small amounts of dissolved ions. The tritium (e.g. 31+/-2 TU) and stable isotope (e.g. $\delta D = -80.5$ ppt; $\delta^{18}O = -12.1$ ppt) contents are usual for recharge meteoric waters in this part of Sweden (Saxena, 1984).

Vertical trends in groundwater chemistry from boreholes KFI09 and BFI01 (Appendix 8:3) show the clear distinction between the non-saline (calcium-bicarbonate type) and saline waters via a transition zone of mixing (i.e. Zone 2). This is readily indicated by the conductivity values. The pH, in contrast, shows a perceptible decrease with depth from just above Zone 2, which is contrary to that normally indicated by Swedish groundwaters at increasing depths.

Of the cations, Ca^{2+} , Na^{+} and Mg^{2+} show marked increases with depth; K^{+} is less emphasised. Of the anions, HCO_3^{-} typically decreases with depth accompanied by sympathetic increases of Cl^{-} and SO_4^{2-} ; increases in Br^{-} , I^{-} and F^{-} (not plotted) are also present.

The stable isotope data (Appendix 8:2) show very little variation with depth and can be considered to be meteoric in origin. Radioisotope data, i.e. percentage modern carbon and tritium contents, clearly indicate the extent of the young, near-surface derived fresh water component (down to approx. 100 m depth) characterised by high amounts of modern-derived carbon (e.g. 85.30% representing an apparent age of less than 2000 years) and significant tritium contents (8-36 TU). With increasing depth and salinity the groundwaters rapidly exhibit a reduction in modern-derived carbon (e.g. 22.60-37.45%) with minima at the lower horizons of Zone 2 (i.e. apparent ages greater than 12 000 years). At these depths no significant tritium has been detected.

From borehole locations KFI09 to BFI01, i.e. a distance of approx. 830 m in a northwest direction, Zone 2 gently descends from a depth of 134-205 m at KFI09 to 234-353 m at BFI01. By comparing the data in Appendices 8:2 and 8:3 there is some evidence that the salinity below Zone 2 increases. This is most readily seen by the conductivity values which reflect small increases in Na, Mg and Cl. Ca, K and HCO_3 remain constant and SO_4 shows a significant decrease. Above Zone 2, within the non-saline groundwaters, some differences are also observed. At borehole KFI09 the demarcation between non-saline and saline

groundwater at the Zone 2 contact is sharp, whilst at BFI01 the transition is less distinct. This is believed to have resulted from an incursion of more saline water from depth via conducting fractures during pumping for sampling purposes.

6.1.2 Redox character of the groundwaters

The redox conditions of the groundwaters are best defined by the Eh and the contents of ferrous iron, uranium and dissolved oxygen. Each of these parameters are individual signatures for the prevailing conditions. Oxidising groundwater conditions are characterised by dissolved oxygen, high uranium, positive Eh and low ferrous iron concentrations. Reducing conditions by an absence of oxygen, negative Eh, low uranium and high ferrous iron. Intermediate conditions are defined by no oxygen, zero Eh values and appreciable uranium and ferrous iron concentrations.

Table 6.1. Redox-sensitive parameters of the Finnsjön groundwaters at increasing depths; see text for explanation (boreholes BFI01 and KFI09). From Smellie and Wikberg (1989).

Sample	Depth (m)	pH	Eh (mV)	Fe(II) (mg/l)	Fe(tot) (mg/l)	U (ppb)	234U/238U Activity Ratio.
BFI01	71- 84	6.9	+40	8.86	9.01	4.57	1.6
BFI01	169-192	7.7	-320	0.50	0.51	12.78	2.2
BFI01*	234-247	7.7	-270	0.87	0.90	3.90	3.3
BFI01*	284-294	6.8	+400	0.009	0.022	114.32	1.7
BFI01*	335-385	7.3	+340	0.009	0.029	10.70	2.0
BFI01	439-460	7.0	+400	0.005	0.016	15.63	1.9
KFI09	94	7.3	-245	0.13	0.52	2.1	4.1
KFI09*	114	7.5	-300	0.36	0.36	-	-
KFI09*	182	7.7	-212	0.19	0.94	1.6	3.1
KFI09	360	7.4	-	0.05	0.35	3.1	5.0

* sampled intervals completely or mostly within Zone 2.

Table 6.1 compares the redox-sensitive parameters from the air-flush percussion borehole (BFI01) with those from the water-flush rotary borehole (KFI09) at different depths; Zone 2 is intercepted at a shallower depth by KFI09.

The most striking feature is the highly oxidising character of the groundwaters sampled from Zone 2 in borehole BFI01 compared

with borehole KFI09. This is attributed to perturbations during drilling when air at high pressure was forced along the conductive fissure systems comprising Zone 2. Although a negative result from a contamination viewpoint, it is interesting to note the extent that the uranium concentrations have increased during the relatively short time period when air has affected the redox conditions (i.e. 2-6 weeks). The Fe(II)/Fe(tot) ratio has also been influenced varying from near unity above Zone 2 to 0.3 to 0.5 within and below the zone.

Borehole KFI09 provides a more normal situation with negative Eh readings, low uranium contents and higher activity ratio values characterising the deeper, older saline groundwaters. The iron oxidation ratios are variable due to some minor drilling water contamination.

It is worth noting here that not only are the redox conditions affected by the incursion of air into the groundwater system. A close look at the pH values show a significant reduction of pH at those levels of artificially induced high uranium content (pH 6.6 to 6.9) when compared to the other undisturbed deep levels in both BFI01 and KFI09 (pH 7.1 to 7.7). This is believed to be due to increased dissolution of carbon dioxide during percussion drilling.

6.1.3 Groundwater flow.

Using available hydrochemical data a simplistic groundwater flow model can be created in the near-vicinity of the two sampled boreholes. As indicated above, the upper (100 m) part of the rock is characterised by groundwater of calcium-bicarbonate type which has a fairly short residence time. The presence of sodium and chloride, however, shows that some water (containing approx. 1% saline water from below Zone 2) has been transported from lower levels. For example, in borehole BFI01, the sampling at 169 m shows an increase in the salinity of the water during the sampling period, confirming the possibility of conducting fractures transporting saline water. A later tritium analysis than presented in Appendix 8:3 gave a value of less than 3 TU which further confirms the assumption that the groundwater sampled in this section was pumped up from deeper levels and therefore more ancient in origin. Under unperturbed conditions the sodium and chloride concentrations at this level would probably be much lower.

Within the upper part of Zone 2 the salinity increases drastically. The composition is constant throughout the sampling period indicating that the mixing is not artificially produced by pumping. This upper part could therefore be considered as a "sump" whereupon saline water from below Zone 2 is mixed with non-saline water from above the zone. Interestingly, the mixed water in the upper part of Zone 2 has a similarly high carbonate content as the non-saline water. This implies the water has been subject to carbon dioxide diffusion after mixing with the saline water. It is not possible to decide exactly how this process has occurred; it is however obvious that the process is continuous or that it has

occurred during a long period of time. Below Zone 2 the water has a constant composition which indicates that there is very little, if any, flow. This is supported by the moderate to high 234U/238U activity ratios (3-5) recorded from borehole BFI09 (Table 6.1) which suggest long residence times enabling a build-up of recoil-loss 234U at the rock/water interfaces.

The presence of Zone 2 thus appears to represent a structural/hydraulic boundary to the bedrock groundwater cells of circulatory movement. As a result, the downward moving non-saline water preferentially spreads out along the upper, more conductive levels of Zone 2, rather than continue to deeper levels to mix with the older saline waters. Similarly, the more sluggish upward moving saline water will do likewise. Zone 2 is therefore a horizon along which groundwaters of considerably contrasting age and chemistry come into contact and partially mix with one another.

6.1.4 Equilibrium modelling of the groundwaters

The computer code PHREEQE has been used for groundwater modelling (Laaksoharju, 1988, written comm.). The computation of the saturation index with respect to calcite shows an index variation ranging from -1 to +0.5 logarithmic units (Appendix 8:4). The undersaturation in the uppermost sampled section (i.e. 71-84 m) can be explained by the short residence time of the non-saline groundwaters. The undersaturation computed for the deeper sections (i.e. 284-460 m) is thought to be the result of drilling activity. These low conducting sections are also associated with high uranium concentrations and positive Eh readings in the sampled waters as a result of the drilling activity (see section 6.1.2).

During percussion drilling there is an enhanced carbon dioxide concentration in the compressed air due to combustion. In the downhole contact between the air and groundwater, dissolution of carbon dioxide in the groundwaters results in a significantly lower pH than in the unperturbed situation. The pH values should be about half a pH unit higher.

The highest saturation index is obtained from water sampled from the upper part of Zone 2. This water has a chloride concentration of 1500 mg/l, i.e. it is diluted by a factor of three to four compared to the saline water below the zone. The supersaturation of 0.5 logarithmic units indicates that calcite is precipitating in this part of the fracture system. With time, precipitation will effectively help to seal off the upper non-saline water rockmass from the saline rockmass below.

Puigdomenech and Nordstrom (1987) using data from earlier groundwater analyses from Finnsjön have shown how the mixing of non-saline and saline water has resulted in a highly supersaturated water even though the initial starting waters are at equilibrium with respect to calcite. A similar mixing calculation is reported here from borehole KFI09 (BFI01 was not considered because of the above-mentioned perturbances). The plotted data (Appendix 8:4) illustrate the fact that even

though the end member waters are undersaturated, the resulting mixtures are supersaturated by a factor of 0.5 logarithmic units.

6.2 Changes of water conductivity during hydraulic interference tests

During the hydraulic interference tests carried out by pumping borehole BFI02, some additional parameters were monitored, e.g. the electrical conductivity of the discharged water at the surface (Andersson et al 1989a). The changes of electrical conductivity during interference tests 1, 2 and 3B are shown in Appendix 8:5. During these tests, the lower, upper and the full extent of Zone 2 was pumped (see section 4.3.2). The groundwater discharge rate, downhole water temperature, and the atmospheric pressure during the different interference tests, are also shown. The figures show that the temperature of the groundwater was relatively stable during the interference tests.

A rough estimation of the leakage flow rate from the upper part of Zone 2 to the lower part during interference test 1 (and vice versa during test 2) was made by Andersson et al. (1989) on the basis of the measured changes of electric conductivity of the discharged water. Knowing the initial water conductivities in the upper and lower parts of Zone 2, and assuming that the discharged water is a mixture of these two sources only, the leakage flow rates from the unpumped to the pumped parts of Zone 2 may be estimated by simple balance calculations. The measured electric conductivity of the discharged water from the pumping borehole and the estimated discharge from the upper and lower parts of Zone 2 by the end of each test are shown in Table 6.2.

Table 6.2 Initial and final values of the electric conductivity (EC) of the discharged water, total flow rates used (Q) and estimated discharge (Q_s) from the upper (U) and lower (L) parts of Zone 2 during the different hydraulic interference tests. From Andersson et al. (1989).

Test no	Part of Zone 2	Q (l/min)	Initial EC (mS/m)	Final EC (mS/m)	Q _s (l/min)
1	lower	500	1250	1150	U = 62 L = 438
2	upper	500	450	720	U = 331 L = 169
3B	whole	700	970	880	U = 324 L = 376

7. LINEAMENTS AND FRACTURES

7.1 Introduction

The objective of this chapter is to give location of lineaments (coordinates) and statistical representation (length, orientation, relative length per azimuth intervals) of lineaments and fractures in the Finnsjön site and its surroundings, Figure 7.1. The basis for this report are lineament analysis presented in Ahlbom and Tirén (1991) and fracture analysis presented in Ahlbom et al. (1988).

Structural information on four different scales are treated:

- o 50 x 50 km, scale 1:250 000 - Regional area
- o 10 x 10 km, scale 1:50 000 - Semi-regional area
- o 2 x 2,5 km, scale 1:10 000 - Local area
- o outcrops, scale 1:1

7.2 Definition of terms and description of methods

7.2.1 Lineament maps

Hobbs (1904) introduced the term lineament to characterize the spatial relationship of generally rectilinear Earth surface features. In 1912 he gave a more restricted definition of the term: "significant lines of landscape which reveal the hidden architecture of the basement are described as lineament." A lineament is a 1-D structure and a lineament map is a 2-D representation of the intersection of discontinuities in the bedrock and the ground surface.

The lineament map of northern Uppland, Figure 7.1, has been interpreted from a grey-toned, 1:250 000 topographical map contoured every 12,5 m. The map comprises an area of 50 x 50 km.

Lineaments constituting rock block boundaries on semiregional scale, 1:50 000, Figure 7.5, has been interpreted from the topographical map 12 I Östhammar NV contoured every 5 m. Mapped area is 10 x 10 km.

Lineaments on local scale, Figure 7.9, has been interpreted from detailed topographical maps on scale 1:10 000 contoured every one metre. The map area is 2,5 x 2 km.

7.2.2 Lineaments of different orders

Lineaments are classified according to their topographical expressions (see legends in Figures 7.2, 7.5 and 7.9). Qualitative description of structures forming the lineaments exists only for some structures in the Forsmark, Finnsjön and Dannemora areas. Notable is that a single structure may continue from a higher order lineament into a lower order lineament.

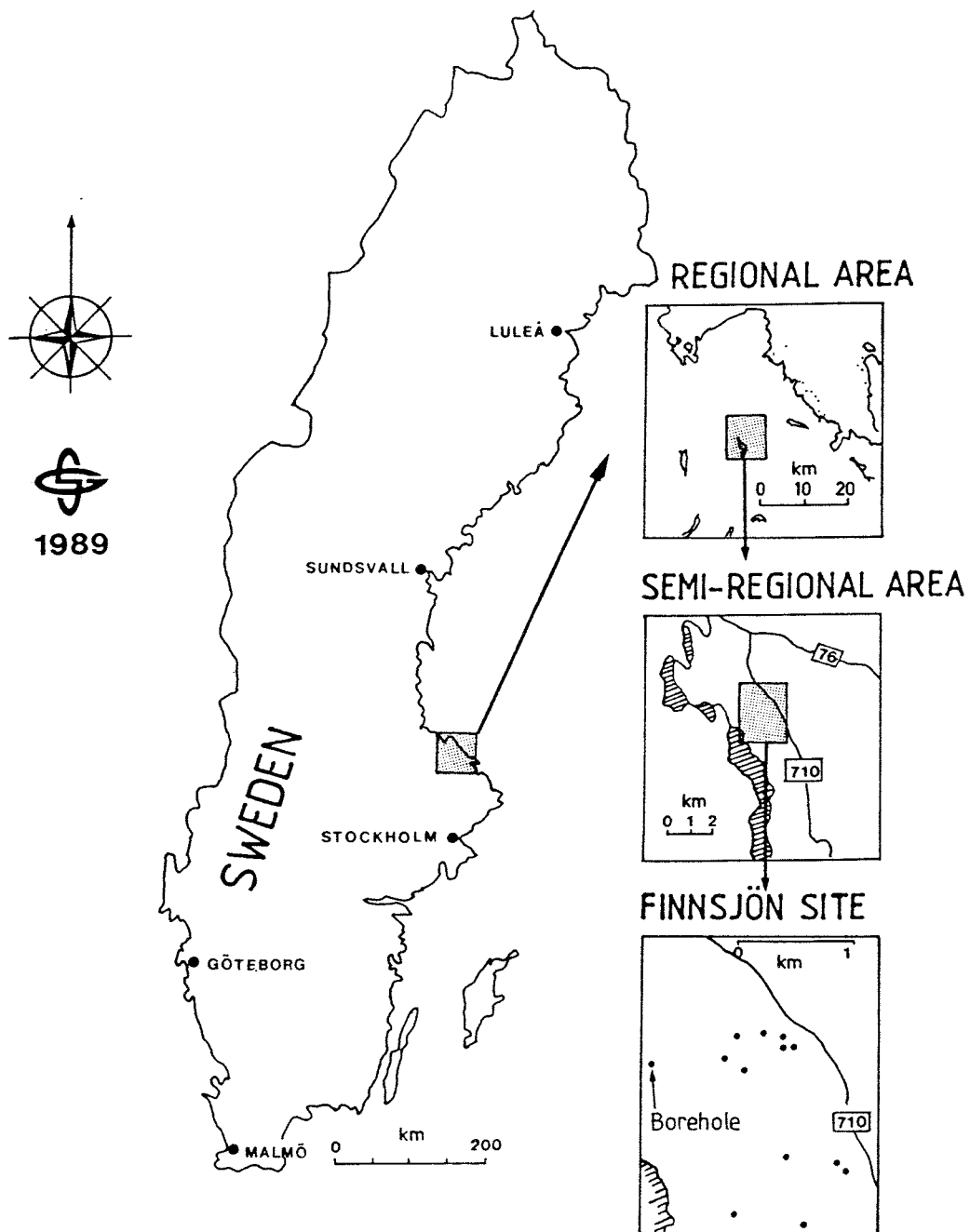


Figure 7.1 Location of the regional area (northeastern Uppland), the semi-regional area (Gävastbo area), and the local area (Finnsjön site).

Rock block maps are given for the semi-regional and local areas. Rock blocks are rock volumes outlined by tectonic discontinuities i.e. zones of low tensile strength, such as fracture zones and faults (Tirén and Beckholmen 1989). The formations of rock blocks engages only some or parts of some of the discontinuities (Dershowitz 1984). This imply that a rock block map is a refinement of ordinary lineament maps in that sence that only structures constituting block boundaries are considered.

7.2.3 Location, length and orientation of lineaments

The locations of the lineaments are presented on maps and their coordinates (RAK) are given in tables in Appendix 9:1.

The length and orientation of lineaments are calculated from rectilinear representations of the structures, i.e. the coordinates of the end points of a lineament is connected by a straight line. Length of lineaments are given as the trace length of such line. Orientation of lineaments are measured in an analogue way. In a separate diagram the relative length of lineaments per cell (50 cell width) are presented. In diagrams, displaying length distributions notations are made if one or both endings of a lineament is outside the map area. However, some of the lineaments are curved, why maps/models showing the rectilinear representation of the lineaments are presented to elucidate the differences, bias, in location, orientation and length presented in the statistical data compared with original maps.

7.2.4 Fractures

Fracture statistics are based on field surveys within a minor part of the Finnsjön site (Brändan area, c.f. Ahlbom et al. 1988). Detailed fracture information has been obtained by mapping all fractures in a 1 x 48 m cell within an excavated N40E trending trench (ca 5 x 90 m) close to borehole KF111.

7.3 Lineaments of northeastern Uppland

7.3.1 Lineament pattern

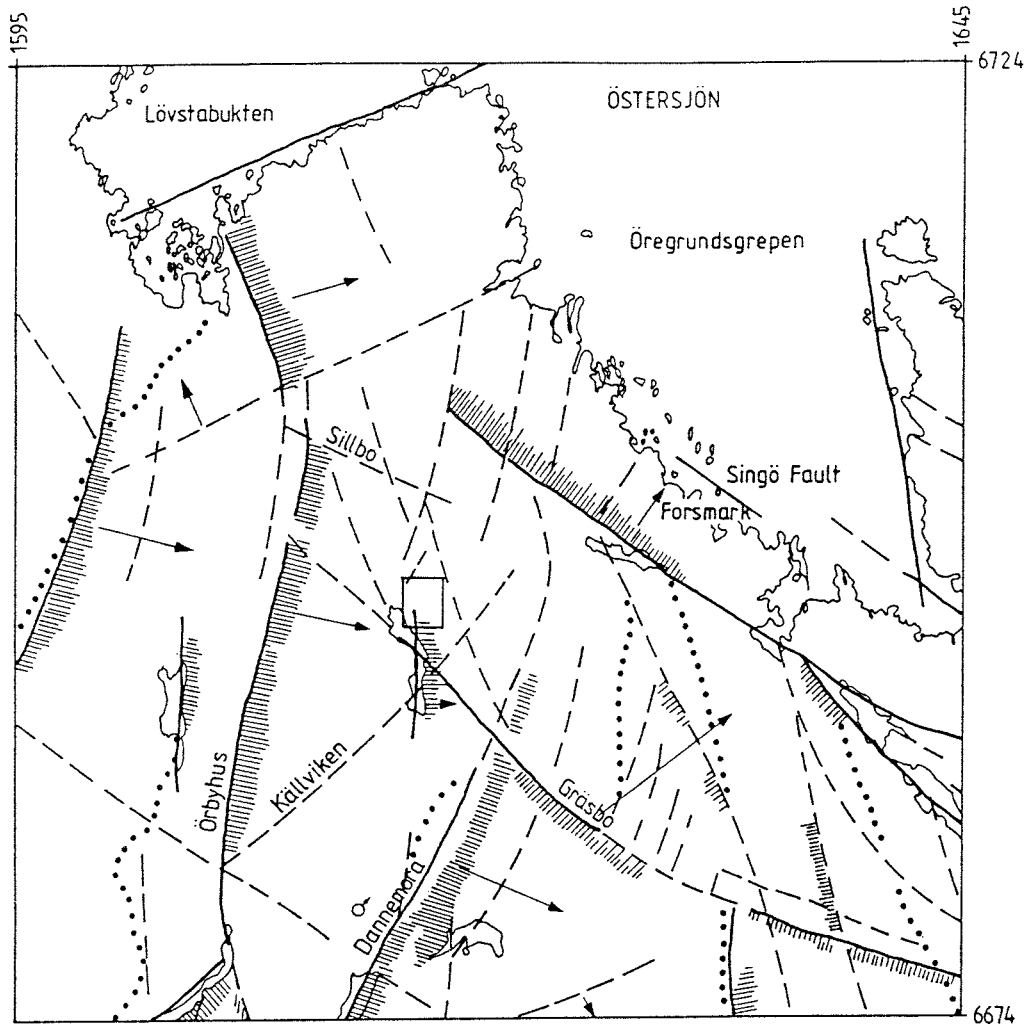
Northeastern Uppland is transected by a regional WNW-trending shear zone, the Östhammar Faults Zone (Tirén in Ahlbom and Smellie, eds., 1989), which is some 25 km wide and traceable some 200 km. The internal structure of this zone, formed c. 1.7 Ga ago, is an anastomosing network of shears enveloping lensoidal blocks, Figure 7.2. These WNW shears are intersected by another set of shears, trending north. These shears envelope regional N-S trending lensoidal blocks.

The Finnsjön site is situated in the southern part and close to the boundary of the Östhammar Fault Zone.

7.3.2 Lineament characteristics


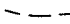





Lineaments of the regional area, Figure 7.2, have been divided into two groups/orders: well expressed and less well expressed (Tables 1.1 and 1.2 in Appendix 9:1 and Figures 7.2 and 7.3). The well expressed lineaments outline boundaries of tilted (up to 2⁰) regional blocks.

Three lineament orientations are dominant: N55W, N5-20E, and N20-25W (Figure 7.4a). The length distribution of lineaments are given in Figure 7.4b and c. About 24% of all lineaments have one end outside the area and 2% of the lineaments transect the area. The lineaments are often curved. NW-trending lineaments are concave SW-wards, while NE to N-S trending lineaments are windling (wave length longer than 30 km).



LINEAMENT MAP, NORTHEASTERN UPPLAND

REGIONAL AREA

-  Lineament, well expressed
-  Lineament, less well expressed
-  The elevated side of the rock block are marked with a line screen
-  Dip direction of the ground surface
-  Glaciafluvial deposits, eskers
-  Dannemora mine
-  Finnsjön site

The glacial striation is north-south

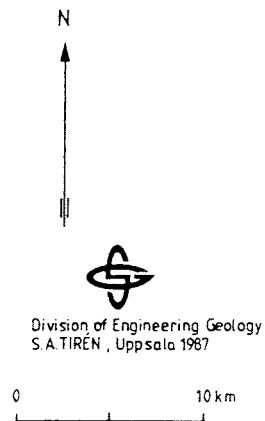


Figure 7.2 Lineament map of northeastern Uppland.

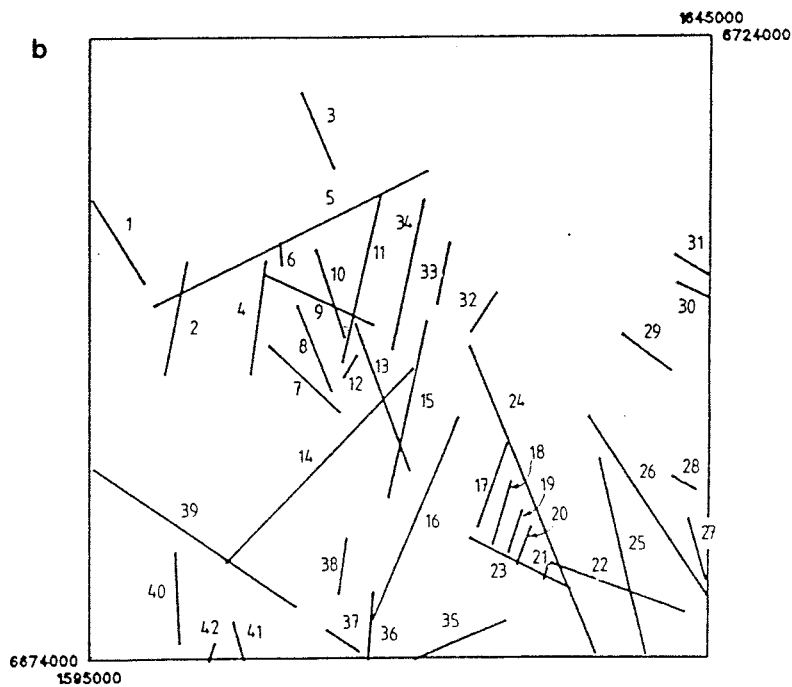
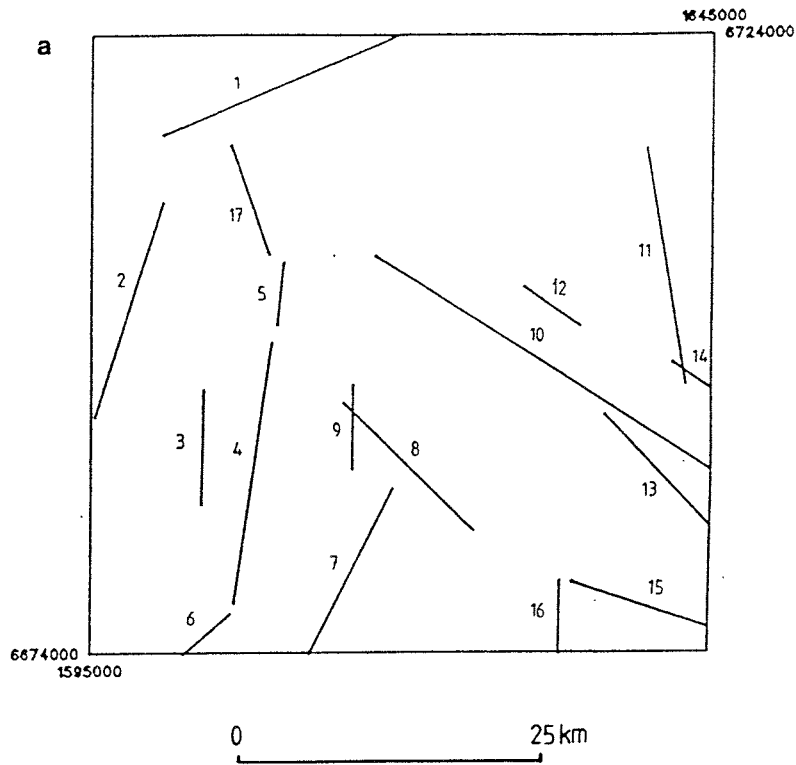


Figure 7.3 Map of rectilinear presentation of lineaments in northeastern Upland: a. well expressed lineaments (first order), and b. less well expressed lineaments (second order). Numbers refer to Table 1.1 - 1.2 in Appendix 9:1.

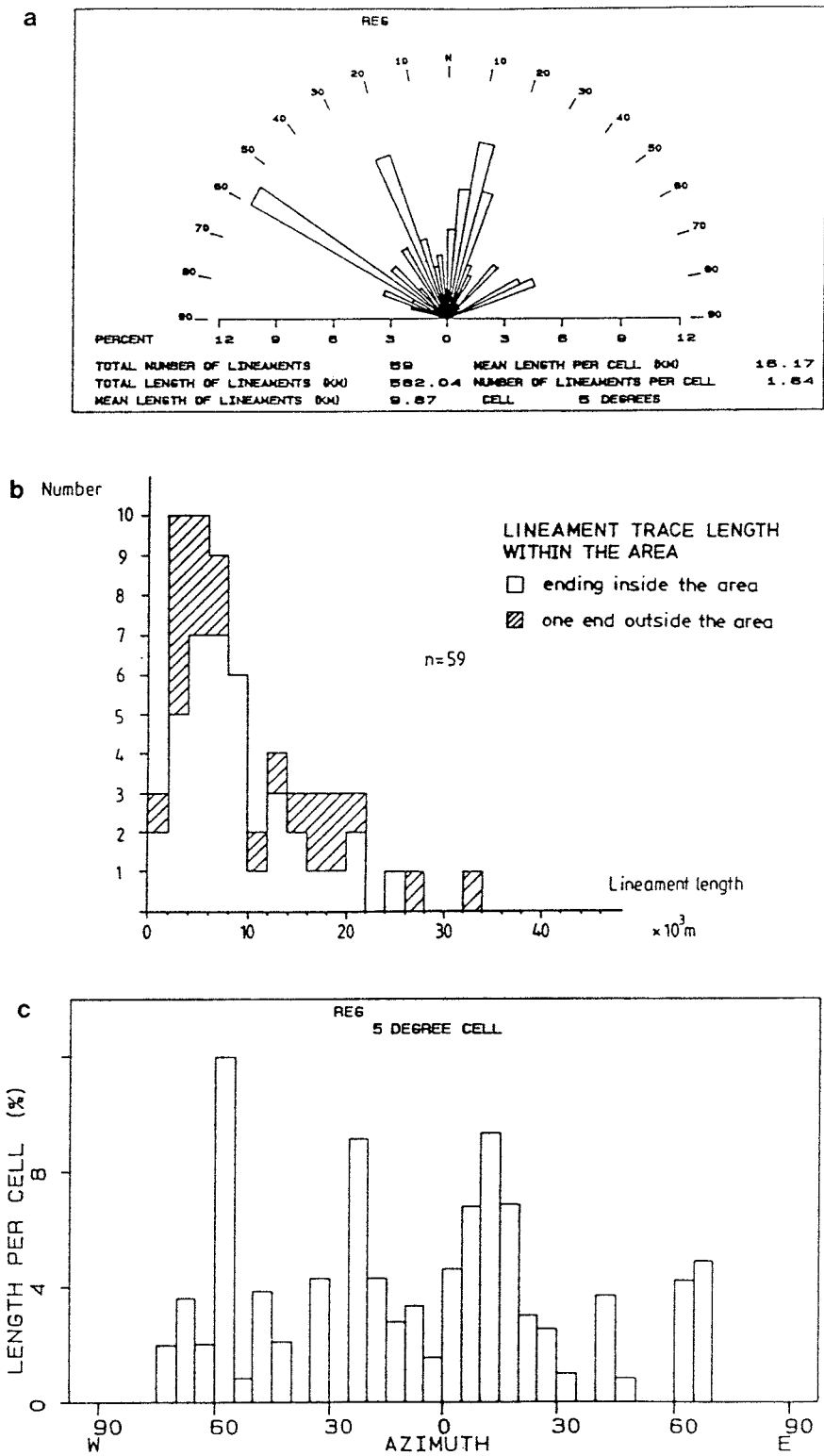


Figure 7.4 Statistical presentation of lineaments in northeastern Upland: a. rosettediagram, b. distribution of lineament lengths, and c. length distribution of lineaments relative to their orientation (5° sectors).

7.4 Lineaments of the Gåvastbo area

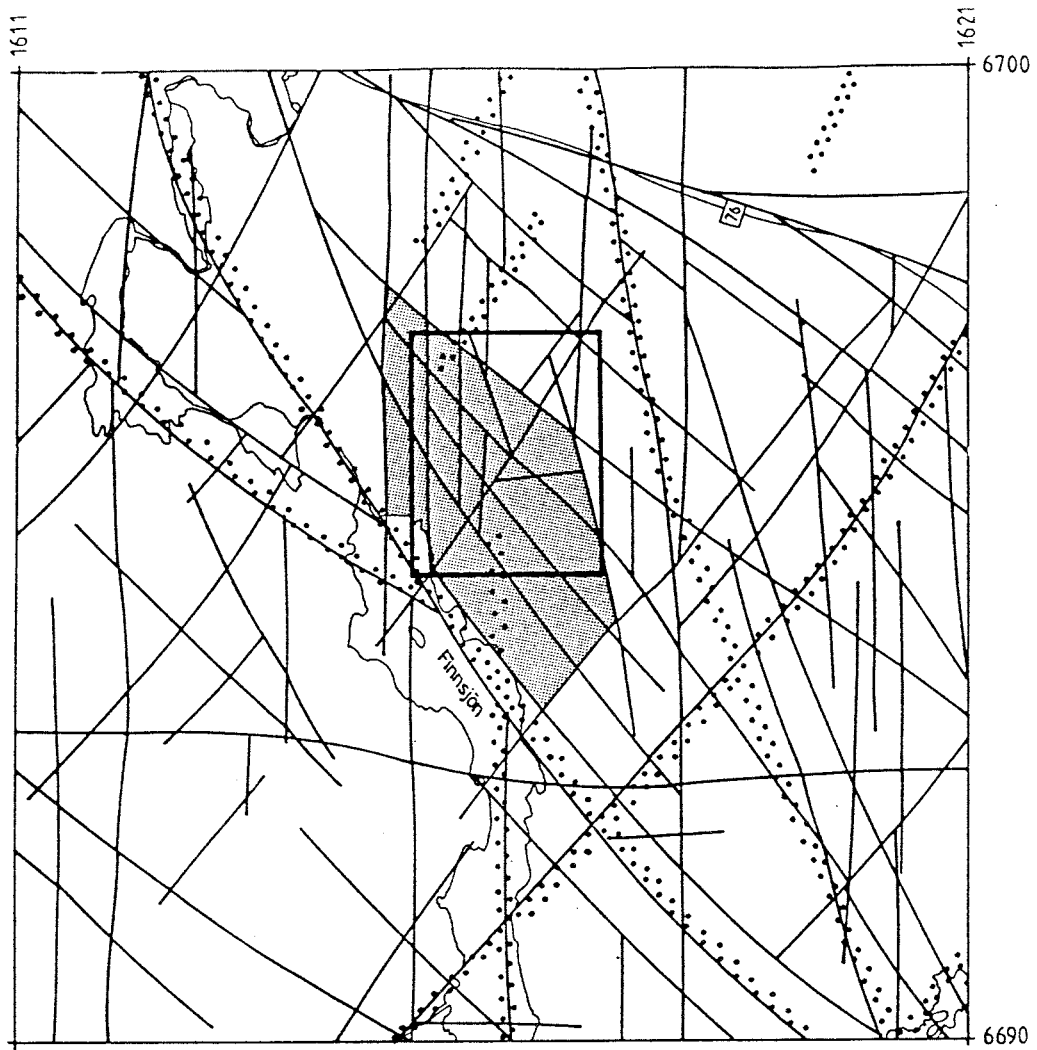
A rock block map of the Gåvastbo area is shown in Figure 7.5. The rock blocks boundaries of the Gåvastbo area are divided in four groups (orders) relative to their topographical appearance (width, depth and extension), Figure 7.6 and 7.7. The length and orientation of lineaments is given in Figure 7.8.

The first order structures are related to the regional WNW trending Östhammar Fault Zone, see Figure 7.6a and Table 2.1 in Appendix 9:1, and they transect the Gåvastbo area.

Second order structures comprise some additional lineaments belonging to the Östhammar Fault Zone, Fig. 7.6b and Table 2.2 in Appendix 9, but also slightly curved NE lineaments and an orthogonal overprinting system of relative straight lineaments oriented in N-S and E-W. The curved NE lineaments are related to regional N-S trending shears, possibly conjugate shears to the Östhammar Fault Zone. The orthogonal system overprint the shears and thereby is considered to be younger. Dolerite dykes (c. 1.5 Ga) trending E-W occur in Uppland, although they are most frequent in the Mälaren region.

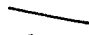


The third order structures are dominantly related to the NW and NE shears (e.g. the Brändan fracture zone; No 18 in Figure 4.3c) and N-S structures, Figure 7.6c and Table 2.3 in Appendix 9.

The fourth order structures, Figure 7.6d and Table 2.4, show an areal distribution which most presumably is related to the degree of exposure. The lowest order structures are conform with the configuration of higher order structures.

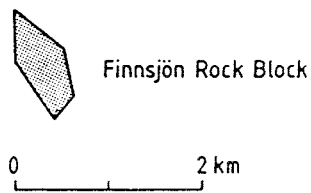


ROCK BLOCK MAP , GÅVASTBO AREA

SEMI-REGIONAL AREA

-  Rock block boundary
-  Position of lineaments interpreted on regional scale
-  Finnsjön site

The glacial striation is north-south



Division of Engineering Geology
S.A. TIRÉN, Uppsala 1989

Figure 7.5 Rock block map of the Gåvastbo area.

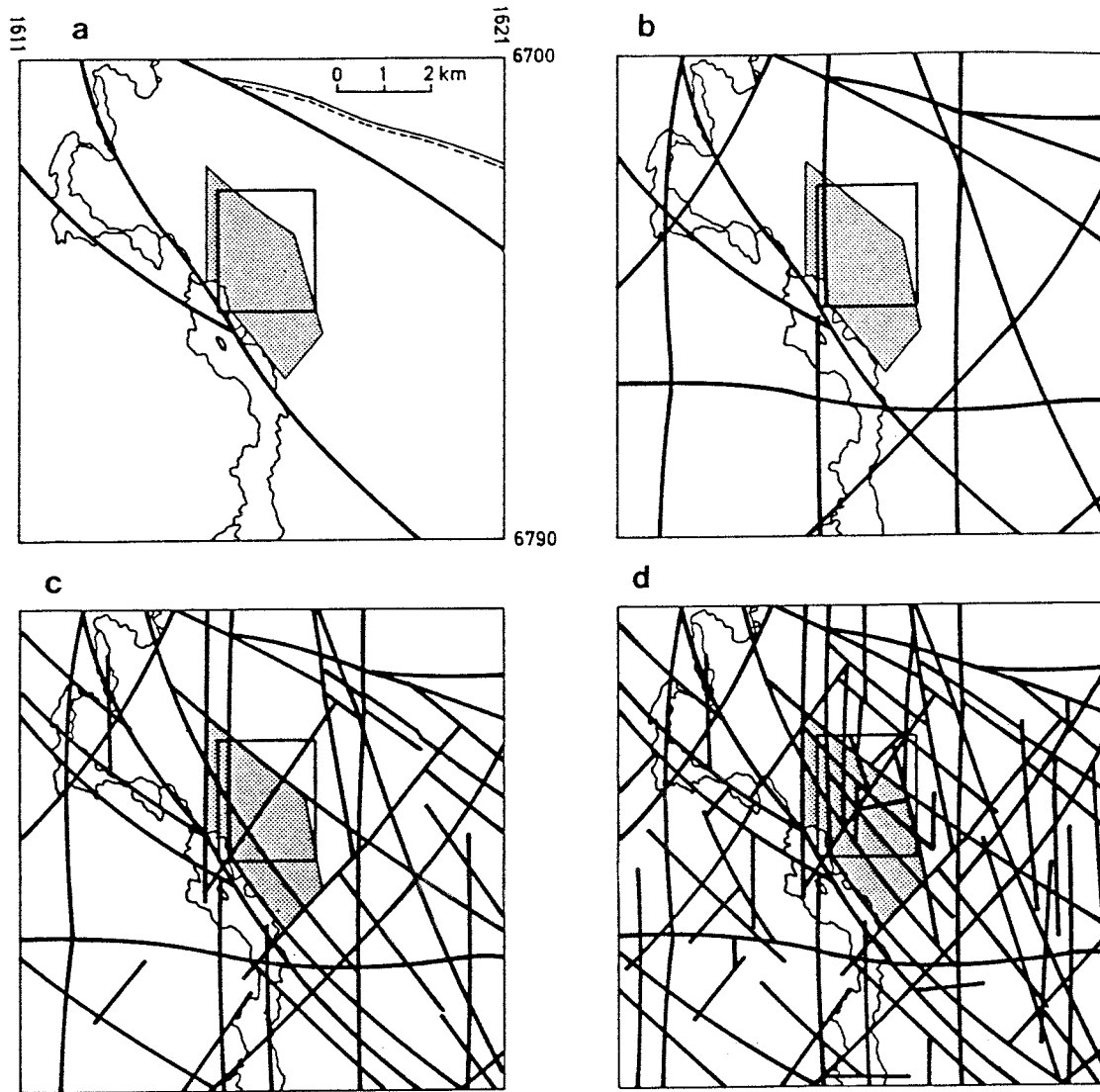


Figure 7.6 Four orders of rock block boundaries in the Gåvastbo area: a. first order structures b. with second order structures added c. third order added and d. all four order structures compiled. After Ahlbom and Tirén (1991).

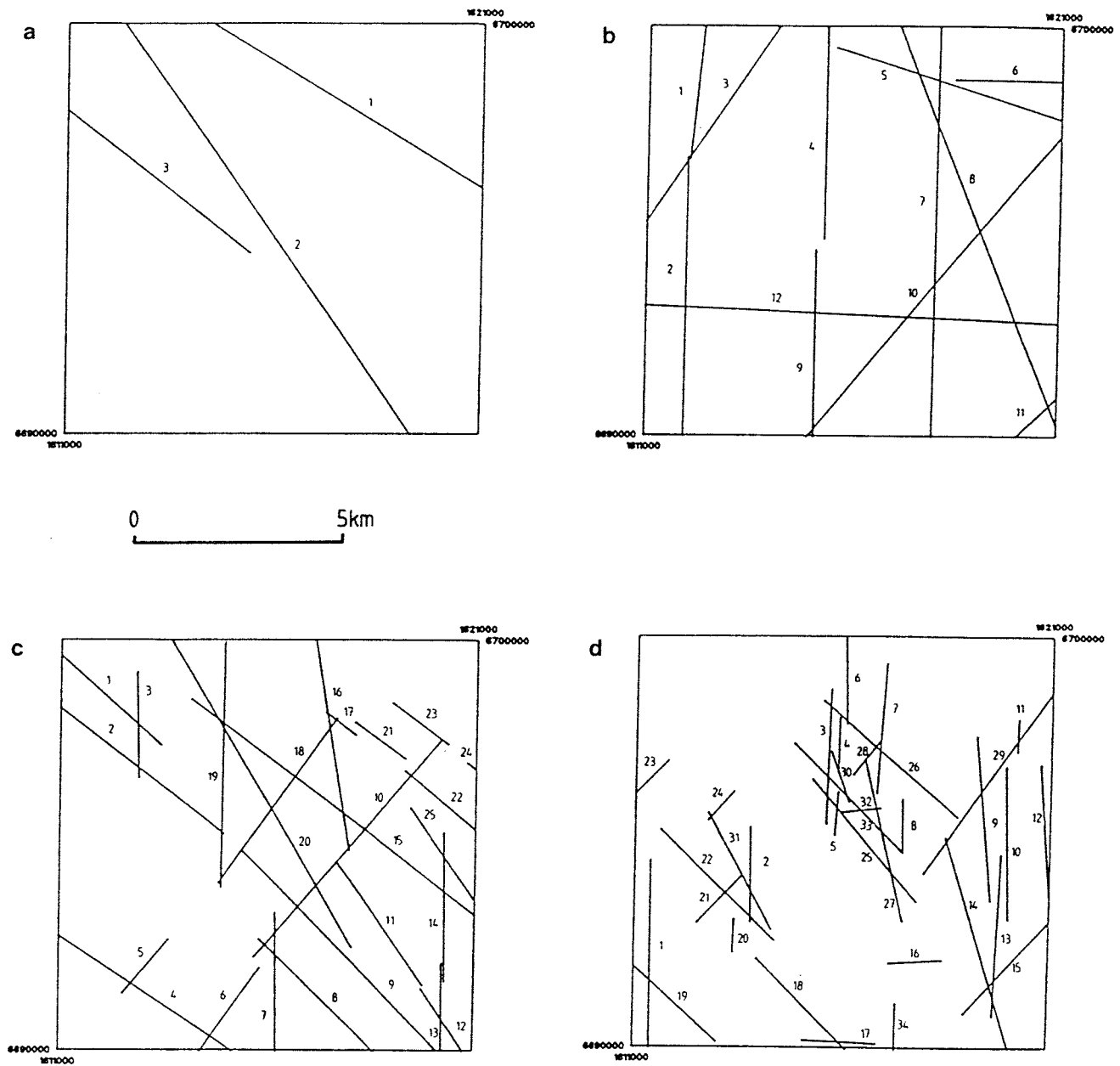


Figure 7.7 Maps of rectilinear presentation of lineaments in the Gävastbo area: a. first order b. second order c. third order and d. fourth order. Numbers refer to Table 2.1 - 2.4 in Appendix 9:1.

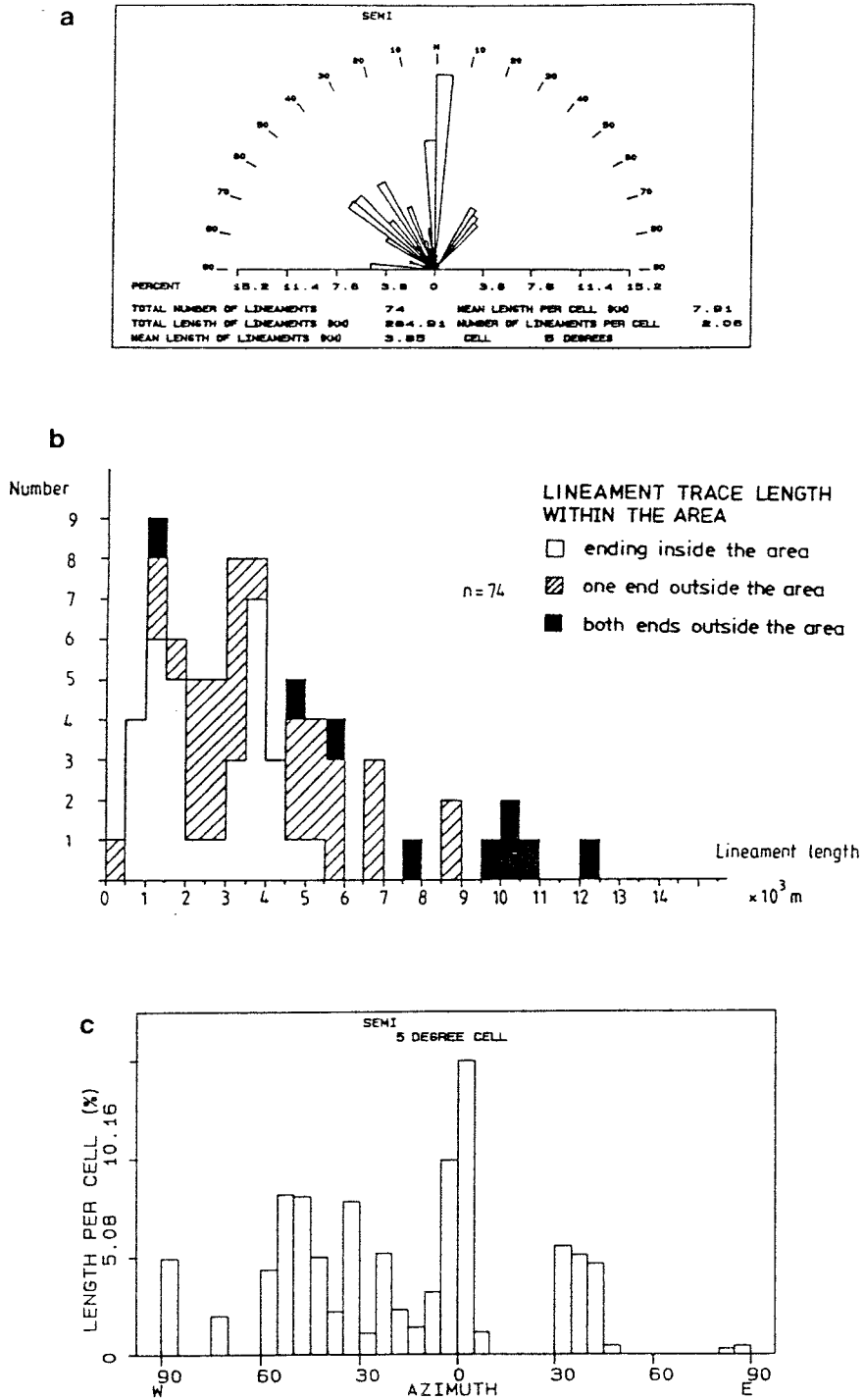


Figure 7.8 Statistical presentation of lineaments (n=74) in the Gävstbo area: a. rosette-diagram, b. distribution of lineament lengths and c. length distribution of lineaments relative to their orientation (5°-sectors).

7.5 Lineaments of the Finnsjön site

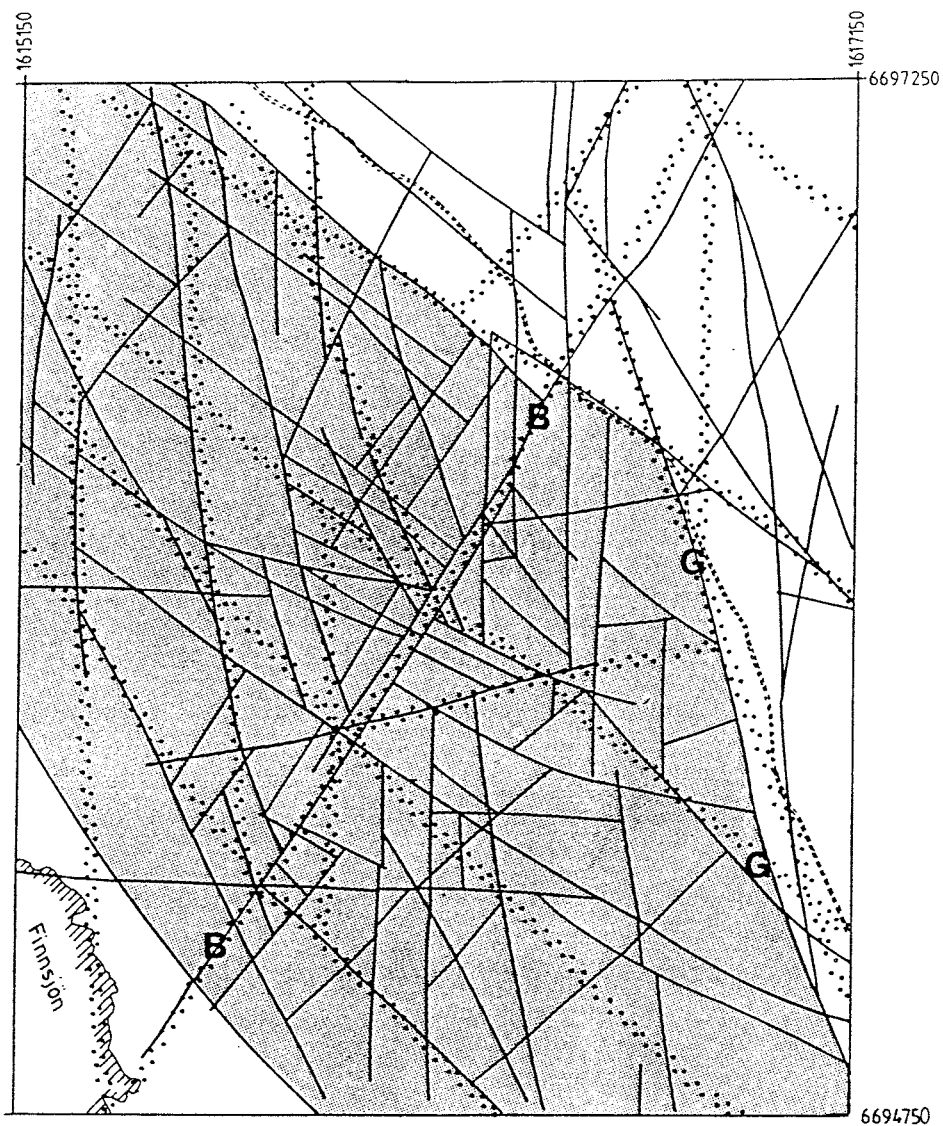
Rock block boundaries/lineaments of the Finnsjön site are shown in Figures 7.9-12. They are sub-divided into four orders, see Figures 7.10 - 7.11 and Table 3.1 - 3.4 in Appendix 9:1. Length and orientation of lineaments in the Finnsjön site is given in Figure 7.12.

The first order structures are associated with the Gåvastbo fracture zone (Figure 7.10a; lineament No 6) or regional NW-shears. Branching (e.g. horse tail structures) is typical for the brittle shears.

Second order lineaments are dominantly related to the NW shears. A transecting fault, the Brändan fracture zone (Figure 7.10b; lineament No 1) transect the area.

For the third order structures it should be noted that some lineaments (Figure 7.10c; lineaments No 1 and No 2) outline most probably the boundaries of a single zone (approx. 200 m lateral width).

The map of fourth order lineaments (Figure 7.10d) shows a high density of NE and NW structures north of the Brändan fracture zone compared to the structures of the southern side.



ROCK BLOCK MAP, FINNSJÖN SITE

LOCAL AREA

- Rock block boundary
- Position of rockblock boundaries interpreted on semi-regional scale

The glacial striation is north-south



0 500m



Division of Engineering Geology
S.A. TIRÉN, Uppsala 1989

Figure 7.9 Rock block map of the Finnsjön site.
B=Brändan fracture zone (Zone 1)
G=Gåvastbo fracture zone (Zone 3)

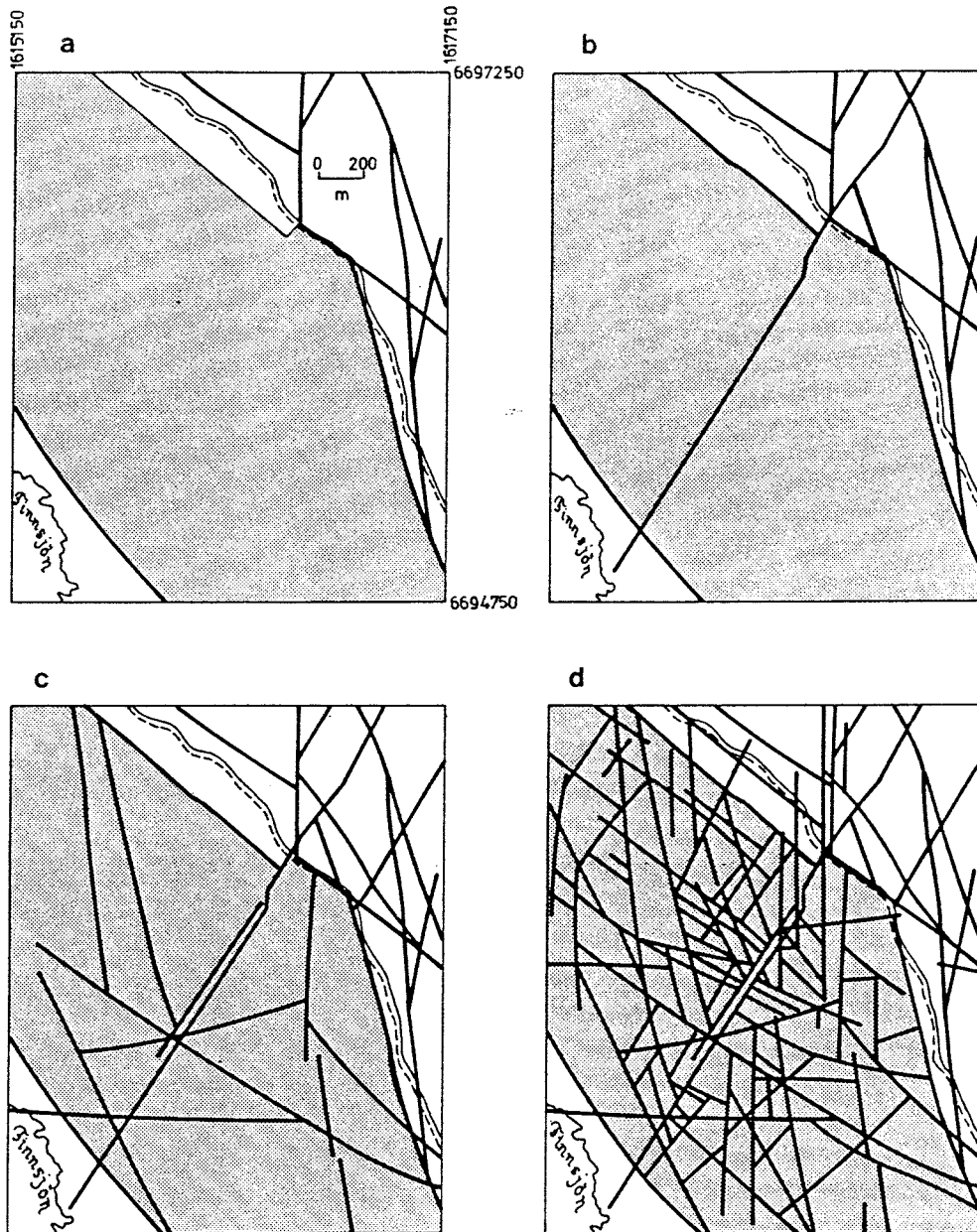


Figure 7.10 Four orders of rock block boundaries in the Finnsjön site: a. first order structures b. with second order structures added c. third order added and d. all four order structures compiled. After Ahlbom and Tirén (1991).

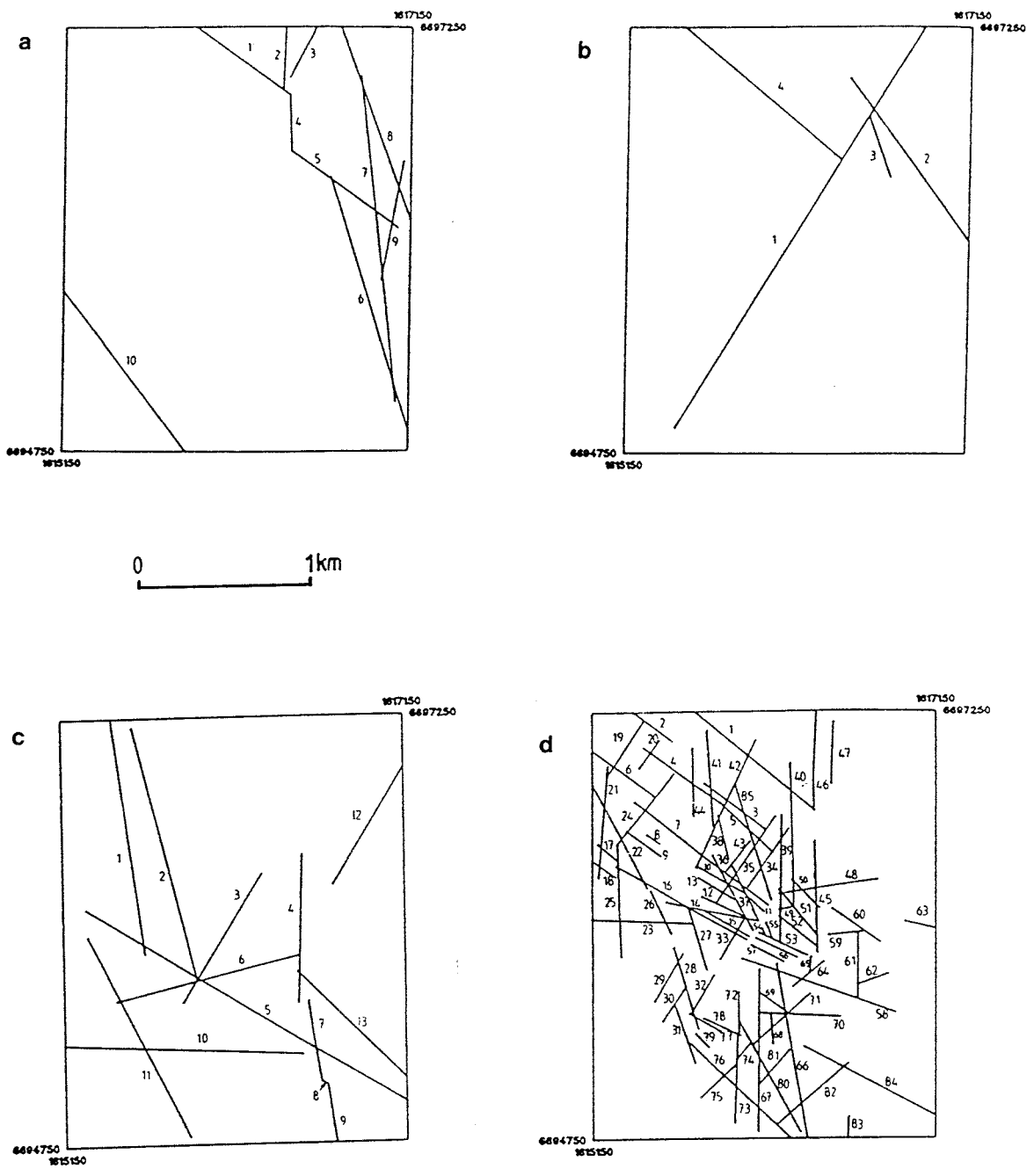


Figure 7.11 Maps of rectilinear presentation of lineaments in the Finnsjön site: a. first order, b. second order, c. third order, and d. fourth order. Numbers refer to Table 3.1 - 3.4 in Appendix 9:1.

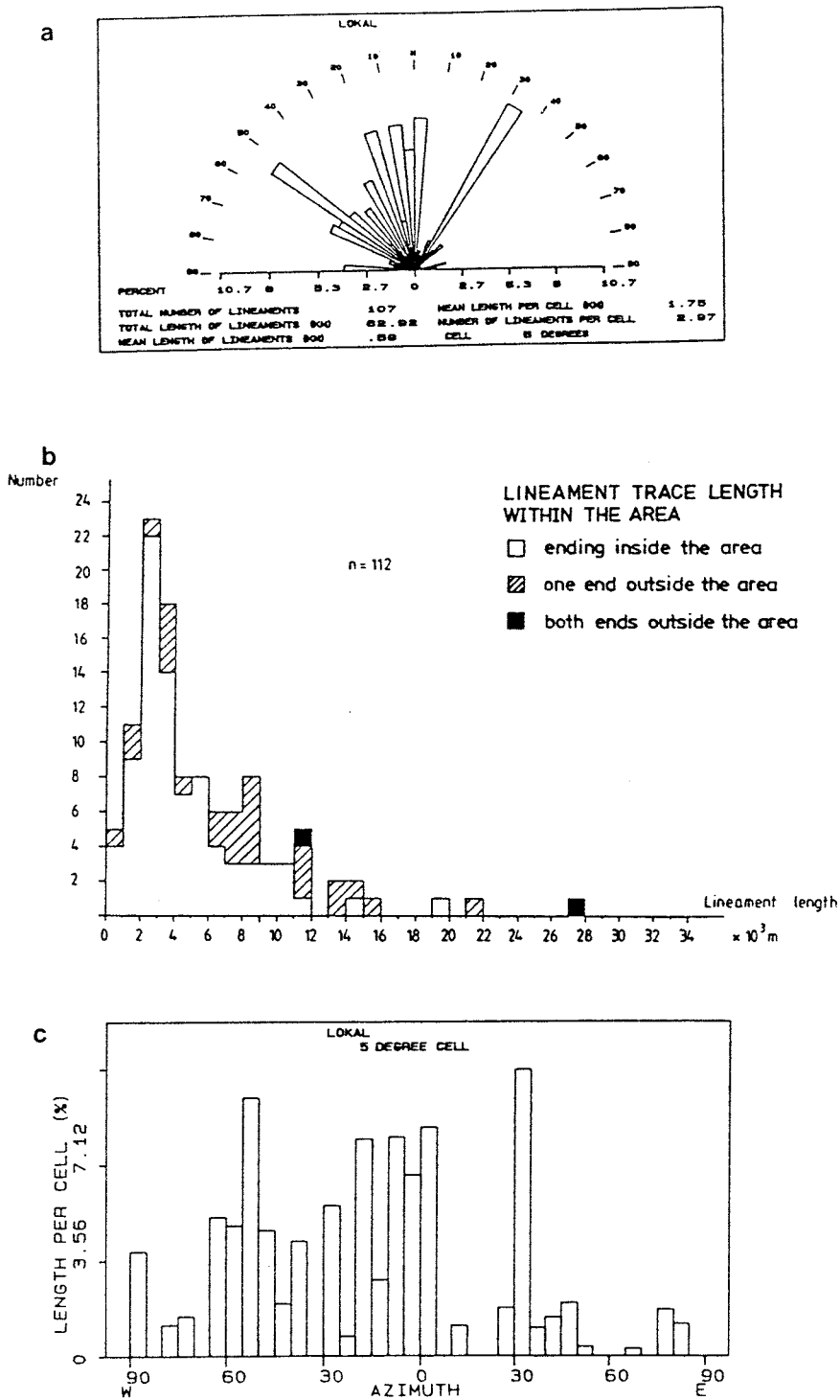


Figure 7.12 Statistical presentation of lineaments (n=112) of the Finnsjön area: a. rosette diagram, b. distribution of lineament lengths, and c. length distribution of lineaments relative to their orientation (5° sectors).

7.6 Fracture mapping in the Finnsjön site

During the site characterization work in 1977-1978 fracture mapping was performed along two stripes, oriented in N-S and E-W, respectively, across the Finnsjön site. The fracture recordings included 73 outcrops on each of which at least two perpendicular fracture scan-line surveys were performed. Fracture mapping south of Zone 1 is given in Appendix 9:2.

A qualitative notation of fracture distribution in a minor part of the Finnsjön site, the Brändan area (c. 1 km²), was performed during the Fracture Zone Project initiated in 1984. Geological mapping and fracture notation was carried out along 50 m wide stripes parallel to the base line of the local grid system (see Appendix 9:2). The separation between the central lines of the stripes was 50 m, i.e. the mapping comprised a complete cover of the area. Notations of fractures south of Zone 1 are given in Appendix 9:2 as the fracture configuration in this part of the Brändan area resembles that in Zone 2.

7.7 Detailed fracture mapping in an excavated trench

A c. 90 m long N40E trending trench has been excavated close to borehole KFI11, Figure 7.13. The trench, c. 5 m wide, is situated in a local rock block and reflects the fracturing in the rock mass away from fracture zones.

Detailed mapping has been performed in a 1 x 48 m cell, Figure 7.14, while line mapping has been done along the remaining 40 m of the trench. Orientation of mapped fractures are presented in Figure 7.15. Detailed notations of fracture characteristics are given in Appendix 9:2. The fractures can be grouped into two groups according to their orientations: N20-75E/ 70-90 and N30-80W/ 60-90. The length distributions for fractures of the two groups are shown in Figure 7.16. The representation of open fractures of the two groups are equal, but N30-80W/60-90 fractures are the far more extensive compared to the N20-75E/70-90 group of fractures. Types of terminations of fractures belonging to the two groups are given in Table 7.1.

Table 7.1 Character of termination of fractures in the 1 x 48 m cell (c.f. Figure 7.14).

Termination	Group of fractures	
	N30-80W %	N20-75E %
Both ends inside the cell	68	87
One end inside	16	12
Both ends outside	16	< 2
Blind terminations	22	54
One end blind	22	36
Both ends against other fractures	22	6

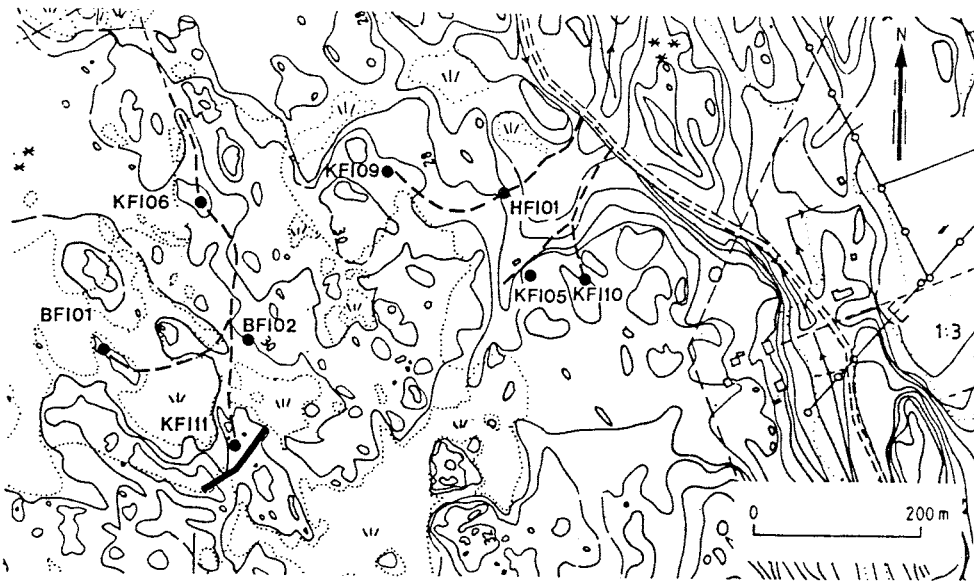


Figure 7.13 Location of excavated trench, just SE of borehole KFI11 (KFixx, BFixx and HFixx are different types of boreholes).

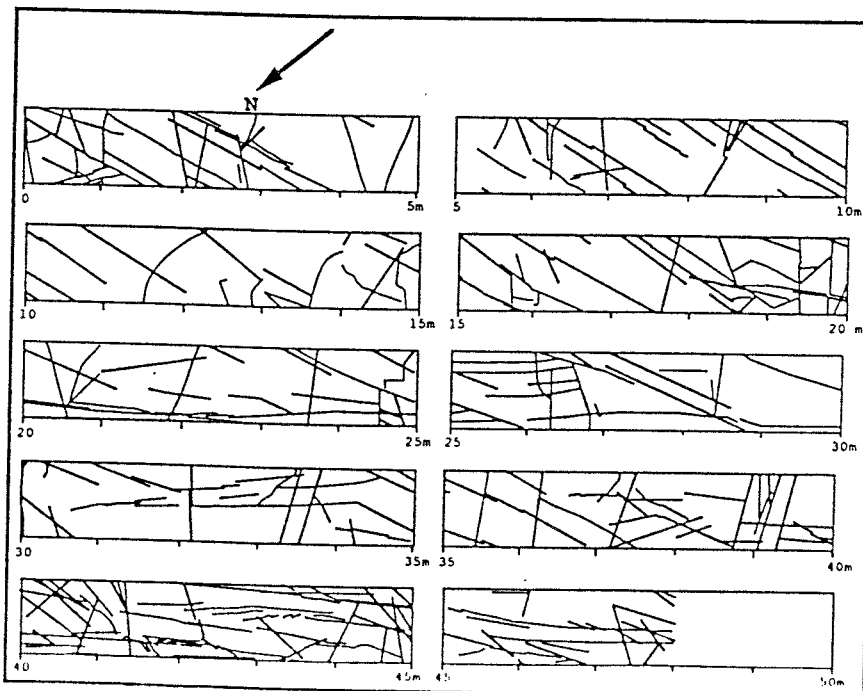


Figure 7.14 Fracture map of the 1 x 48 m cell. (See also Appendix 9:2).

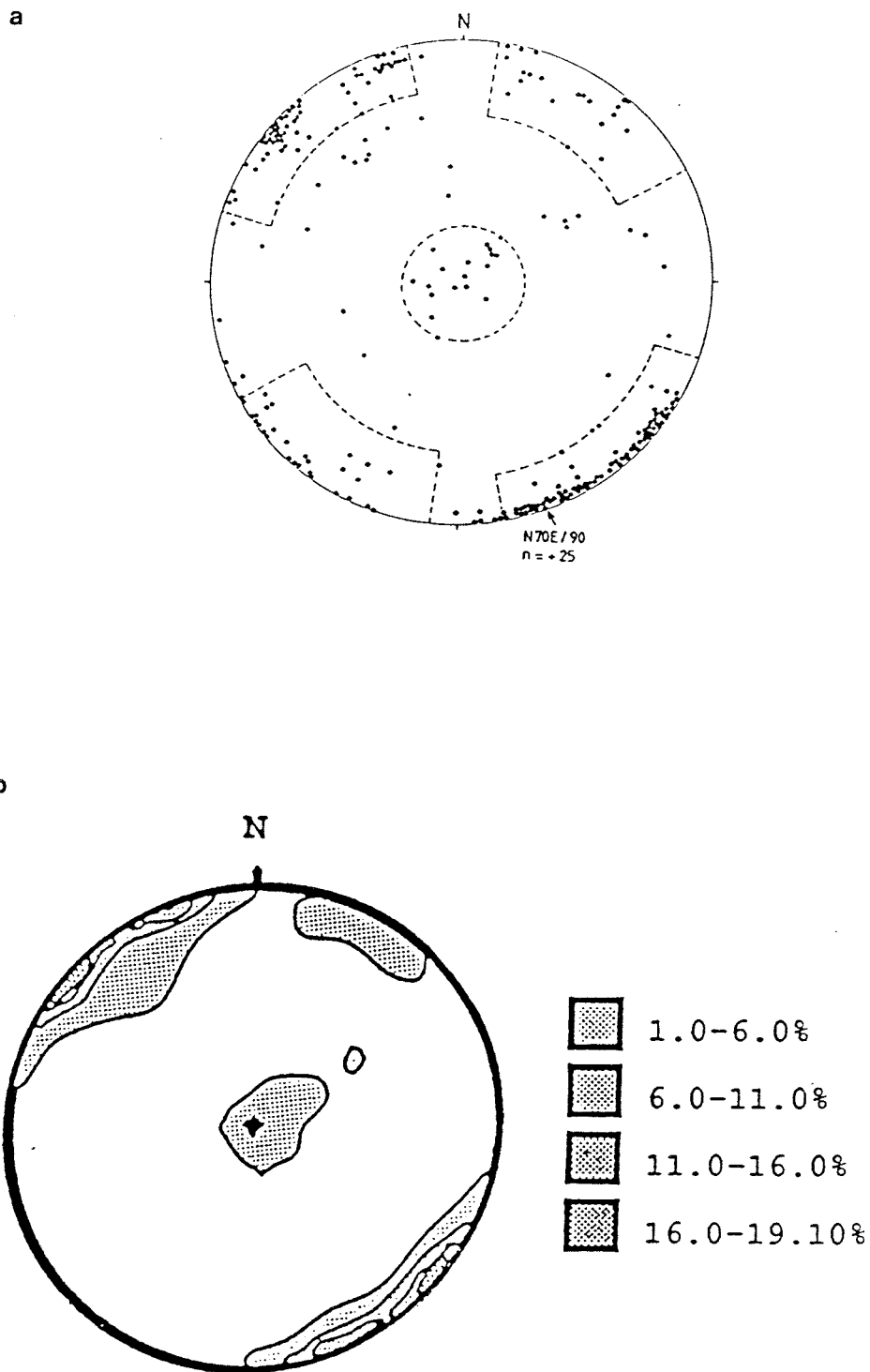


Figure 7.15 Orientation of fractures, Schmidth net lower hemisphere projection.
 a. Inside the 1 x 48 m cell, n = 272
 b. Mapped fractures mapped in the 90 m trench, contoured plot, n = 335.

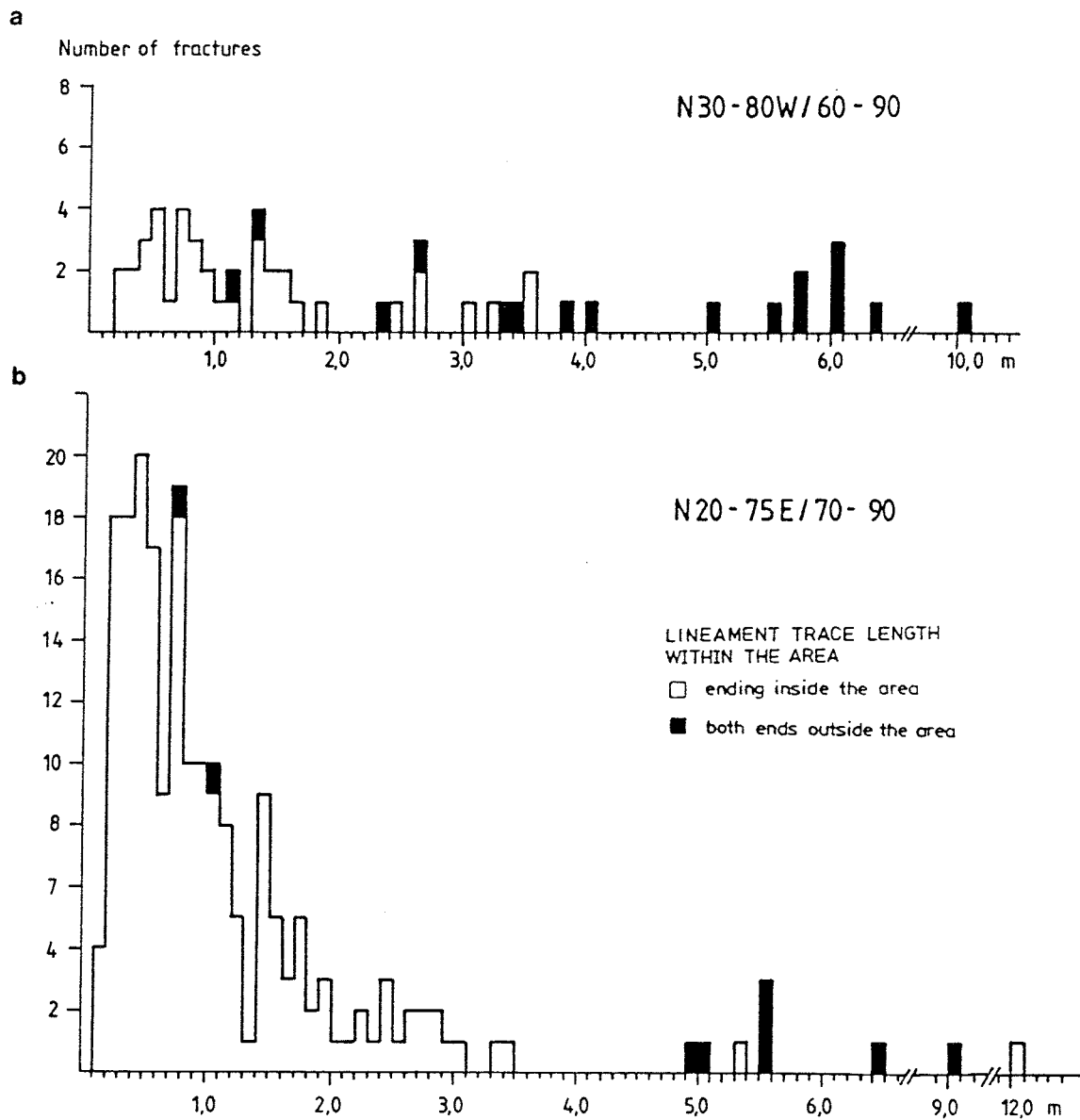


Figure 7.16 Length distribution of fractures. Trace length of a fracture ending outside the profile (ends not exposed) is infilled.

a. N30-60W fractures

b. N20-75E

8. PREVIOUS NUMERICAL MODELLING OF THE FINNSJÖN AREA

This chapter summarizes the results of previous modelling performed within the Finnsjön area and surroundings. The numerical models include both flow and transport in regional and local scales. The models are described in chronological order.

8.1 Preliminary regional and local groundwater flow models

In the KBS 3-project preliminary groundwater flow simulations were performed by Carlsson et al. (1983) using a 3D-model based on the Finite Element Method (FEM). This modelling was merely carried out to gain experience of modelling flow in crystalline rock. The groundwater head distribution and flow field in vertical sections; the groundwater flow at the repository level and groundwater recharge were calculated at steady-state conditions. Three model meshes were generated in successively smaller areas but only the results from the smallest mesh (FINC) were presented. Selected model runs together with a brief description of the runs are shown in Table 8.1. Different functions of hydraulic conductivity versus depth, based on a power function of the form shown in Eqn (8.1), were used.

$$K_e = A z^{-b} \quad (z > 0) \quad (8.1)$$

K_e is the effective hydraulic conductivity, z is vertical depth and A and b are constants. Different depth functions were used for the rock mass and fracture zones. In the FINCL-run the hydraulic conductivity was assumed to be constant for the uppermost 120 m. In the FINCHT-run the fracture zones were assumed to have the same hydraulic conductivity as the rock mass (Table 8.1).

Table 8.1 Description of selected model runs with the FINC-mesh at Finnsjön. From Carlsson et al. (1983).

Run	Coefficients used in equation (8.1)				Conditions at vertical boundaries
	Rock mass		Fracture zones		
	A	-b	A	-b	
FINC (Z>25m)	$1.3 \cdot 10^{-2}$	2.49	0.1	2.0	Non-flow
FINCL (Z>120m)	$1.3 \cdot 10^{-2}$	2.49	0.1	2.0	"
FINCK x)	$1.3 \cdot 10^{-2}$	2.49	0.1	2.0	"
FINCHT	$1.3 \cdot 10^{-2}$	2.49	Not applicable		Hydrostatic pressure
FINCL2 (Z>25 m)	$7.5 \cdot 10^{-6}$	1.30	0.005	2.15	Non-flow

Z=depth in m

x) The function has been averaged within the elements so that each element has a constant permeability.

8.2 Local modelling of the Brändan area (Zone 2)

A series of numerical simulations of the groundwater flow in Zone 2 within the Brändan area at Finnsjön were performed by Andersson and Andersson (1987). The objectives of the simulations were to assist in the planning, design and evaluation of the tracer tests (described in Chapter 5) and hydraulic interference tests in Zone 2 (described in Chapter 4). The simulations were made with the 2D finite element code SUTRA (Voss, 1984) and were restricted to steady-state flow conditions under natural hydraulic gradients and different pumping strategies. Simulations were made both in a vertical cross-section of Zone 2 and in a horizontal plane of the zone using different outer boundary conditions.

In the vertical cross-section, pumping was simulated in the upper highly conductive part of Zone 2 under different outer boundary conditions. The idealized hydraulic conductivity distribution used for these simulations is shown in Figure 8.1. The upper part of Zone 2 was represented as a thin, high-conductivity layer. The computational domain of the horizontal plane was a 600 x 800 m rectangle, in which the right hand side coincides with the Brändan Zone (Zone 1).

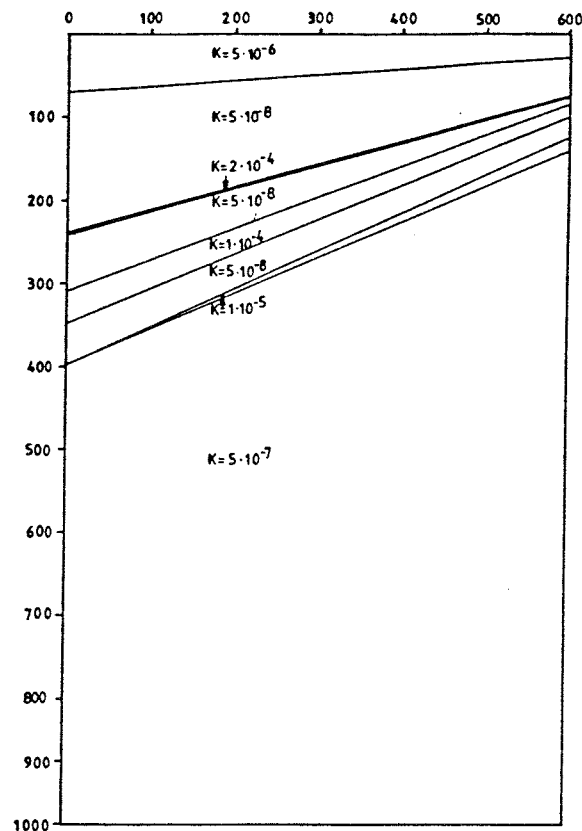


Figure 8.1 Idealized hydraulic conductivity distribution used for the simulations in the vertical cross-section. (From Andersson and Andersson, 1987).

The simulations showed that the planned tracer experiment in Zone 2 was feasible regarding transport distances and pumping rates anticipated. It was concluded that the natural groundwater flow in Zone 2 is relatively important and should be accounted for when selecting pumping boreholes and rates. The simulations in the vertical cross-section supported modelling of Zone 2 as a two-dimensional confined aquifer.

8.3 Modelling of the hydraulic interference tests

Numerical modelling to predict borehole responses and assist in the design of the planned hydraulic interference tests in Zone 2, described in Chapter 4, was performed by Nordqvist and Andersson (1987). After the interference tests, numerical flow modelling was performed to verify geological interpretations and analytical evaluation of the interference test data (Andersson et al. 1989). Both model campaigns were performed using a transient flow equation which was solved numerically by the two-dimensional finite element simulation code SUTRA (Voss, 1984).

8.3.1 Predictive modelling

The predictive modelling of the hydraulic interference tests was performed in a vertical profile, assuming radial symmetry around the pumped borehole, BFI02. The computational domain and its assumed hydraulic parameter distribution are shown in Figure 8.2, where Zone 2 is modelled as more or less permeable layers between depths of approximately 150 and 250 metres. Compared to the model domain shown in Figure 8.1, the cross-section was extended across the Brändan Zone (the interval 600-900 m in Figure 8.2). The hydraulic conductivity distribution was primarily obtained from single-hole injection tests whereas the values on the specific storativity were estimated. In addition, some model calibration was carried out based on very limited drawdown data (from borehole KFI09) from pumping during drilling of borehole BFI01. Fluid discharge was distributed along the left side boundary in Figure 8.2 in accordance with the extent of the simulated pumped section for each test. Different pumping scenarios and boundary conditions were simulated.

Predicted versus measured drawdown time series (primary responses) in observation boreholes KFI11 and HFIO1 during interference test 3B are compared in logarithmic diagrams in Figures 8.3-4. Also included are predicted responses above Zone 2, shown as solid lines without symbols. The magnitude of the total drawdowns are relatively accurately predicted only for borehole HFIO1 farthest away from the pumped borehole. At shorter distances (KFI11), predicted drawdowns are significantly higher than measured. In addition, the general shape of the predicted drawdown curves in the observation boreholes does not conform to the measured.

The first observation might be explained by the fact that the values of transmissivity within Zone 2 used for the predictive modelling were too small (c.f. Section 4.3.2). The difference

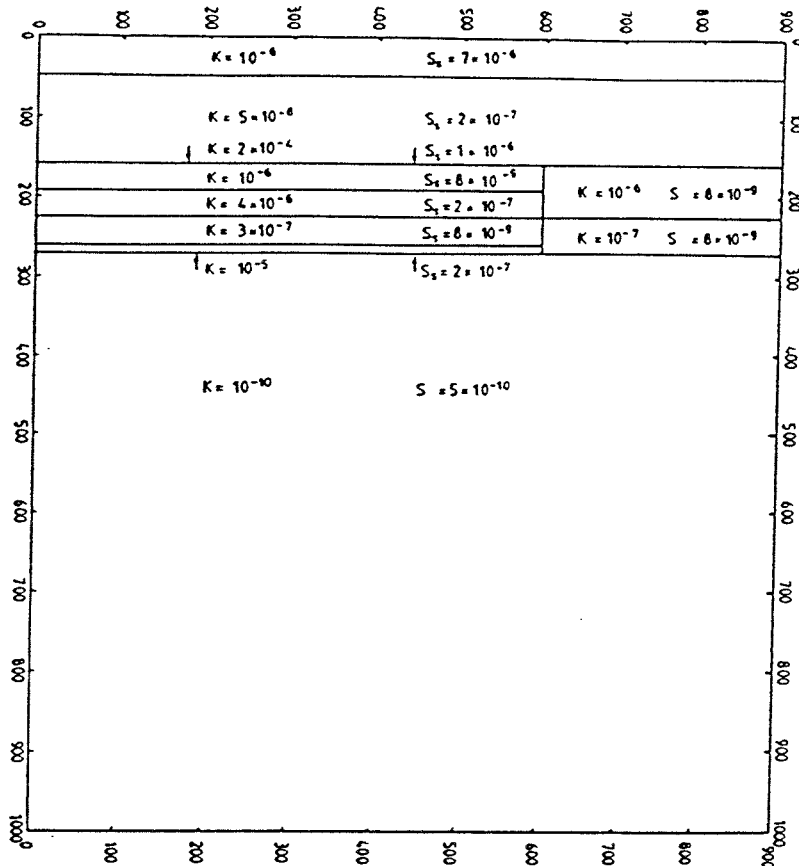


Figure 8.2 Parameter distribution used for the predictive model prior to the hydraulic interference tests. (From Nordqvist and Andersson, 1987).

in shape of the drawdown curves indicates that the physical geometry of the modelled region was not sufficiently detailed. Apparently, the hydrogeological outer boundaries of the model region are more complex than what the relatively simple model geometry accounted for.

8.3.2 Model calibration after interference tests

In order to obtain an updated and improved groundwater flow model for the Brändan area, more detailed geological features were incorporated into the model (Andersson et al., 1989). This resulted in a computational domain as shown in Figure 8.5, where Zone 2 was modelled as a sub-horizontal plane. Note that the north is directed downward in the Figures 8.5-7. Zone 2 is generally surrounded by less transmissive rock and appears as a triangular-shaped area in the middle of the figure. The two vertical fracture zones, the Brändan and Gåvastbo zones (Zone 1 and 3), were also represented as physical entities. Boundaries to Zone 2 are either no-flow or semi-permeable. It can be noted that boundary conditions for the entire computational

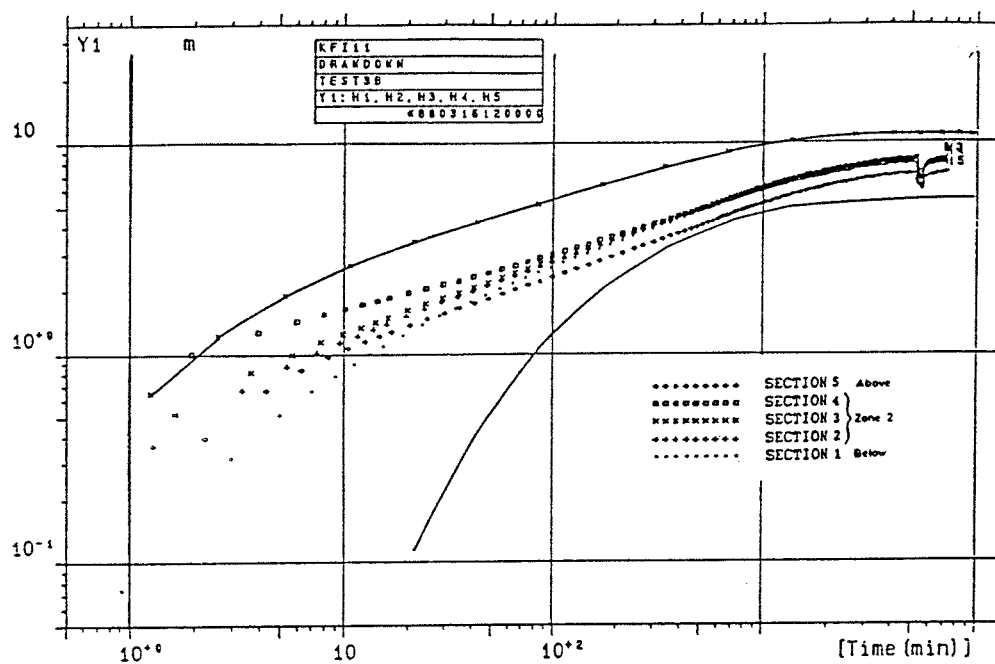


Figure 8.3 Predicted (solid lines) and measured drawdown responses in observation borehole KFI11 during interference test 3B. (From Andersson et al., 1989).

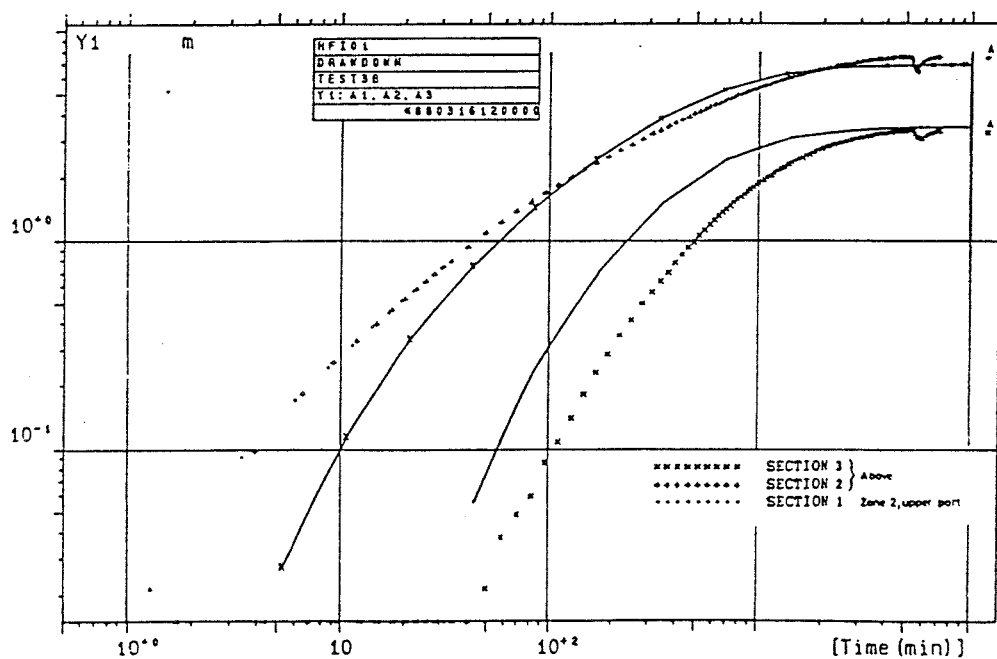


Figure 8.4 Predicted (solid lines) and measured drawdown responses in observation borehole HF101 during interference test 3B. (From Andersson et al., 1989).

domain thus were either no-flow or constant hydraulic head (Fig 8.5).

Groundwater recharge was modelled as lateral inflows to the computational domain through constant head boundaries. Thus, no areal vertical leakage from the rock mass above or below Zone 2 was considered. The entire Zone 2 was modelled, rather than separate subzones, since the results from the interference tests indicated that three-dimensional effects within Zone 2 may be important when pumping in only one of the subzones. Thus, test 3B was the test actually modelled. The hydraulic parameters for the updated model were determined by trial-and-error calibration of the numerical model, supported by analytical aquifer analyses of the hydraulic interference tests (see Section 4.3.2).

The resulting parameter distribution and the resulting computed drawdown distribution is shown in Figures 8.6 and 8.7, respectively. The transmissivity value for Zone 2 was $3 \times 10^{-3} \text{ m}^2/\text{s}$, which is significantly higher than was used in the predictive modelling. Comparison of measured and simulated drawdown curves in observation boreholes HF101 and KF111 are presented in Figures 8.8-9. For most boreholes, the simulated and measured responses were practically identical, the main exception being borehole BF101, where the simulated steady-state drawdowns were somewhat larger than measured. This can not be accurately modelled without significantly altering the geological description of the fracture zone, or introducing some local heterogeneities which may or may not be artificial. Some attempts to improve model performance by assuming a general horizontal anisotropy of the transmissivity in Zone 2 were made, but with inconclusive results (Andersson et al., 1989). Also for the other observation boreholes in the near-region, e.g. KF111, there were some differences between simulated and measured drawdowns.

It should be pointed out that the model calibration described has not been verified, i.e., tested during different hydraulic events (for example pumping in a different borehole). Thus, there is significant uncertainty as to the uniqueness of the obtained hydraulic parameters and flow geometry. An additional factor of uncertainty is that spatial data are somewhat sparse. However, the flow modelling has proven to be extremely valuable for understanding the flow conditions in the Brändan area, as well as for verification of geological and hydrogeological interpretations and for predictive modelling of the tracer tests.

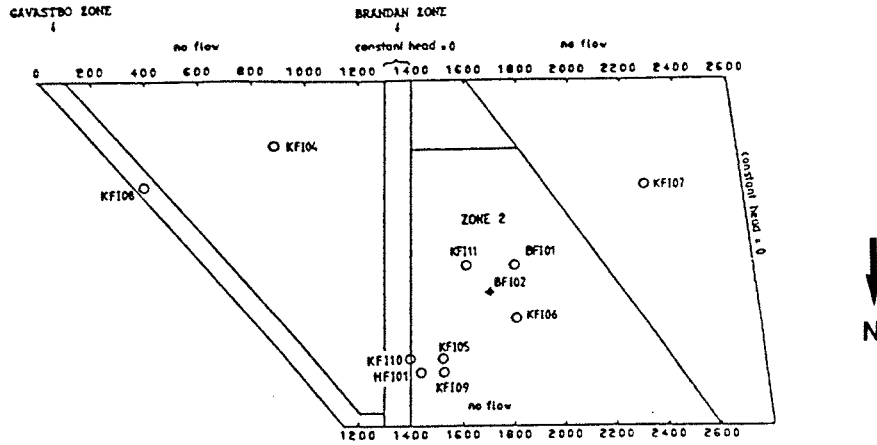


Figure 8.5 Layout and boundary conditions applied for the calibrated numerical model. Andersson et al. (1989).

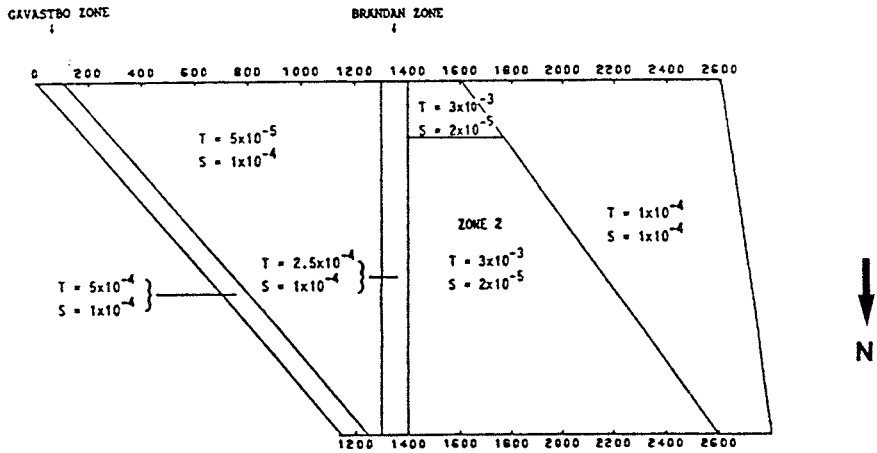


Figure 8.6 Parameter distribution used for the calibrated numerical model. From Andersson et al. (1989).

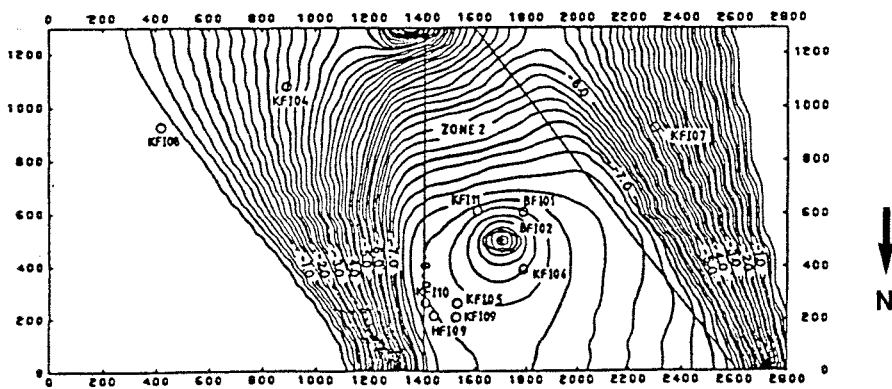


Figure 8.7 Contour map of the drawdown distribution at steady-state according to the calibrated numerical model. Equipotential = 0.20 m. Andersson et al. (1989).

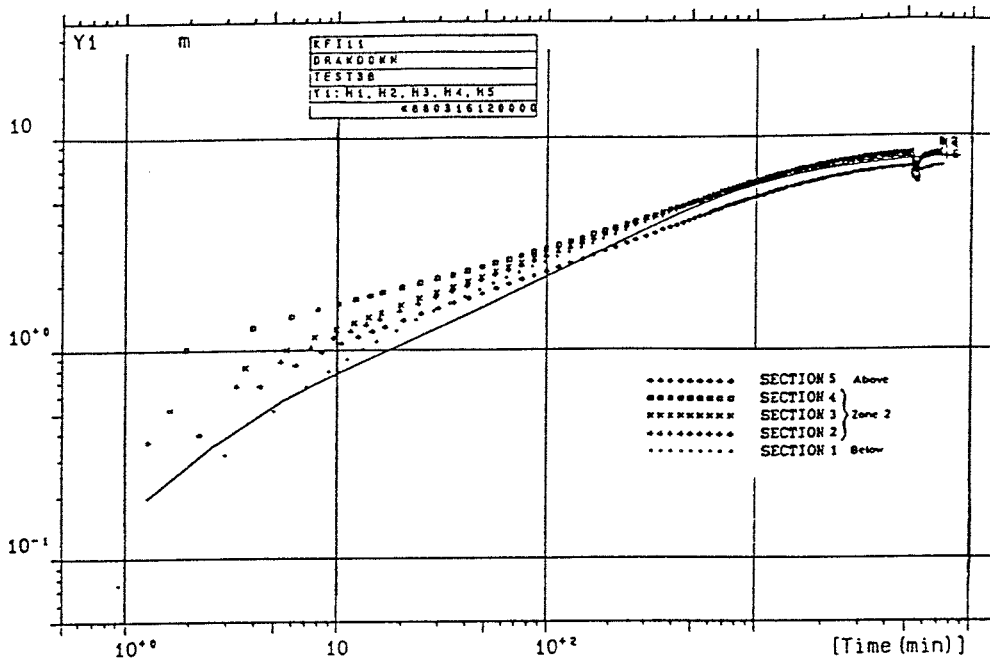


Figure 8.8 Predicted (solid line) and measured drawdown responses in observation borehole KFI11 during interference test 3B according to the calibrated numerical model. From Andersson et al. (1989).

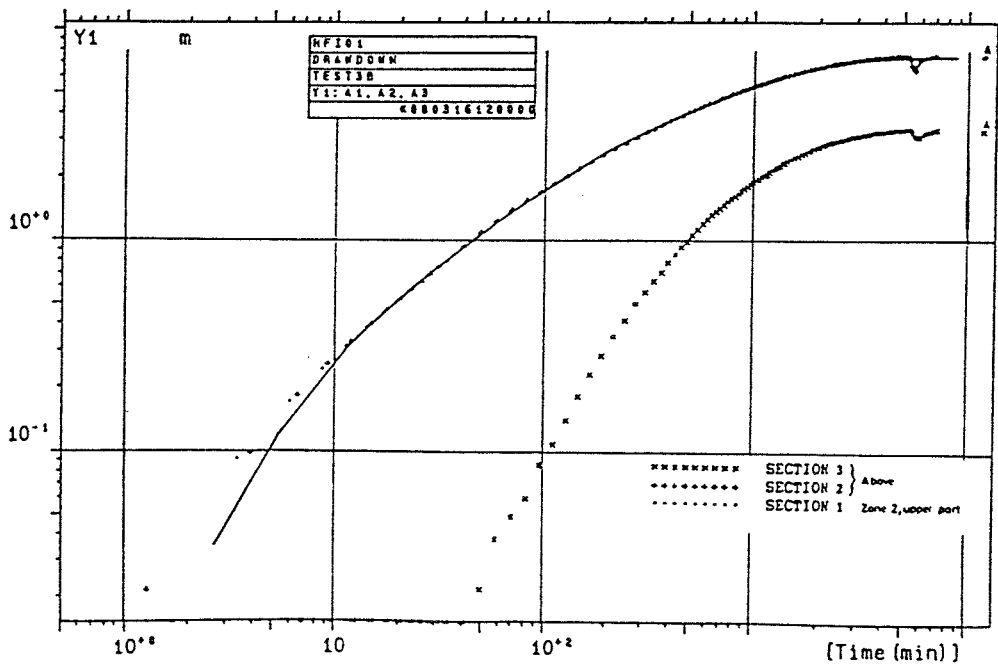


Figure 8.9 Predicted (solid line) and measured drawdown responses in observation borehole HFI01 during interference test 3B according to the calibrated numerical model. From Andersson et al. (1989).

8.4 Modelling of radially converging tracer test

The results of the radially converging tracer test at Finnsjön are presented in Section 5.2. Predictive modelling of this test was performed by Gustafsson et al. (1989). Assessment of the model performance and comparisons between predicted and tracer breakthrough curves are presented in Gustafsson et al. (1989). In both cases, the flow and transport equations were solved numerically by the two-dimensional finite element code SUTRA (Voss, 1984).

8.4.1. Predictive modelling

In the first step of predicting the transport of the tracers, the updated and calibrated groundwater flow model used to simulate the hydraulic interference test responses, described in the previous section, was used. Additional information needed in order to predict solute transport in separate subzones consists of hydraulic conductivities, flow porosities, longitudinal and transverse dispersivities and geometry of tracer injection. Of these parameters, only hydraulic conductivities could be estimated a priori with some confidence, based on measurements from single-hole injection tests. Very little was known about porosities and dispersivities. A porosity value of $3.0E-04$, obtained from Ahlbom et al., (1986) was used. Assigned dispersivities were somewhat arbitrary. The predictions were divided into two "extreme cases". One assuming a high hydraulic conductivity and one with a low hydraulic conductivity. The parameters shown in Table 8.2 were used.

Table 8.2 Parameter values used in prediction of the radially converging tracer test at Finnsjön. After Gustafsson et al. (1989).

Hydraulic unit	K (m/s)	\emptyset (-)	α_L (m)	α_T (m)
High-conductivity zones	3.5E-3	3E-4	10.0	3.0
Low-conductivity zones	7.0E-5	3E-4	10.0	3.0

In Table 8.2, K denotes hydraulic conductivity, \emptyset porosity, α_L and α_T transverse and longitudinal dispersivity, respectively. The actual breakthrough curves were obtained by scaling the simulated observations at the point of observation (BF102) according to some assumptions about the dilution effects in the sampling sections. In this case, a flux-averaging of sample concentration was assumed, with fluxes assigned according to the assumed transmissivities for each layer.

8.4.2 Comparison between predicted and observed results

By comparing predicted and observed results it is important that both hydraulic gradients and breakthrough curves are

predicted satisfactorily. Table 8.3 summarizes measured hydraulic head differences (prior to the detailed sampling) between the injection intervals and the pumping interval together with the predicted head differences. The measured values were estimated from time series of head differences calculated from manually levelled (generally once a day) hydraulic heads.

Table 8.3 Comparison of measured and predicted head differences in the injection intervals. From Gustafsson et al. (1989).

Borehole	Section	Hydraulic head difference (m)		
		Measured	Average	Predicted
KFI06	Lower	0.62	0.62	0.42
	Middle	0.64		
	Upper	0.59		
KFI11	Lower	0.81	0.77	0.47
	Middle	0.74		
	Upper	0.77		
BFI01	Lower	1.14	1.27	0.46
	Middle	1.25		
	Upper	1.41		

Table 8.3 again confirms that the present groundwater flow model does not explain hydraulic heads in borehole BFI01. For boreholes KFI06 and KFI11 the agreement was significantly better, although also here a certain discrepancy can be noted.

Table 8.4 presents a comparison between measured and predicted first arrival times, as obtained for the measured and predicted breakthrough curves. In general, the middle section is considered to be part of a low conductivity zone, while the upper and lower are considered to be located in high conductivity zones. Regarding the predicted first arrival times, the high conductivity zones are considered more accurate with respect to the actual hydraulic conductivities given as input. Table 8.4 shows that the predicted arrival times are significantly underestimated for all sections.

The steady state concentrations for tracers injected in the different injection sections, as well as actual measured values are compared to predicted concentrations in Table 8.5. The table shows that predicted steady-state concentrations, as sampled in BFI02, are significantly overestimated. An assessment of the overall model performance in predicting flow and tracer transport is given in Gustafsson et al. (1989).

Table 8.4 Comparison of measured and predicted first arrival times (t hours). From Gustafsson et al.(1989).

Borehole	Section	Measured t	Predicted t
KFI06	Lower	194	1
	Middle	1250-1350	50
	Upper	106	1
KFI11	Lower	3600	1
	Middle	850	50
	Upper	24	1
BFI01	Lower	1250	1
	Middle	700	50
	Upper	75	1

Table 8.5 Comparison of calculated, measured and predicted steady-state tracer concentrations (C ppb). From Gustafsson et al. (1989).

Borehole	Section	Calculated C	Measured C	Predicted C
KFI06	Lower	4.2-5.1	4.5	85
	Middle	54-71	4.5	1144
	Upper	NA	NA	NA
KFI11	Lower	56-58	NS	8360
	Middle	16-31	NS	750
	Upper	47	45	178
BFI01	Lower	68-70	NS	9670
	Middle	127-154	NS	979
	Upper	19	12-18	36

NA = Not Applicable

NS = No Steady state reached

9. CONCEPTUAL MODEL OF THE FINNSJÖN AREA

9.1 General

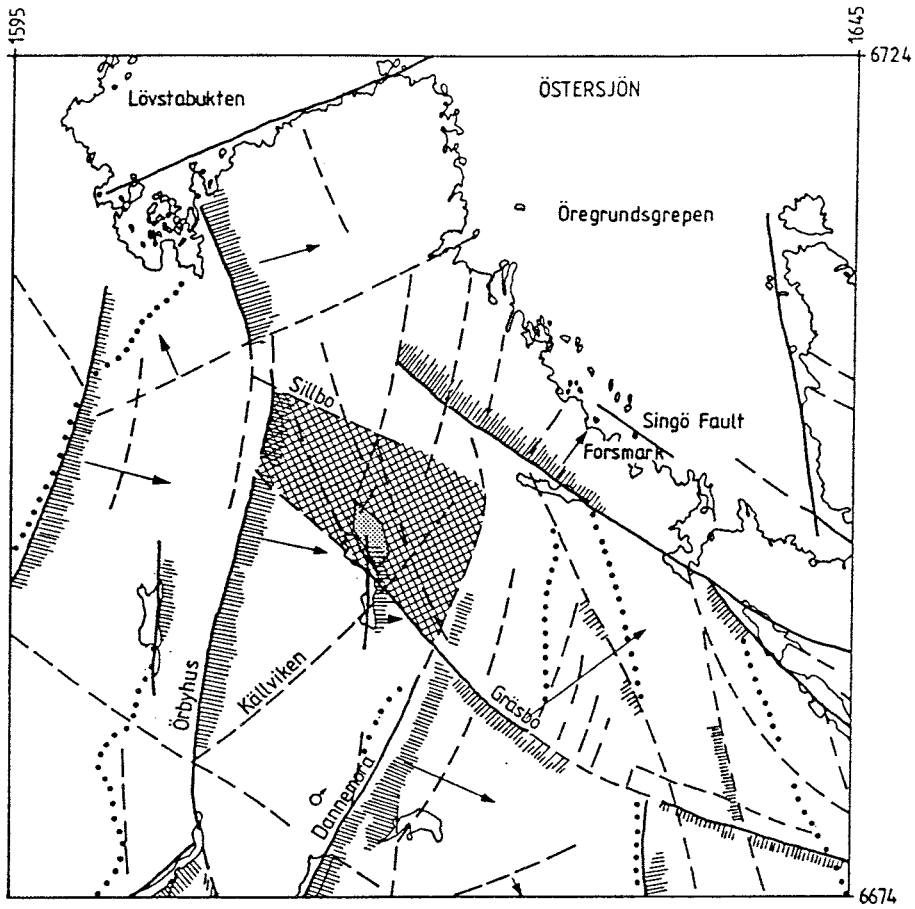
In this chapter conceptual models of the hydrogeological conditions on different scales in the Finnsjön area are presented. Based on the conceptual models the appropriate model code(s) should be selected to meet the specific conditions in the Finnsjön area and to fulfil the stated objectives of the modelling. It is intended that the information supplied in this report will provide a sufficient basis for a variety of models to be used in the synthesis. As a first step in the modelling, specific model lay-outs should be established for each type, e.g. 2D and 3D continuum models, discrete fracture network models etc. This chapter is mainly focussed on continuum models.

9.2 Modelling strategy

The basic concept is to perform modelling on different scales in successively smaller areas. The ultimate goals of the modelling are to investigate the groundwater and transport conditions in the vicinity of the hypothetical repository. The models increase in detail with decreasing areal coverage. Modelling a very large area may be too generalized and provide little information on the conditions of the area of special interest. Therefore, it is suggested that the first model effort should include an area of a size comparable to the semi-regional area defined by Ahlbom and Tirén (1989, 1991) shown in Figure 1.3. On this scale of modelling only major hydraulic units should be included, i.e. regional fracture zones and rock mass. One of the objectives of the (semi)-regional modelling is to obtain appropriate boundary conditions for the more detailed models. The semi-regional area proposed for modelling is shown in Figure 9.1.

The next phase involves modelling of the local area on a block scale, i.e. the Finnsjön Rock Block, defined by Ahlbom and Tirén (1989, 1991), see Figure 9.2. In the local model, the local fracture zones should also be included.

Finally, detailed modelling of specific areas of the repository and adjoining parts will also be required. In the detailed modelling, all available information on all scales should be included. The local model will provide appropriate boundary conditions to the detailed model(s).



LINEAMENT MAP, NORTHEASTERN UPPLAND

REGIONAL AREA

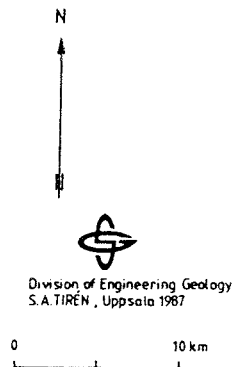
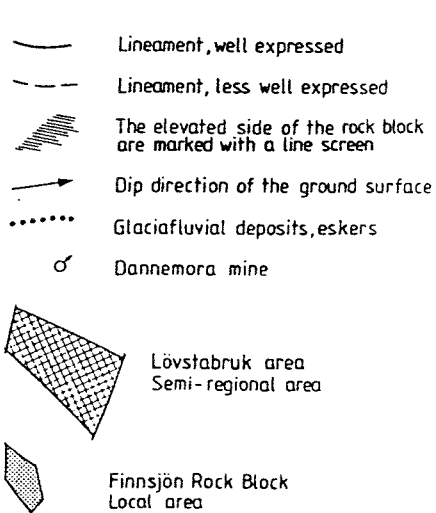
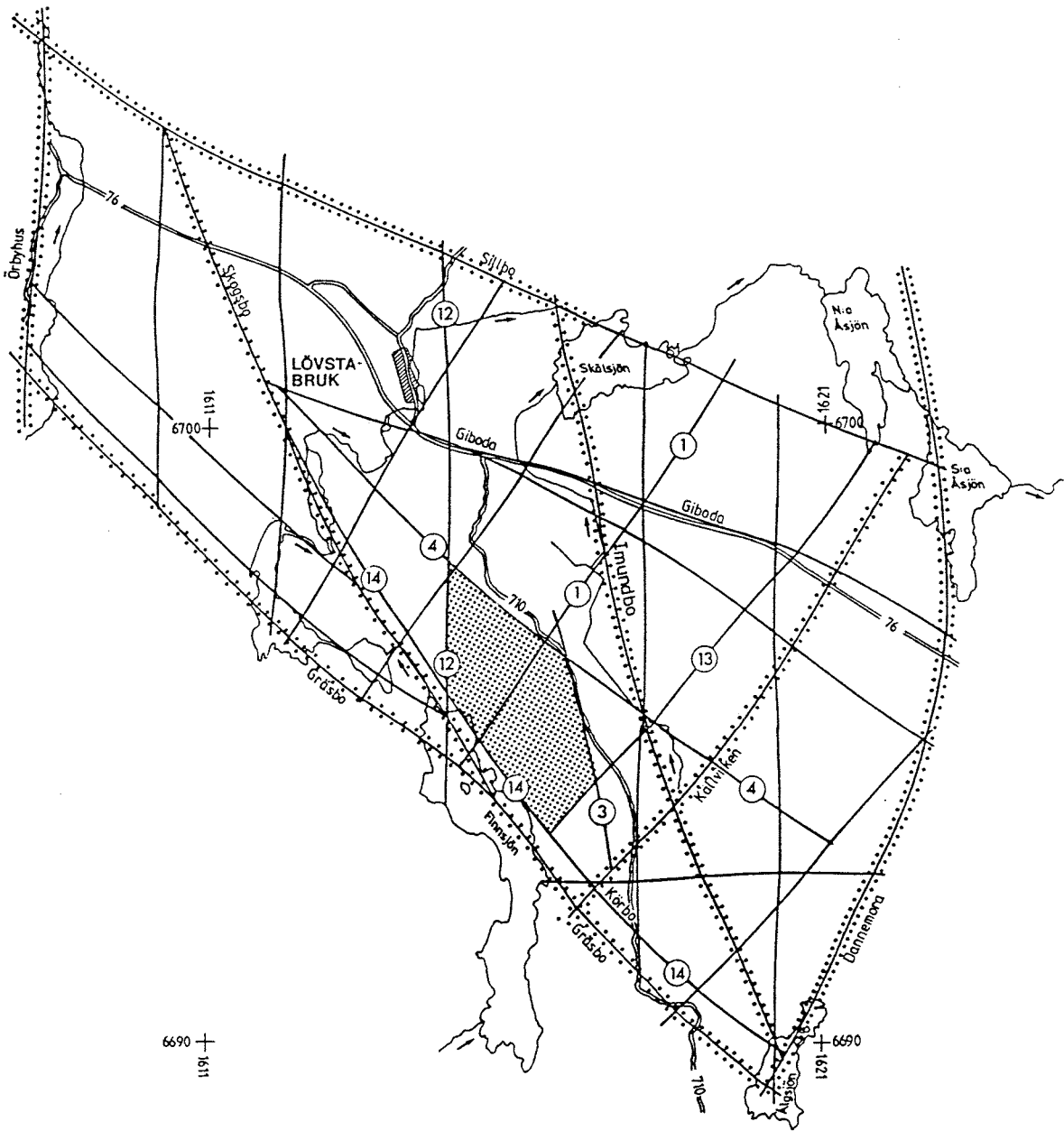
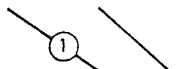
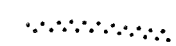
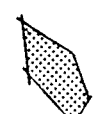


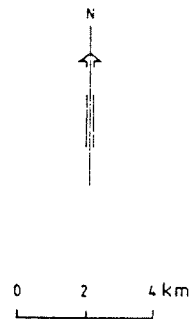
Figure 9.1 Lineament map showing the suggested delimitations of the semi-regional and local model area.



SIMPLIFIED ROCK BLOCK MAP, LÖVSTABRUK AREA

-  Fracture zones
-  Position of lineaments interpreted on regional scale
-  Finnsjön Rock Block

The glacial striation is north-south




 SWEDISH GEOLOGICAL CO
DIVISION OF ENGINEERING
GEOLOGY, Uppsala 1989
S. A. Tirén

Figure 9.2 Rock Block map of the proposed semi-regional model (Löfstabruk area) including the Finnsjön Rock Block (rastered).

9.3 Semi-regional model

The semi-regional model should preferably be delimited by major, well expressed lineaments. The suggested delimitations of the semi-regional model (Lövstabruk area) all constitute major lineaments. This area is part of a major shear lense (Ahlbom and Tirén, 1989, 1991), see Figure 9.1 and 9.2. The assumed orientation and order of the lineaments outside the Finnsjön Rock Block is presented in Table 9.1.

Table 9.1 Assumed orientations and order of the lineaments outside the Finnsjön Rock Block.

Lineament	Orientation strike	dip	Order of lineament	Limits semi- regional area in
Sillbo	N65W	90	Reg./Semireg.	North
Giboda	N60W	90	Semiregional	
Gräsbo	N40W	90	Regional	South
Skogsbo	N30W	90	Regional	
Källviken	N40E	75-90SE	Regional	
Dannemora	N25E	90	Regional	East
Imundbo	N15W	90	Regional	
Örbyhus	N-S	90	Regional	West

The size of the Lövstabruk area is in the order of 100 km². A prerequisite regarding the size of the semi-regional model area is that the groundwater recharge within the area must exceed the estimated natural groundwater flow within Zone 2, see Section 5.4.2. Assuming a recharge rate of 10 mm/year (which is considered as a conservative estimate) and the same proportions between recharge and discharge areas (70% and 30% respectively) as reported by Carlsson and Gidlund (1983) for northern Uppland (Section 2.4), the groundwater recharge within the Lövstabruk area may be estimated to about 700 000 m³/year. This flow rate is higher than the maximal estimate of the groundwater flow within Zone 2 presented in Section 5.4.2.

Considering the small area constituted by Zone 2 (see Appendix 5) in comparison to the Lövstabruk area, areal recharge may not entirely account for the estimated flow in Zone 2. Other sources of recharge to Zone 2 are possible. During the hydraulic interference tests (e.g. test 2) approximate steady-state conditions occurred by the end of the tests, indicating a major source of recharge to the zone (Section 4.3.2). As discussed by Andersson et al. (1989), Zone 2 may be in hydraulic contact with Lake Finnsjön, possibly via other fracture zones. During long-term pumping in conjunction with the radially converging tracer test (Gustafsson et al., 1989) the electric conductivity of the discharged water was decreasing successively, indicating recharge from a major source of fresh water, possibly Lake Finnsjön.

The groundwater flow across the delimiting major lineaments of the semi-regional area (Table 9.1) is likely to be rather small. However, significant groundwater flow is assumed to occur along the lineaments. The semi-regional area should include the regional fracture zones, delimiting the Finnsjön Rock Block together with the numbered fracture zones outside this Block, see Figure 9.2.

No borehole information is available from the lineaments constituting the outer boundaries of the semi-regional model area. The hydraulic properties of one (Zone 3) of the regional fracture zones in the Finnsjön area, estimated from available hydraulic test data, are described in Section 4.3.1, see Table 9.2.

For regional fracture zones from which no borehole information is available, the hydraulic properties of regional zones with similar genesis in adjacent areas, e.g. the Singö Fault, should be used. Hydraulic properties of the upper part of the Singö Fault used in the modelling of SFR (Carlsson et al., 1987) are also included in Table 9.2. The average hydraulic conductivity of the Singö Zone was estimated at $8E-7$ m/s in the regional conceptual model of SFR and in the local conceptual model ranging from $5E-7$ m/s to $5E-6$ m/s in different parts of the zone. In the regional modelling an effective hydraulic conductivity of $1E-5$ m/s was assigned to the Singö and Forsmark zones.

Fracture zones with a preferred orientation of about N30W are found in the Forsmark region (Carlsson et al., 1987). Pumping tests in the surficial part of one of these zones indicated a transmissivity of $5E-4$ m²/s (Andersson and Olsson, 1978). In the Finnsjön area these zones are associated with splays connected to the Gräsbo lineament.

The NW-striking major fracture zones (Gräsbo, Skogsbo, Imundbo, Giboda, Sillbo and Zones 4 and 14) constitute very old shear zones which are part of a major structural unit to which also the Singö Fault is related. As a first approximation, the same hydraulic properties as of the latter zone could be assigned to the Gräsbo and Sillbo lineaments and Zone 14. The remainder of the NW-striking zones could be expected to have similar hydraulic properties as those of Zone 5 (Table 9.3).

The NE-striking major zones (Örbyhus, Dannemora, Källviken and Zone 13) constitute younger, brittle shear zones. The magnitude of the first two zones are at least as the Singö Fault and their hydraulic properties can thus be expected to be in the same order as of the latter zone or higher. The hydraulic properties of the Källviken lineament and Zone 13 can be expected to be similar to those of Zone 1. The N-S and E-W striking major fracture zones (Zone 12 and the other non-named zones in Figure 9.2) constitute young tension zones. The hydraulic properties of these zones are unknown.

Too few data from regional fracture zones exist to establish the variation of the hydraulic parameters in the vertical and lateral directions of the zones. As a first approximation, the

same depth-dependence as determined for the rock mass may be used for the regional zones, see Section 4.4. The total widths of the lineaments delimiting the semi-regional model area may be estimated to 100-200 m and of the zones delimiting the Finnsjön Rock Block to 20-100 m.

Table 9.2 Estimated transmissivity (T) and average hydraulic conductivity (K) and width of regional fracture zones.

Fracture zone	Vertical depth (m)	Width (m)	Inclin. (degrees)	T (m^2/s)	K (m/s)
3	30-120	50	80SW	1-5E-4	1-10E-6
Singö	Upper 100 m	120	90	1-5E-4	1-10E-6

The hydraulic conductivity of the rock mass may be expressed by the depth-relationships described in section 4.4 for the different parts of the Finnsjön Rock Block. The relationship derived from the southern part of the Block, which is assumed to be more representative due to the absence of Zone 2 in this part, may be used as a general expression of the hydraulic conductivity of the rock mass in the semi-regional model.

The sensitivity of the boundary conditions calculated from the semi-regional model, to be used in the local modelling, should be tested by also including Zone 2 (and possibly also Zone 1) in the semi-regional model as a specific hydraulic unit. If the boundary conditions turn out to be sensitive to the presence of Zone 2 (and Zone 1), this zone must be incorporated in the semi-regional model.

9.4 Local and detailed models

The local model area may be defined as the Finnsjön Rock Block. The major lineaments surrounding this area are suggested as potential outer boundaries for the local model (Fig. 9.2). The Finnsjön Rock Block has an area of 5.6 km² (Ahlbom and Tirén, 1989). As can be seen from Figure 9.2 the Finnsjön Rock Block is delimited by fracture Zone 3 (Gåvastbo zone) and Zone 4 in northeast and north, Zone 12 (Bredmossen) and 14 (Körbo) in west and southwest and by Zone 13 (Gruvskogen) in southeast. A generalized map of fracture zones in the Finnsjön Rock Block is shown in Figure 9.3.

The Finnsjön Rock Block is intersected by several fracture zones, e.g. Zone 1 (Brändan Zone) and Zone 2. In addition, several other internal fracture zones have been defined in the local scale, i.e. Zones 5 - 11, see Figure 9.3. All these zones

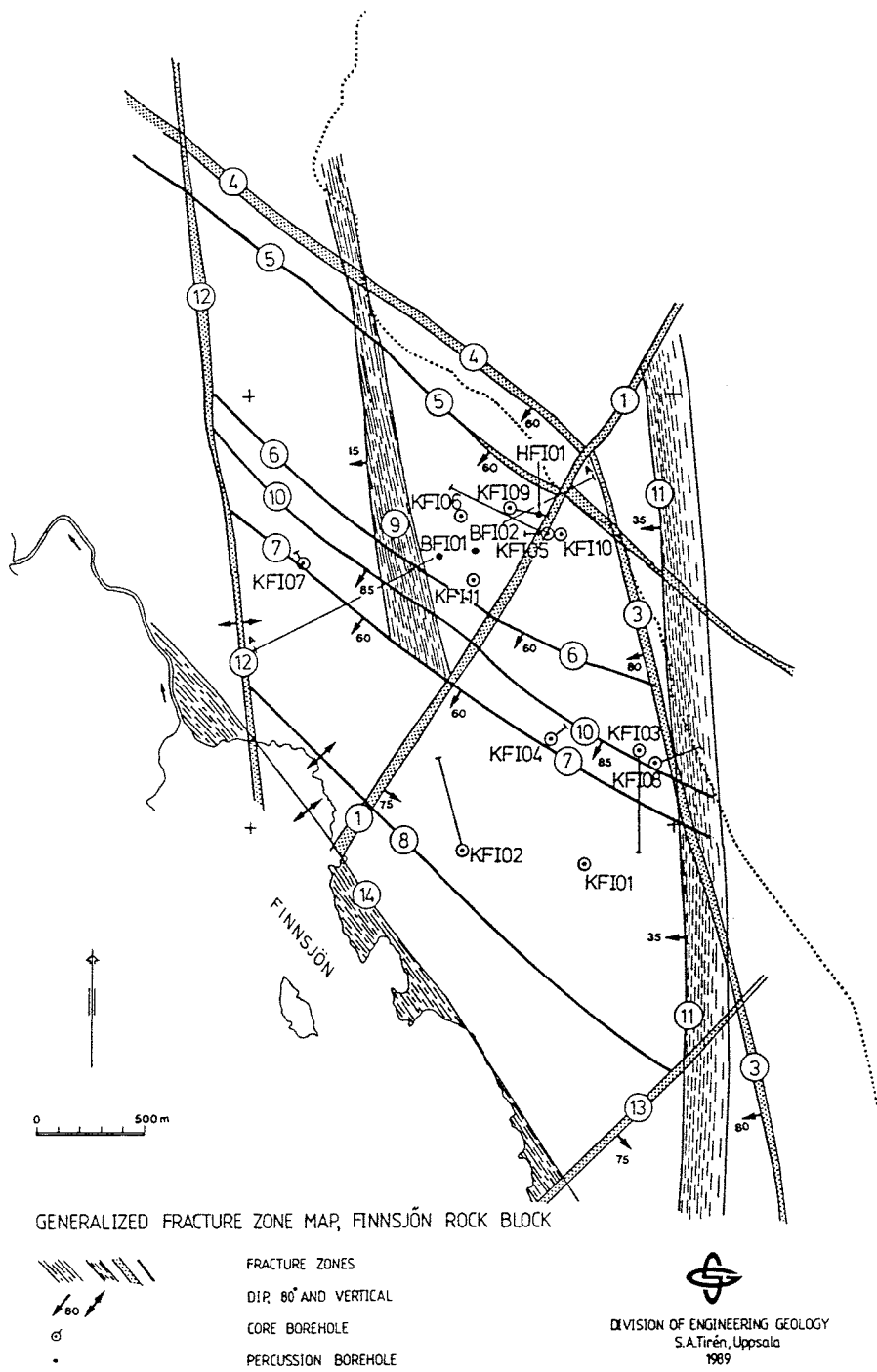


Figure 9.3 Generalized fracture zone map of the Finnsjön Rock Block. From Ahlbom and Tirén (1991).

constitute ductile shear zones. The regional modelling should provide appropriate boundary conditions of the delimiting fracture zones of the Finnsjön Rock Block in the local model. Only a few data of the hydraulic properties of these zones are available, see Table 9.2. The hydraulic properties of the local fracture zones within the Finnsjön Rock Block, estimated from available hydraulic test data, are presented in Table 4.4. A summary is presented in Table 9.3 together with interpreted geometrical properties of the zones according to Ahlbom and Tirén (1991). The hydraulic properties of Zones 7 and 8, from which no borehole information is available, can be estimated as an average of the properties of Zones 5, 6 and 10.

Table 9.3 Estimated transmissivity (T) and average hydraulic conductivity (K) of local fracture zones at different depths (m.b.g.l.) together with estimated gross width/thickness of the zones.

Fracture zone	Vertical depth(m)	Width (m)	Inclin. (degrees)	T (m ² /s)	K (m/s)
1	55-75	20	75SE	1-5E-4	5-25E-6
2	100-300	100	16SW	2-4E-3	2-4E-5
5	170-180	5	60SW	5-15E-5	5-50E-6
	320-350			1-2E-5	1-5E-6
	550-560			1-2E-6	1-5E-7
6	515-520	5	60SW	1-5E-8	1-10E-9
9	105-160	50	15SW	1-5E-6	1-10E-8
10	45-48	5	85SW	1-5E-8	1-10E-9
11	16-120	100	35SW	1-5E-4	1-5E-6
	82-174			5-10E-4	5-10E-6
	364-394			1-5E-4	1-5E-6
	364-436			5-10E-7	5-10E-9

As stated above, the widths of the fracture zones delimiting the Finnsjön Rock Block may be estimated to 20-100 m. The widths of the relatively steep, local fracture zones within the Rock Block striking in northwest, i.e. Zones 5, 6, 7, 8 and 10 are assumed to be in the order of 5 m. The thicknesses of the subhorizontal Zones 9 and 11 are in the order of 50 and 100 m, respectively. Since Zones 1 and 2 are considered of special importance in the local modelling, they are described separately in the next two sections. The sensitivity of the extension of Zone 2 in the subhorizontal direction should be tested in the local model, see Section 9.6.

The statistical analyses in Section 4.4 indicate that there are differences in the hydraulic conductivity distributions of the rock mass in the southern and northern parts of the Finnsjön Rock Block, particularly in the interval below 200 m, i.e. below Zone 2. Therefore, the sensitivity of using different conductivity distributions in the southern and northern part of the Block in the local model, according to Eqns.(4.2-3), should be tested. The sensitivity of using alternative statistical representations of the hydraulic conductivity distributions, e.g. step functions, should also be assessed.

As the final step in the modelling, detailed models of the hypothetical repository area and surroundings are required to achieve the ultimate goals, i.e. to calculate the groundwater flow and transport times at the repository depth. The detailed modelling should take all information available and the results of the previous modelling efforts on larger scales into account.

On the detailed scale, stochastic modelling may be used and based on the introductory geostatistical analyses presented in Section 4.5. In this process, these analyses must be extended to also include the horizontal correlation properties of the rock together with regularization of hydraulic conductivity data as suggested by Neuman (1988). The geostatistical analysis should be focussed on the rock below Zone 2, i.e. on the rock between the hypothetical repository and the zone.

9.5 Hydraulic properties of Zone 1

The modelling of the steeply dipping Zone 1 and the sub-subhorizontal Zone 2 is regarded of special importance in the local model. Concerning Zone 1, some debate exists about its hydraulic properties. The fact that saline groundwater only has been found in the northern part of the Finnsjön Rock Block (except in borehole KFI08) may be interpreted as Zone 1 being rather tight (perpendicular to the zone). On the other hand, the hydraulic interference tests in Zone 2 showed that drawdown responses occurred across Zone 1 in open boreholes in the southern part of the Block, indicating a certain hydraulic interaction between the two parts of the Block (Andersson et al., 1989). This may seem contradictory but may be explained as follows.

The drawdown responses in the boreholes in the southern part of the Finnsjön Rock Block occurred after long times of pumping during the interference tests. For example, the drawdown response in the observation borehole KFI04 during interference test 2 occurred after about 1500 minutes (25 hours) after start of pumping (Andersson et al, 1989, Appendix 7.2). This is much later than would be expected if the response between the pumping borehole BFI02 and borehole KFI04 had occurred along a deep high-conductivity fracture zone between the boreholes. For example, if Zone 2 is assumed to continue across Zone 1 into the southern part of the Block and the response were propagated directly along this zone, the response in KFI04 would have

occured at about 0.5-1 hour after start of pumping, assuming constant hydraulic properties of Zone 2.

This indicates that the responses across Zone 1 are indirect and probably transmitted along surficial parts of the bedrock. This is also supported by the observed (small) response in the shallow percussion borehole HGB02 (Andersson et al., 1989, Appendix 7:3), see Fig. 1.1, indicating surficial hydraulic communication between the two parts of the Finnsjön Rock Block. This assumption is further supported by the fact that significant drawdowns of the groundwater level (above the uppermost packer) occurred in most of the observation boreholes within the Brändan area during the interference tests (Andersson et al., 1989, Appendix 6). Thus, it is concluded that the responses across Zone 1 most likely occurred along surficial parts of the bedrock. At greater depths, little hydraulic communication across Zone 1 is likely to occur. This may possibly explain the different salinities observed in boreholes in the two parts of the Finnsjön Rock Block, see Section 9.7.

The hydraulic interference tests also indicated that Zone 2 is surrounded by outer (barrier) boundaries. Such effects will occur if the contrast in transmissivity between the aquifer and the surrounding rock (or fracture zones) is about one order of magnitude or higher (Fenske, 1984). By the numerical simulation of the interference tests a transmissivity of $2.5 \text{ E-}4 \text{ m}^2/\text{s}$ was assigned to Zone 1, i.e. about one order of magnitude lower than that for Zone 2, and $5 \text{ E-}5 \text{ m}^2/\text{s}$ to the bedrock in the southern part of the Finnsjön Rock Block (Fig. 8.6). Using these transmissivity values, the measured drawdown responses in most observation boreholes within Zone 2 could be reasonable reproduced by the model. This shows that Zone 1 need not be tight (perpendicular to the zone) to act as a hydraulic (barrier) boundary to groundwater flow across the zone at some depth.

9.6 Modelling of Zone 2

The interpreted extension of Zone 2 in the subhorizontal direction is shown in the CAD-projection of the zone from above in Appendix 5. The maximal extension of Zone 2 is considered to be defined by the area delimited by Zones 1, 4, 12 and 14 extending to Lake Finnsjön. Fracture Zone 2 should be modelled as a separate hydraulic unit in the local model. By the analytical interpretation of the hydraulic interference tests, Zone 2 was represented by a leaky aquifer system (Section 4.3.2). This turned out to be a satisfactory representation in the near-region around the pumping borehole. However, in the distant-region, Zone 2 almost behaved as an equivalent single hydraulic unit with averaged hydraulic properties although slight effects of vertical anisotropy were observed. This indicates that hydraulic interaction in the vertical direction of the zone is significant. This is also supported by the radially converging tracer test (Section 5.2).

Since the local modelling preferably should represent the natural (long-term) groundwater conditions, average hydraulic properties of the zone should be used, i.e. the properties determined from the distant-region boreholes. In the local model, Zone 2 may therefore be represented as a single, vertically anisotropic aquifer unit with a transmissivity of $3E-3 \text{ m}^2/\text{s}$ in the subhorizontal direction and a storativity of $2E-5$. These values of the hydraulic parameters of Zone 2 were used by the final simulation of the hydraulic interference tests (Section 8.3.2).

As an initial estimate of the average hydraulic conductivity in the vertical direction of the zone, the values calculated from the interference tests may be used, i.e. $K_z = 1-5E-6 \text{ m/s}$. This value represents the hydraulic properties of an equivalent porous confining layer. To account for the fractured nature of Zone 2 with possible high-conductivity interconnections in the subvertical direction of the zone, this value probably must be significantly altered locally. Alternatively, the average (equivalent) value of the vertical hydraulic conductivity of the zone should be altered. However, with this representation of Zone 2, a perfect agreement between simulated and measured responses in the observation boreholes used during the interference tests cannot be expected, particularly not for the near-region observation boreholes, due to local heterogeneities in this region (Section 4.3.2).

A possible modification of the modelling of Zone 2 would be to treat the uppermost part of the zone as a separate, high-transmissivity aquifer unit with uniform hydraulic properties and the remainder of the zone as another aquifer unit with hydraulic anisotropy in the vertical direction. Such an approach seems to be justified regarding the results of the hydraulic interference tests and tracer tests.

Furthermore, as pointed out by Ahlbom and Tirén (1989), Zone 2 is probably faulted in the area between boreholes BFI01 and KFI07 (see Appendix 5). The hydraulic interference tests (and tracer tests) also indicate a possible fault between boreholes BFI01 and BFI02 (Sections 4.3.2 and 5.2). The latter, assumed, fault is however not likely to affect the long-term hydraulic conditions within the zone.

9.7 Tentative model of groundwater circulation at Finnsjön

A possible explanation of the different salinities observed from groundwater in the southern and northern parts of the Finnsjön Rock Block is presented here. The theory is based on the groundwater conditions at greater depths. If the differences of hydraulic conductivity of the rock mass, calculated for the northern and southern parts in Section 4.4, are assumed to be significant, this may have implications on the groundwater circulating system at depth.

In Section 4.4 it was indicated that the hydraulic conductivity of the rock mass is higher in the northern part (where Zone 2

is present) than in the southern part, particularly at deeper parts, i.e. 500-600 m. This may possibly indicate that deeper, saline groundwater can migrate upward towards Zone 2 where it is flushed away in the uppermost, highly conductive part by the natural groundwater flow in the zone. Possibly, this circulating process of groundwater would be initiated and maintained by the groundwater flow in Zone 2.

Figure 9.4 shows a tentative model of groundwater flow in Zone 2 and adjacent rock. The above interpretation is also supported by tracer tests and hydrochemical investigations (Section 6.1.3). The hydraulic interference tests also showed that deep saline water below Zone 2 was rapidly transmitted upward to the upper parts of the zone during pumping (Section 6.2). The piezometric borehole measurements discussed in Section 3.2 also seem to support this theory. In most boreholes in the northern part of the Block, the estimated potential gradient below Zone 2 is directed upward as was also pointed out in Ahlbom et al. (1988). However, the piezometric measurements also showed that the potential gradients below Zone 2 are very small, indicating a slow migration of groundwater flow to Zone 2 from below under natural conditions.

In this process, Zone 1 may then act as a hydraulic barrier between the two parts of the Finnsjön Rock Block (as discussed above) to prevent saline water to penetrate across Zone 1. However, saline water may also be present in the southern part of the Block at depths greater than penetrated by boreholes. Although somewhat uncertain, the piezometric borehole measurements also indicated that the natural potential gradient in the horizontal direction of Zone 2 is directed towards Zone 1, which may act as a drain of groundwater from Zone 2 in the lateral direction. The natural groundwater flow in Zone 2 and adjacent parts is discussed in Section 5.4.2.

The saline groundwater flow conditions in the northern and southern parts of the Finnsjön Rock Block are discussed in more detail by Ahlbom and Tirén (1991).

9.8 Available data for model calibration and validation

Firstly, the local model can be calibrated against the estimated pressure differences along the boreholes, presented in Appendix 3. The local model should also reasonably describe the transient groundwater flow conditions within the Finnsjön Rock Block. To validate the model, the measured time series of head changes (drawdown/recovery) during the hydraulic interference tests (in particular test 3B) should be reasonably reproduced by the model. Data files have been prepared on diskettes with drawdown/recovery data versus time during interference test 3B (entire Zone 2 pumped).

In addition, the groundwater flow in Zone 2 under natural conditions (magnitude and vertical distribution within the zone) as determined from the dilution tests (Section 5.4.2), should be accurately modelled. This may require a model taking

the variations of the groundwater salinity into account. Finally, the last validation criterium may be to simulate the measured changes of the electric conductivity of the discharged water during the interference tests, shown in Appendix 8:5.

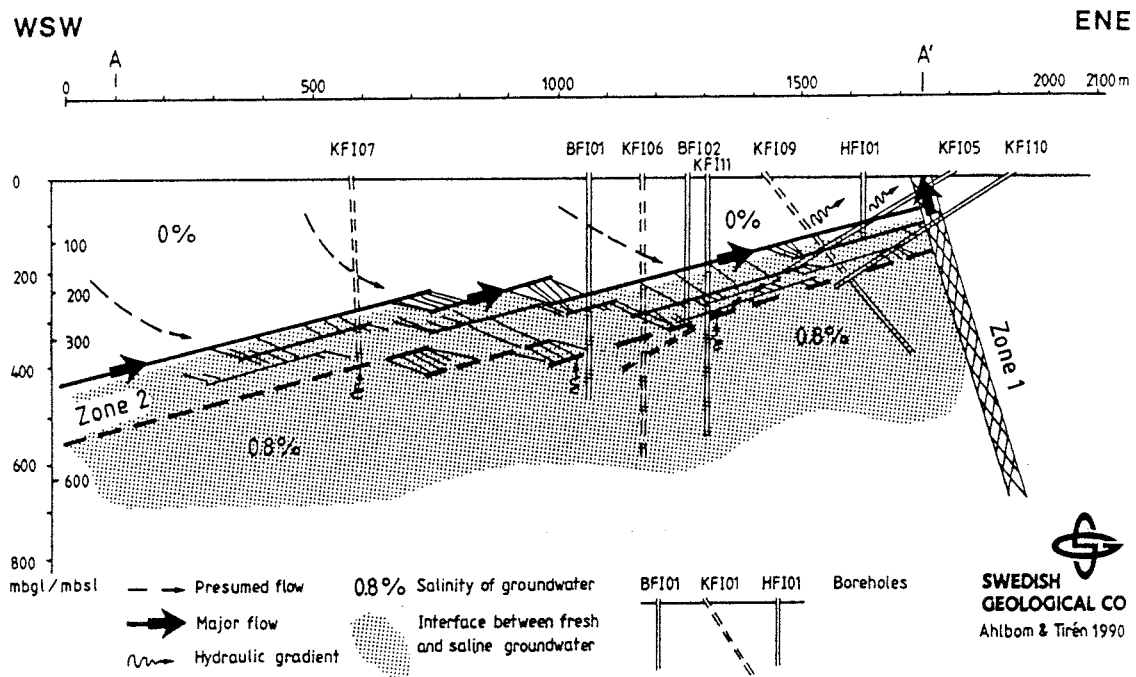


Figure 9.4 Tentative model of groundwater flow in Zone 2 and adjacent rock at Finnsjön.

10. DATA SUMMARY

In this Chapter, a summary of data available from the different tests is compiled. References are given to the appropriate sections in the report and in the Appendices. The actual storage of the data is also described. A compilation of investigations in the Finnsjön area during the period 1977-1988 is presented by Ekman (1989).

10.1 Groundwater head conditions

The preparation of the contour maps of the groundwater table for the semi-regional and local model area is described in Section 3.1. The maps are shown in Appendix 2:1 and 2:2, respectively. Data are available in digitalized form on diskettes.

The long-term piezometric measurements in boreholes are described in Section 3.2.1 and Appendix 3:1. The data are available on protocols.

The estimated natural pressure differences along boreholes in 2 m and 20 m sections in connection with single-hole hydraulic tests are presented in Section 3.2.2 and in Appendix 3:2 and 3:3, respectively. The data are stored in the GEOTAB database. The data from the 2 m sections (DPOPI) are found in HYDRO (subject) > SHSINJ (method) > SHSINJD (table). The data from the 20 m sections (DPOPI=PO-PI or DPSPI=PS-PI according to Appendix 3:3) are found in HYDRO > SHTINJ > SHTINJD.

10.2 Hydraulic parameters

Values on the hydraulic conductivity determined from single-hole tests and interference tests are described in Section 4.1. The hydraulic conductivity distributions along the boreholes with different packer spacings are presented in Appendix 4. The data are stored in the GEOTAB database. The data from tests in 2 m and 3 m sections are found in HYDRO > SHSINJ > SHSINJCD. The data from tests in 20 m sections are found in HYDRO > SHTINJ > SHTINJCD.

Interpreted hydraulic parameters from the interference tests are presented in Section 4.3.2 and stored in the GEOTAB > INTER > INTRCD. Time-drawdown/recovery data from interference test 3B are available on diskette.

The estimations of the conductive fracture frequency are described in Section 5.5. The results are available on protocols.

10.3 Parameters from tracer tests

The parameters determined from the preliminary tracer test during the hydraulic interference tests are presented in Section 5.1; from the radially converging tracer test in Section 5.2; from other tracer tests in Section 5.3 and finally, from the dilution test in Section 5.4. The results are available on protocols.

10.4 Hydrochemical parameters

The major chemical parameters from groundwater from Finnsjön are presented in Section 6.1 and Appendix 8:1 and 8:3. Stable isotope data are described in Section 6.1.1 and presented in Appendix 8:2. Saturation index with respect to calcite is described in Section 6.1.4 and presented in Appendix 8:4. The data are available on protocols.

Chemical analyses of groundwater from boreholes KFIO9 and BFIO1 are stored in GEOTAB > CHEMICAL > WATER. Under the method WATER the following tables are available:

REDOX	redox potentials
PHETC	pH, pS, Temp, Cond, Oxygen
MAIN	Na, K, Ca, Mg a.s.o.
REM	phosphate, nitrate, sulphide a.s.o.
EQUIV	same as in MAIN but expressed in milliequivalents

The changes of the electric conductivity of the discharged water during the hydraulic interference tests are described in Section 6.2 and presented in Appendix 8:5. The data are available on raw data files.

10.5 Geological and geometric data of fracture zones

The interpretation of fracture zones is described in Section 4.2. A CAD-model of the Finnsjön Rock Block is presented in Appendix 5 together with geometric data of the fracture zones. The CAD-model is available on data files and the geometric data on diskette.

Data on lineaments and fractures in the Finnsjön area and surroundings are described in Chapter 7. The data, which are presented in tables in Appendix 9, are available on diskettes.

10.6 Borehole data

The borehole coordinates (X, Y, Z) according to the deviation logs are stored in GEOTAB > BGR > BGHOLE > BHCOORD.

11. REFERENCES

- Ahlbom K, Andersson P, Ekman L, Gustafsson E, Smellie J and Tullborg E-L 1986: Preliminary investigations of fracture zones in the Brändan area, Finnsjön study site. SKB Technical Report 86-05.
- Ahlbom K, Andersson P, Ekman L and Tirén S 1988: Characterization of fracture zones in the Brändan area, Finnsjön study site, central Sweden. SKB Progress Report 88-09.
- Ahlbom K and Tirén S 1989: Overview of geologic and hydrogeologic character of the Finnsjön site and its surroundings. SKB Progress Report 89-08.
- Ahlbom K and Tirén S 1991: Overview of geologic and hydrogeologic character of the Finnsjön site and its surroundings. SKB Technical Report 91-08.
- Allard B, Larsson, S-Å and Tullborg E-L 1983: Chemistry of deep groundwaters from granitic bedrock. SKBF/KBS Technical Report 83-59.
- Almén K-E, Andersson J-E, Carlsson L, Hansson K and Larsson N-Å 1986: Hydraulic testing in crystalline rock. A comparative study of single-hole test methods. SKB Technical Report 86-27.
- Andersson J-E and Olsson T 1978: Forsmark Nuclear Power Plant - Fresh-water supply by groundwater extraction in bedrock. Swedish Geological Survey, July 1978. (In Swedish).
- Andersson J-E, Ekman L and Winberg A 1988: Detailed investigations of fracture zones in the Brändan area, Finnsjön study site. Single-hole water injection tests in detailed sections. SKB Progress Report 88-08.
- Andersson J-E and Lindqvist L: Prediction of hydraulic conductivity and conductive fracture frequency by multivariate analysis of data from the Klipperås study site. SKB Technical Report 89-11.
- Andersson J-E, Ekman L, Gustafsson E, Nordqvist R and Tirén S 1989: Hydraulic interference tests and tracer tests within the Brändan area, Finnsjön study site. SKB Technical Report 89-12.
- Andersson J-E, Nordqvist R, Nyberg G, Smellie JAT and Tirén S 1989b: Hydrogeological conditions in the Finnsjön area - Compilation of data and conceptual model. SKB Progress Report 89-24.
- Andersson J and Andersson P 1987: Flow simulations in a fracture zone in the Brändan area, Finnsjön. SKB Progress Report 87-26.

Axelsson C-L 1986: Modelling of groundwater flow with salt-water interface at the final repository for reactor waste (SFR). Report compiled for the National Institute of Radiation Protection, Stockholm.

Carlsson L, Gentzschein B, Gidlund G, Hansson K, Svenson T och Thoregren U 1980: Supplementary permeability measurements in the Finnsjön area. (In Swedish). SKBF-KBS Technical Report 80-10.

Carlsson L and Gidlund G 1983: Evaluation of the hydrogeological conditions at Finnsjön SKBF-KBS Technical Report 83-56.

Carlsson L, Winberg A and Grundfeldt B 1983: Model calculations of the groundwater flow at Finnsjön, Fjällveden, Gideå and Kam-lunge. SKBF-KBS Technical Report 83-45.

Carlsson L, Winberg A and Rosander B 1984: Investigations of hydraulic properties in crystalline rock. Mat Res Soc Symp Proc Vol 26, Boston, Elsevier.

Carlsson L, Winberg A and Arnefors J 1986: Hydraulic modelling of the final repository for reactor waste (SFR) - Compilation and conceptualization of available geological and hydrogeological data. SKB Progress Report SFR 86-03.

Carlsson L, Winberg A and Grundfelt B 1987: Hydraulic modelling of the final repository for reactor waste (SFR) - Evaluation of the groundwater flow situation at SFR. SKB Progress Report SFR 86-07.

Cvetkovic V and Kung C-S 1989: Variogram analysis of single-hole packer test data from the Finnsjön site. SKB Progress Report 89-17.

Dershowitz, W.S., 1984: Rock joint systems. Unpubl. Ph. D. thesis, Massachusetts Institute of Technology, Massachusetts, 764 pp.

Ekman L, Andersson J-E, Andersson P, Carlsten S, Eriksson C-O, Gustafsson E, Hansson K and Stenberg L 1988: Documentation of borehole BFI02 within the Brändan area, Finnsjön study site. SKB Progress Report 89-21.

Ekman L 1989: Compilation of geo-investigations within the Finnsjön area during the period 1977-1988. SKB Progress Report 89-09. (In Swedish).

Fenske P R 1984: Unsteady drawdown in the presence of a linear discontinuity. In Rosenheim: Groundwater Hydraulics. AGU Water Resources Monograph 9.

Gelhar L 1987: Applications of stochastic models to solute transport in fractured rocks. SKB Technical Report 87-05.

- Gustafsson E and Klockars C-E 1981: Studies on groundwater transport in fractured crystalline rock under controlled conditions using nonradioactive tracers. SKBF-KBS Technical Report 81-07.
- Gustafsson E and Andersson P 1989: Groundwater flow conditions in a low-angle fracture zone at Finnsjön, Sweden. In Ahlbom and Smellie (Eds.) 1989: Characterization of fracture zone 2, Finnsjön study-site. SKB Technical Report 89-19.
- Gustafsson E, Andersson P, Eriksson C-E and Nordqvist R 1989: Radially converging tracer experiment in a low-angle fracture zone at the Finnsjön site, central Sweden. SKB Progress Report 90-27.
- Hobbs W H 1904: Lineaments of the Atlantic border region. Geol. Soc. Am. Bull. 15, 483-506.
- Hobbs W H 1912: Earth fractures and their meaning. Macmillan Co., New York, 506 pp.
- Hult A, Gidlund G and Thoregren U 1978: Permeability determinations. KBS Technical Report 61. (In Swedish).
- Hultberg B, Larsson S-Å och Tullborg E-L 1981: Groundwater in crystalline rock - chemical composition and isotope conditions in groundwater from Finnsjön, Kråkemåla och Sternö. (In Swedish) SKBF/KBS Progress Report 81-29.
- Jacobsson J-Å, Larsson N-Å 1980: Hydrological surface mapping of the Finnsjön area. (In Swedish). SKBF-KBS Progress Report 80-10.
- Laurent S 1982: Analysis of groundwater from deep boreholes in Kråkemåla, Sternö and Finnsjön. SKBF-KBS Technical Report 82-23.
- Magnusson K-Å and Duran O 1978: Geophysical borehole measurement. KBS Technical Report 61. (In Swedish).
- NCSS 1987: Reference manual.
- Neuman S P 1988: A proposed conceptual framework and methodology for investigating flow and transport in Swedish crystalline rocks. SKB Progress Report 88-37.
- Nordqvist R and Andersson J-E 1987: Transient flow simulations in a fracture zone in the Brändan area, Finnsjön. SKB Progress Report 88-11.
- Olkiewicz A, Scherman S and Kornfält K-A 1979: Complementary bedrock investigations within the Finnsjön and Karlshamn areas. SKBF-KBS Technical Report 79-05. (In Swedish).
- Osnes J D, Winberg A and Andersson J-E 1988: Analysis of well test data - Application of probabilistic models to infer hydraulic properties of fractures. SKB/OWTD joint report in prep.

Puigdomenech I and Nordstrom K 1987: Geochemical interpretation of groundwaters from Finnsjön, Sweden. SKB Technical Report 87-15.

Saxena R K 1984: Surface and groundwater mixing and identification of local recharge-discharge zones from seasonal fluctuations of oxygen-18 in groundwater in fissured rock. Div. Hydrol. Uppsala Univ.

Smellie J A T and Wikberg P 1989: Hydrochemical investigations at Finnsjön, Sweden. In Ahlbom and Smellie (Eds.) 1989: Characterization of fracture zone 2, Finnsjön study-site. SKB Technical Report 89-19.

Tirén S A and Beckholmen M 1989: Block faulting in southeastern Sweden interpreted from digital terrain models. Geol. För. Stockholm. Förh. 111, 171-179.

Tirén S A and Stark T 1989: Tentative model of hydraulically conductive fracture zones in the Finnsjön site, Sweden. SGAB IRAP 89346.

Tirén S A 1989: Geological setting and deformation history of a low angle fracture zone at Finnsjön, Sweden. In Ahlbom and Smellie (Eds.) 1989: Characterization of fracture zone 2, Finnsjön study site. SKB Technical Report 89-19.

Tullborg E-L and Larson S-Å 1982: Fissure fillings from Finnsjön and Studsvik Sweden. Identification, chemistry and dating. SKBF-KBS Technical Report 82-20.

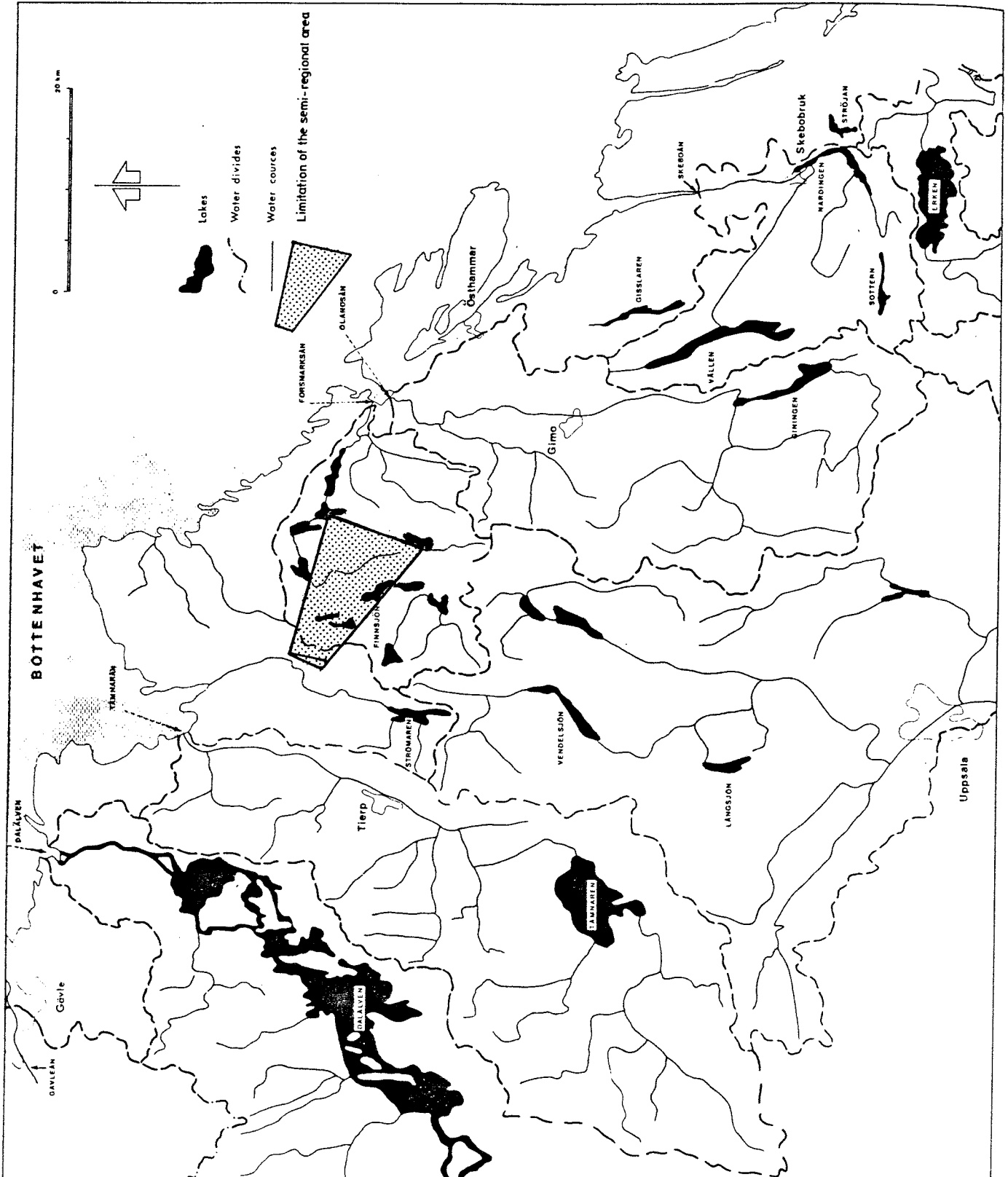
Voss C 1984: A finite-element simulation model for saturated-unsaturated fluid-density-dependent groundwater flow with energy transport or chemically reactive single species solute transport. USGS Water Res Invest Report 84-4369.

Winberg A and Carlsson L 1987: Calculations of conductive fracture frequency and description of skin effects around tunnels in the rock cavern area, SFR, Forsmark. Report in Swedish prepared for SKB.

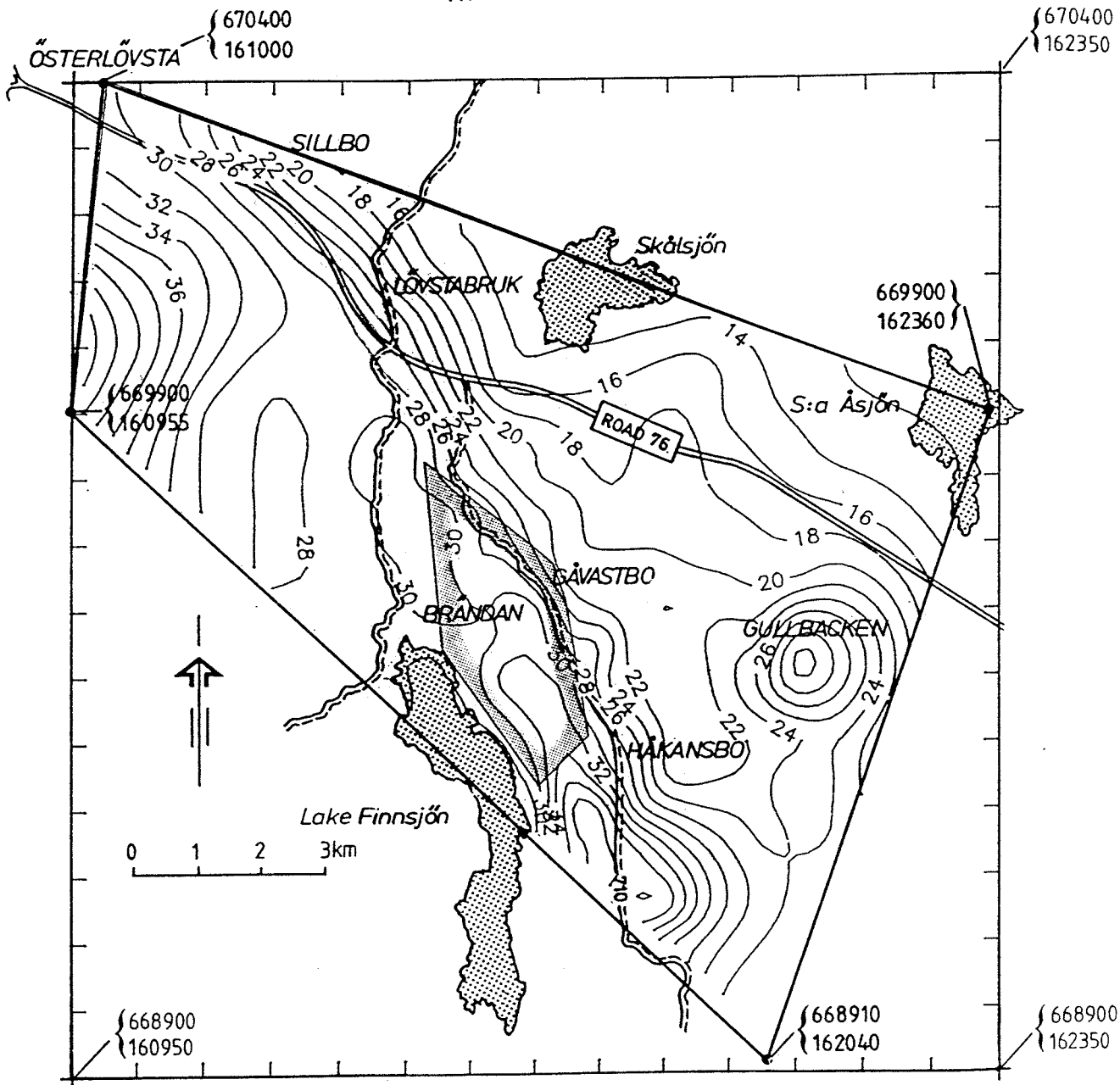
LIST OF APPENDICES

	Page
Appendix 1 Drainage basins and larger lakes in Northern Uppland	A1
Appendix 2 Contour maps of the groundwater table	
2:1 Semi-regional model area	A2
2:2 Local model area	A3
Appendix 3 Groundwater head conditions	
3:1 Piezometric measurements in multiple-borehole sections	A4
3:2 Pressure differences in 2 m borehole sections	A8
3:3 " 20 m "	A10
Appendix 4 Hydraulic conductivity distributions along the boreholes from single-hole tests	A11
Appendix 5 CAD-model and geometric data of the Finnsjön Rock Block	
5:1 CAD-pictures from different views	A17
5:2 Geometric data of fracture zones	A22
Appendix 6 Statistical analysis of the hydraulic conductivity distributions of the rock mass	
6:1 Mean of log(K) + standard deviation in 100 m intervals displayed in a Box Plot	A26
6:2 Regression analysis of rock mass data	A29
6:3 Plots showing the 95% confidence interval	A31
Appendix 7 Geostatistical analysis of hydraulic conductivity data	A33
Appendix 8 Groundwater chemical parameters	
8:1 Major chemical parameters	A44
8:2 Isotope analyses	A47
8:3 Chemical parameters from KFI09 and BFI01	A49
8:4 Saturation index with respect to calcite	A51
8:5 Changes of electric conductivity of discharged water during the hydraulic interference tests	A52
Appendix 9 Data on lineaments/fracture zones and fractures in the Finnsjön site and surroundings	
9:1 Lineament/fracture zone data	A55
9:2 Fracture data	A64

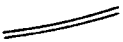
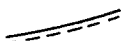
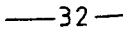
DRAINAGE BASINS AND LARGER LAKES IN NORTHERN UPPLAND



GROUNDWATER TABLE
Semi-regional model area
The Lövstabruk Area



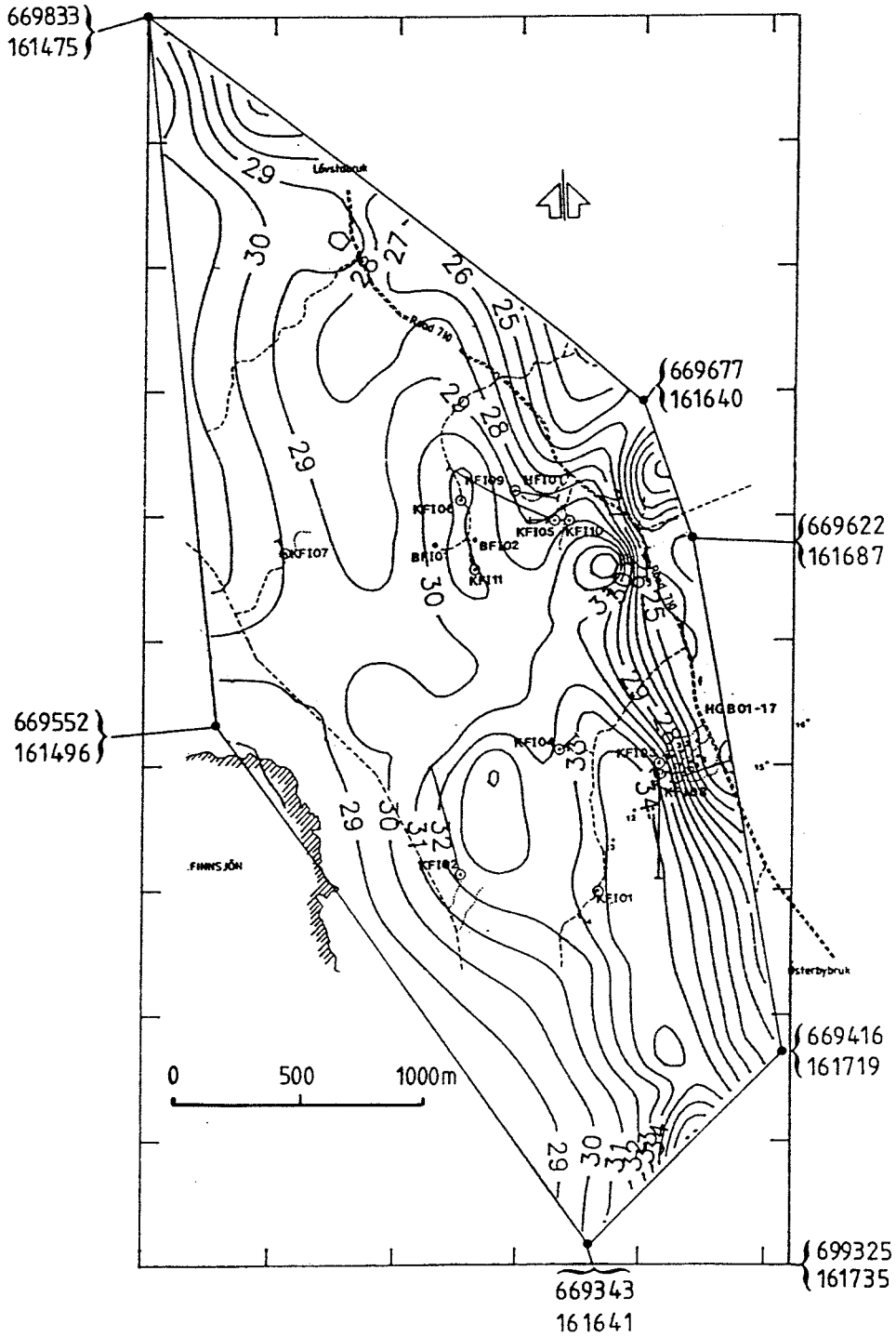
LEGEND:

- Road 
- Minor road 
- Groundwater table contour 

Local model area



GROUNDWATER TABLE
Local model area
The Finnsjön Rock Block



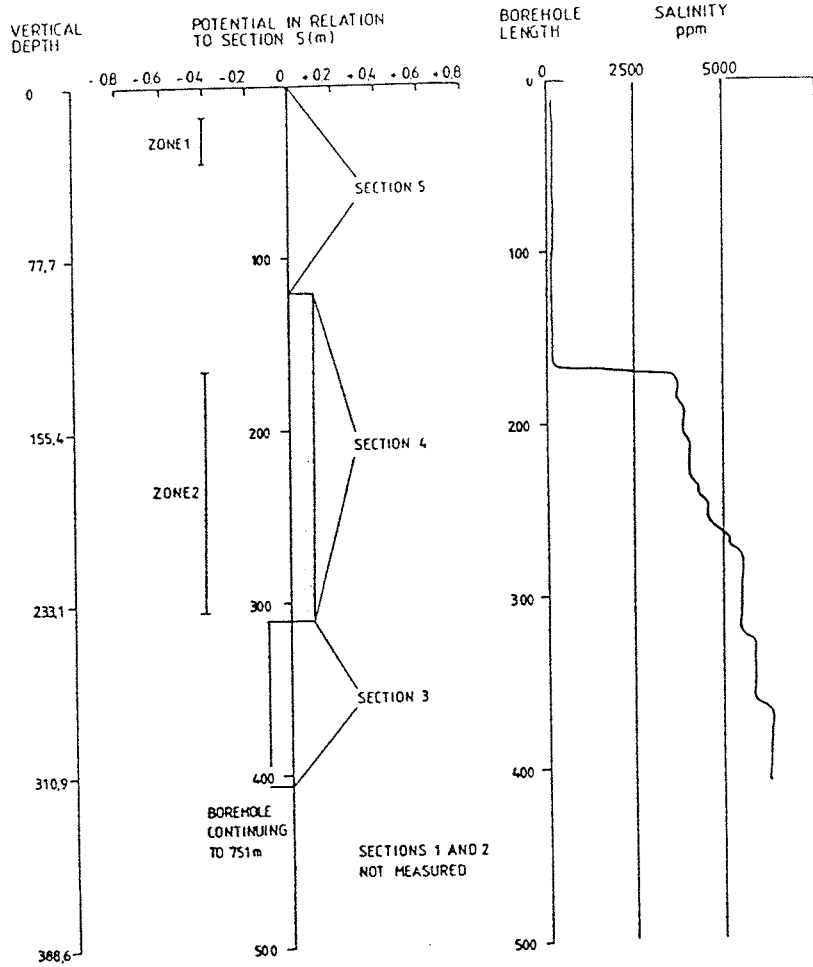
LEGEND:

- Road =====
- Minor road -----

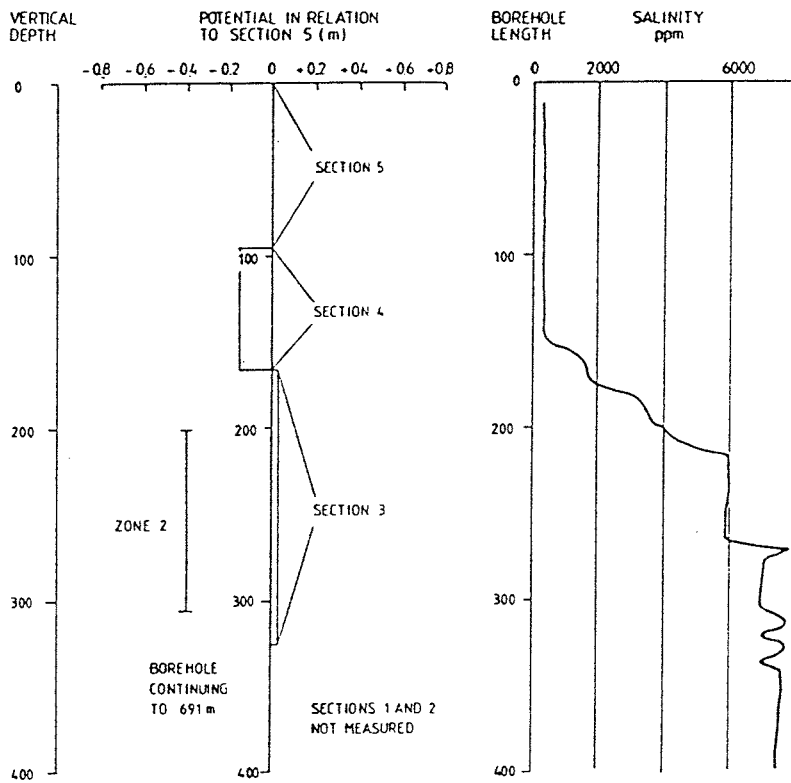
- Core borehole ○
- Percussion borehole ●
- Groundwater table contour -32-

KFIO5 Manual levelling

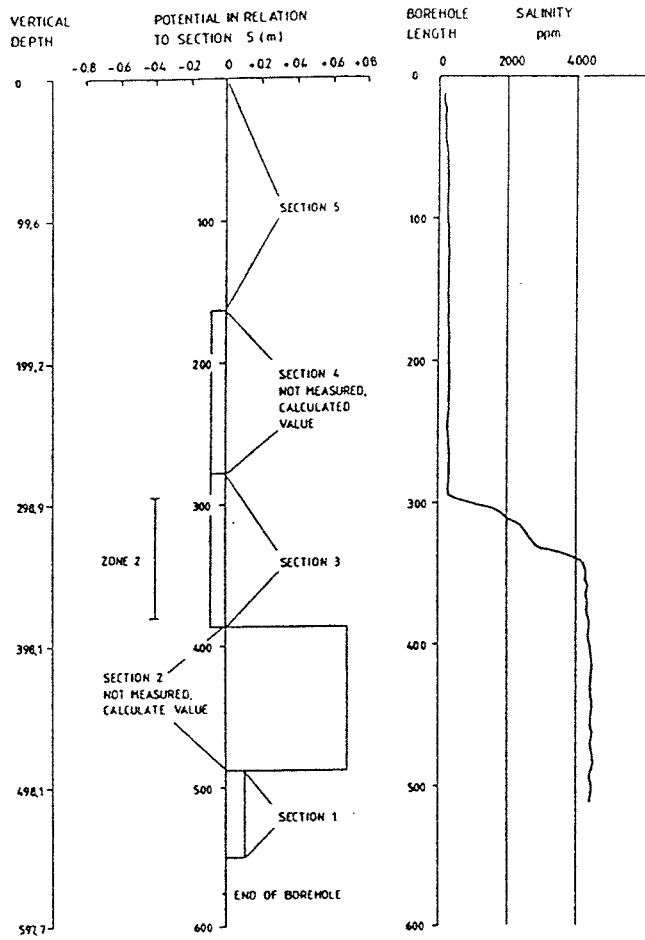
3:1



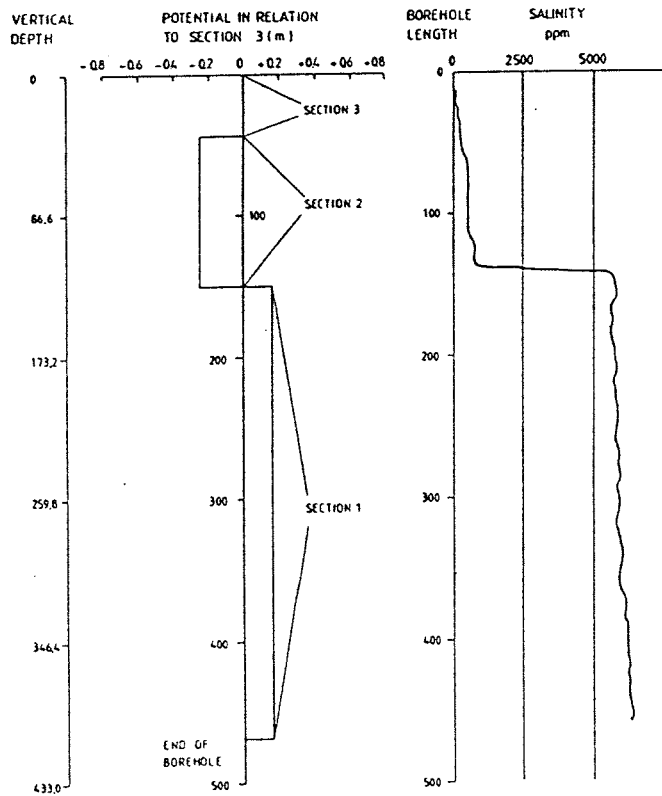
KFIO6 Manual levelling



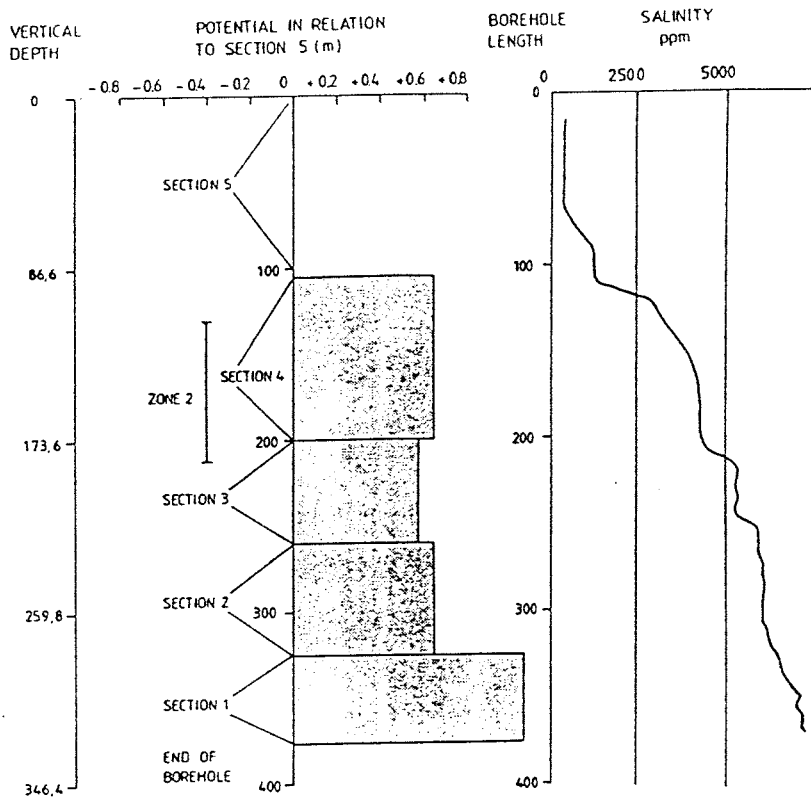
KFIO7 Manual levelling



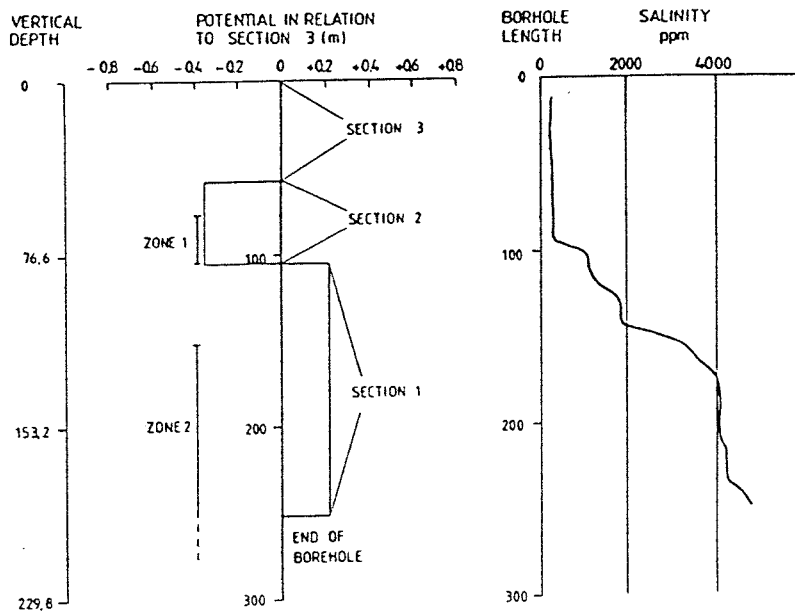
KFIO8 Manual levelling



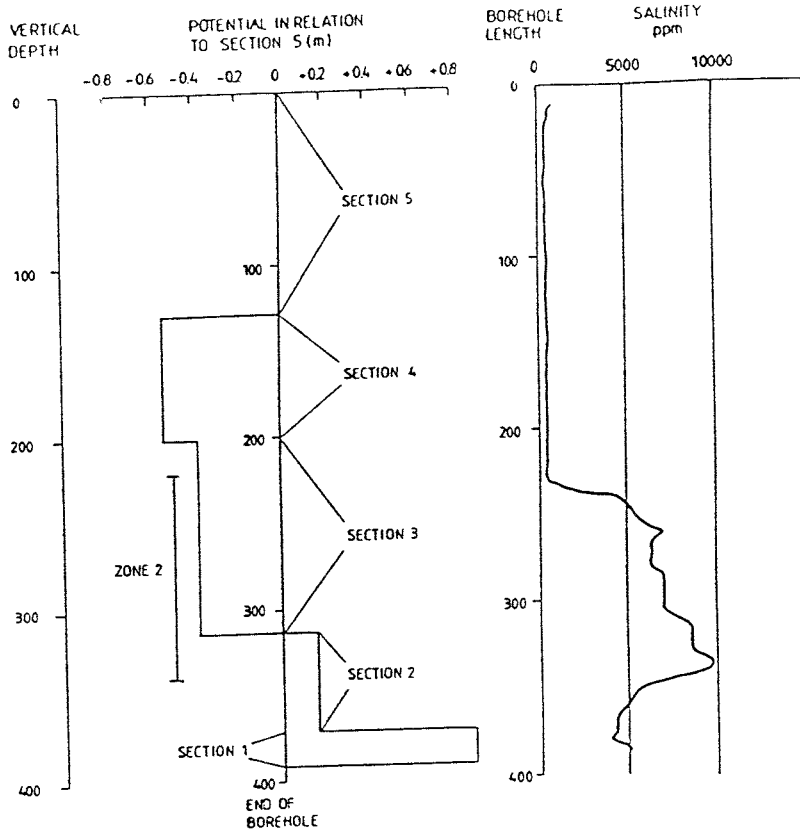
KFI09 Automatic registration



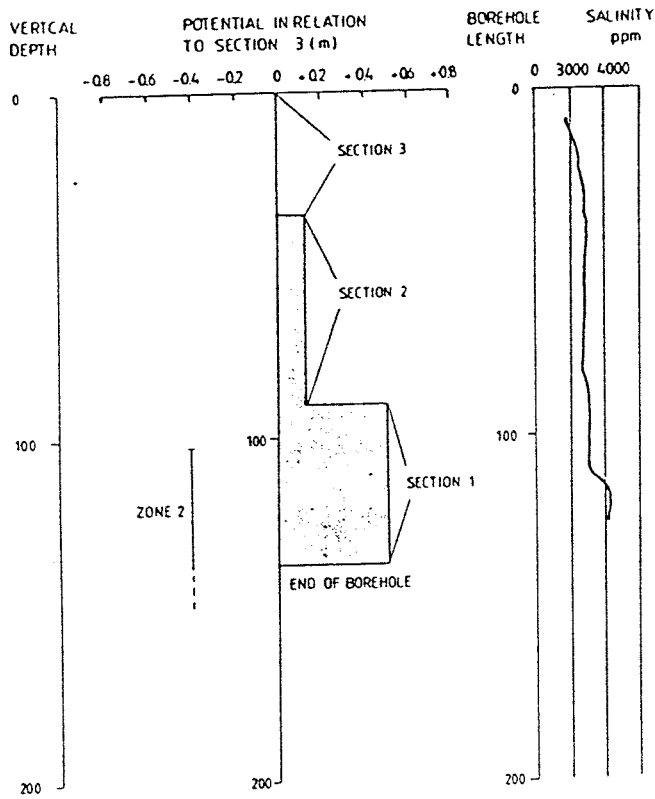
KFI10 Manual levelling

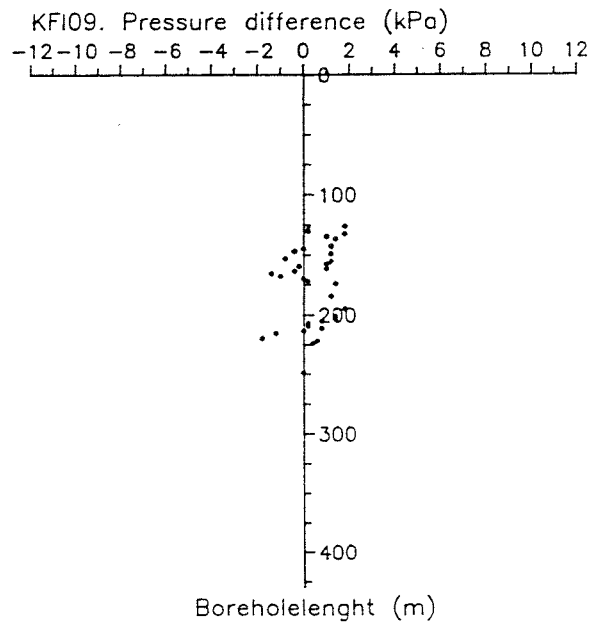
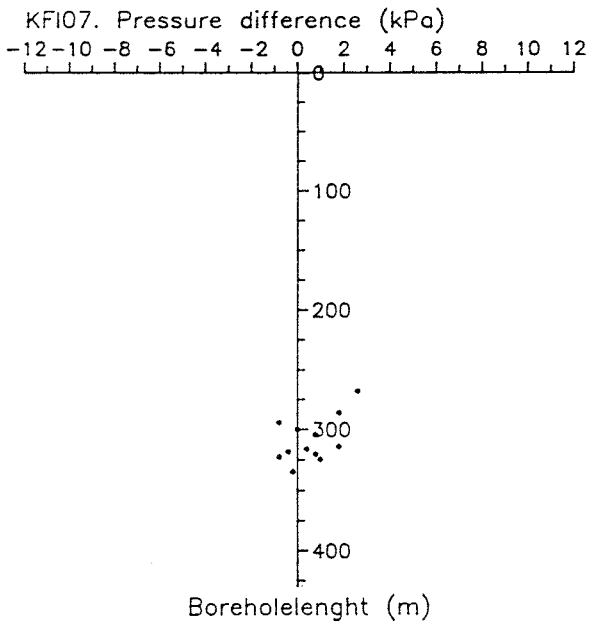
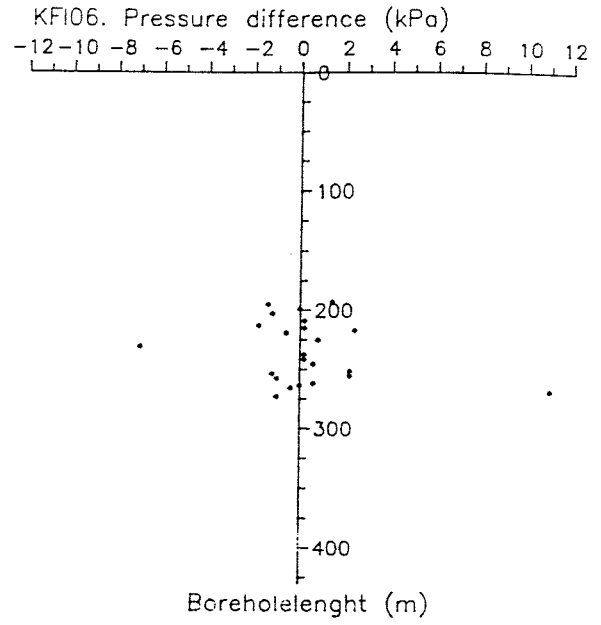
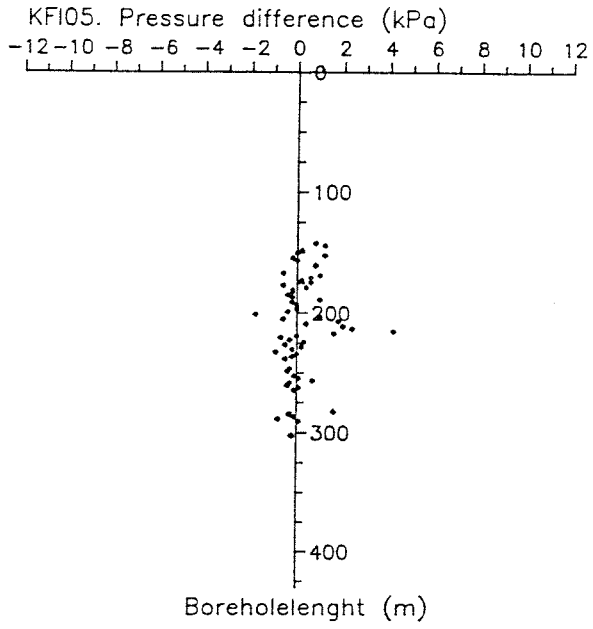


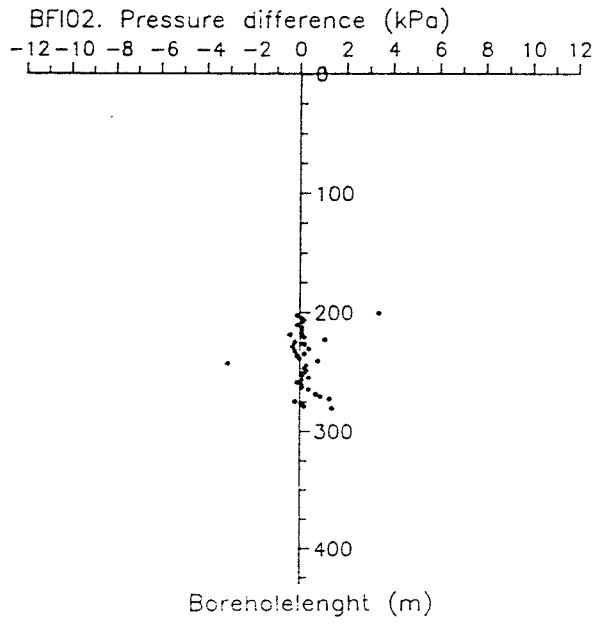
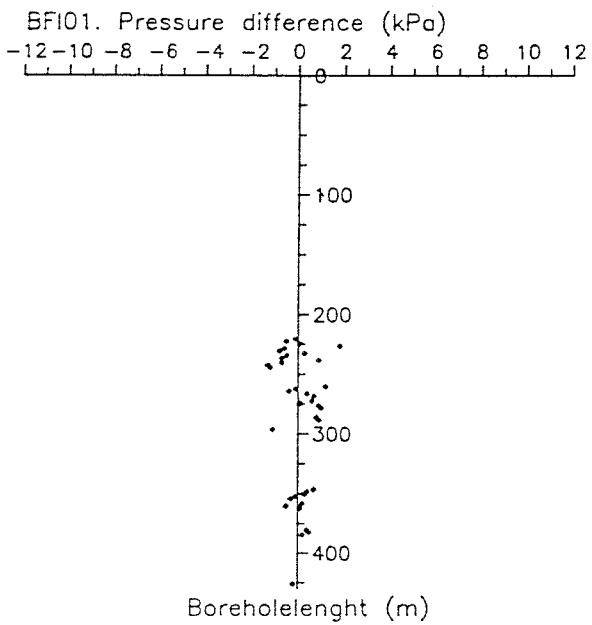
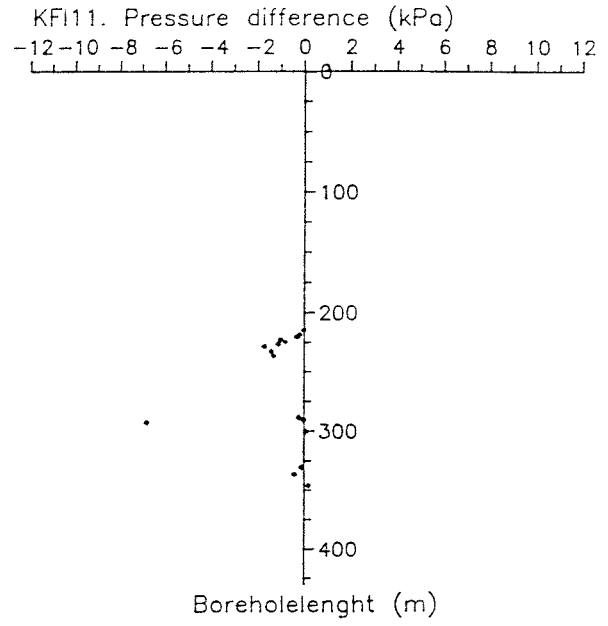
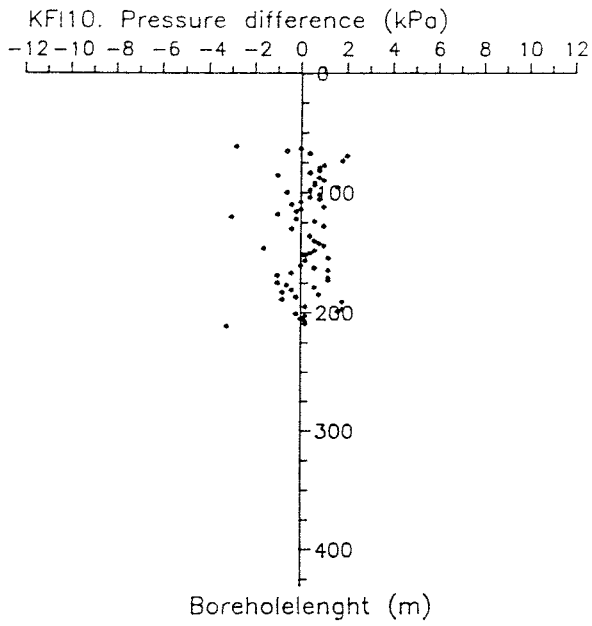
KFI11 Automatic registration

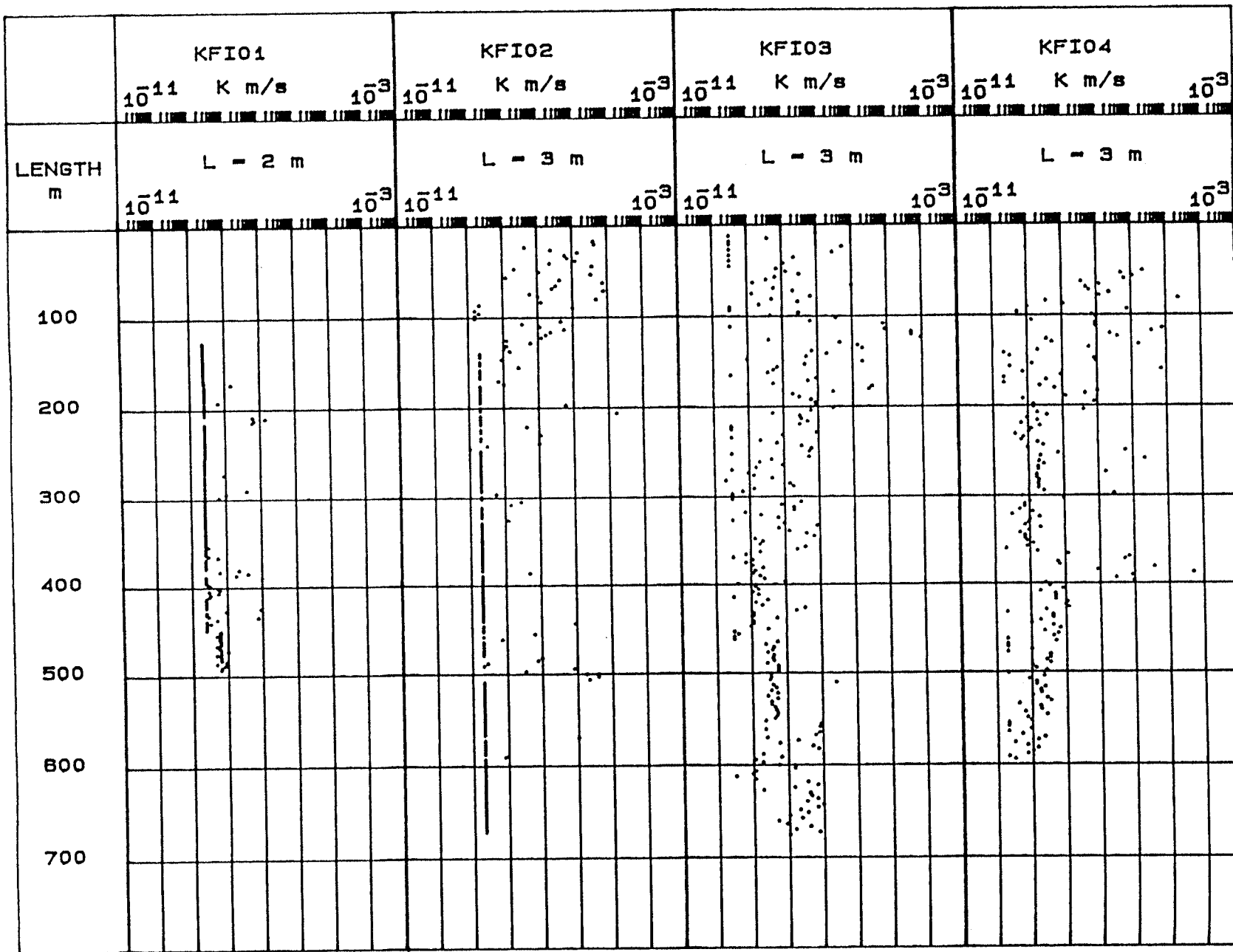


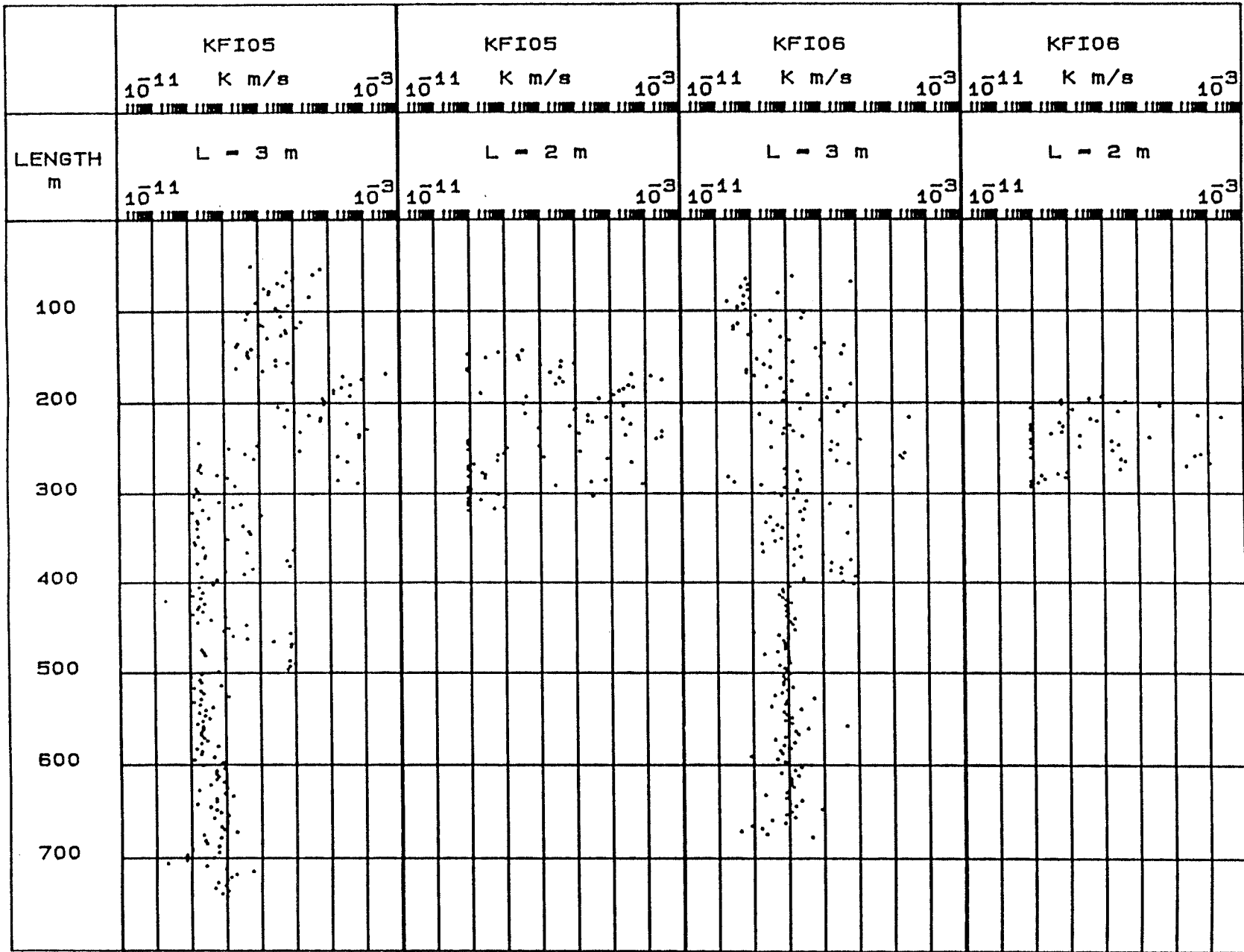
HFIO1 Manual levelling

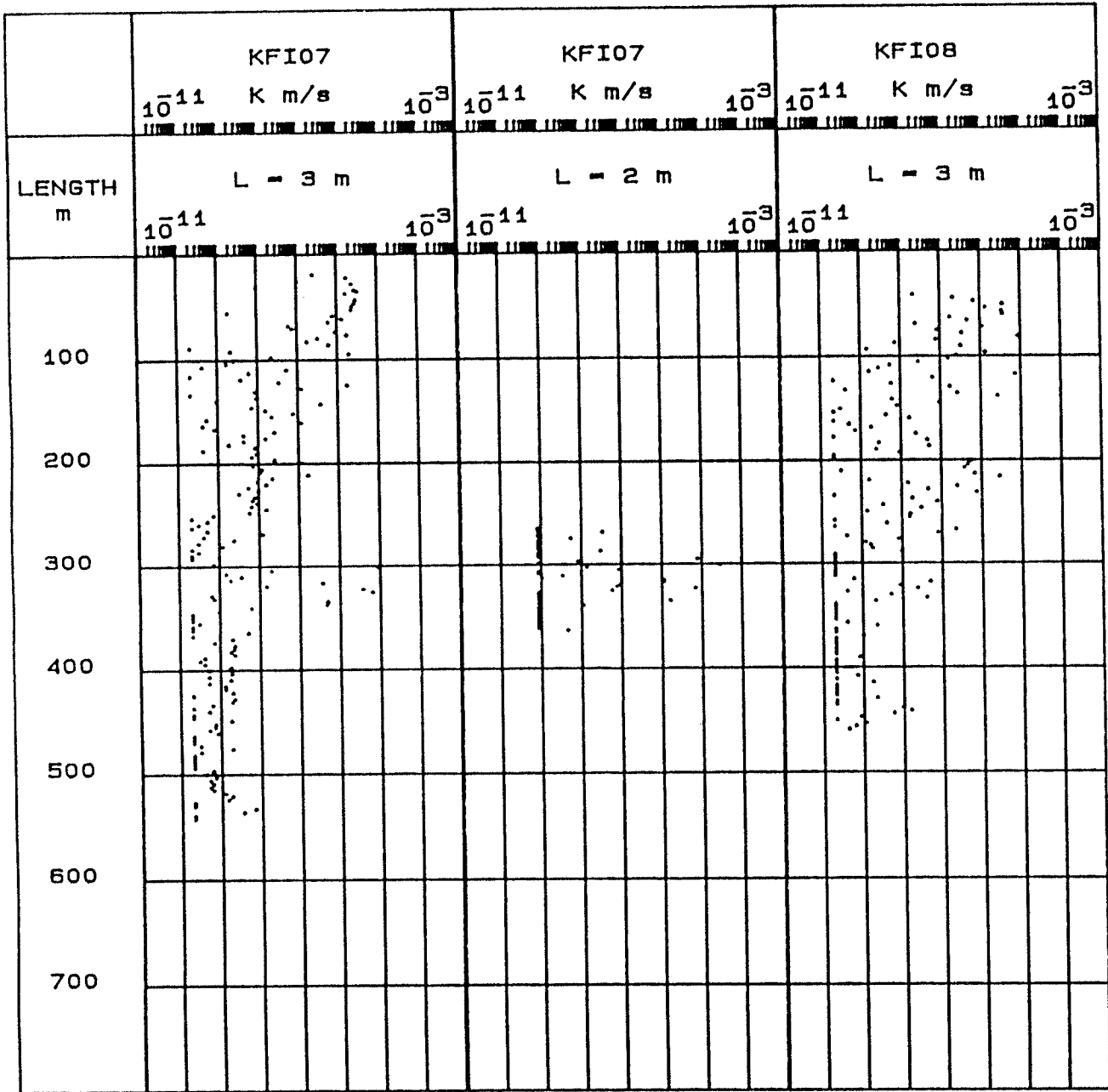


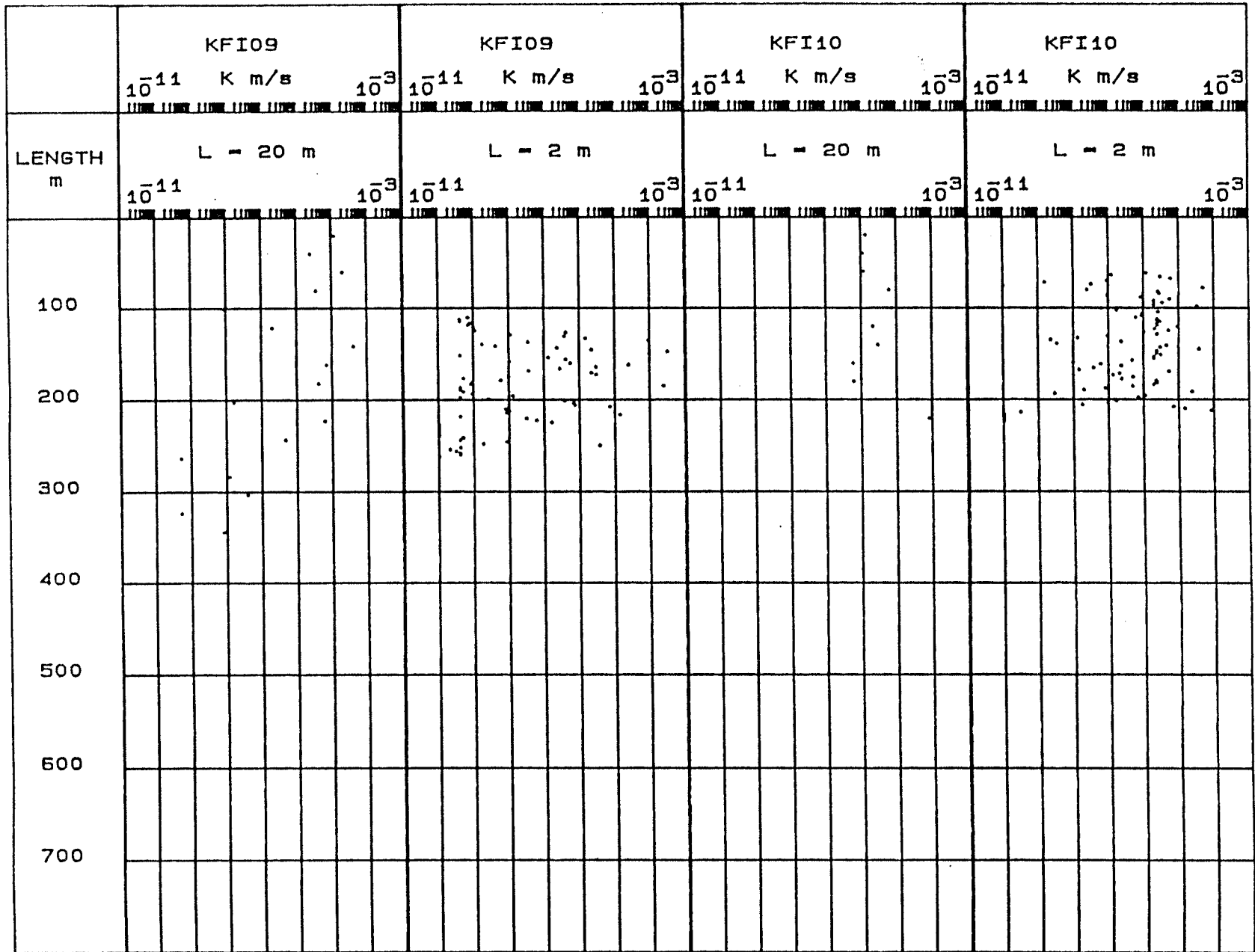


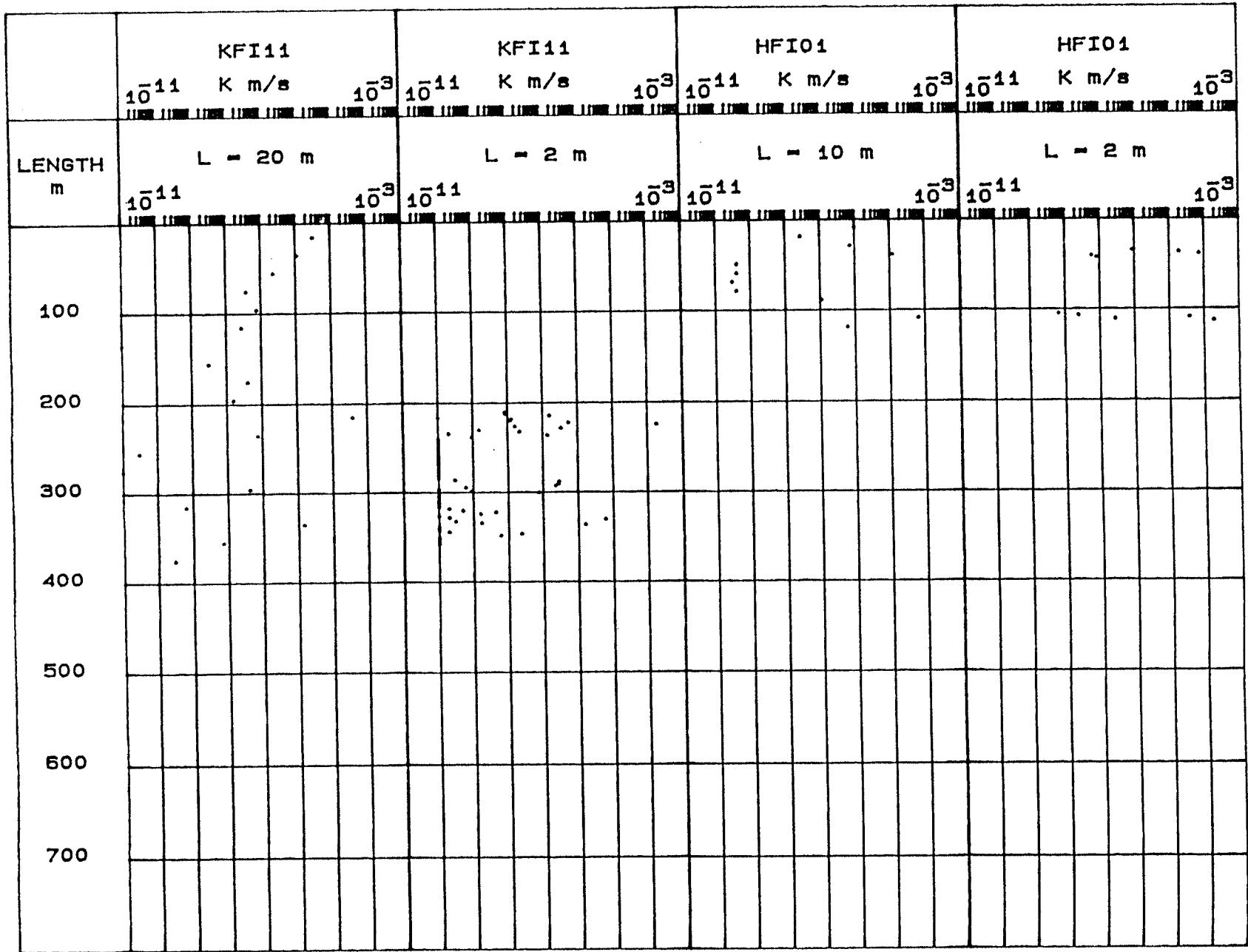


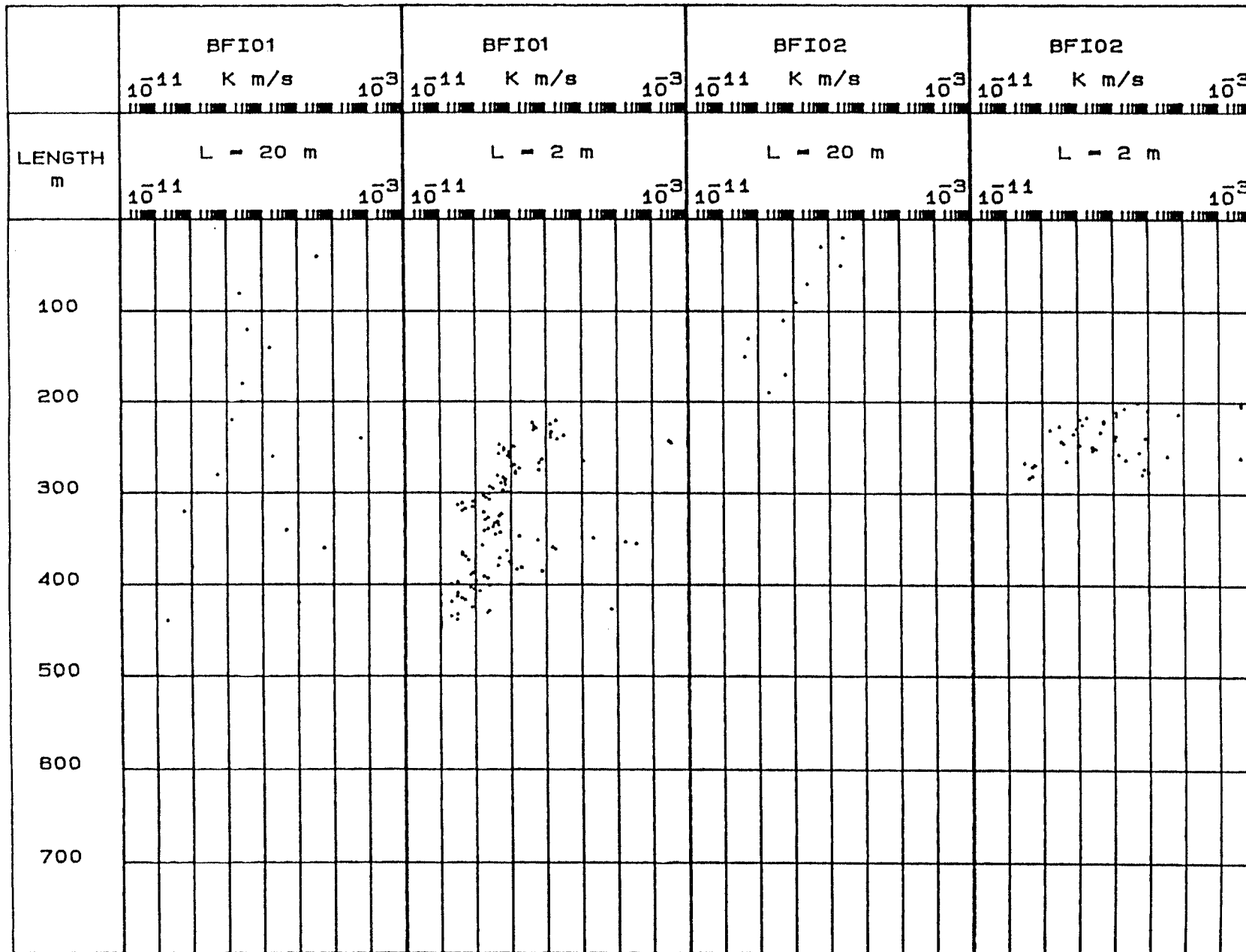


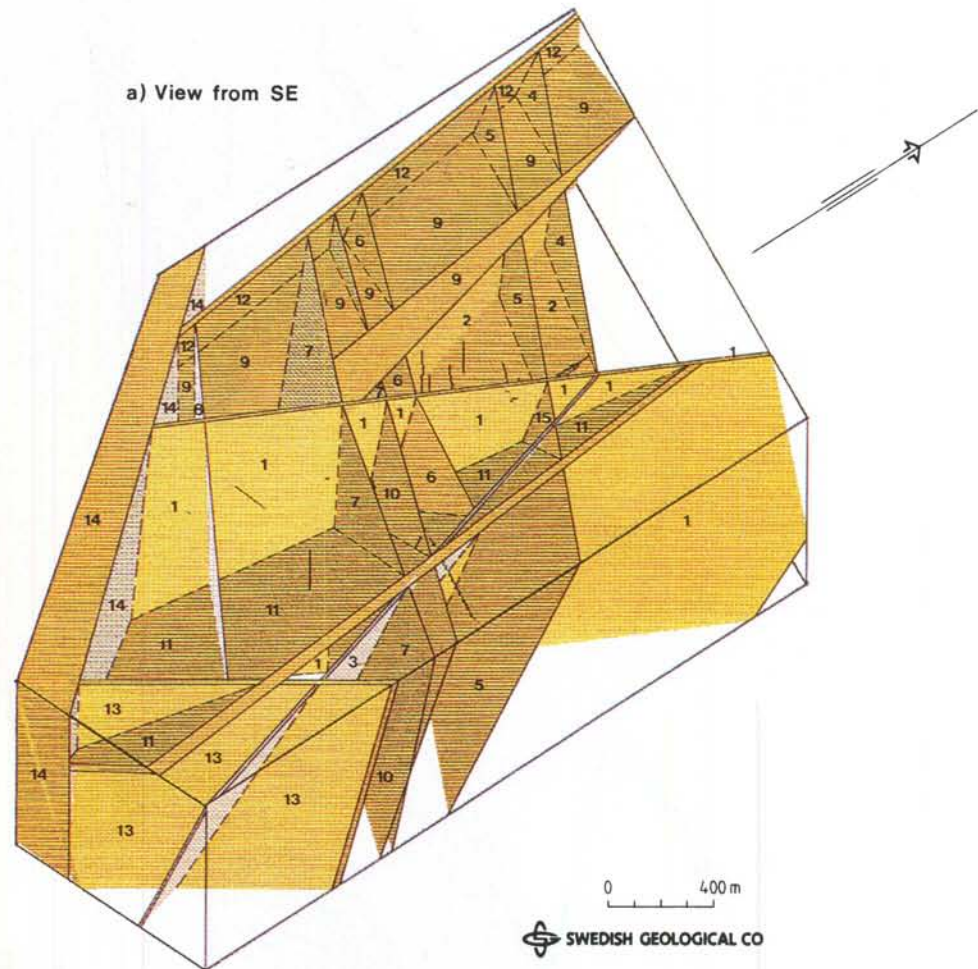




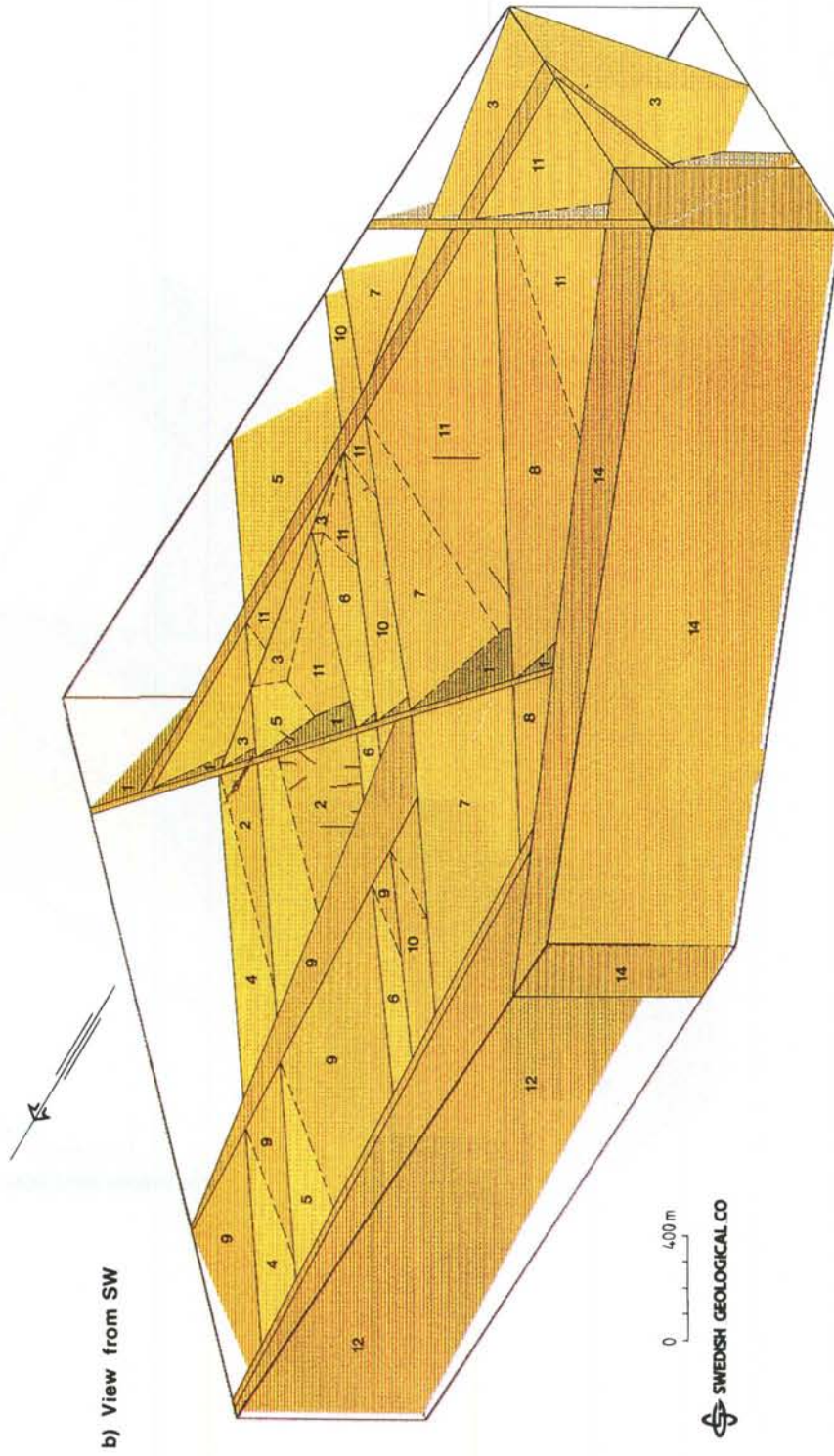




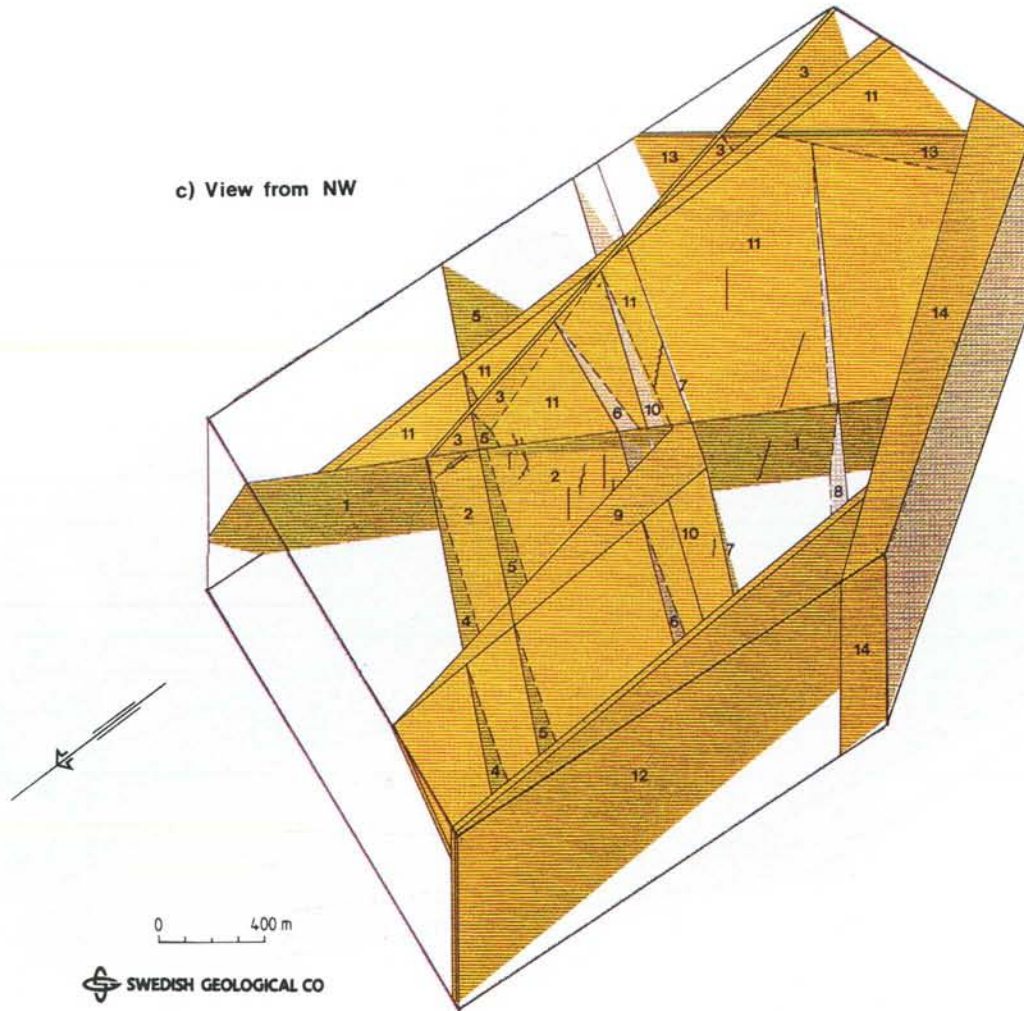




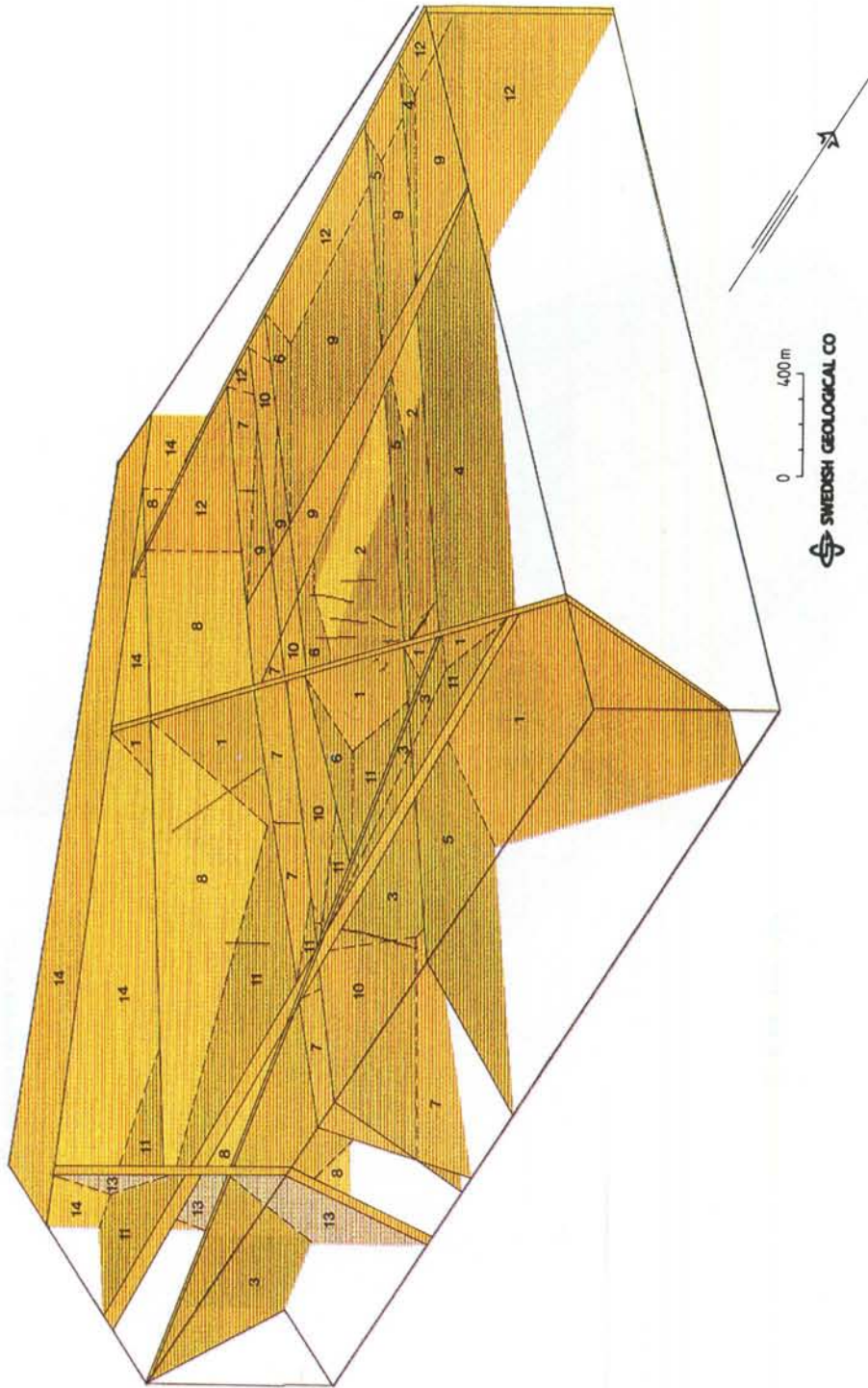
Figures 1a,b,c,d,e 3D-model of the Finnsjön Rock Block. The view of the model is inclined 40° in a,b,c,d and vertical in e. The direction of the view is SE in a, SW in b, NW in c, and NE in d. Equations of fracture zones and their intersections are given in tables.



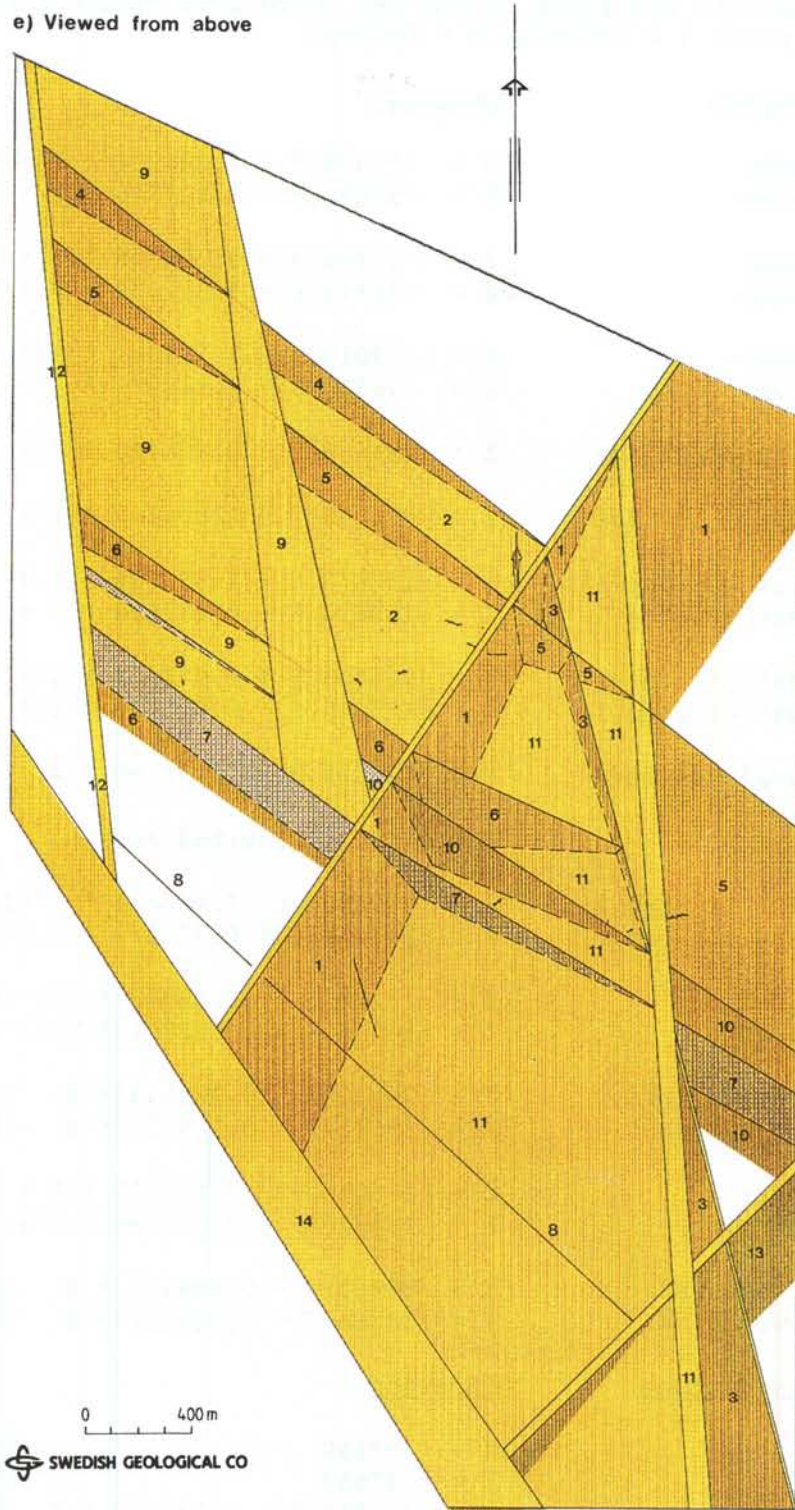
c) View from NW



d) View from NE



e) Viewed from above



Equations for upper and lower boundaries of fracture zones at the Finnsjön site.

The equations are given in the RAK coordinate system with offset in the point Y = 1600000, X = 6600000

<u>Zone Surface</u>	<u>Equation</u>
1 Upper	$Z = -57939.7 - 1.204254 * Y + 0.806301 * X$
Lower	$Z = -57876.8 - 1.203346 * Y + 0.805116 * X$
2 Upper	$Z = -16704.3 + 0.250798 * Y + 0.129853 * X$
Lower	$Z = -22170.6 + 0.342498 * Y + 0.170248 * X$
3 Upper	$Z = -93018.9 + 2.231941 * Y + 0.578364 * X$
Lower	$Z = -94336.8 + 2.242979 * Y + 0.590052 * X$
4 Single surface	$Z = -124628.9 + 0.884799 * Y + 1.136467 * X$
5 Single surface	$Z = -124108.2 + 0.884107 * Y + 1.134914 * X$
6 West of Zone 1	$Z = -157875.6 + 1.031736 * Y + 1.471614 * X$
East of Zone 1	$Z = -142423.6 + 0.613828 * Y + 1.381111 * X$
7 West of Zone 1	$Z = -149503.3 + 1.036978 * Y + 1.390081 * X$
East of Zone 1	$Z = -155865.0 + 0.900979 * Y + 1.479273 * X$
8 Single surface	$Y = 123628.8 - 1.136259 * X$ (Vertical)
9 -	Not defined, faulted zone
10 West of Zone 1	$Z = -1098072.0 + 7.466671 * Y + 10.209540 * X$
East of Zone 1	$Z = -1012283.0 + 6.37267 * Y + 9.493081 * X$
11 Upper	$Z = -17242.3 + 0.734073 * Y + 0.050388 * X$
Lower	$Z = -16538.7 + 0.698541 * Y + 0.048014 * X$
12 Towards East	$Y = 25431.5 - 0.109049 * X$ (Vertical)
Towards West	$Y = 25172.7 - 0.106779 * X$ (Vertical)
13 Upper	$Z = -196045.6 - 2.574173 * Y + 2.555830 * X$
Lower	$Z = -196219.7 - 2.571535 * Y + 2.555830 * X$
14 Towards NE	$Y = 80832.3 - 0.689417 * X$ (Vertical)
Towards SW	$Y = 88266.2 - 0.769231 * X$ (Vertical)
<u>Boundary surface</u>	<u>Equation</u>
South	$X = 93140$ (Vertical)
East	$Y = 17560$ (Vertical)
North	$Y = 234140.0 - 2.227273 * X$ (Vertical)
West	$Y = 14620$ (Vertical)
Southwest	$Y = 75009.8 - 0.630769 * X$ (Vertical)
Top	$Y = 30$ (Horizontal)
Bottom	$Y = 1000$ (Horizontal)

Coordinates for upper and lower surfaces of fracture zones at the Finnsjön site.

The coordinates are given in the RAK coordinate system with offset in the point Y= 1600000, X = 6600000

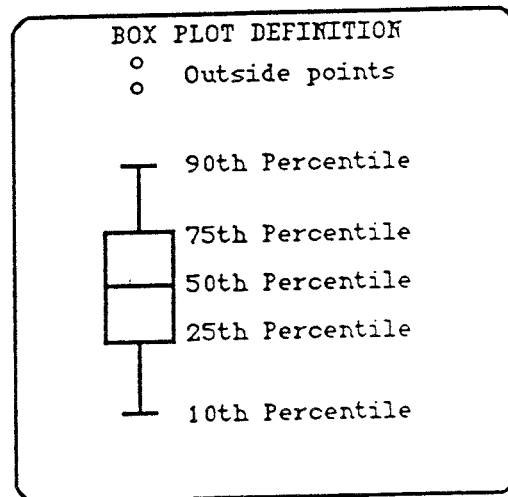
Zone Surface		X	Y	Z		
1	Upper, towards Zone 14	94903	15405	30		
		94273	15838	-1000		
	towards northern boundary	97444	17105	30		
		96844	17560	-1000		
	Lower, towards Zone 14	94925	15389	30		
		94295	15824	-1000		
	towards northern boundary	97455	17082	30		
		96890	17560	-1000		
2	East part, upper,	towards 4/1	96746	16613	25	
		towards 7/1	95535	16044	-275	
		under 9 towards 4	97388	15605	-144	
		under 9 towards 7	95544	16023	-279	
	lower,	towards 4/1	96710	16627	-11	
		towards 7/1	95459	16106	-403	
		under 9 towards 4	97266	15633	-257	
		under 9 towards 7	95512	16002	-429	
	West part, upper,	towards 4/12	98530	14687	-102	
		towards 7/12	96362	14925	-325	
		under 9 towards 4	97628	15420	-36	
		under 9 towards 7	95698	15858	-178	
		lower,	towards 4/12	98530	14687	-148
			towards 7/12	96336	14929	-438
			under 9 towards 4	97631	15389	-61
			under 9 towards 7	95736	15787	-247
3	Upper, towards Zone 1	96732	16618	30		
		95331	16525	-1000		
	towards southern boundary	93140	17556	30		
		93140	17095	-1000		
	Lower, towards Zone 1	96734	16627	30		
		95333	16534	-1000		
	towards southern boundary	93140	17560	30		
		93140	17106	-1000		
4	Towards Zone 1	96755	16614	30		
		95721	16778	-1000		
	Towards Zone 12	98232	14719	30		
		97242	14826	-1000		
5	Towards Zone 12	97886	14756	30		
		96893	14866	-1000		
	Towards eastern boundary	95701	17560	30		
		94794	17560	-1000		

6	West of Zone 1, towards Zone 1	96005	16112	30		
		95120	16375	-1000		
	towards Zone 12		96877	14868	30	
			96119	14950	-1000	
	East of Zone 1, towards Zone 1	95685	15928	30		
towards Zone 3		95116	16403	-1000		
95627		16907	30			
		95018	16606	-1000		
7	West of Zone 1, towards Zone 1	95703	15910	30		
		94783	16150	-1000		
	towards Zone 12		96446	14914	30	
			95638	15002	-1000	
	East of Zone 1, towards Zone 1	95685	15928	30		
		towards E boundary		94820	16205	-1000
		94691	17560	30		
		93995	17560	-1000		
8	Towards Zone 12	95596	15007	30		
			95596	15007	-1000	
	Towards Zone 13	93864	16975	30		
			93676	17188	-1000	
9	Upper, towards Zone 7	95899	15646	30		
		towards Zone 7/12		96404	14919	-170
	towards northern boundary		98214	15390	30	
	towards N boundary/Zone 12		98530	14687	-169	
	Lower, towards Zone 7	95636	16001	30		
		towards Zone 7/12		96393	14920	-198
		towards northern boundary		98214	15390	30
towards N boundary/Zone 12		98530	14687	-130		
10	West of Zone 1, towards Zone 1	95833	16030	30		
		95405	16567	-330		
	towards Zone 12		96666	14891	30	
			96548	14903	-381	
	East of Zone 1, towards Zone 1	95864	16048	30		
		towards E boundary		95393	16588	-1000
		94849	17561	30		
		94742	17560	-1000		
11	Upper, towards Zone 1	97088	16865	30		
		towards southwestern boundary		94067	15651	-963
		towards southern boundary		93140	17136	30
			93140	16260	-582	
	Lower, towards Zone 1	97330	17029	30		
		towards southern boundary		94239	15787	-986
		93140	17317	30		
		93140	16260	-709		
12	Towards East, towards N boundary	98529	14687	30		
		towards S boundary		98529	14687	-1000
		95026	15069	30		
			95026	15069	-1000	
	Towards West, towards N boundary	98546	14650	30		
		towards S boundary		98546	14650	-1000
		95109	15017	30		
		95109	15017	-1000		

13	Upper, towards Zone 14	93140	16306	30
		93140	16706	-1000
	towards eastern boundary	94403	17560	30
		94000	17560	-1000
	Lower, towards Zone 14	93143	16258	30
		93143	16656	-1000
	towards eastern boundary	94453	17560	30
		94050	17560	-1000
14	Towards NE, towards western boundary	96041	14620	30
		96041	14620	-1000
	towards southern boundary	93140	16620	30
		93140	16620	-1000
	Towards SW, towards western boundary	95740	14620	30
		95740	14620	-1000
	towards southern boundary	93140	16260	30
		93140	16260	-1000
<u>Boundary surfaces</u>		<u>X</u>	<u>Y</u>	<u>Z</u>
South		93140	16260	30
		93140	16260	-1000
		93140	17560	30
		93140	17560	-1000
East		93140	17560	30
		93140	17560	-1000
		97240	17560	30
		97240	17560	-1000
North		97240	17560	30
		97240	17560	-1000
		98560	14620	30
		98560	14620	-1000
West		98560	14620	30
		98560	14620	-1000
		95740	14620	30
		95740	14620	-1000
Southwest		95740	14620	30
		95740	14620	-1000
		93140	16260	30
		93140	16260	-1000

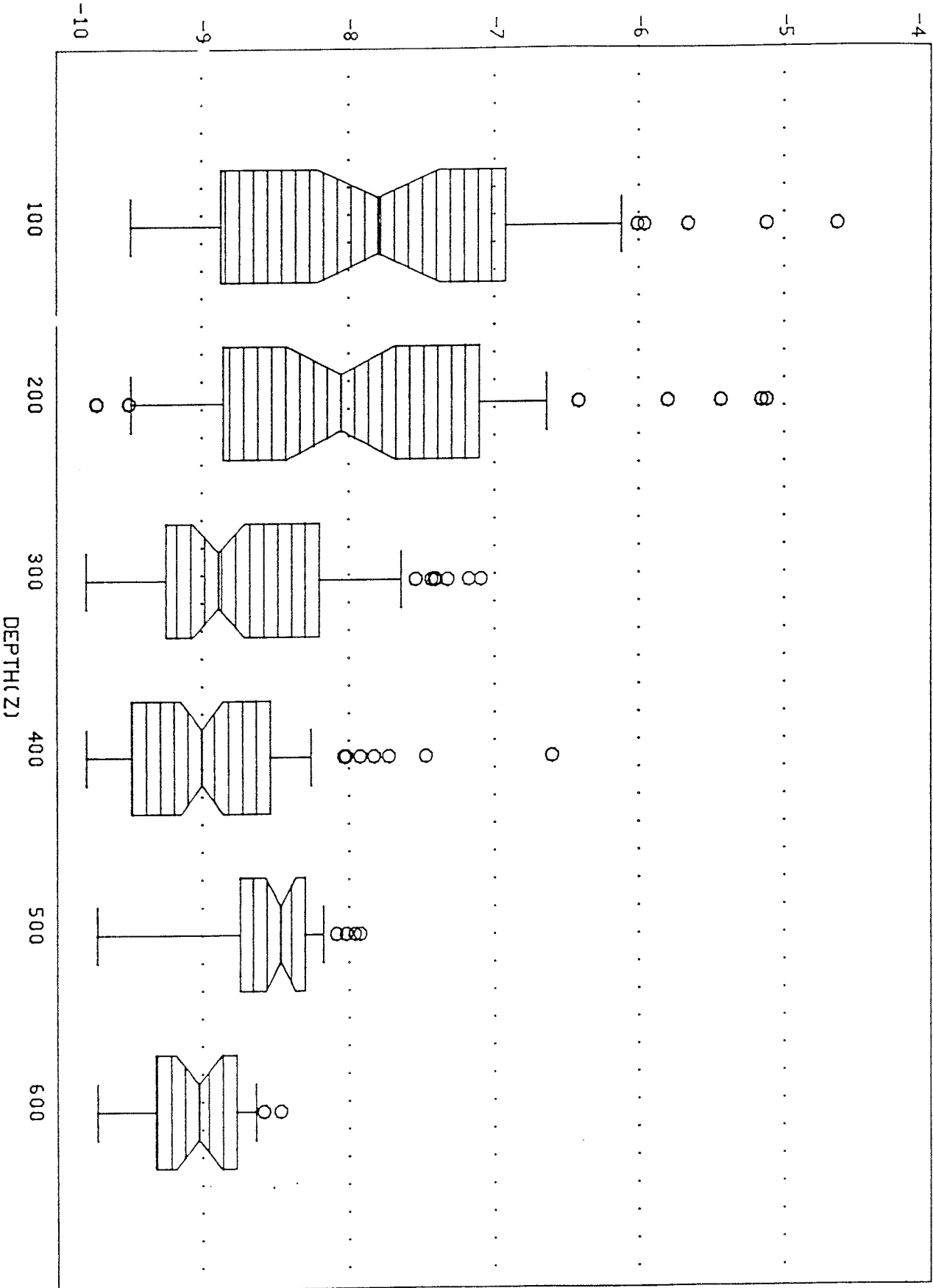
Table 1 Mean of $\log(K)$ of the rock mass and standard deviation in 100 m depth intervals for the southern and northern parts of the Finnsjön Rock Block (n= number of data).

Region/ boreholes	Interval (m.b.g.l)	Mean of $\log(K)$	St. dev.	n
Southern KFI03,04, 08	0-100	-7.78	1.29	52
	100-200	-7.93	1.19	53
	200-300	-8.76	0.75	85
	300-400	-8.98	0.63	105
	400-500	-8.62	0.50	45
	500-600	-9.07	0.37	30
Northern KFI05,06, 07	0-100	-6.92	1.28	68
	100-200	-7.99	0.93	61
	200-300	-8.25	0.92	76
	300-400	-8.30	0.91	85
	400-500	-8.59	0.61	114
	500-600	-8.35	0.56	69
	600-700	-8.10	0.51	26



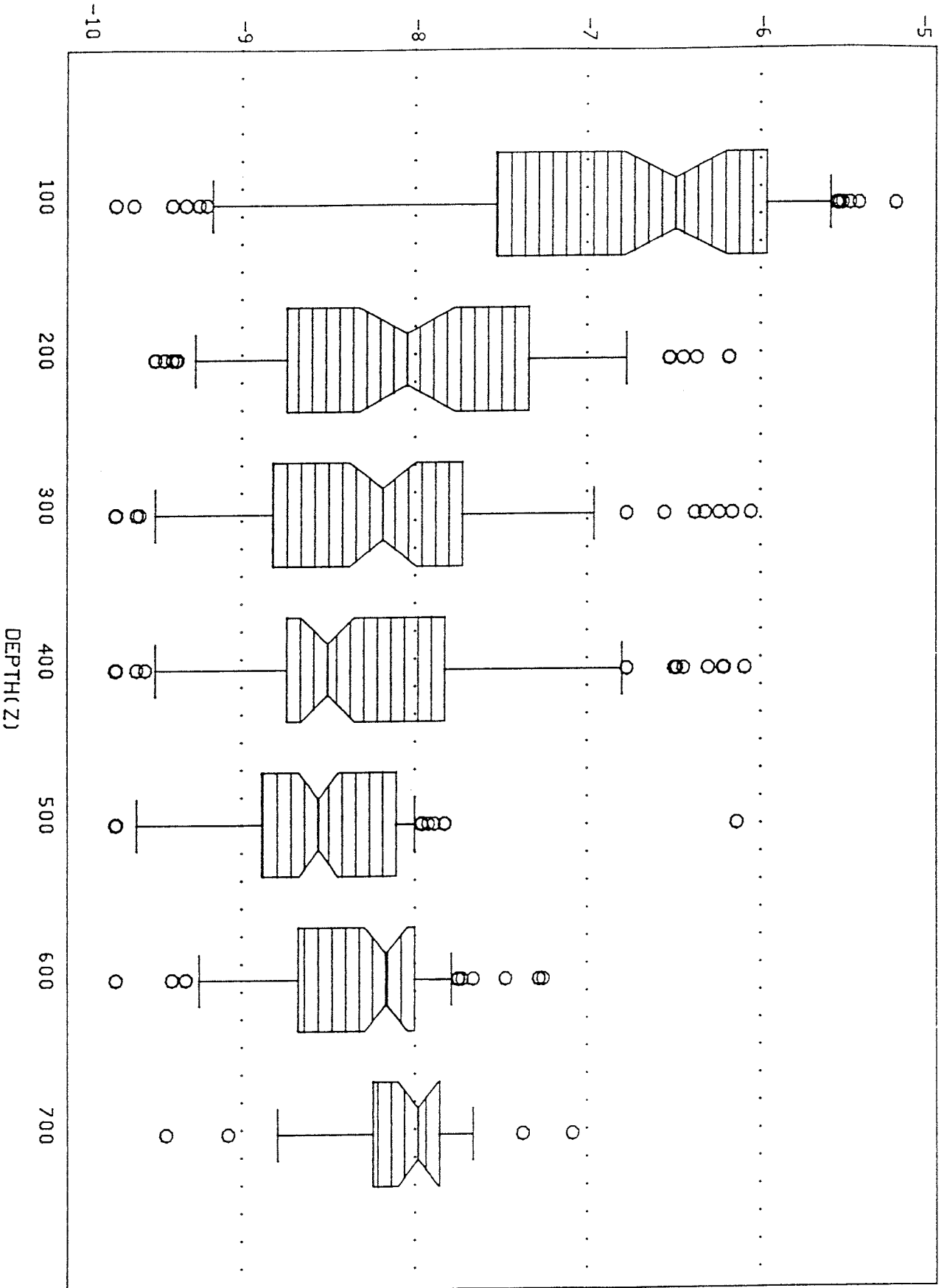
LOG(K)

Box plot for boreholes KFI03, KFI04 and KFI08



LOG(K)

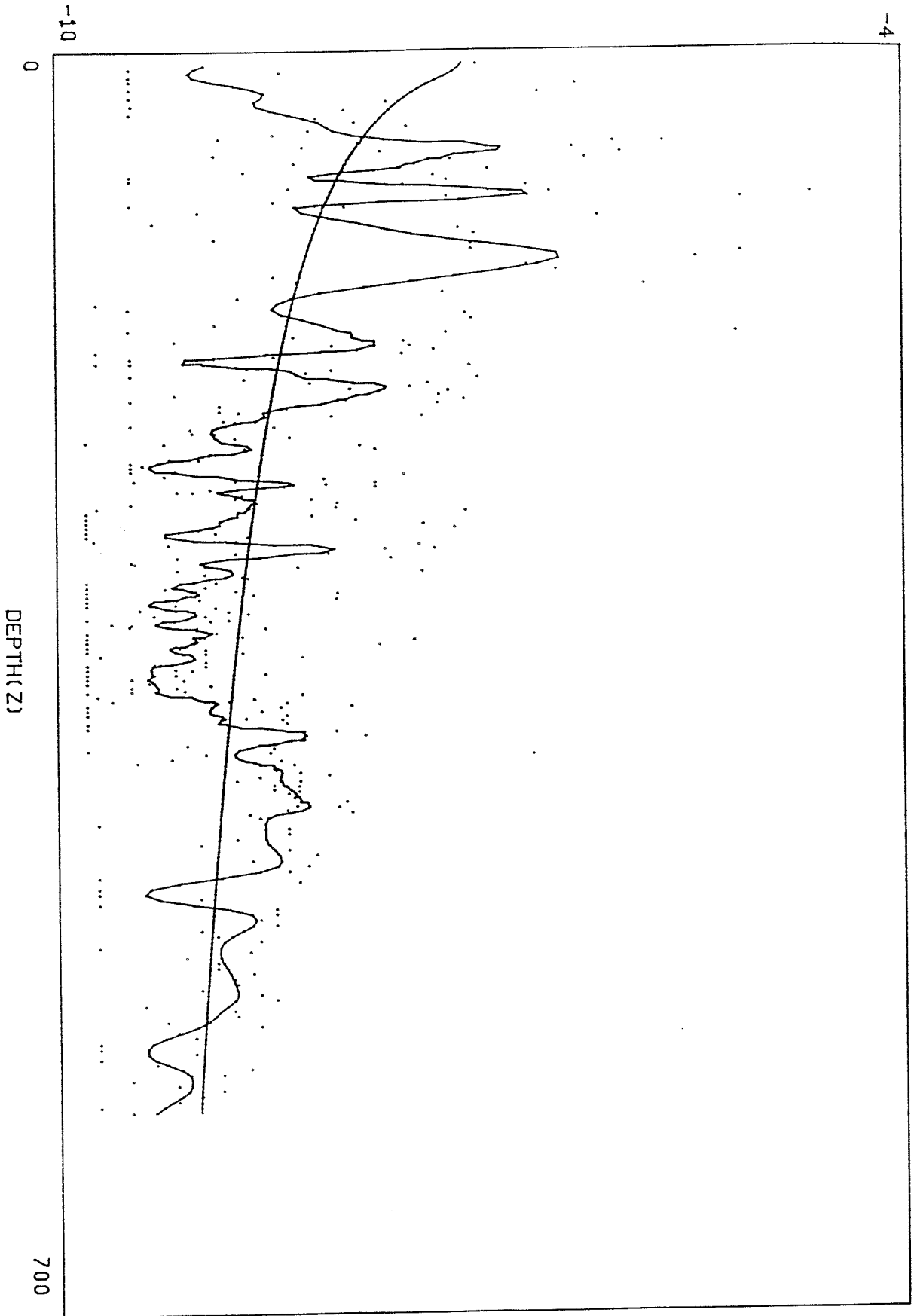
Box plot for boreholes KFI05, KFI06 and KFI07



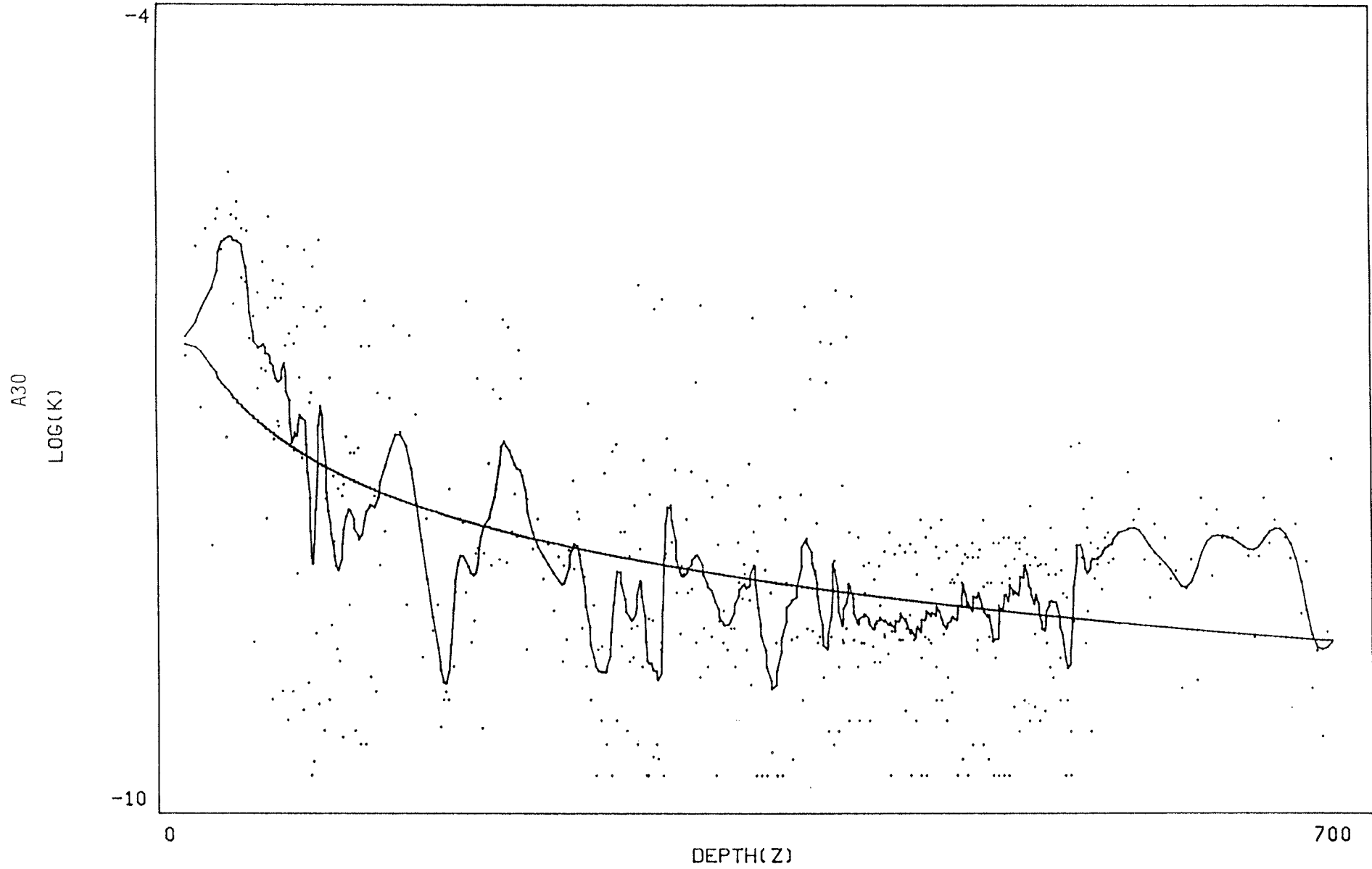
A29
LOG(K)

6:2

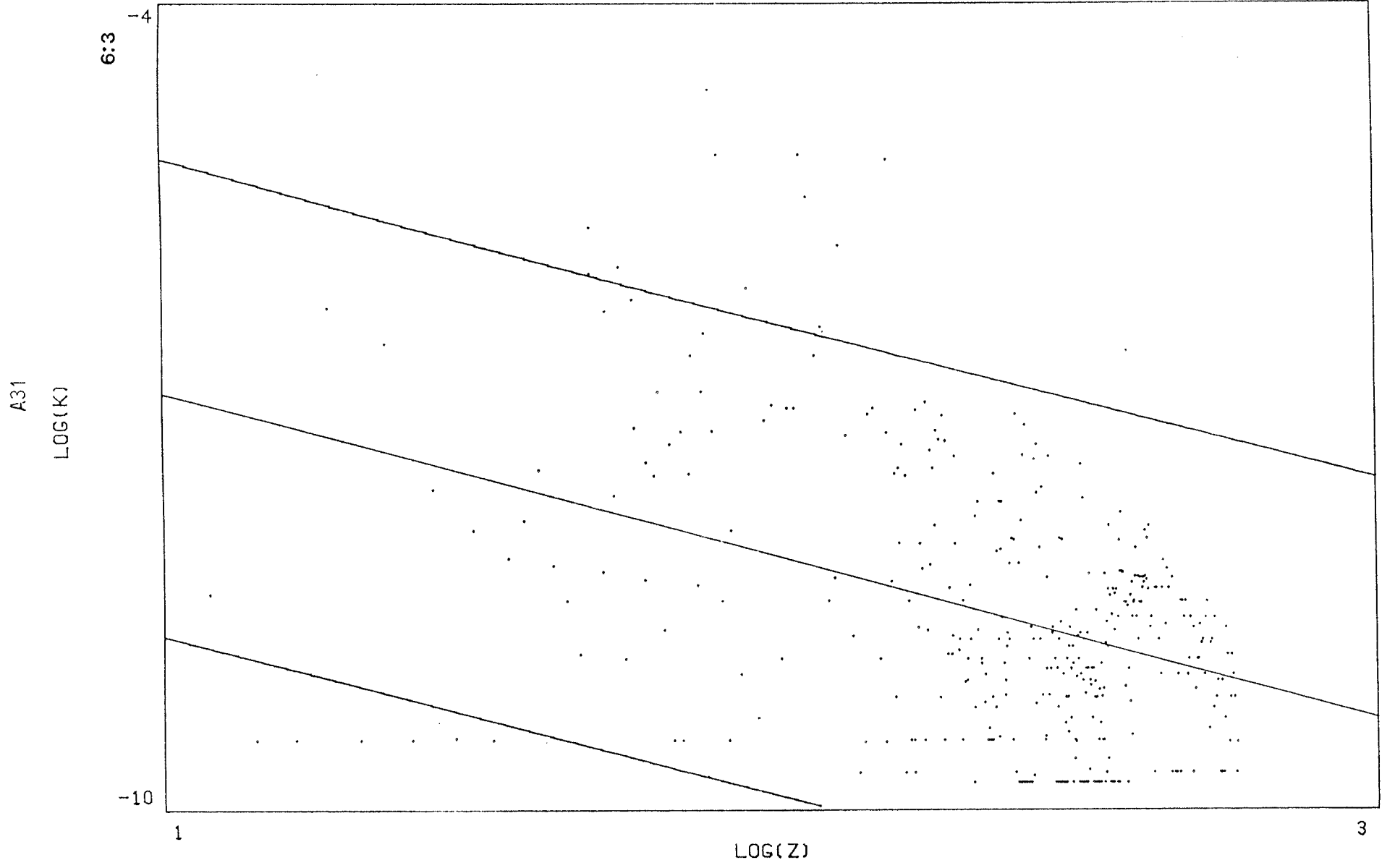
Boreholes KFI03, KFI04 and KFI08



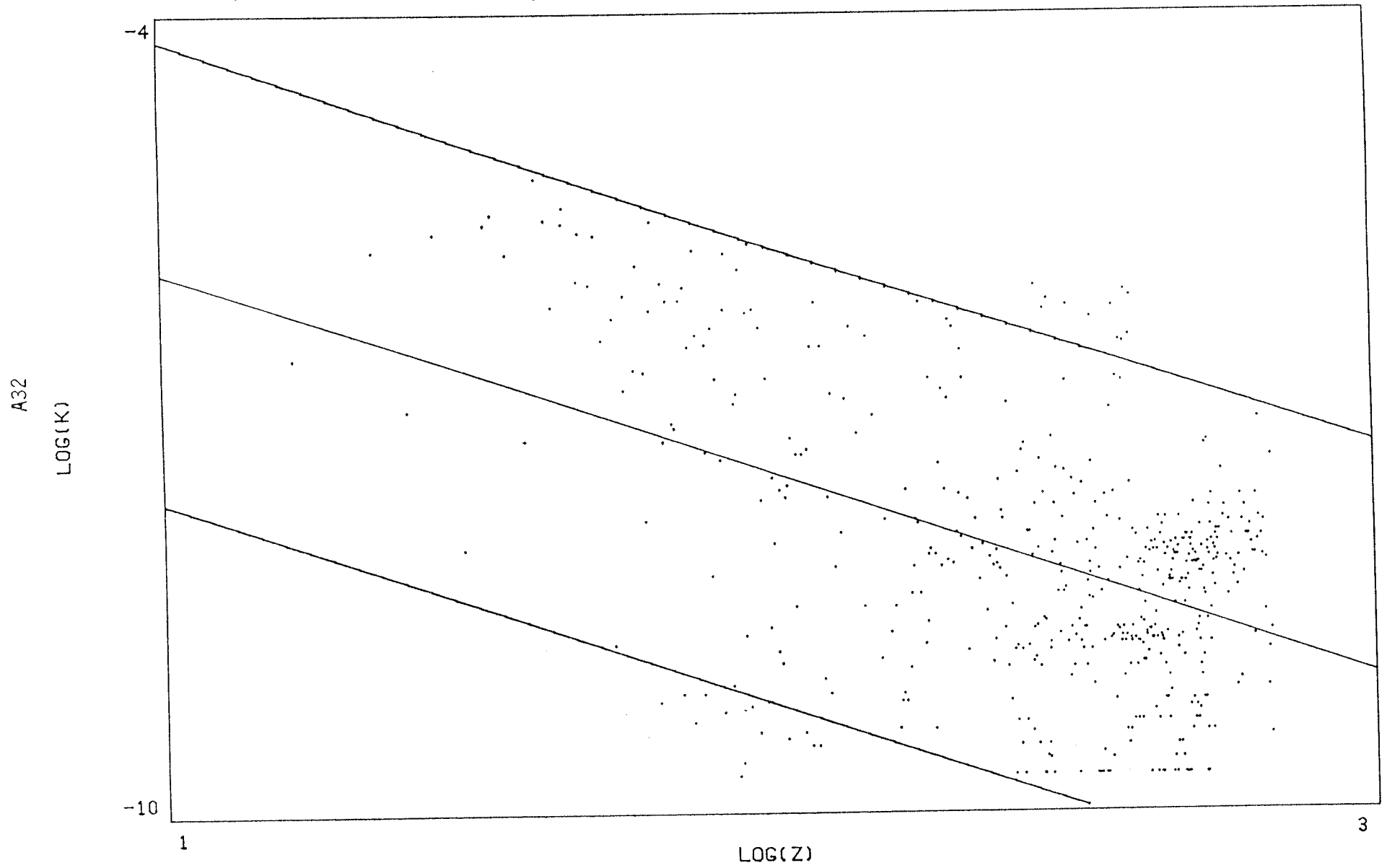
Boreholes KFI05, KFI06 and KFI07

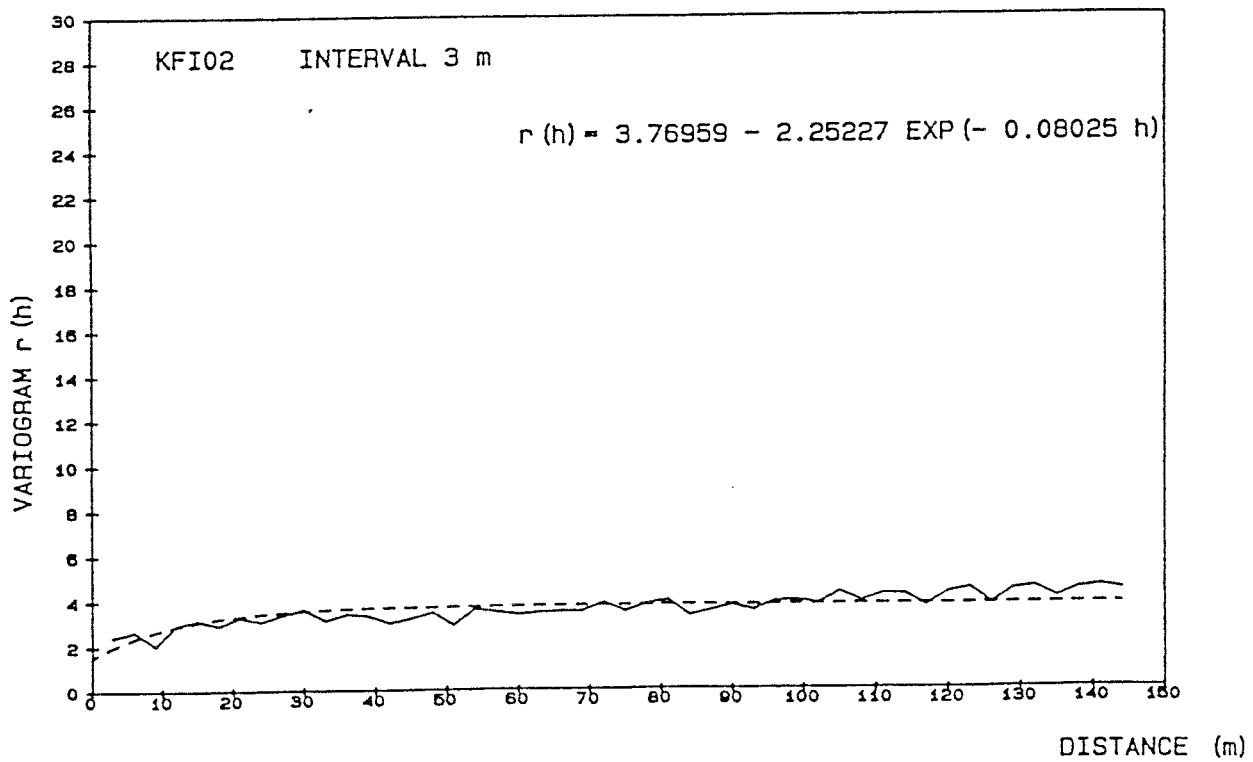
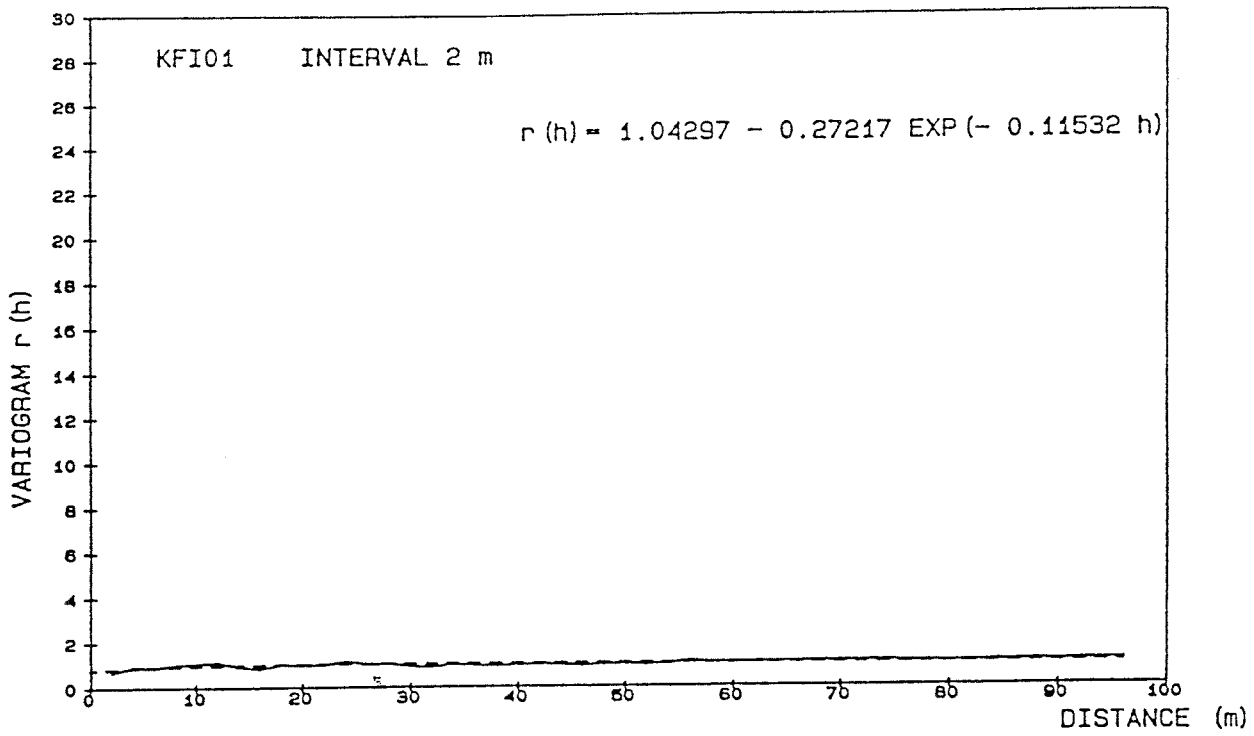


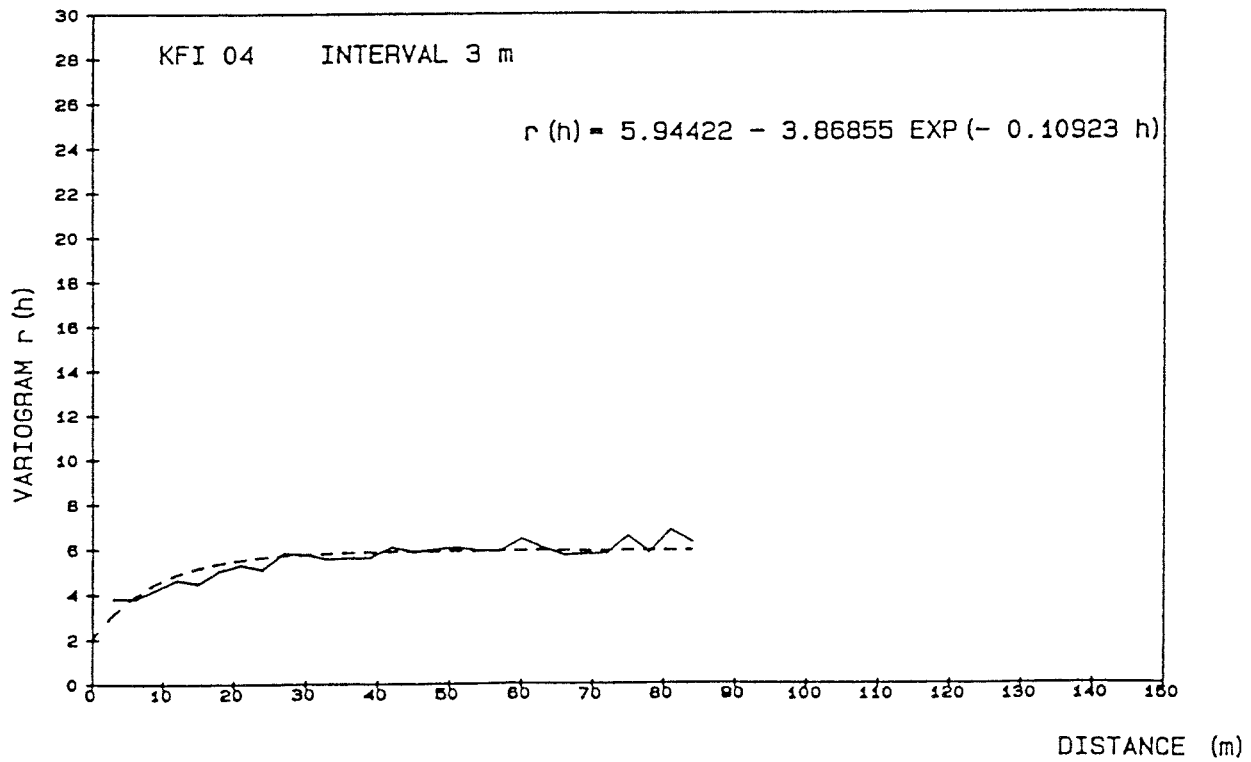
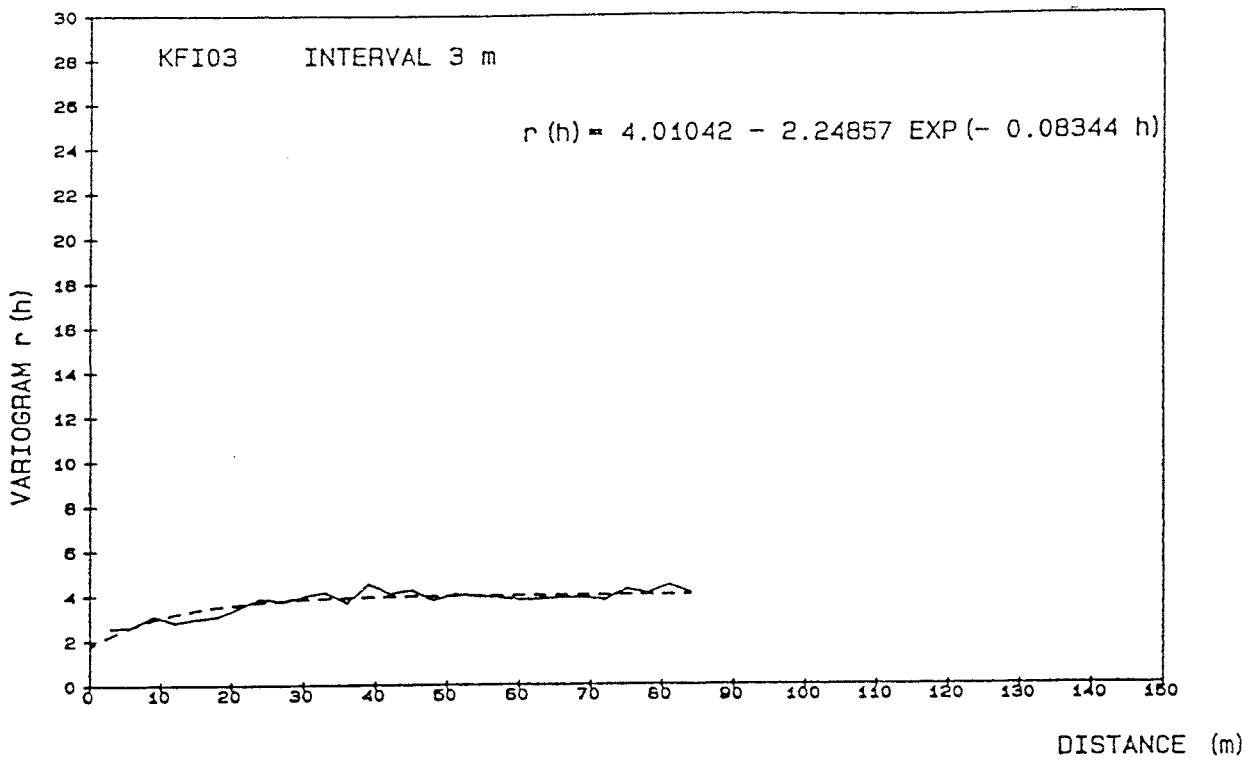
Boreholes KFI03, KFI04 and KFI08

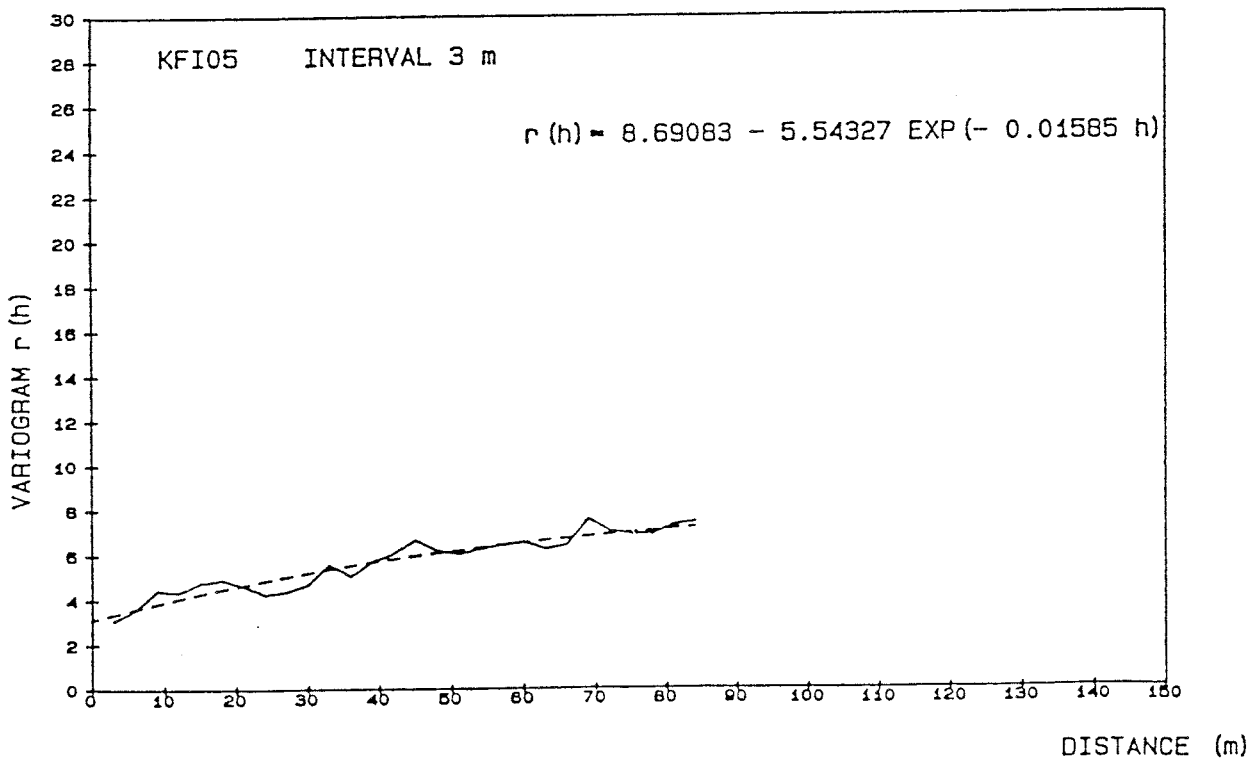
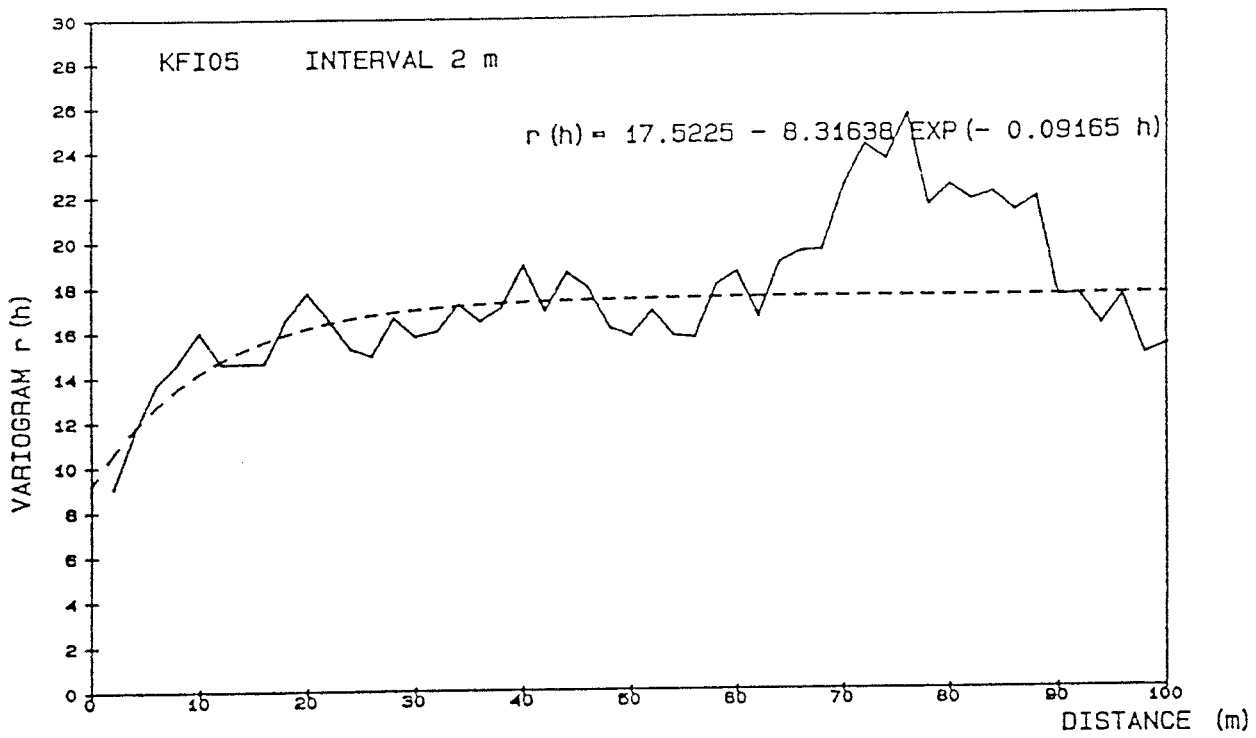


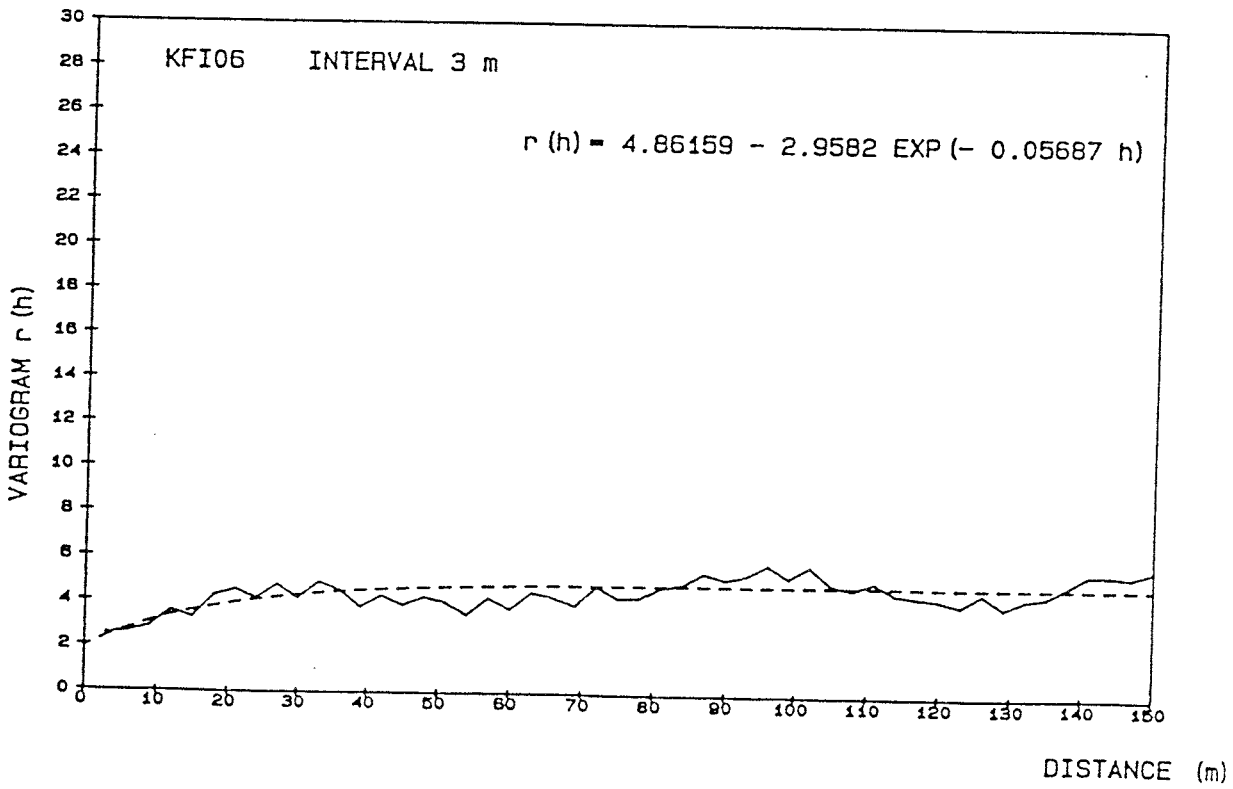
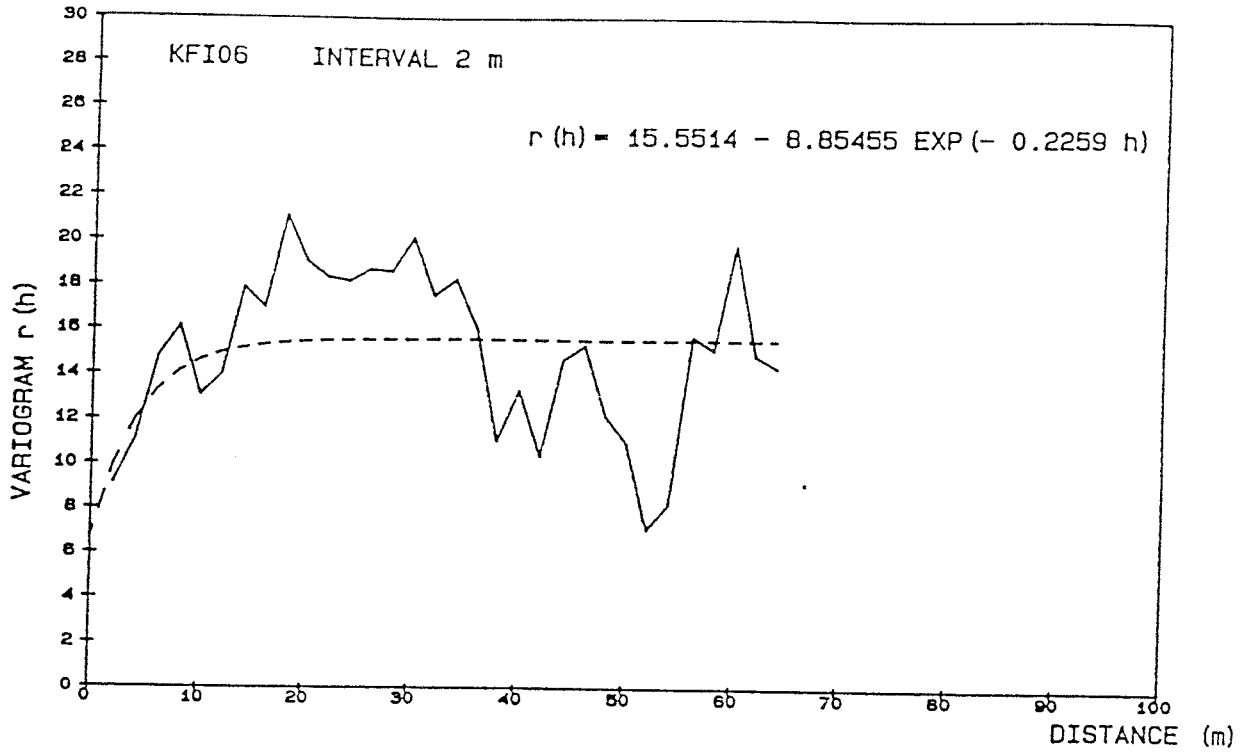
Boreholes KFI05, KFI06 and KFI07

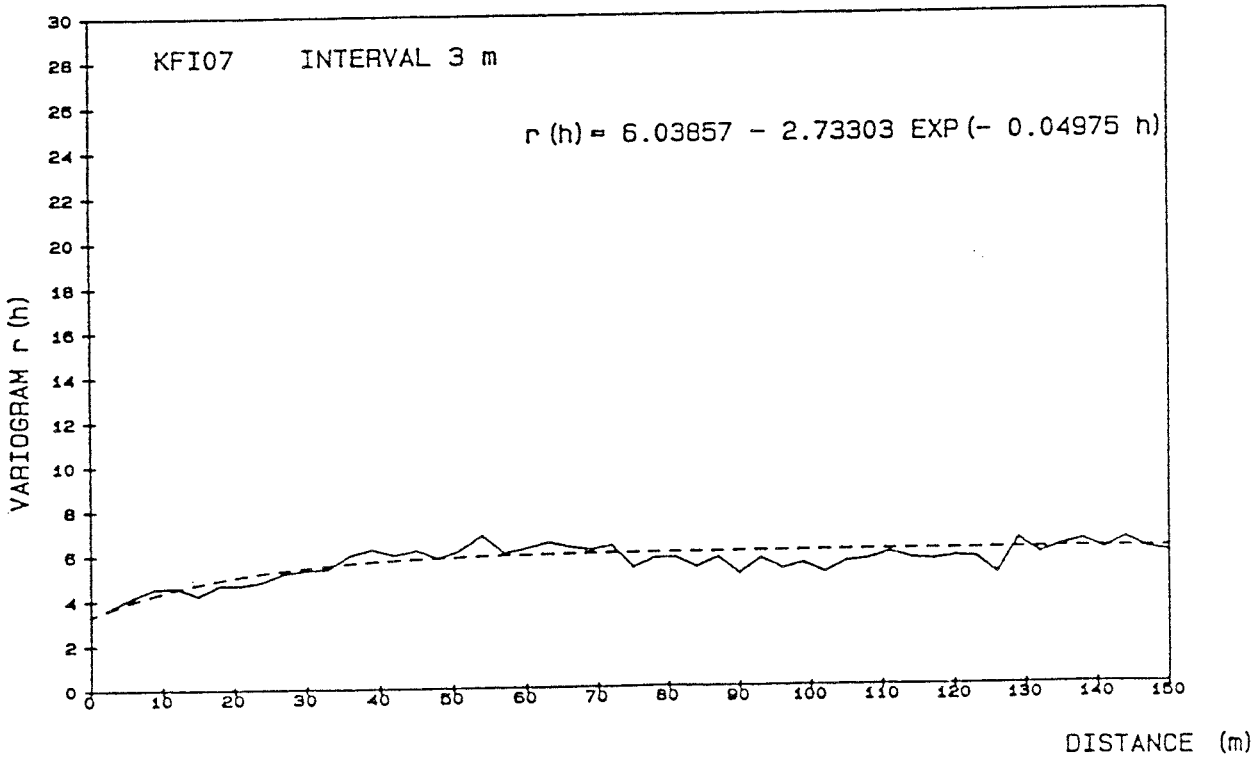
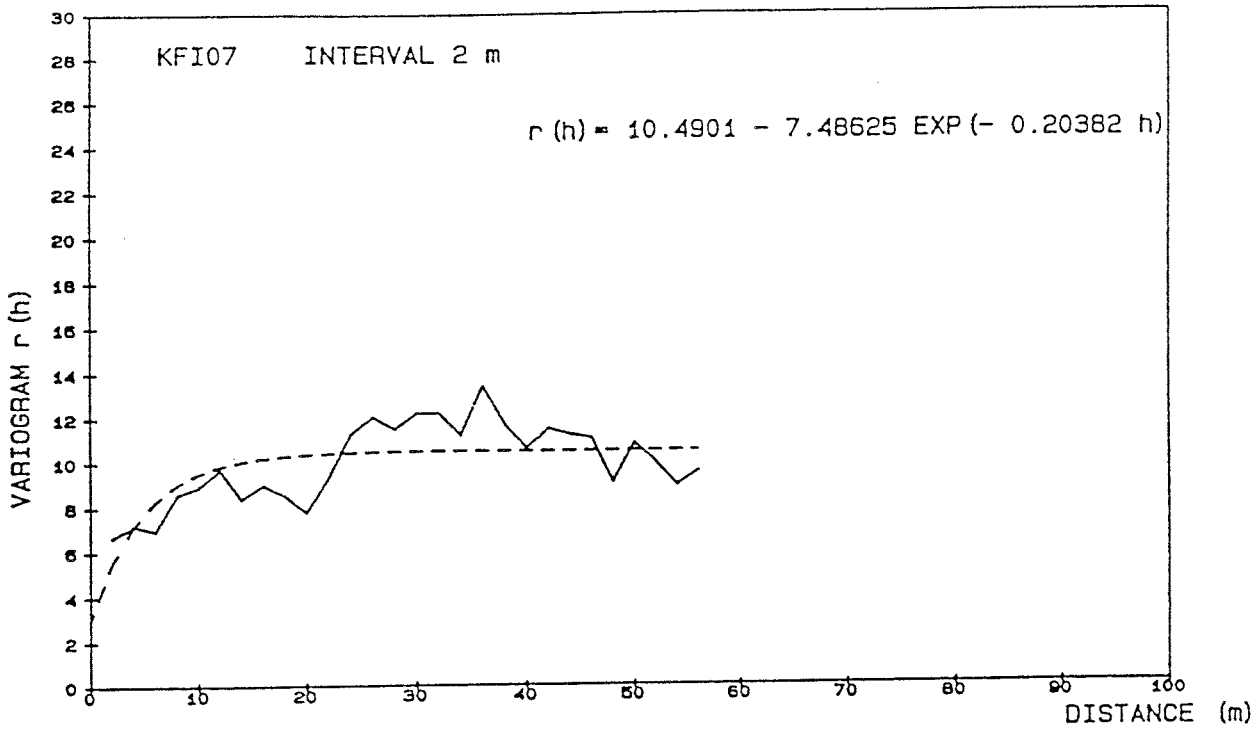


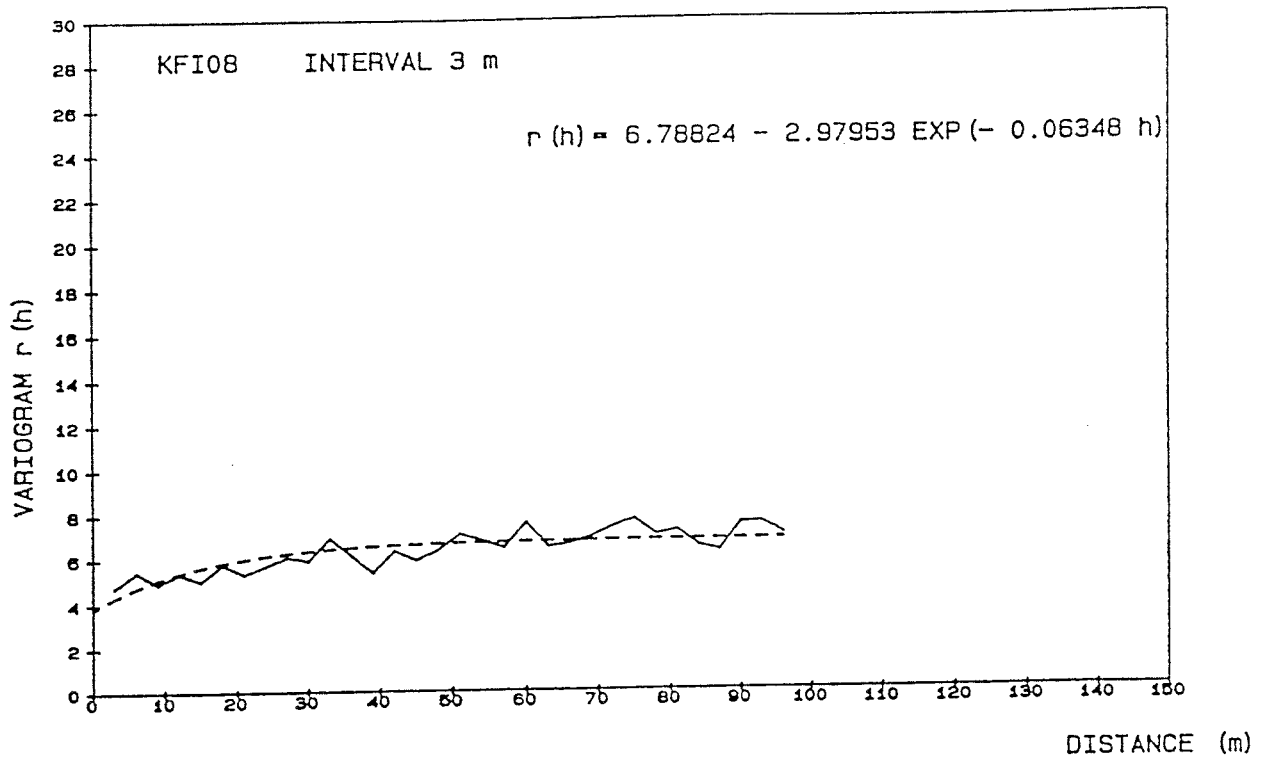


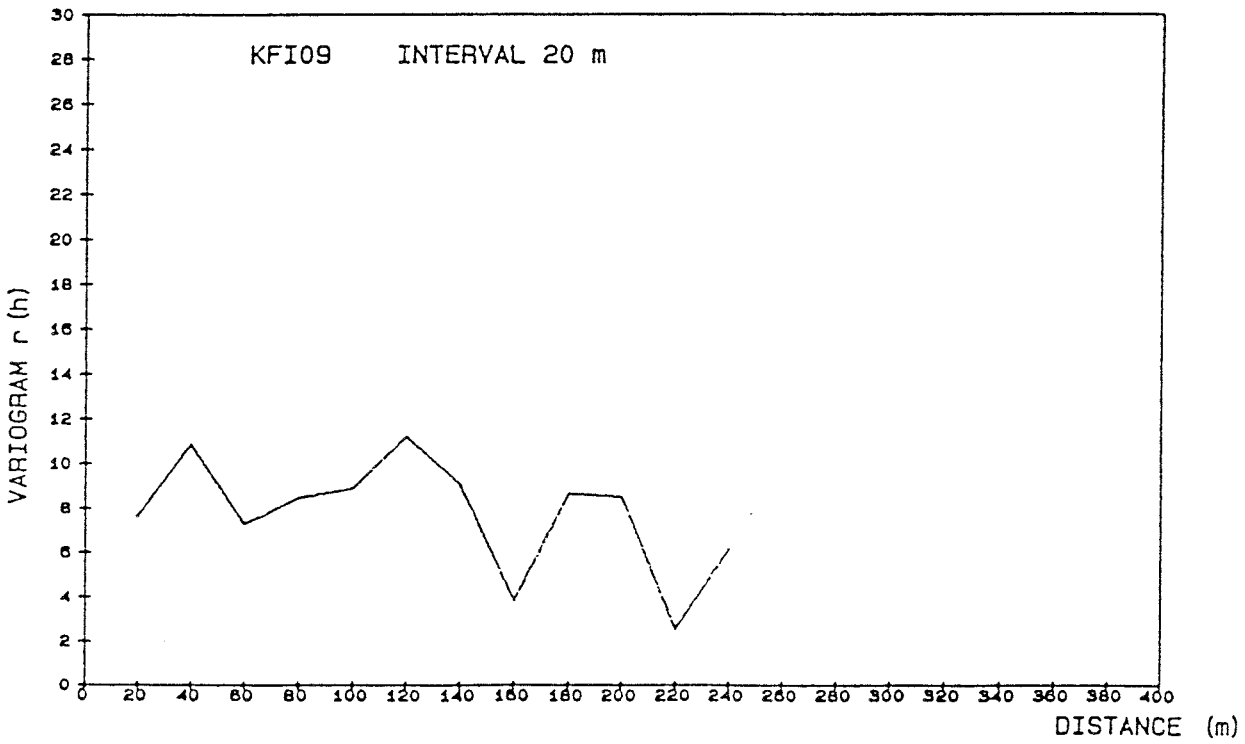
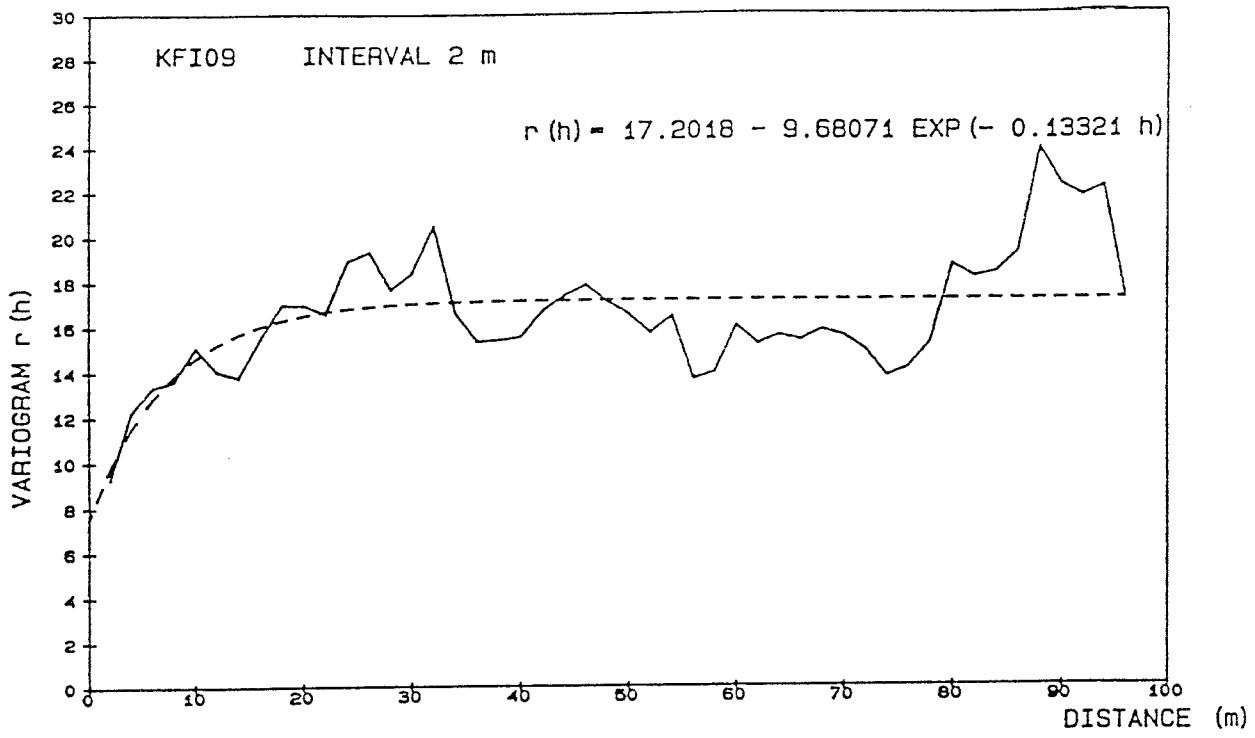


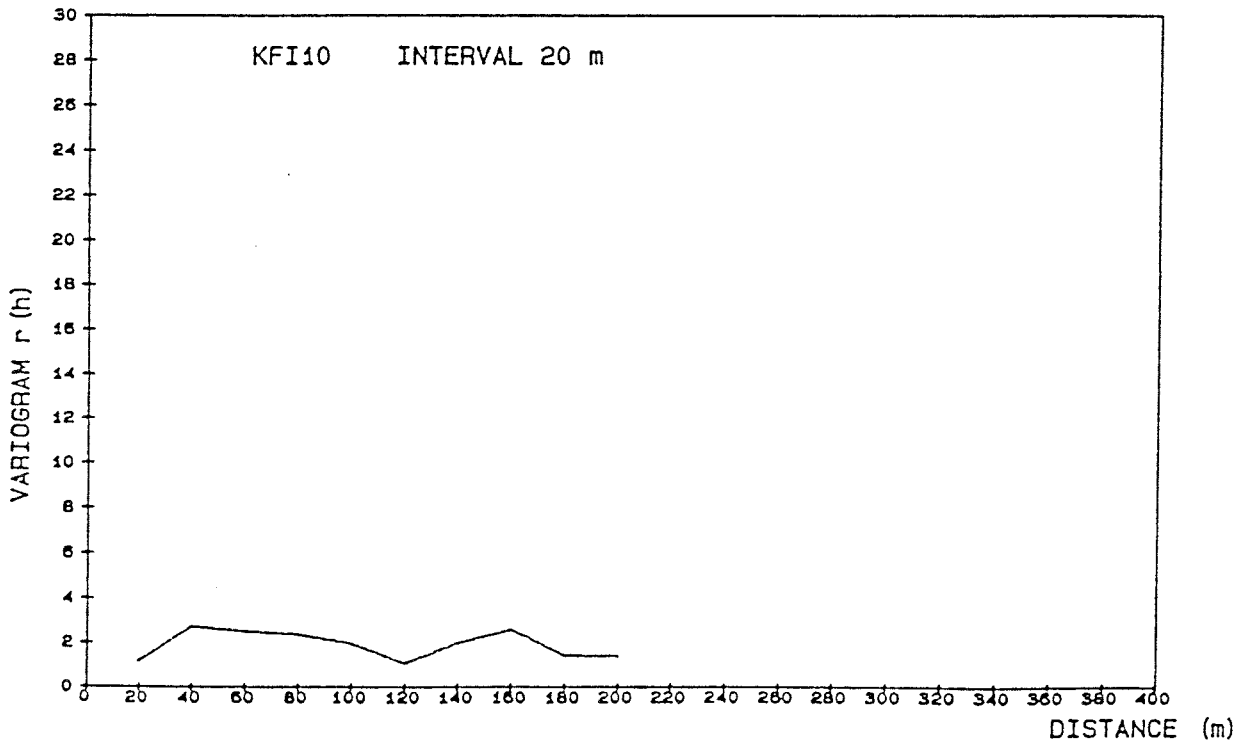
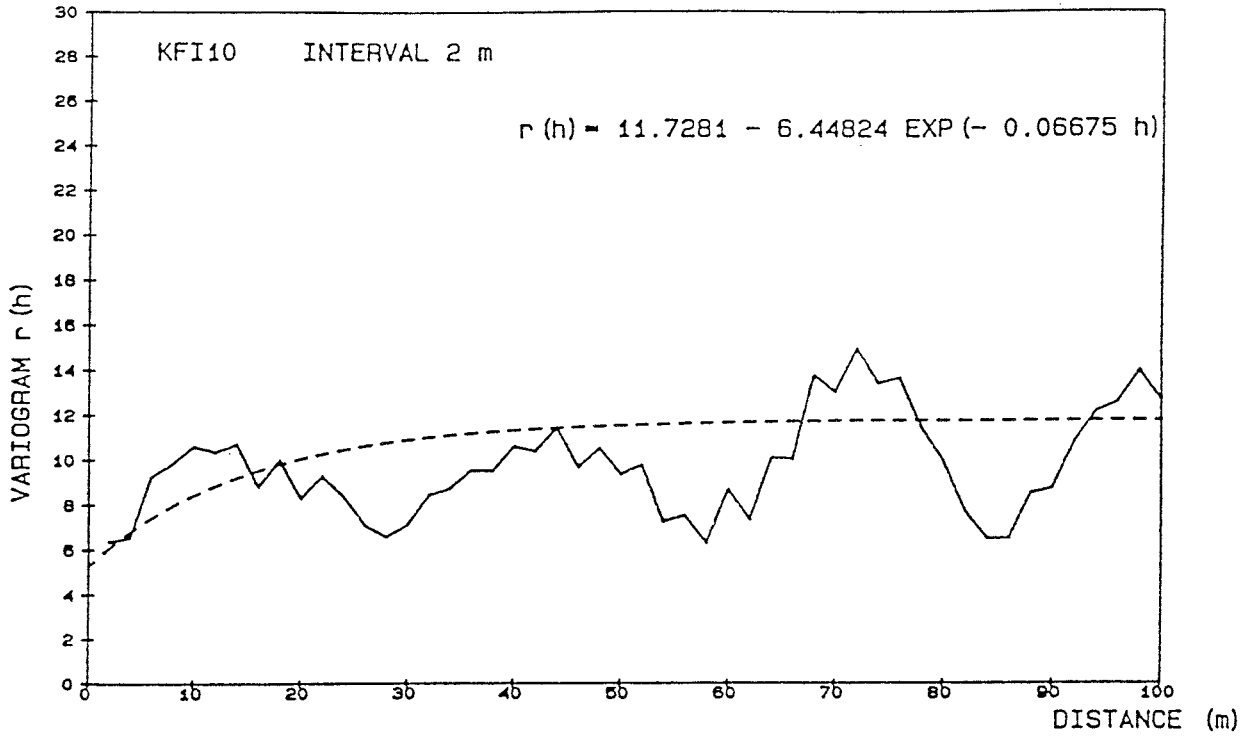


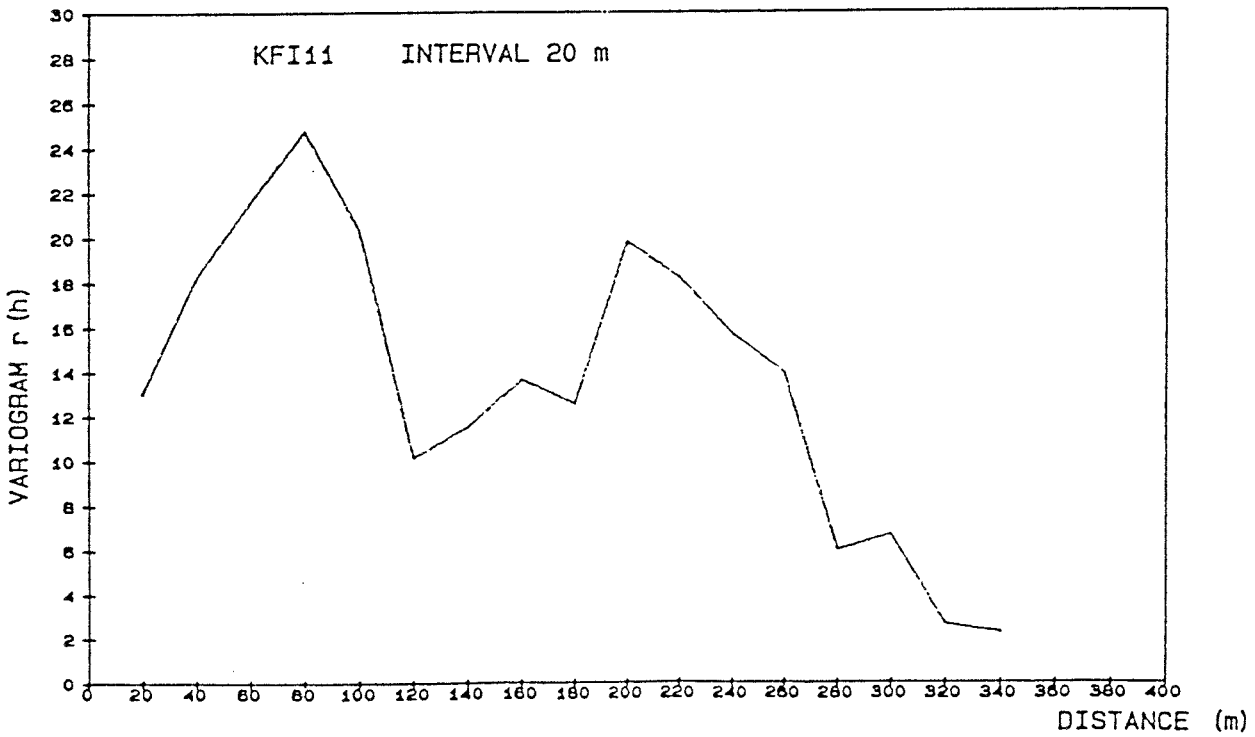
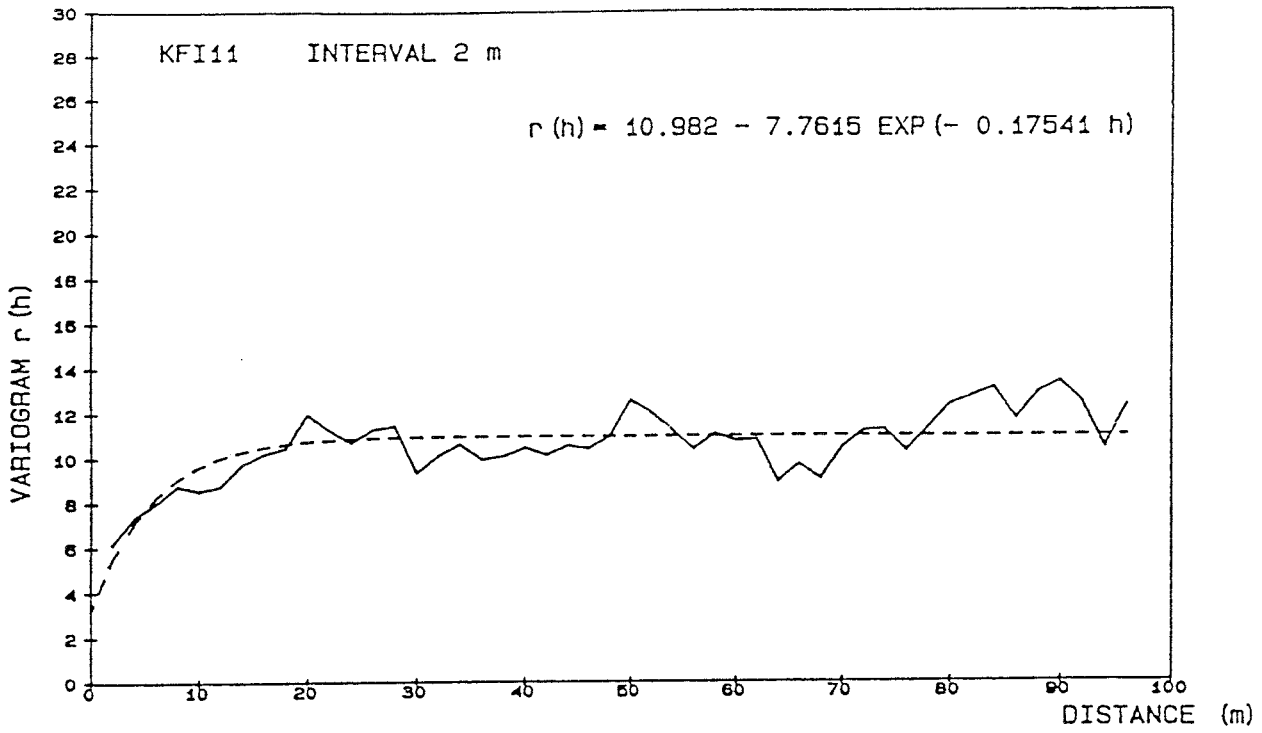


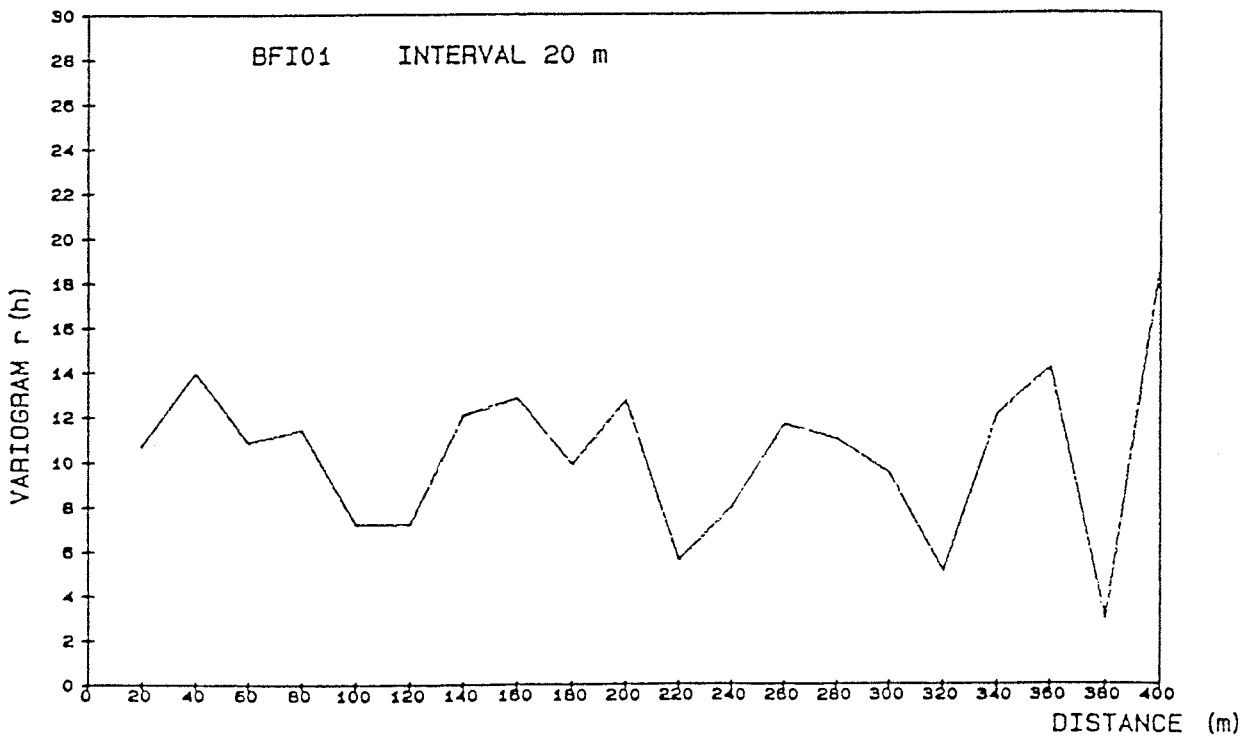
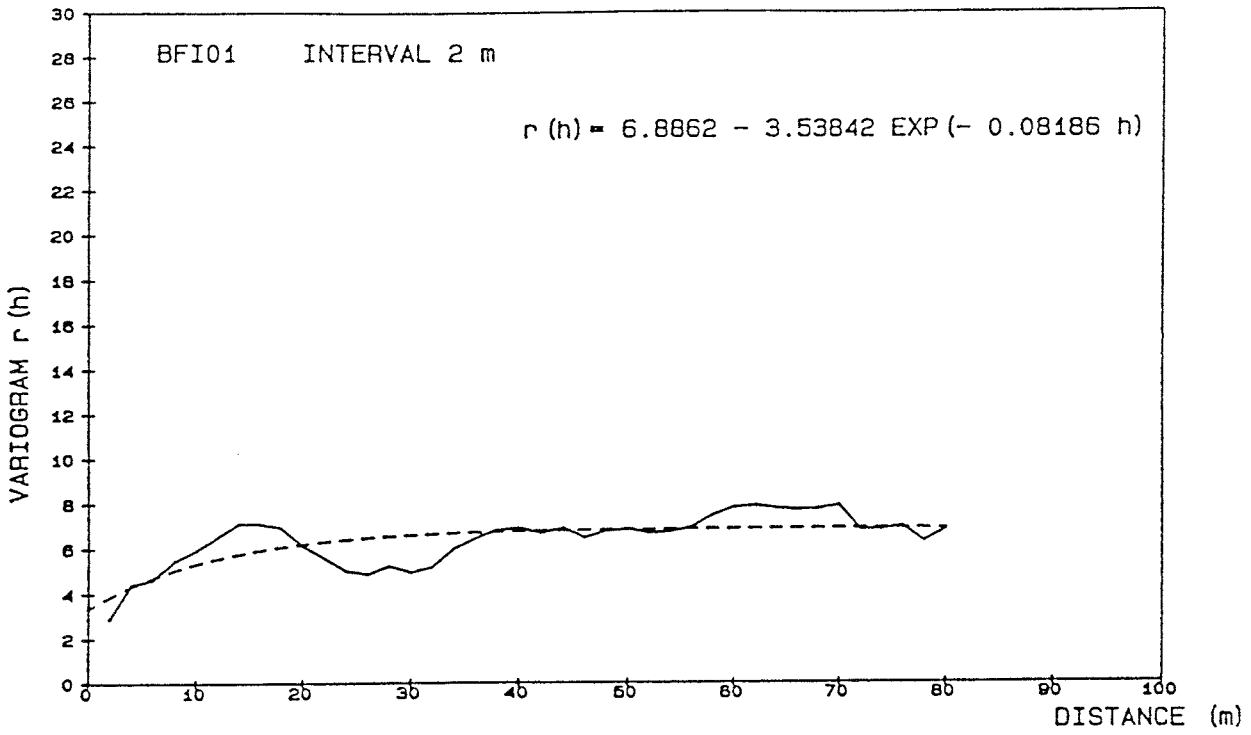


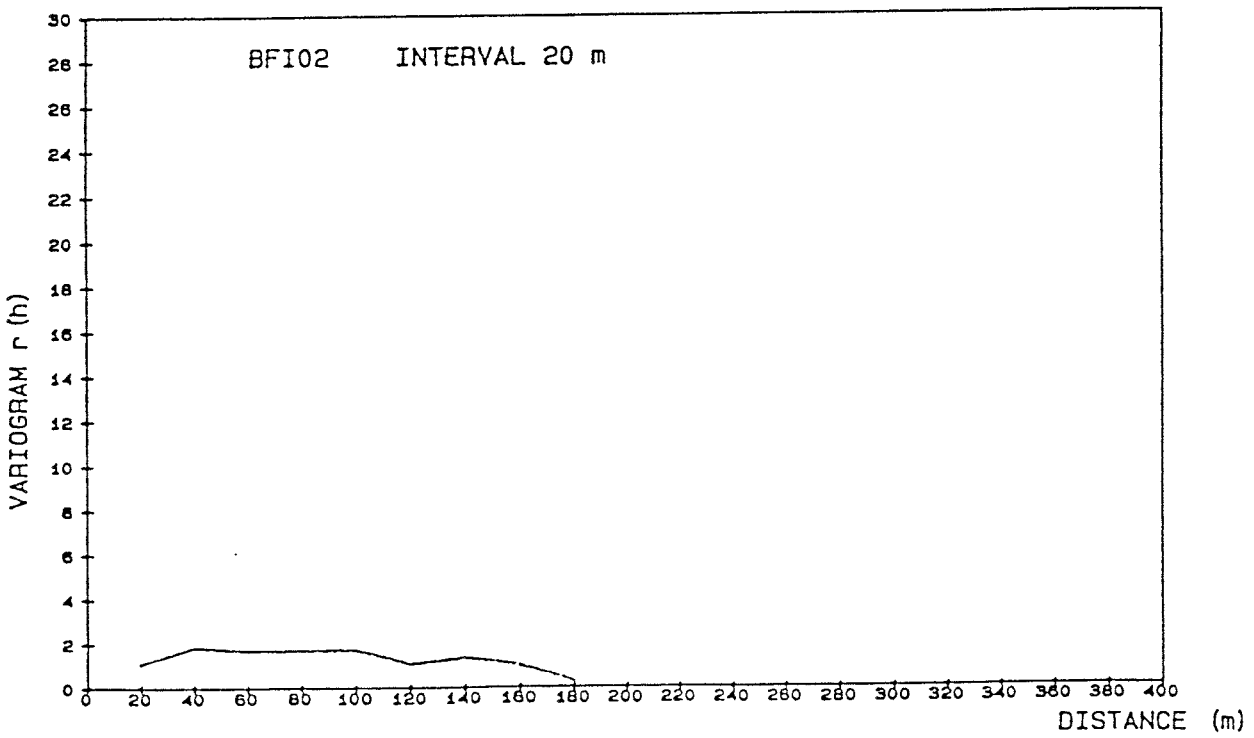
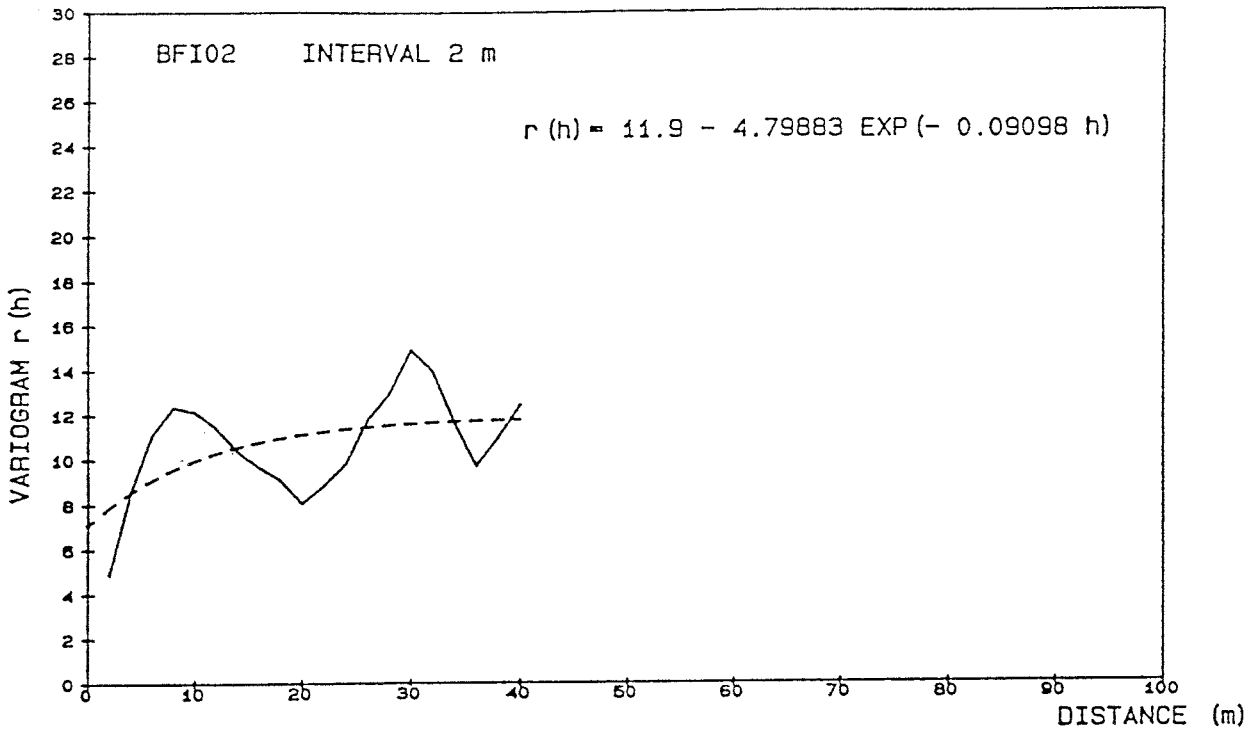












Bore- hole	Depth m	Date	Ca mg/l	Mg mg/l	Na mg/l	K mg/l	Mn mg/l	Fe2+ mg/l	Fe,tot mg/l	NH4 mg/l	HCO3 mg/l	Cl mg/l	F mg/l	SO4 mg/l	PO4 mg/l	NO3 mg/l	NO2 mg/l	SiO2 mg/l
KFI01	206	801009	59	7.5	44	2.5	.36	24	24	.05	314	10	1.4	1	.10	4.3	.07	17
		801014	61	7.0	45	2.5	.33	18	19	.03	320	11	1.3	1	.11	.13	<.01	18
		801021	60	7.0	50	2.7	.31	17	17	.06	322	13	1.4	1	.11	.09	<.01	18
KFI01	293	801030	58	8.0	50	2.8	.35	23	30	.07	325	9	1.3	1	.14	.06	<.01	17
		801105	59	7.5	56	2.9	.35	17	28	.04	325	18	1.5	1	.25	.07	<.01	18
		801111	50	6.5	88	2.8	.29	20	21	.06	350	37	1.5	1	.26	.03	<.01	16
KFI02	385	771203	30	4.5	92	4.4	.14		6.6	.11	325	24	1.5	2.1	<.01	.18	<.01	6.2
		771207	30	4.0	96	5.6	.10		7.8	.08	320	32	1.5	2.4	<.01	.22	<.01	6.0
KFI04	152	791026	23	6.0	180	2.9	.05		2.4	.13	383	136	3.3	47	.09	.04	.02	15
		791030	25	4.0	225	3.0	.04	1.8	1.8	.17	386	127	3.5	44	.07	.08	<.01	14
		791204	24	5.5	225	3.1	.06	4.8	5.1	.20	390	133	3.5	48	.06	.20	.01	13
		791212	23	9.5	210	3.1	.05	3.3	3.4	.17	389	124	3.5	46	.05	.10	.01	14
KFI04	247	800117	40	7.0	215	3.0	.06	3.2	3.2	.26	360	200	2.5	40	.06	.01	.01	14
		800123	76	10	275	4.0	.11	5.8	5.8	.29	335	360	2.5	51	.06	<.01	.02	10
		800229	24	4.0	170	2.8	.08	6.1	6.1	.20	390	74	2.1	30	.16	.09	<.01	16
KFI04	368	800314	23	4.0	165	2.7	.07	3.8	3.8	.21	388	72	2.1	30	.16	.09	<.01	16
		800328	23	4.0	165	2.8	.05	3.0	3.0	.20	387	70	2.1	28	.22	.09	<.01	17
		800426	22	4.0	165	2.8	.08	1.9	9.2	.24	397	72	2.6	25	.09	.04	<.01	13
		800429	22	4.0	165	2.7	.08	7.8	9.7	.23	395	72	2.0	29	.09	.04	<.01	15
KFI04	534	800507	22	4.0	165	2.9	.08	7.3	8.0	.23	395	75	2.2	29	.09	.02	.03	12
		800514	22	4.0	170	2.8	.07	6.8	6.8	.23	393	75	2.2	29	.08	.03	.03	13
		800521	22	4.0	170	2.8	.05	2.4	7.9	.22	393	75	3.0	19	.09	.03	.03	13
		800528	22	4.0	170	2.7	.06	5.9	5.9	.27	393	75	3.0	19	.08	.03	.03	14

A44

Bore- hole	Depth m	Date	Ca mg/l	Mg mg/l	Na mg/l	K mg/l	Mn mg/l	Fe2+ mg/l	Fe, tot mg/l	NH4 mg/l	HCO3 mg/l	Cl mg/l	F mg/l	SO4 mg/l	PO4 mg/l	NO3 mg/l	NO2 mg/l	SiO2 mg/l
KFI05	141	790814	650	89	900	10	.71		2.9	1.34	151	2650	.90	224	.05	.07	.02	8.6
		790911	640	89	900	10	.75		2.8	1.38	166	2520	1.1	225	.06	.05	.03	11
		791003	641	62	875	9.1	.75		3.1	1.37	161	2700	1.1	224	.05	.05	.02	12
		791018	643	79	900	9.1	.75		2.7	1.32	161	2700	1.1	197	.07	.03	.02	12
		791206	630	70	1000	10	.74	7.4	9.2	1.40	161	2580	1.2	236	.10	.11	.02	10
KFI05*	205	800118	955	110	1100	10	.59	3.2	3.7	.75	70	3500	.74	300	.13	<.01	.04	5.0
		800125	875	130	1100	10	.65	2.9	3.1	.85	84	3400	.90	325	.13	<.01	.03	10
		800129	875	110	1100	10	.66	3.0	3.0	.86	85	3400	.86	325	.14	<.01	.02	9.0
		800208	875	140	1100	10	.67	2.7	3.1	.87	85	3400	.82	320	.14	<.01	.03	10
		800215	900	110	1100	9.4	.67	3.4	6.2	.03	83	3450	.74	325	.13	.10	2.2	9.5
KFI05	297	800320	1440	100	1250	7.6	.41	3.5	3.5	.21	39	4580	.74	325	.16	.10	.02	9.5
		800328	1450	100	1300	7.5	.44	2.9	3.1	.21	39	4700	.75	330	.18	.10	.03	11
		800411	1530	80	1380	7.3	.46	2.2	2.5	.20	38	4500	1.2	288	.16	.02	.01	11
		800417	1500	70	1380	7.2	.47	2.4	2.4	.21	39	4650	1.3	300	.15	.04	.01	11
		800422	1500	70	1320	7.2	.50	2.5	7.0	.20	33	4650	1.3	300	.39	.02	.01	7
		800428	1500	80	1320	6.9	.47	2.2	2.2	.21	39	4750	1.4	300	.15	<.01	.01	11
KFI05	384	800514	1730	125	1480	8.0	.70	2.5	3.0	.44	39	5650	1.1	312	.16	.02	<.01	12
		800521	1790	100	1500	8.3	.70	2.4	3.4	.44	44	5650	1.1	324	.19	.02	<.01	11
		800528	1790	90	1460	8.2	.83	2.8	3.4	.48	41	5500	1.1	312	.17	<.01	<.01	12
KFI06	184	810716	554	69	922	16	.54		.91	.41	123	2500	.97	205	<.03		<.005	17
		810726	542	67	859	15	.55		.60	.43	122	2480	.96	207	<.03		<.005	17
		810730	555	67	866	15	.58		.39	.31	124	2480	.98	204	<.03		<.005	17
		810806	573	68	870	15	.57		.83	.40	124	2500	.89	204	<.03		.012	17
KFI06	250	810818	1219	120	1140	37	1.3		2.1	2.1	59	4650	1.2	340	<.02	<.1	<.005	14
		810908	1183	112	1134	34	1.2		1.8	2.1	75	4650	1.2	330	<.02	<.1	<.005	14
KFI06	398	810916	1893	24	1138	19	.08		.22	.02	9	5650	1.2	270	<.02	<.1	<.005	7
		811007	1936	31	1146	21	.17		.24	.09	16	5900	1.3	280	<.02	<.1	.005	9
KFI06	688	811022	1900	74	1520	28	.59		3.2	.13	36	5700	1.4	320	<.03	<.1	<.005	10
		811103	1900	75	1520	29	.60		2.3	.16	38	5800	1.5	320	<.02	<.1	<.005	12

Bore- hole	Depth m	Date	Ca mg/l	Mg mg/l	Na mg/l	K mg/l	Mn mg/l	Fe2+ mg/l	Fe,tot mg/l	NH4 mg/l	HCO3 mg/l	Cl mg/l	F mg/l	SO4 mg/l	PO4 mg/l	NO3 mg/l	NO2 mg/l	SiO2 mg/l
KFI07	123	800902	36	5.5	94	1.4	.13	2.9	2.9	.07	333	23	2.0	7.0	.03	.92	.12	16
		800919	23	4.0	118	1.2	.06	2.4	2.4	.06	332	29	2.0	10	.02	.12	<.01	14
		800927	32	4.0	105	1.4	.09	2.5	2.5	.08	334	27	2.3	8.0	.02	.12	<.01	16
KFI07	301	800910	57	7.5	164	1.6	.12	4.8	4.8	.09	314	173	1.6	18	.05	.93	.01	14
		800917	51	7.0	140	1.6	.14	4.6	5.0	.07	321	122	2.1	18	.06	.07	<.01	15
		801008	114	18	390	2.9	.06	.53	.57	.03	233	665	2.3	71	.03	1.78	.05	7.7
KFI07	322	801015	122	15	240	1.8	.12	.85	4.9	.04	283	445	2.0	38	.05	.04	<.01	10
		801022	96	13	195	1.7	.12	5.8	5.8	.05	300	320	2.1	32	.05	.04	<.01	14
		801028	107	16	224	1.8	.12	4.1	5.2	.04	292	380	2.0	35	.05	.05	<.01	14
KFI07	511	801105	145	18	280	2.2	.14	3.0	7.4	.03	278	545	1.5	51	.08	<.01	.01	12
		801111	149	14	275	2.1	.13	3.2	6.8	.02	277	555	1.5	47	.09	<.01	.02	12
		801119	142	17	275	2.0	.13	1.8	7.0	.11	278	555	1.5	49	.12	<.01	.04	12
KFI08	103	810716	37	12	286	12	.11		3.2	<.02	263	440	2.3	42	<.03		.37	12
		810726	40	12	295	12	.10		.95	.12	264	450	2.4	44	.04		.005	13
		810731	35	12	283	12	.11		2.9	<.02	257	400	2.3	41	.04		.005	13
KFI08	196	810818	1000	9.0	702	16	.19		2.2	<.02	68	3000	1.8	100	<.02	<1	.10	11
		810902	1200	12	872	12	.21		3.1	<.02	79	3400	1.8	110	<.02	<1	.043	10
		810908	1550	7.5	1042	9.7	.21		.95	<.02	30	4300	1.6	130	<.02	<1	<.005	10
KFI08	283	810923	1630	7.2	922	13	.22		.68	<.02	18	4550	1.4	140	<.02	<1	<.005	9
		811012	1664	6.7	919	13	.23		.84	<.02	13	4500	1.4	130	<.02	<1	<.005	9
KFI08	395	820113	1783	4.2	903	13	.14		.70	<.02	21	4600	1.6	130	<.02	<1	<.005	7
		820121	1807	4.4	943	13	.14		.10	<.02	25	4650	1.6	140	.02	<1	<.005	7
		820128	1761	4.0	962	12	.14		.25	<.02	21	4400	1.6	140	.03	<1	<.005	8
		820203	1625	3.5	1001	11	.13		.20	<.02	11	4400	1.6	120	<.02	<1	<.005	8
FS	993	780502	16	1.5	3	.7	.10		.78	.19	37	5	.10	7.2	.01	.57	.01	4.8
		780502	16	1.5	2	.6	.23		.78	.21	37	5	.10	6.6	.01	.63	.01	5.2
		780502	16	1.5	3	.7	.23		.78	.21	38	5	.10	7.2	.01	.66	.01	5.2

FINNSJON - Dating parameters

Bore-hole	Depth m	Date	Age BP year	Age BP corr C13 year	$\delta^{13}\text{C}$ o/oo	δ^{18} carbonate o/oo	$\delta^{18}\text{O}$ water o/oo	Tritium TU	Deuterium o/oo
KFI01	206	801011	1760	2035	-8.2		-11.6	38	-87
KFI01	206	801014	1825	2065	-10.3	11.8	-11.6	40	-88
KFI01	206	801022	1935	2185	-9.7	13.4	-11.6	50	-90
KFI01	293	801104	2275	2505	-10.8	4.2	-11.6	46	-88
KFI01	293	801111	2305	2570	-8.9	9.8	-11.6	40	-87
KFI02	385	771203		3730	-12.9	9.8			
KFI02	385	771207		3785	-11.9	13.5			
KFI02	504	771203		3730	-13.0	9.8			
KFI04	152	791029	6815	7035	-11.7		-11.3	6	
KFI04	152	791203	6850	7055	-12.5		-11.3	7	
KFI04	152	791214	6590	6805	-11.8		-11.3	6	-83
KFI04	152	791221	6555	6775	-11.7	10.4	-11.4	6	-63
KFI04	247	791221	6555	6775	-11.7	10.4			
KFI04	247	800117	5835	6035	-12.6	7.8	-11.7	10	
KFI04	247	800125	5920	6125	-12.3	9.2	-11.7	7	
KFI04	247	800229	5340	5540	-12.8	8.4	-11.5	11	-81
KFI04	368	800427	5205	5410	-12.3	10.8	-11.4	13	-85
KFI04	368	800429	5185	5385	-12.6	10.4	-10.9	14	-85
KFI04	534	800507	5295	5505	-12.2	11.1	-11.3	13	-85
KFI04	534	800514	5182	5380	-12.7	8.1	-11.5	14	-85
KFI04	534	800521	5050	5250	-12.8	9.2	-11.4	10	-85
KFI04	534	800529	5100	5310	-12.2	9.8	-11.6	13	-85
KFI05	141	790912	9350	9595	-10.1	5.2		<3	
KFI05	141	791002	10490	10730	-10.3	3.8		<3	
KFI05	141	791018	9700	9925	-11.3	4.8	-11.6	<3	
KFI05	205	800129	10465	10715	-9.7	4.6	-10.5	7	-86
KFI05	205	800215	10240				-10.9	7	-86
KFI05	297	800417	4345	4510	-14.6	1.6	-11.8	5	-88
KFI05	384	800520	10380				-12.2	<3	-88

FINNSJÖN - Dating parameters

Bore-hole	Depth m	Date	Age BP year	Age BP corr C13 year	$\delta^{13}C$ o/oo	$\delta^{18}O$ carbonate o/oo	$\delta^{18}O$ water o/oo	Tritium TU	Deuterium o/oo
KFI06	184	810716				17.6		4	
KFI06	184	810718	8913	9145	-10.9	3.4			
KFI06	184	810806	13150			17.6		<3	
KFI06	250	810818				18.4		<3	
KFI06	250	810908				18.7		<3	
KFI06	398	810916				17.8		<3	
KFI06	398	811007				17.8		<3	
KFI06	688	811022				17.7		<3	
KFI06	688	811104				17.7		<3	
KFI07	123	800827	3765	3935	-14.3	12.0	-11.8	11	-86
KFI07	123	800831	3760	3930	-14.4	11.3	-11.8	11	-87
KFI07	123	800902	3735	3925	-13.3	13.3	-11.6	13	-87
KFI07	301	800913	3910	4080	-14.5	8.0	-11.8	10	-87
KFI07	301	801008	4515	4700	-13.6	10.2	-11.7	3	-90
KFI07	301	801018	4225	4400	-14.0	9.8	-11.8	12	-87
KFI07	322	801023	4590	4785	-13.1		-11.8	11	-88
KFI07	322	801028	4005	4200	-13.1	12.0	-11.8	11	-88
KFI07	511	801106	4085	4265	-13.9	6.3	-12.0	10	-89
KFI07	511	801111	4275	4365	-14.0	1.8	-11.9	11	-89
KFI07	511	801119	4440	4610	-14.6	3.0	-11.9	8	-89
KFI08	103	810716	5770	5960	-13.4	18.2		17	
KFI08	103	810731				18.3			
KFI08	103	810806	5530	5715	-13.7	5.9			
KFI08	103	810807						15	
KFI08	196	810818	6360	6550	-13.2	3.5			
KFI08	196	810818				17.8		6	
KFI08	196	810909				17.2		<3	
KFI08	283	810922				17.0		<3	
KFI08	283	811013				17.1		<3	
KFI08	395	820115				17.1		<3	
KFI08	395	820203				17.3		<3	

Groundwater physico-chemical parameters from boreholes KFI09 and BFI01, Finnsjön.

Borehole	Surface Water	KFI09	KFI09	KFI09	KFI09	BFI01	BFI01	BFI01	BFI01	BFI01	BFI01
Sampling Int (m)	0	94	114	182	360	71-85	169-191	234-247	284-294	335-385	439-459
Date Collected	841112	850311	850224	850215	850205	860408	860507	860528	861112	860625	861025
Temperature (°C)	7.0										
pH (lab)	5.9	7.3	7.4	7.7	7.4	6.9	7.2	7.6	6.9	7.1	6.6
pH (field)	ND	7.3	7.5	7.4	7.6	6.9	7.7	7.7	6.8	7.3	7.0
Cond. (mSm)	4.12	270	656	860	1410	54	415	531	1570	1650	1660
Eh (mV)	ND	-245	-300	-212	ND	+40	-320	-270	+400	+340	+400
Alkalinity (mg/l HCO ₃ ⁻)	7	285	116	160	32	220	200	260	59	59	48
Dissolved O ₂ (mg/l)	ND	0	0	0	0	0	0	0	7	2	4
Element	mg/l										
Ca	5.9	115	ND	700	1691	76	270	320	1500	1500	1600
Mg	8.81	16	ND	91	84	6.3	36	40	126	140	120
Na	2.6	415	ND	960	1510	23	610	650	1600	1700	1700
K	0.04	5.8	ND	15	7.4	3.2	6.5	8.7	15	15	13
Fe (II)	0.58	0.56	0.36	1.07	0.34	8.86	0.50	0.87	0.009	<0.01	0.005
Fe (tot)	0.97	0.56	0.35	1.08	0.35	9.01	0.51	0.90	0.022	0.01	0.016
Al	0.8	0.02	ND	0.003	0.18	0.06	0.006	0.013	0.024	0.16	0.022
Mn	0.006	0.19	0.45	0.82	0.36	0.50	0.37	0.42	1.2	1.0	0.8
SO ₄	4.7	175	ND	210	326	8.3	150	140	380	400	380
F	0.13	3.4	ND	7.2	9.1	0.6	1.8	2.3	1.1	1.2	1.2
Cl	2	680	2125	2800	5150	61	1310	1500	5200	5500	5500
Br	-	2.03	ND	13.5	27.1	0.3	4.5	7.0	26.0	29.0	29.0
I	<0.01	0.01	ND	0.03	0.07	<0.002	0.020	0.035	0.070	0.120	0.120
NO ₃	0.28	0.02	ND	0.019	0.01	0.006	<0.005	0.005	<0.005	<0.005	<0.005
PO ₄	0.01	0.001	0.002	0.003	0.004	0.001	0.001	<0.002	<0.005	0.002	<0.005
NH ₄	ND	0	ND	1.1	ND	0.15	0.34	0.63	0.45	0.71	0.35
S	ND	0.22	ND	0.44	0.03	<0.01	0.01	<0.01	0.01	<0.01	<0.01
Si	2.8	7.6	1.75	4.6	7.6	6.2	8.3	7.5	5.5	6	5.4
TOC	62	18	ND	7.5	1.0	16	12	6.9	68	4.2	18
U (ppb)	ND	2.1	ND	1.6	8.2	4.57	12.78	3.90	114.32	10.70	15.63
²³⁴ U/ ²³⁸ U	ND	4.1	ND	3.1	5.0	1.6	2.2	3.3	1.7	2.0	1.9
² H (‰)	-80.5	-79.0	ND	-86.4	-89.9	-88.2	-85.2	-85.7	-89.0	-86.9	-88.7
				-86.8							
				-84.0	-87.4						
¹⁸ O (‰)	-12.1	-9.8	ND	-10.4	-11.2	-12.0	-11.6	-11.7	-11.5	-11.8	-11.8
				-10.9							
				-11.0	-11.1						
³ H (TU)	31±2	8±1	ND	<3	<3	36±3	5±2	<3	<3	<3	<3
¹⁴ C (‰ modern)	ND	ND	ND	22.60	ND	85.30	33.02	37.45	ND	19.07	28.75

ND = Not determined

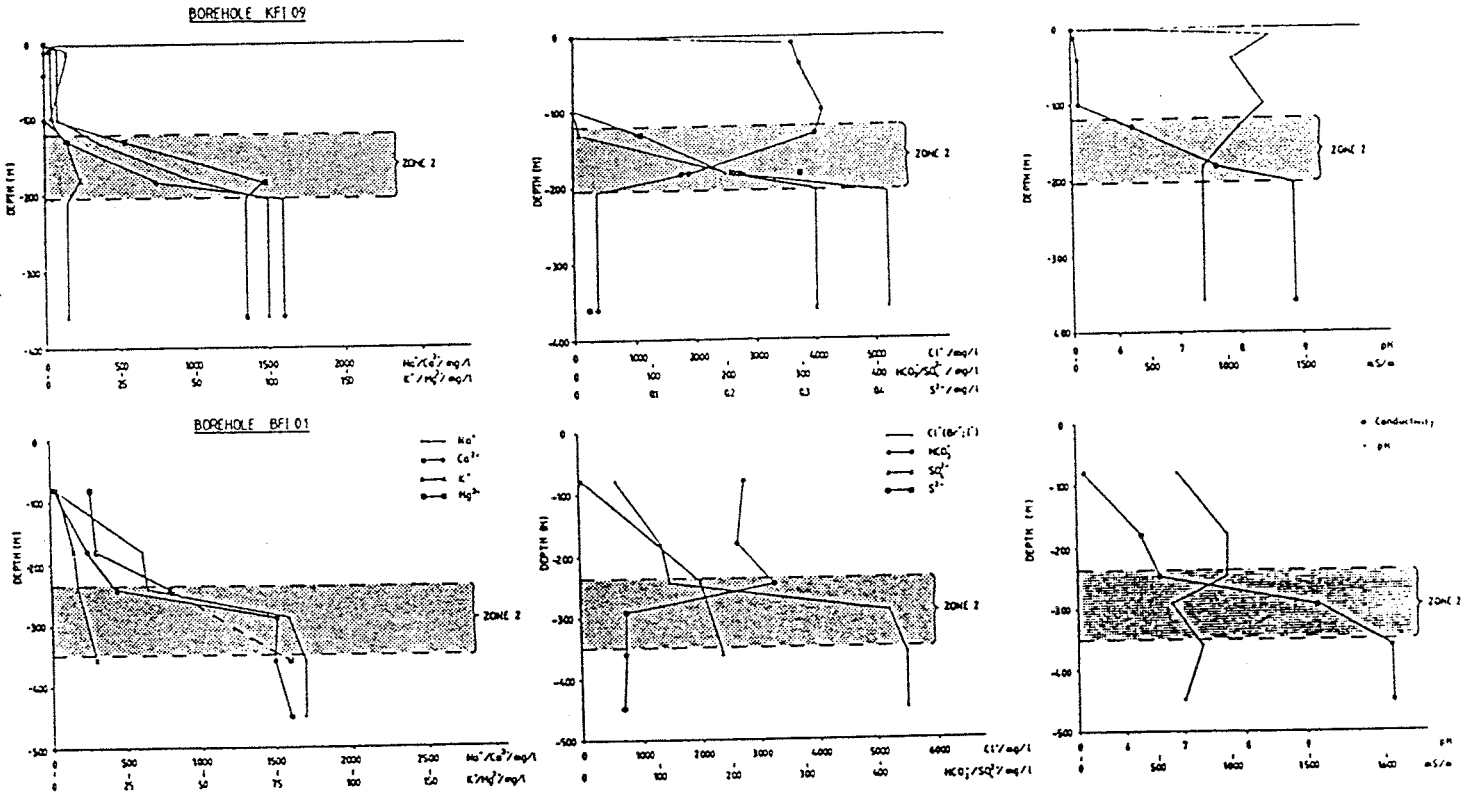
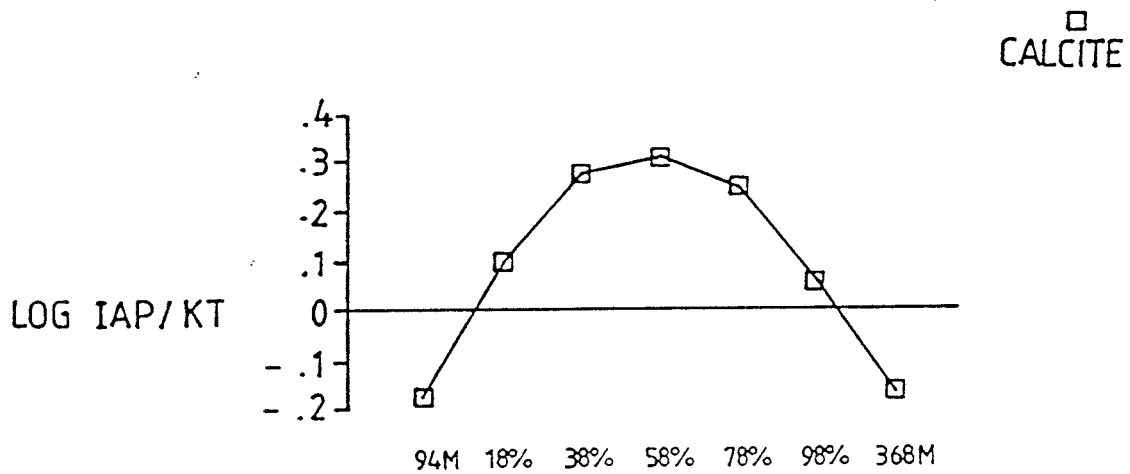
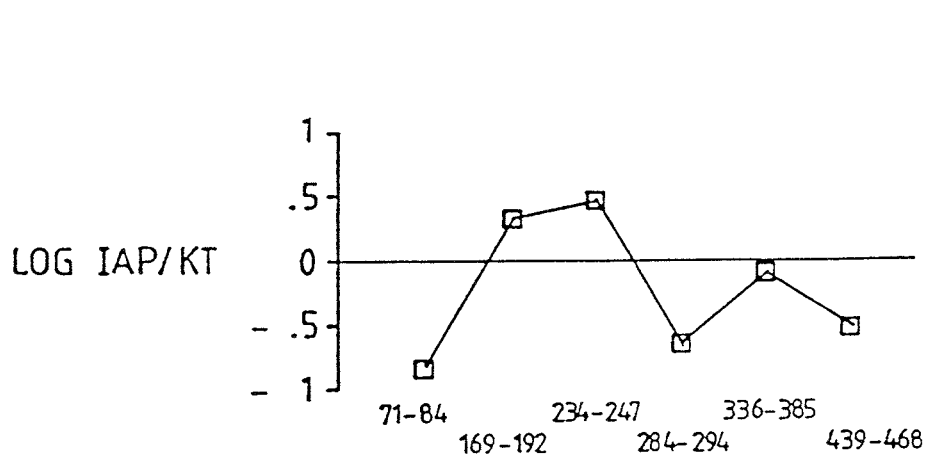


Fig. 4. Variation of pH, conductivity and selected ions with depth (Boreholes KFI09 and BFI01).



Upper plot: computation of the saturation index with respect to calcite. (Borehole BFI01; 71 to 468 m).

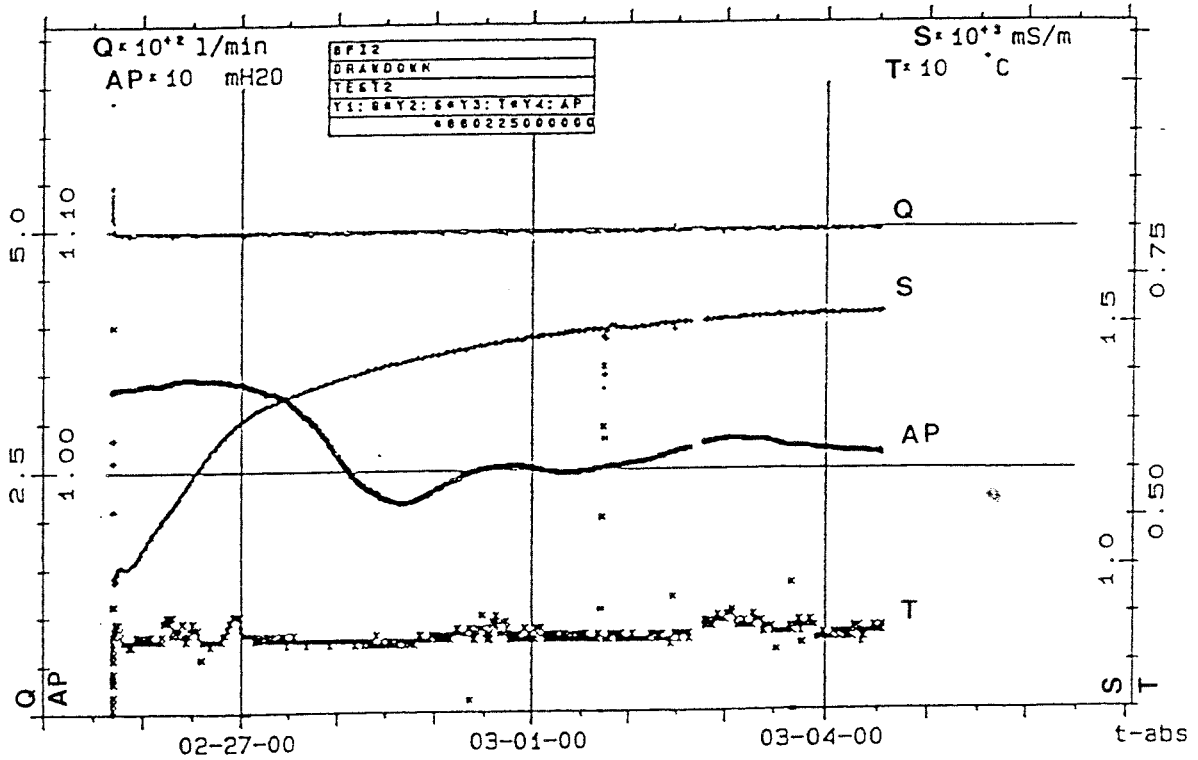
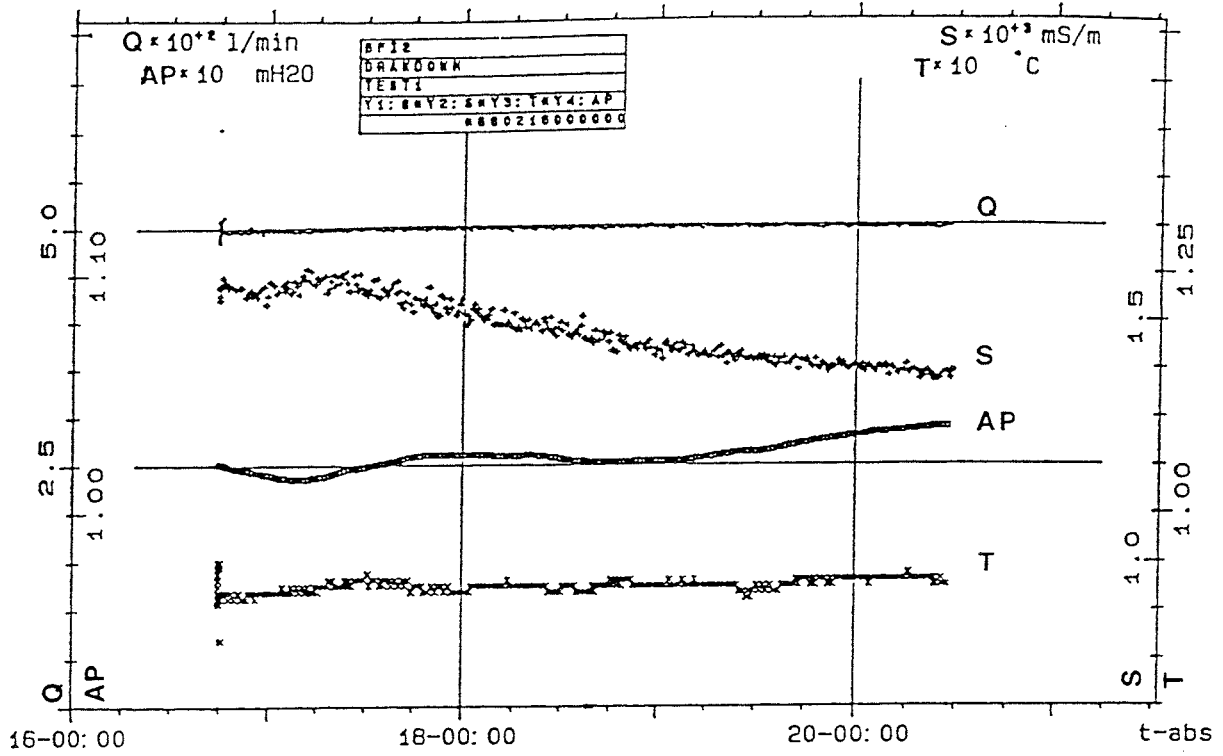
Lower plot: mixing computation between non-saline and saline groundwaters with respect to calcite saturation. (Borehole KFI09; 94 to 368 m).

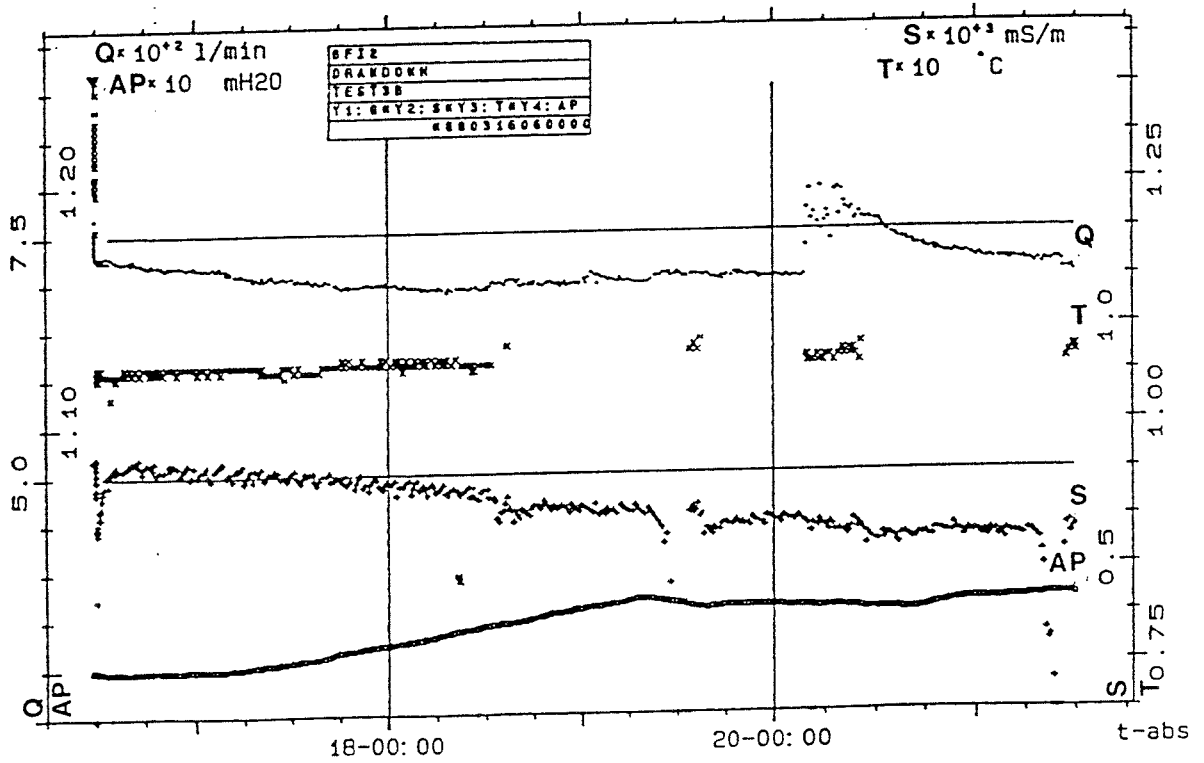
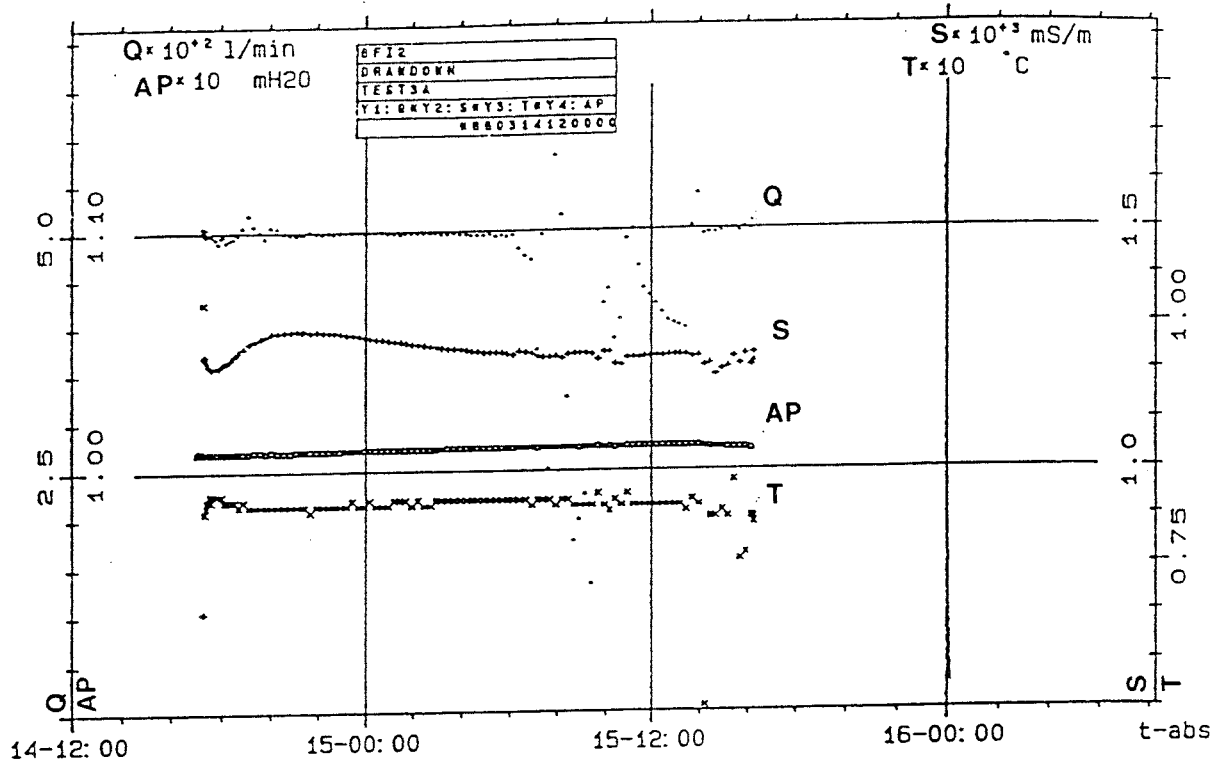
LEGEND

Symbols used for parameters measured in the pumping borehole BFI02.

Pumping borehole

.	flow rate(Q)
+ + + + +	electric conductivity(S)
□ □ □ □ □	barometric pressure head(AP)
x x x x x	temperature(T)





LINEAMENT DATA

In Appendix 9:1 base data of lineaments presented in Figures 7.2-7.3, 7.5-7.7, and 7.9-7.11 are summarized in Tables 1.1-3.4 below.

Table 1.1 First order lineament of northeastern Upland (Fig. 7.2 and 7.3a).

No	Start coord. in RAK		End coord. in RAK		Length (m)	Azimuth (degrees)
	Y	X	Y	X		
1	1600604	6715784	1619626	6723946	20699	66.8
2	1595266	6692760	1600625	6710220	18264	17.1
3	1603728	6685824	1603863	6694963	9140	0.8
4	1606388	6677951	1609330	6698762	21018	8.0
5	1609765	6700223	1610254	6705259	5060	5.5
6	1602330	6673860	1606089	6677086	4953	49.4
7	1612487	6673859	1619267	6687035	14818	27.2
8	1625881	6683695	1615193	6693882	14765	-46.4
9	1615948	6688603	1615970	6695334	6731	0.2
10	1644936	6688549	1617745	6705780	32191	-57.6
11	1642980	6695351	1639769	6714626	19541	-9.5
12	1634417	6700081	1629897	6703172	5476	-55.6
13	1644989	6684075	1636477	6692887	12252	-44.0
14	1644973	6694988	1641917	6697116	3724	-55.1
15	1644949	6676027	1633946	6679582	11563	-72.1
16	1632954	6673883	1632969	6679650	5767	0.1
17	1609122	6705946	1606036	6714956	9524	-18.9

RAK = Coord. system used on Swedish topographical maps defined by the Survey office of Sweden (RAK), the present National Land Survey of Sweden.

Y = East-west axis of the coordinate system.

X = North-south axis of the coordinate system.

The coordinates of the lineament endings are given with an accuracy of one metre. The precision is ca 100 m (scale 1:250 000) to 5 m (scale 1:10 000).

Table 1.2 Second order lineament of northeastern Uppland (Fig. 7.2 and 7.3b).

No	Start coord. in RAK		End coord. in RAK		Length (m)	Azimuth (degrees)
	Y	X	Y	X		
1	1599291	6704303	1595218	6710960	7804	-31.5
2	1600984	6696966	1602705	6705929	9127	10.9
3	1614655	6713434	1612044	6719533	6634	-23.2
4	1607908	6696962	1609122	6705946	9066	7.7
5	1600165	6702472	1622291	6713183	24582	64.2
6	1610417	6705691	1610317	6707427	1739	-3.3
7	1615193	6693882	1609442	6699206	7837	-47.2
8	1614549	6695562	1611717	6702420	7420	-22.4
9	1617928	6700864	1609103	6704907	9707	-65.4
10	1615600	6699893	1613250	6706882	7374	-18.6
11	1615435	6697889	1618524	6711262	13725	13.0
12	1615531	6696648	1616611	6698394	2053	31.7
13	1620953	6689204	1616507	6700953	12562	-20.7
14	1605984	6681825	1621145	6697305	21668	44.4
15	1619267	6687035	1622288	6701129	14414	12.1
16	1618034	6677113	1624846	6693370	17626	22.7
17	1626523	6684588	1628789	6691350	7132	18.5
18	1627711	6683179	1629138	6688235	5254	15.8
19	1628995	6682518	1630027	6685873	3510	17.1
20	1629686	6681561	1630758	6684549	3174	19.7
21	1631836	6680350	1632197	6681456	1163	18.1
22	1632437	6681648	1643088	6677646	11378	-69.4
23	1633946	6679582	1625894	6683695	9042	-62.9
24	1635981	6674340	1625813	6699069	26738	-22.4
25	1640002	6674235	1636203	6690045	16260	-13.5
26	1644944	6678955	1635307	6693460	17415	-33.6
27	1644809	6680272	1643410	6685165	5089	-16.0
28	1643953	6687539	1642057	6688638	2191	-59.9
29	1641917	6697116	1638019	6700010	4855	-53.4
30	1644988	6702909	1642394	6704142	2872	-64.6
31	1644952	6704722	1642178	6706371	3227	-59.3
32	1625882	6700261	1627930	6703345	3702	33.6
33	1623193	6702493	1624152	6707369	4969	11.1
34	1619525	6698888	1622051	6710861	12237	11.9
35	1621465	6673873	1628763	6676927	7911	67.3
36	1617648	6673840	1618059	6679281	5457	4.3
37	1616883	6674518	1614210	6676269	3195	-56.8
38	1615206	6679218	1615838	6683685	4511	8.1
39	1611675	6678161	1595311	6689452	19881	-55.4
40	1602194	6675266	1601858	6682626	7368	-2.6
41	1607427	6673866	1606546	6676925	3183	-16.1
42	1604575	6673803	1605048	6675227	1501	18.4

Table 2.1 First order lineaments in the Gåvastbo area. (Fig. 7.6a and 7.7a).

No	Start coord. in RAK		End coord. in RAK		Length (m)	Azimuth (degrees)
	Y	X	Y	X		
1	1620991	6695984	1614509	6699959	7604	-58.5
2	1619314	6689997	1612348	6699975	12169	-34.9
3	1615419	6694359	1610992	6697865	5647	-51.6

Table 2.2 Second order lineaments in the Gåvastbo area. (Fig. 7.6b and 7.7b).

No	Start coord. in RAK		End coord. in RAK		Length (m)	Azimuth (degrees)
	Y	X	Y	X		
1	1612024	6696733	1612335	6699980	3262	5.5
2	1611946	6689964	1611968	6696773	6809	0.2
3	1610980	6695208	1614145	6699985	5730	33.5
4	1615307	6694783	1615310	6699986	5203	0.0
5	1615533	6699475	1620996	6697742	5731	-72.4
6	1620968	6698680	1618437	6698701	2531	-89.5
7	1618051	6699996	1618005	6689978	10018	0.3
8	1621002	6690254	1617068	6699991	10502	-22.0
9	1615115	6689959	1615115	6694524	4565	0.0
10	1614948	6689959	1620990	6697308	9514	39.4
11	1620034	6689982	1620989	6690935	1349	45.1
12	1620997	6692752	1610978	6693159	10027	-87.7

Table 2.3 Third order lineaments in the Gåvastbo area. (Fig. 7.6c and 7.7c).

No	Start coord. in RAK		End coord. in RAK		Length (m)	Azimuth (degrees)
	Y	X	Y	X		
1	1613370	6697430	1610995	6699623	3233	-47.3
2	1614888	6695238	1610988	6698343	4985	-51.5
3	1612854	6696615	1612795	6699208	2594	-1.3
4	1615140	6689970	1611003	6692776	4999	-55.9
5	1612509	6691384	1613585	6692685	1688	39.6
6	1614352	6689971	1615776	6692003	2481	35.0
7	1616183	6689965	1616140	6693331	3366	-0.7
8	1618558	6689969	1615759	6692699	3910	-45.7
9	1620104	6690025	1615358	6694806	6737	-44.8
10	1615645	6692259	1620173	6697561	6972	40.5
11	1619764	6691589	1617614	6694563	3670	-35.9
12	1620775	6689993	1619723	6691512	1848	-34.7
13	1620250	6689998	1620227	6692125	2127	-0.6
14	1620304	6691678	1620255	6695273	3595	-0.8
15	1620994	6693292	1614090	6698554	8681	-52.7
16	1617917	6694831	1617058	6699990	5230	-9.5
17	1618041	6697680	1617325	6698238	908	-52.1
18	1614761	6694040	1617593	6698100	4950	34.9
19	1614830	6693934	1614877	6699928	5994	0.4
20	1617991	6692497	1613609	6699977	8669	-30.4
21	1619279	6697092	1618032	6697995	1540	-54.1
22	1620987	6695360	1619282	6696795	2229	-49.9
23	1620334	6697443	1618962	6698475	1717	-53.0
24	1620986	6696834	1620797	6696990	245	-50.5
25	1620989	6693653	1619430	6695878	2717	-35.0

Table 2.4 Forth order lineaments in the Gåvastbo area. (Fig. 7.6d and 7.7d).

No	Start coord. in RAK		End coord. in RAK		Length (m)	Azimuth (degrees)
	Y	X	Y	X		
1	1611398	6689975	1611375	6694532	4557	-0.3
2	1613817	6693025	1613792	6695351	2326	-0.6
3	1615620	6695435	1615695	6698710	3276	1.3
4	1615897	6696777	1615910	6698025	1248	0.6
5	1615825	6695164	1615898	6696211	1050	4.0
6	1616090	6697883	1616032	6699943	2061	-1.6
7	1616842	6696182	1617035	6699339	3163	3.5
8	1617476	6694743	1617462	6696042	1299	-0.6
9	1619607	6693568	1619221	6697579	4030	-5.5
10	1620033	6693116	1619942	6696837	3722	-1.4
11	1620204	6697209	1620229	6698021	812	1.8
12	1620995	6693727	1620759	6696887	3169	-4.3
13	1619701	6690771	1619848	6694691	3923	2.1
14	1620092	6689993	1618496	6695112	5362	-17.3
15	1619010	6690829	1620990	6693047	2973	41.8
16	1618459	6692120	1617200	6692049	1261	86.8
17	1616917	6690099	1615138	6690173	1781	-87.6
18	1616178	6689958	1613977	6692154	3109	-45.1
19	1613040	6690135	1611006	6691969	2739	-48.0
20	1613398	6692292	1613425	6693102	810	1.9
21	1612536	6693020	1613575	6694135	1524	43.0
22	1614401	6692590	1611617	6695284	3874	-45.9
23	1610995	6696158	1611776	6696967	1124	44.0
24	1612778	6695508	1613386	6696213	931	40.8
25	1617821	6693538	1615282	6696518	3915	-40.4
26	1618780	6695603	1615514	6698440	4326	-49.0
27	1617499	6693059	1616549	6697020	4073	-13.5
28	1616269	6696638	1616915	6697467	1051	37.9
29	1617984	6694233	1620996	6698619	5321	34.5
30	1616172	6695974	1615721	6697215	1320	-20.0
31	1614324	6692855	1612786	6695691	3226	-28.5
32	1616016	6695720	1616935	6695816	924	84.0
33	1617481	6694746	1614822	6697407	3762	-45.0
34	1617361	6689946	1617372	6691073	1127	0.6

Table 3.1 First order lineament in the Finnsjön site. (Fig. 7.10a and 7.11a).

No	Start coord. in RAK		End coord. in RAK		Length (m)	Azimuth (degrees)
	Y	X	Y	X		
1	1616448	6696851	1615911	6697249	668	-53.5
2	1616411	6696878	1616422	6697241	363	1.7
3	1616448	6696953	1616598	6697247	330	27.0
4	1616459	6696523	1616449	6696853	330	-1.7
5	1617078	6696066	1616461	6696522	767	-53.5
6	1617150	6694868	1616687	6696367	1569	-17.2
7	1617075	6695039	1616857	6696964	1937	-6.5
8	1617148	6696120	1616741	6697247	1198	-19.9
9	1616982	6695755	1617109	6696462	718	10.2
10	1615867	6694754	1615150	6695697	1185	-37.2

Table 3.2 Second order lineaments in the Finnsjön site. (Fig. 7.10b and 7.11b).

No	Start coord. in RAK		End coord. in RAK		Length (m)	Azimuth (degrees)
	Y	X	Y	X		
1	1615449	6694897	1616881	6697247	2752	31.4
2	1617150	6695992	1616451	6696947	1183	-36.2
3	1616690	6696366	1616563	6696723	379	-19.6
4	1616400	6696475	1615490	6697243	1191	-49.8

Table 3.3 Third order lineaments in the Finnsjön area. (Fig. 7.10c and 7.11c).

No	Start coord. in RAK		End coord. in RAK		Length (m)	Azimuth (degrees)
	Y	X	Y	X		
1	1615629	6695867	1615445	6697235	1380	-7.7
2	1615936	6695721	1615568	6697198	1522	-14.0
3	1615854	6695581	1616327	6696322	879	32.6
4	1616532	6695568	1616562	6696436	869	2.0
5	1617152	6694980	1615283	6696130	2194	-58.4
6	1615460	6695596	1616534	6695844	1102	77.0
7	1616660	6695109	1616589	6695581	477	-8.6
8	1616660	6695109	1616695	6695091	39	-62.8
9	1616695	6695091	1616741	6694759	335	-7.9
10	1616553	6695270	1615152	6695342	1403	-87.1
11	1615887	6694797	1615291	6695970	1316	-26.9
12	1616738	6696252	1617147	6696935	796	30.9
13	1617149	6695118	1616531	6695753	886	-44.2

Table 3.4 Forth order lineaments in the Finnsjön area. (Fig. 7.10d and 7.11d).

No	Start coord. in RAK		End coord. in RAK		Length (m)	Azimuth (degrees)
	Y	X	Y	X		
1	1616456	6696674	1615762	6697250	902	-50.3
2	1615626	6697074	1615391	6697248	292	-53.5
3	1616175	6696562	1615817	6696833	449	-52.9
4	1615930	6696704	1615448	6697042	589	-55.0
5	1616218	6696428	1615929	6696701	398	-46.6
6	1615513	6696759	1615151	6697024	449	-53.8
7	1616190	6696118	1615396	6696726	1000	-52.6
8	1615546	6696482	1615468	6696534	94	-56.3
9	1615554	6696409	1615347	6696556	254	-54.6
10	1616058	6696185	1615775	6696350	328	-59.8
11	1616165	6696080	1616059	6696181	146	-46.4
12	1615993	6696152	1615782	6696283	248	-58.2
13	1616051	6696052	1615803	6696170	275	-64.6
14	1616133	6696024	1615588	6696139	557	-78.1
15	1616079	6695932	1615822	6696085	299	-59.2
16	1616065	6695913	1615288	6696353	893	-60.5
17	1615288	6696389	1615180	6696483	143	-49.0
18	1615280	6696289	1615152	6696385	160	-53.1
19	1615235	6696877	1615452	6697202	391	33.7
20	1615423	6696921	1615547	6697085	206	37.1
21	1615183	6696283	1615238	6696934	653	4.8
22	1615469	6696221	1615152	6696826	683	-27.7
23	1615751	6696011	1615152	6696040	600	-87.2
24	1615293	6696482	1615634	6696886	529	40.2
25	1615293	6696482	1615313	6695815	667	-1.7
26	1615618	6695949	1615490	6696207	288	-26.4
27	1615832	6695734	1615723	6696107	389	-16.3
28	1615782	6695390	1615634	6695869	501	-17.2
29	1615513	6695552	1615687	6695833	331	31.8
30	1615563	6695437	1615709	6695642	252	35.5
31	1615762	6695191	1615636	6695540	371	-19.9
32	1615739	6695481	1615873	6695705	261	30.9
33	1615912	6695800	1616055	6696043	282	30.5
34	1616068	6696218	1616308	6696566	423	34.6
35	1615887	6696130	1616231	6696638	614	34.1
36	1616101	6695968	1615866	6696414	504	-27.8
37	1616134	6696024	1615978	6696360	370	-24.9
38	1615961	6696390	1615901	6696644	261	-13.3
39	1616258	6695892	1616268	6696648	756	0.8
40	1616340	6696099	1616318	6696947	848	-1.5
41	1615871	6696581	1615834	6697141	561	-3.8
42	1615770	6696341	1616119	6697081	818	25.2
43	1615947	6696320	1616085	6696493	221	38.6
44	1615756	6696639	1615749	6697040	401	-1.0
45	1616474	6695832	1616450	6696854	1022	-1.3
46	1616450	6696854	1616467	6697250	396	2.5
47	1616553	6696825	1616566	6697185	360	2.1

Table 3.4 (continued)

No	Start coord. in RAK		End coord. in RAK		Length (m)	Azimuth (degrees)
	Y	X	Y	X		
48	1616255	6696184	1616814	6696266	565	81.7
49	1616254	6696091	1616335	6696106	82	79.5
50	1616486	6696098	1616330	6696269	231	-42.4
51	1616468	6695942	1616254	6696211	344	-38.5
52	1616474	6695867	1616254	6696052	287	-49.9
53	1616415	6695819	1616138	6695955	309	-63.9
54	1616172	6695939	1616155	6695979	43	-23.0
55	1616214	6695919	1616177	6696016	104	-20.9
56	1616118	6695923	1616358	6695807	267	-64.2
57	1616091	6695882	1616279	6695785	212	-62.7
58	1616040	6695803	1616919	6695483	935	-70.0
59	1616539	6695937	1616729	6695956	191	84.3
60	1616546	6696103	1616831	6695894	353	-53.7
61	1616703	6695568	1616706	6695952	384	0.4
62	1616704	6695647	1616877	6695709	184	70.3
63	1616975	6696017	1617148	6695974	178	-76.0
64	1616334	6695635	1616510	6695782	229	50.1
65	1616430	6695713	1616437	6695810	97	4.1
66	1616416	6694760	1616239	6695771	1026	-9.9
67	1616133	6694789	1616140	6695739	950	0.4
68	1616218	6695300	1616207	6695484	184	-3.4
69	1616300	6695484	1616137	6695606	204	-53.2
70	1616136	6695485	1616605	6695459	470	-86.8
71	1616432	6695594	1616106	6695301	438	48.1
72	1616020	6695356	1616020	6695608	252	0.0
73	1615995	6694839	1616013	6695358	519	2.0
74	1616008	6695211	1616083	6695300	116	40.1
75	1615793	6694989	1616007	6695185	290	47.5
76	1616315	6694755	1615731	6695308	804	-46.6
77	1615914	6695375	1615726	6695482	216	-60.4
78	1616030	6695350	1615810	6695455	244	-64.5
79	1615843	6695282	1615765	6695364	113	-43.6
80	1616378	6694784	1616021	6695434	742	-28.8
81	1616131	6695058	1616312	6695266	276	41.0
82	1616241	6694831	1616650	6695185	541	49.1
83	1616649	6694747	1616653	6694875	128	1.8
84	1617152	6694878	1616398	6695287	858	-61.5
85	1616210	6696147	1616001	6696818	703	-17.3

FRACTURE DATA

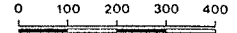
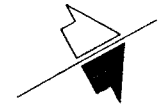
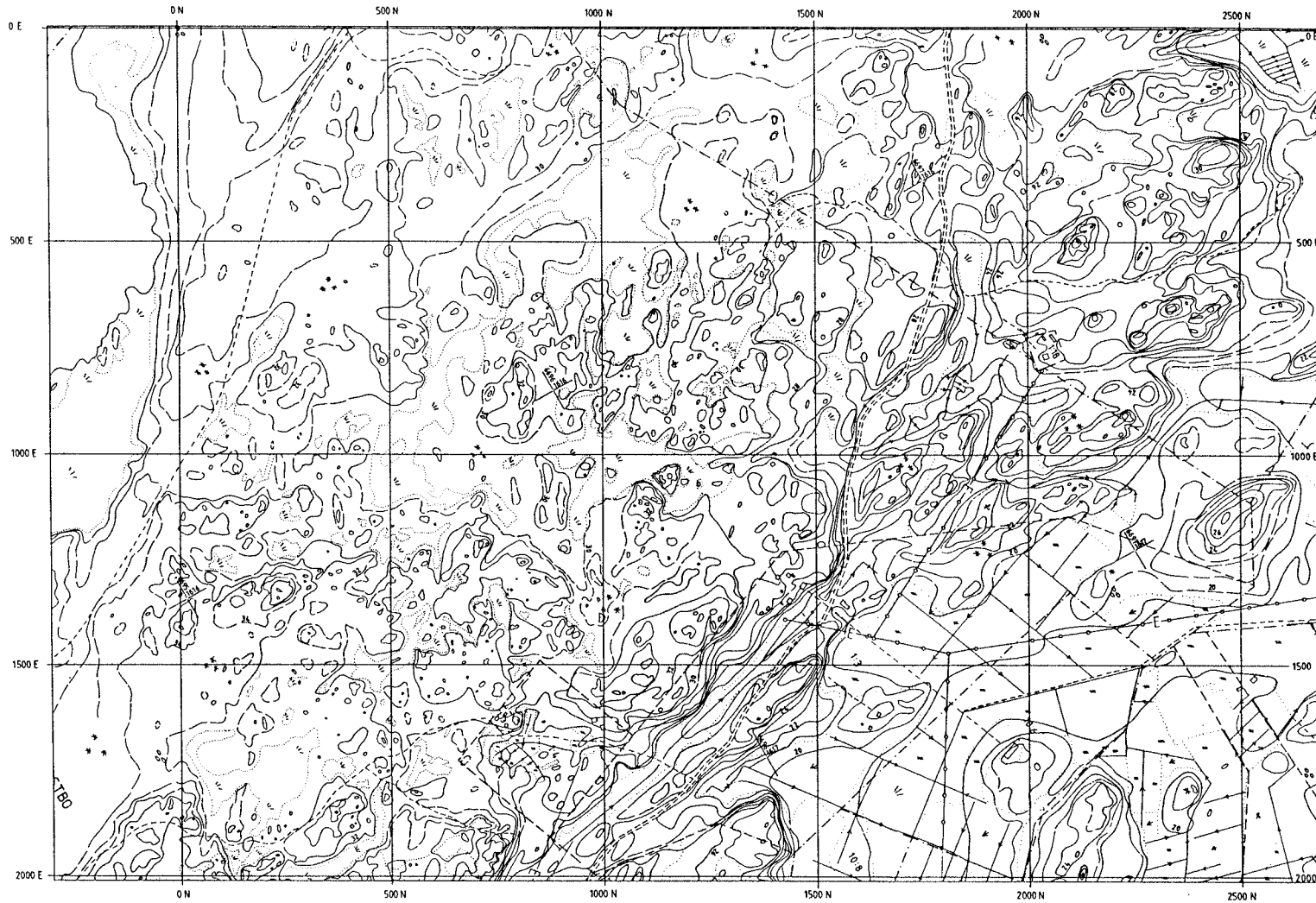
The fracture data presented in Appendix 9:2 constitute a minor part of all fracture mappings performed in the Finnsjön site. The first two sections only comprise fracture data (Tables 4 and 5) assumed to be analogous to the fracturing in Zone 2 while the third section provides detailed information of the sound rock (within block fractures).

Fracture pattern analogous to fracturing in Zone 2

In 1977-1978 fracture mapping was performed along two stripes across the Finnsjön site. The stripes were oriented in N-S and E-W. The study included 73 outcrops on each of which two perpendicular scan-line surveys were performed.

In Table 4 fracture data recorded on 8 outcrops along the N-S stripe, south of Zone 1 to the east of borehole KFI05, are presented.

During the "Fracture Zone Project" a systematic qualitative fracture mapping was performed in a minor part of the Finnsjön site. The recording of fractures was made along 50 m wide stripes parallel to the base line of the local grid (N-axis, Fig.1). The separation of the central lines of the stripes was 50 m, i.e. the area was fully covered. Notations of fractures south of Zone 1 (local grid coordinates: 1000-1500N, 1000-1200E, c.f. Fig. 1) are given in Table 5.



FINNSJÖN, BRÄNDAN
Fracture zone project / SKB

A 65

 **SWEDISH GEOLOGICAL CO**
DIVISION ENGINEERING GEOLOGY

Figure 1: Local grid system, Brändan area, Finnsjön site

Notations and abbreviations in Table 4.

ORIENTATION= the orientation of the scan-line
LENGTH = the length of the scan-line in metres
FRAC = the orientation of fracture
WIDTH = the width of fractures in millimetres
CHART = character, o=open, c=closed
NOTE soil=the fracture is infilled with soil, it is not documented whether the fracture is open, closed or is a fracture zone.
EP=epidote, QZ=quartz, FSP=feldspar, red=the fracture walls (wall rock) is coloured red, peg=pegmatite, amph=amphibolite, metadolerite, dyke.

Table 4. Fracture mapping on outcrops in 8 localities south of Zone 1, just to the east of borehole KFI05, Finnsjön site.

PROFILE	ORIENT	LENGTH	FRACT	WIDTH	CHART	NOTE	PROFILE	ORIENT	LENGTH	FRACT	WIDTH	CHART	NOTE
55A	N60W	13	N75W			soil	56B	NS	9	N15E			soil
			N50E	1	o					N55E/90	1	c	
			N20E		c					N40E		c	red
			N40E		c					N30E		c	
			N80W	5	c	EP				N30E		c	
			N65W		c					N30E		c	
			N15E/60NW	1	o					N65W	1	o	
			N55W		c					N60E/90	1	o	
			N75E		c					N60E/90	1	o	
			NS		c					N25W	1	o	
			N25E		c					N50W		c	
			N10W		c					N45W	500		soil
			N10W	1	c					N60W		c	
			N30E	2	o					N60W		c	
			N30E/60W		c					N50E		c	
			N30W/60W		c					N60W	50		soil
			N20E		c					N60W	20		soil
			N60E		c					N50E		c	red
			N60E		c					N50E		c	red
			N60E		c					N50E		c	red
			N05E		c					EW		c	soil
			N60W	2	o					N60E	20		soil
			N50E		c					N50W	1	o	
			N50E		c					N70E		c	
			N50E		c					EW		c	
			N50E		c					EW/90		c	soil
			N50E		c		57A	N05E	12.5	N70W	10		
			N50E	1	o					N55W		c	
			N50E	1	o					N35E	1	o	red
			N50E	1	o					N35E	1	o	red
			N50E	1	o					N35E	1	o	red
			NS	1	o					N80W		c	
			EW	1	o					N80W		c	
			N20E	2	o					N80W		c	
			N10E		c					N15W		c	FSP
			EW		c	EP				N15W		c	FSP
			N10E/60W		c	soil				N50E		c	
			N10E/60W		c					N75W	1	o	cataclastic
			N75E		c					N75W		c	red
			N80E	1	o					N75W		c	red
			N70E	1	o					N70W		c	
			EW	1	o					N30E	2	o	
			NS	1	o					N30E		c	EP
			NS		c					N30W	1	o	
			N40E		c					N30E	1	o	
			N40E		c					N30E	1	o	
			EW		c					N30E	1	o	
			N85E	2	o					N30E	1	o	red
			N85E		c					EW	1	o	
			N40E	1	o					N10E		c	
			N40E	1	o					EW		c	
55B	N60E	7	N45W		c	soil				EW		c	
			N75W	1	o					EW		c	
			N25E		c					EW		c	
			N25E		c					N45E		c	
			N40E		c					N40E		c	
			N50W		c					N10E	10	c	QZ, EP
			N70W	1	o					N40E		c	
			N60W	50		soil				N35E		c	
			N75E		c					N40E	1	o	
			N30W		c					N40E	1	o	
			N20E		c					N40E	1	o	
			N60E		c					N40W		c	soil
			N45W		c					N80E		c	
			N60W	1	o					N80E		c	
			N60W	1	o					N80E		c	
			EW		c	EP, QZ				N30E		c	
			N40W	1	o					N30E		c	
			N10E		c					N30W	5	c	FSP
			EW		c					N55W		c	
			N15E	2	o					N55E		c	
			EW		c	EP	57B	N85W	15	N55E	1	o	red
			EW		c	EP				N55E	1	o	red
			EW		c	EP				N55E	1	o	red
			N10E	4	o					N40W	7	c	QZ, EP
			N20E		c					N30E		c	
56A	EW	10	N55W		c					N50W		c	soil
			N55W		c					N50W	1	o	
			N55W		c					N50W	1	o	
			N55W		c					N50W	1	o	
			N55W		c					N50W	1	o	
			N20E	1	o					N20E	4	QZ	
			N50E	1	c					N35E		c	
			N50E	1	o					N40E		c	
			N50E		c	1000, soil				N40E	1	o	
			N60E		c					N35E	1	o	
			N40E	2	o					N35E	1	o	
			N60W	1	o					N35E	1	o	
			N50W	1	o					N35E	1	o	
			N60E		c					N35E	7		QZ
			N40W	1	o					N40W	50		soil
			N40W	1	o					N10E	1	o	
			N40W	1	o					N05W		c	
			N40W		c	soil				N60E/50SE		c	
			N40E		c					N60E/50SE		c	
			N50W	1	o					NS		c	
			N40E		c					N40W	10		shearzone

PROFILE	ORIENT	LENGTH	FRACT	WIDTH	CHART	NOTE	PROFILE	ORIENT	LENGTH	FRACT	WIDTH	CHART	NOTE
58A	N50W	17	N45E		c		59A	N70E	9	N30W		c	
			N45E		c					N75W		c	
			N45E		c					N75W		c	
			N45E		c					N15E		c	
			N45E		c					N40E	10	c	
			N50W	25	EP					N80W		c	
			N50W	25	EP					N80E		c	
			N50W		c					N20W		c	
			N50W		c					N80W	6	o	
			N55E			soil				N80W	2	o	
			N40E		c					N80W	2	o	
			N40E		c					N80W	1	o	
			N30E	2						EW	1	o	
			N50E	20	QZ					EW	1	o	
			N75E		red					N55W	2	c	
			NS		c					N80W	2	o	
			NS		c					N30E	1	c	
			N70E		c					N25E	1	o	
			N50W		c					N25E	2	o	
			N80E		c	soil				N25E	3	o	
			N80E		c					N30E		c	
			N55W	1	o	red				N30E		c	
			N30E		c					N30W	1	o	
			N30E		c					N40W	5	o	EP
			N80E		c					N45E		c	
			N80E		c					N60E		c	
			N80E		c					N30W		c	
			N85E	1	o					N80W		c	
			N15W		c					N40E	3	o	
			N75E	1	o					N40E	3	o	
			N35E		c					N40E	2		FSP
			N25E		c					N05W		c	red
			N25W		c					N50E		c	red
			N25W		c					N60E/50SE	2	o	FSP
			N30E	1	o					N30W		c	
			N30E	1	o					N30W		c	
			N70E/70S							N50W	1	o	
			N10W		c					N25W		c	
			N10W		c					N40W		c	soil
			N10W		c					N05E	2	o	
			N70E	1	o					NS	100		peg
			N80E	1	o					N45E		c	
			N10W		c					N45E		c	
			N40E		c					N45E	1	o	
			N10E/50W	1	o					N45E	1	o	
N25E	1	o		N50E	1	o							
N20W		c		N50W		c	soil						
N60E	1	o		N40E		c							
N70E	2	o		N40E		c							
N30E	1	o		N40E		c							
N30E	1	o		N40E		c							
N30E	1	o		N30E		c							
N30E	1	o		N30E		c							
N45E	1	o		N70E		c							
N65E	3	o		N30E	2	o							
NS	2000		soil	N30E	1000		soil						
N50E	1	o		N20E	1	o							
N50E	1	o		N20E	1	o							
N50E	1	o		N20E	1	o							
N25E		c		N20E	1	o							
N45E	1	o		N35E		c							
EW		c		N35E		c							
N40E	2	o		N10E	1	o							
N25W	3	o		N60E/50SE	2	o	red						
N40E		c		N30W	50	c	FSP						
N40E	1	o		N30E	3	o							
N40E	1	o		N30E	3	o							
NS		c	soil	N50E	10		peg						
N50E	20		soil	N30E		c	red						
N50E		c		N30E		c	red						
N80E	1	o		N30E		c	red						
N35E		c		N30E		c	red						
N30E	6	o		N20E		c	red						
N30E		c	soil	N20E		c	red						
N20E	1	o		N20E		c	red						
N20E	1	o		N20E		c	red						
N60W	1	o		N20E		c	red						
N60W	1	o		N60E		c	red						
N60E	1	o	red	N60W		c	red						
N20W	1	o		N30E/80NW	1	o							
N30W		c		N30E/80NW	1	o							
N30W		c		N30E		c							
N50W	1	o		N30E		c							
N50W	1	o		N30E		c							
N50W	1	o		N30E		c							
N10E	2	o		N30E		c							
N20W	10		soil	N30E		c							
NS		c		N40E	13								
N70W		c	EP	N40E		c							
N70W		c	EP	N40E		c							
N40W	2	o		N40E		c							
N80E		c		N40E		c							
NS	20		soil	N40E		c							
N65W		c	red	N85W		c							
N65W		c	red	NS	2	o							

Notations and abbreviations in Table 5.

E	= east coordinates of the observation points given in the local grid system
N	=north coordinates of observation points given in the local grid system
ROCK	grd=granodiorite pegm=pegmatite aplite=aplite
FOLIATION	foliation=gneissosity
FRAC	morph=fractures forming the morphology of the outcrop Char/Infil=character/infillings En ech=en echelon arrangement of fractures (stepped) myl=mylonite pl shear=plastic shear HM=hematite LA=laumontite Striat=striations/slicken sides
FRAC ZONE	=fracture zone width in metres Lineam=lineament, observation point located in a lineament, orientation of the lineament is given
NOTE	a=aperture of fracture 5X12=size of fracture surface in metres=5mX12m

Table 5. Fracture recordings from an area southeast of Zone 1, Finnsjön site.

E	N	ROCK	FOLIAT	FRACTURE			FRAC ZONE			NOTE
				Orient	Morphol	Char/InfiStriat	Orient	Spacing	Width	
1050	1005	grey grd	N53W							
1070	1080	grey grd		N45E		En echl	EW	0.1-0.5		
1070	1090	grey grd		N45E/90					N50E	
1050	1116	red grd		N50E/90					NS	
				NS/90						
				N28W		pl shear				
				N70W/90						
1022	1160	red grd		N30E/90						a<1.5
				N50E/90						
1050	1225	grey grd	N65W/90	N83W/50SW		HM.LA				
				N35E/35SE		HM.LA	N55W/35SE			
				N70W/50SW		HM.LA	N60W/27SE			
				N80E/40SE		HM.LA				
				N20E/60NE		planar				
1050	1315	grey grd		N30E/90						
				N60W/90						
1075	1370	grey grd		N60W/90						a<10-20
				N35E/30SE						
1050	1414	red grd		N25E/90			N30E		>5	
				N58W						
1050	1450	grey grd		N27E/90		HM.LA	N30E			
1050	1462						N30E			
							N60W			
1090	1500	grey grd		N05E/70W	morph					
1100	1515	grey grd	N79W/85N	N79W/85W		myl.shear				
		aplite		N60W						
1100	1493	grey grd		N60W/90	morph					
				N05E/85W	morph					
1100	1383	grey grd		N30E/75W						
1100	1330	grey grd		N35W						
				EW						
1100	1290	grey grd	N70W/80S	N25E/85W						
1100	1265	grey grd		N50W/90			N50W	0.15	1.5	
1100	1235	grey grd		N45E/32SE		HM.LA				
1100	1225	grey grd		N80E/90			N80E		>1	

1100	1150 red grd	N60W		N60W	>1	
1100	1134 grey grd	N80E/20S morph	planar			
1100	1120 grey grd	N50E/80W		N50E	0.05-0.3 >10	N50W
1100	1105	N80E/30S morph	HM		1.0-3.0	
1100	1085 grey grd	N60W/10S morph				
		N50E/40SE	HM. LA			
		N55E/80NE				
1100	1063 grey grd	N50E/30SE morph	HM. LA			
		N72E/35SE	HM. LA			
1100	1010 grey grd	N65W/90 EW/20S morph	HM. LA			5X12
		N05W/20E	HM			
1150	1485 grey grd	N75E/15S	HM			
		N20E/90				
		N70E/90 morph				
1150	1420 red grd	N50E/90		N50E		
1150	1406 grey grd	N50E/54SE	HM. LA			
1150	1400 red grd	N60E/90		N55E		
1150	1395 grey grd	N65E/30SE	HM. LA			
			en echl			
1150	1384 grey grd	N70E/42SE	HM. LA			
	1200					
1150	1341 dolerite	N70W/90			0.5-1.0	
1150	1315 grey grd	N45E/90		N45E	0.5-2.0 >5	
		N45E/90				
1150	1277 grey grd	N60E/32SE	HM. LA			
		N45E/47SE	HM. LA			
		N60E/35SE	HM. LA			
		N32E/90				
		N60W/90			>0.1	
1150	1267 grey grd	N50E/46SE	HM. LA	N60W	1.0	5
1130	1242 grey grd	N25E/90				
1150	1127 grey grd	N75W				N25E
1150	1050 grey grd	N50W				
1150	1020 grey grd	N50W/90		N50W		
1150	969 grey grd	N40W/40NE				
1200	1520 aplite	N20W/22E morph				
		N72W				

1200	1475 red grd	NS/18E morph N70E/85N morph N40W/85SWmorph N60W/90			25X10
1200	1435 aplite	N40E N30E/90			0.05wide, >
1200	1400 grey grd N80W				
1200	1300 grey grd	N80W/16S morph N30E/90			
1200	1258 grey grd	N30E/90			
1200	1200 grey grd	Subhor		>0.15-0.20	
1185	1190 dolerite	N50W			
	grey grd	N38E/42SE			1.0
1220	1135 grey grd	N22E/£SSE	HM.LA		
		N30E/42SE	HM.LA		
1200	1100 grey grd N75W	N30E/90			
		N30E/55SE	HM.La		
1200	1095 grey grd	N67/36SE	HM		
		NS/37E	HM		
		N70E/90			
1200	1075 grey grd N65W/85SW	N30E/50SE	HM.LA		
		N20E/38SE	HM.LA		
1220	1045 grey grd	N42E/43SE	HM.LA		
	pegm	N45E/90			
1200	1015 red grd	N70W/90			0.02wide blocks

A 73

Fracture pattern in sound rock

To study the relation between fractures and morphology, and to obtain fracture data for statistical characterization of the bedrock in the northern block of the Finnsjön Rock Block, the soil was stripped from a ca 90m long and 5-6m wide profile, close to borehole KFI11, Fig. 2 and 3. The rock was cleaned with a high-pressure (150 atm) water hose. In this profile, a detailed fracture mapping was performed within a cell of 1x48m, Fig. 4. For the rest of the profile fractures intersecting a measuring tape were recorded as a scan-line survey. All fractures longer than 0.2m were mapped.

Cell mapping:The following notations of fracture characteristics were made: orientation, trace length, width, terminations, infillings and effects on wallrock, Table 1. If it was possible to stick a ca 0.2mm thick steel blade 2-4cm into the fracture it was denoted as open. 322 fractures were mapped. Both strike and dip were recorded for 272 fractures (84% of all fractures). The result is presented in Table 6.

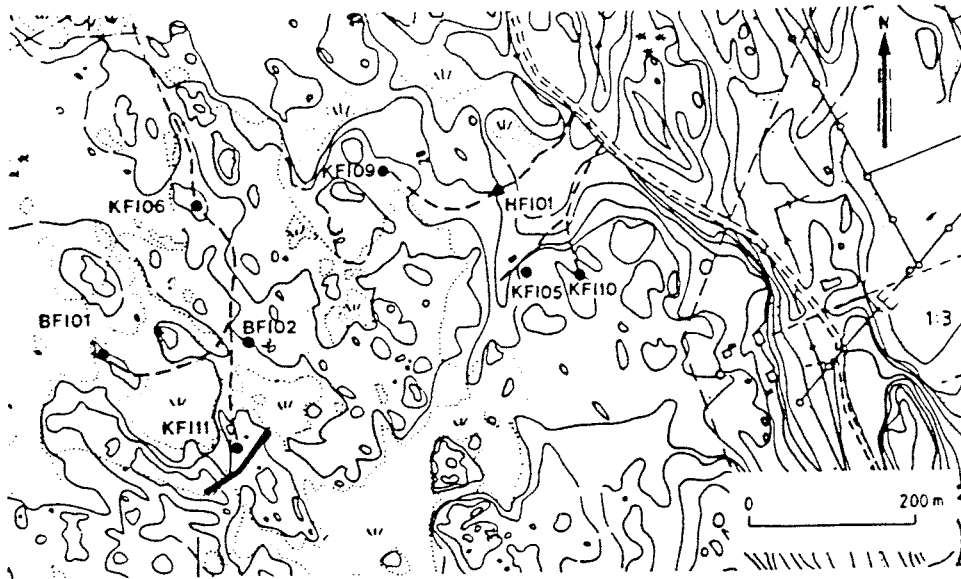


Fig.2 Location of the excavated trench just south of borehole-KF111 (KF1xx, BF1xx and HF1xx are different types of other boreholes). The cell-area is in the eastern part of the trench and the scan-line is in the western part.

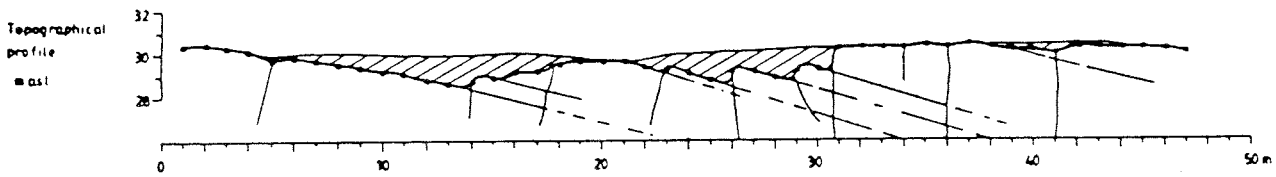


Fig.3 Vertical section along the cell-area showing the relief and larger fractures forming the morphology.

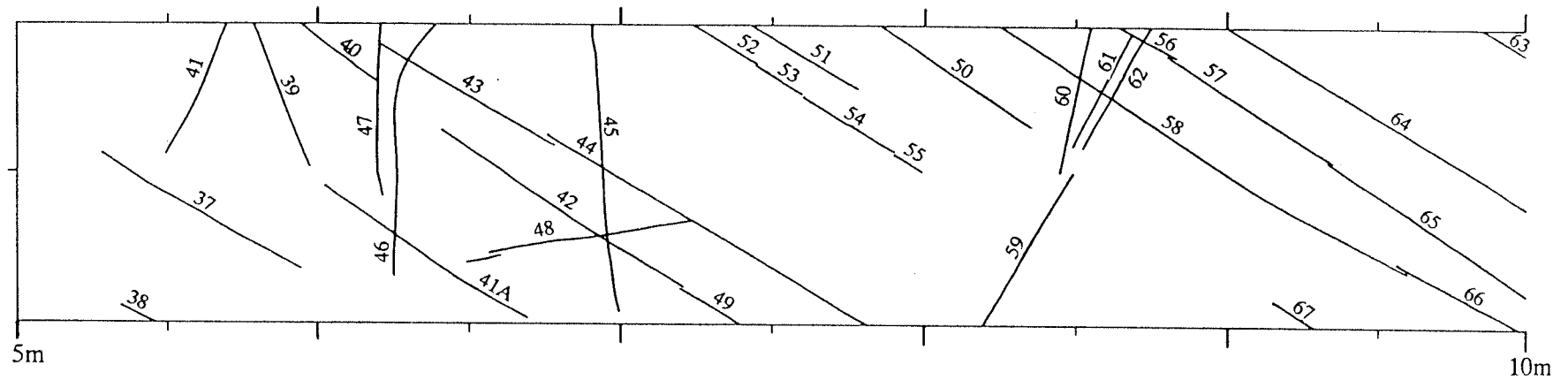
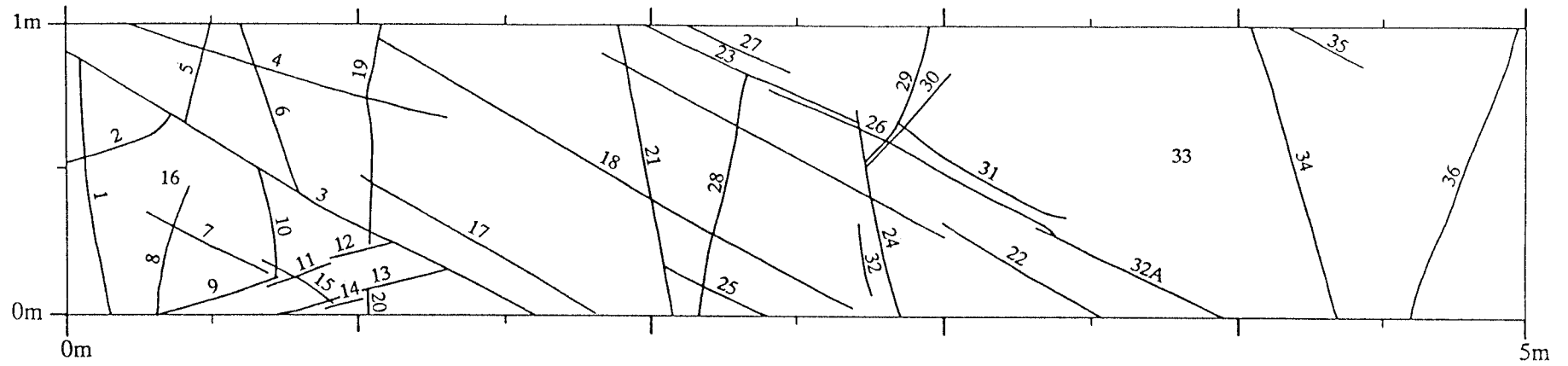
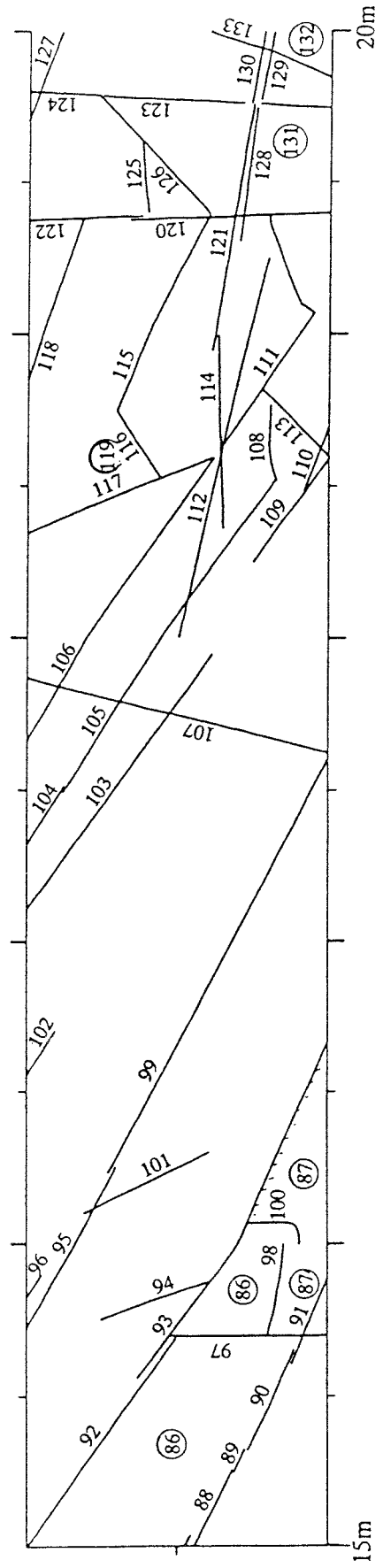
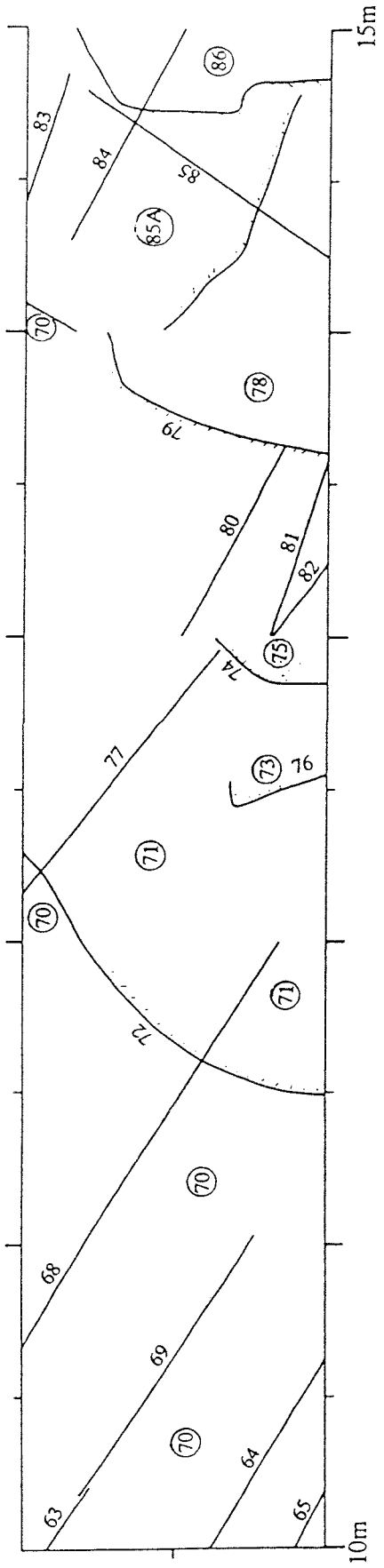
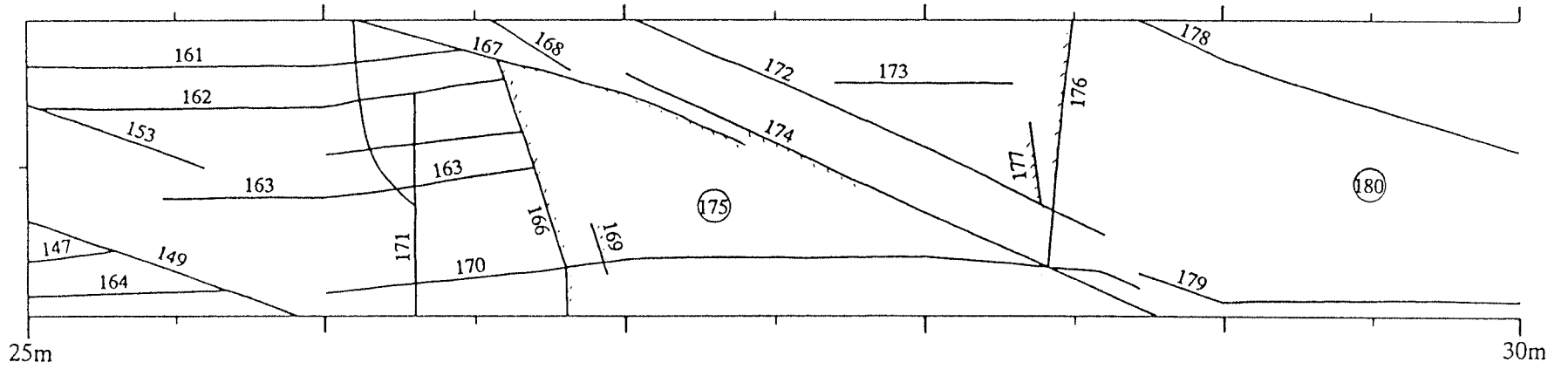
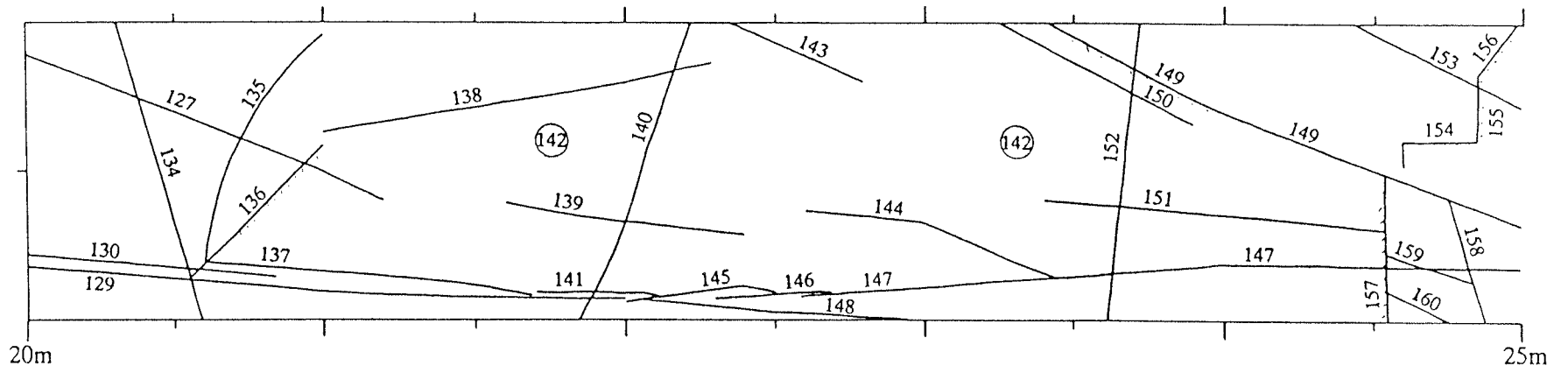
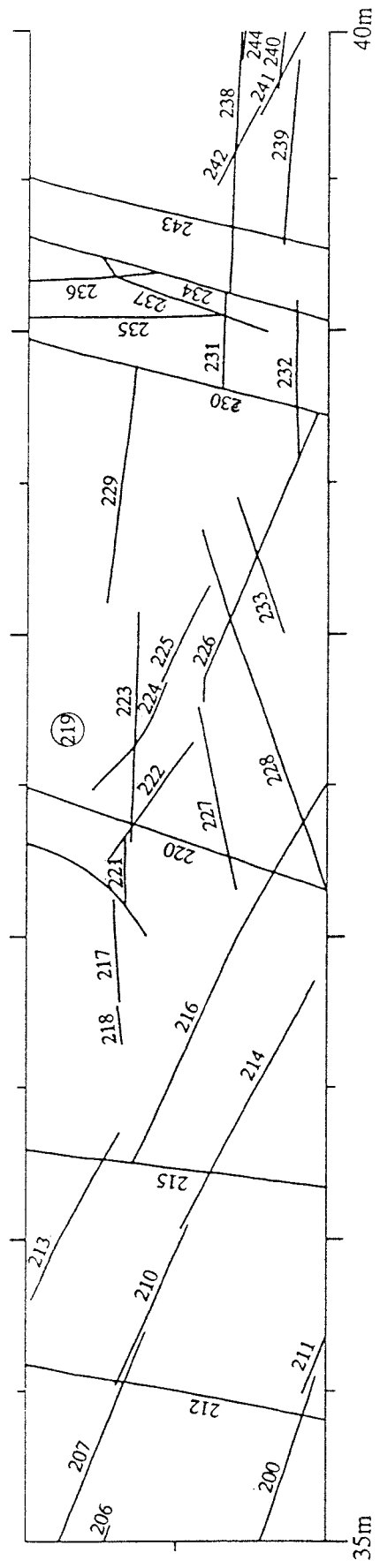
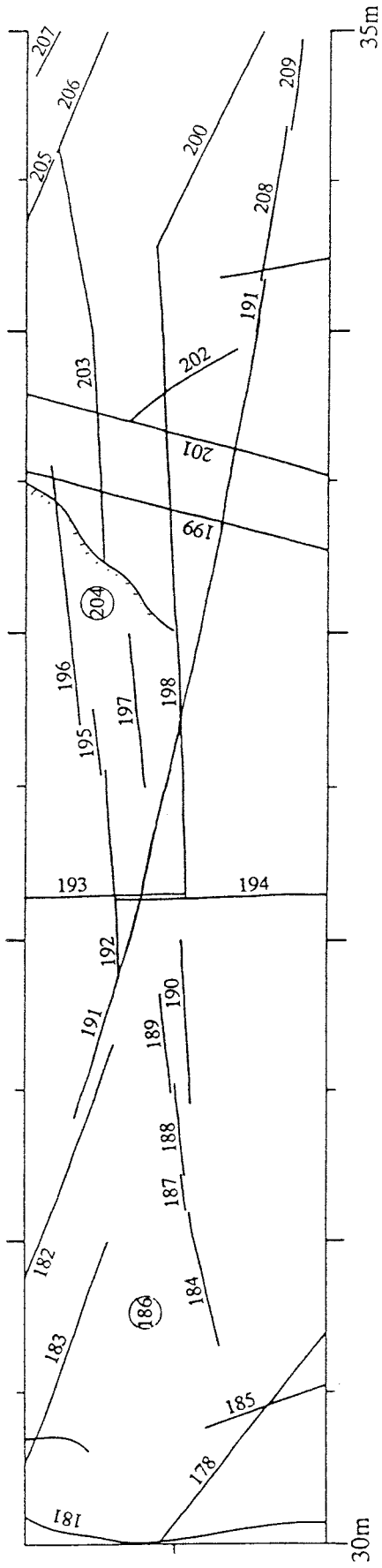
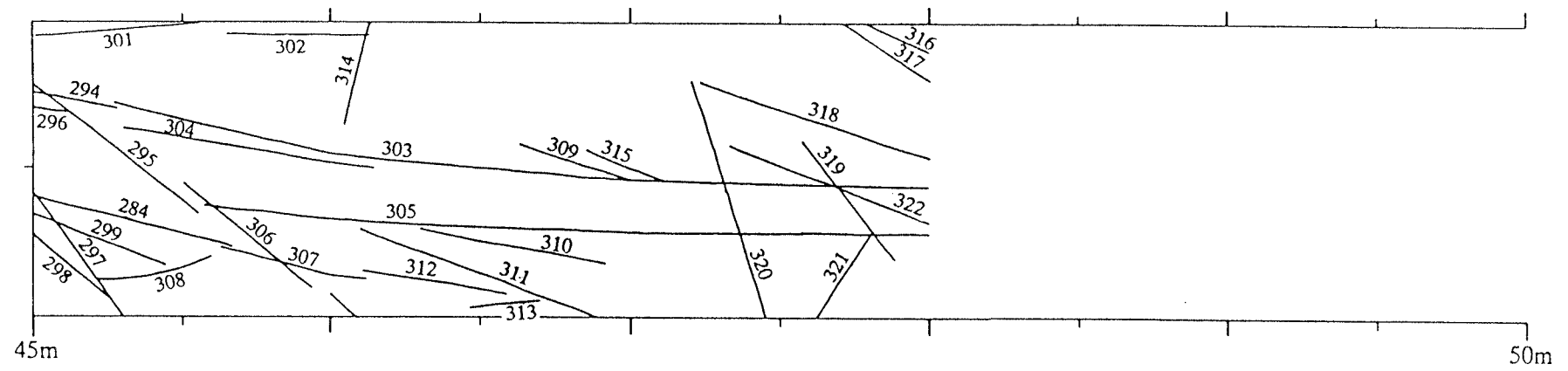
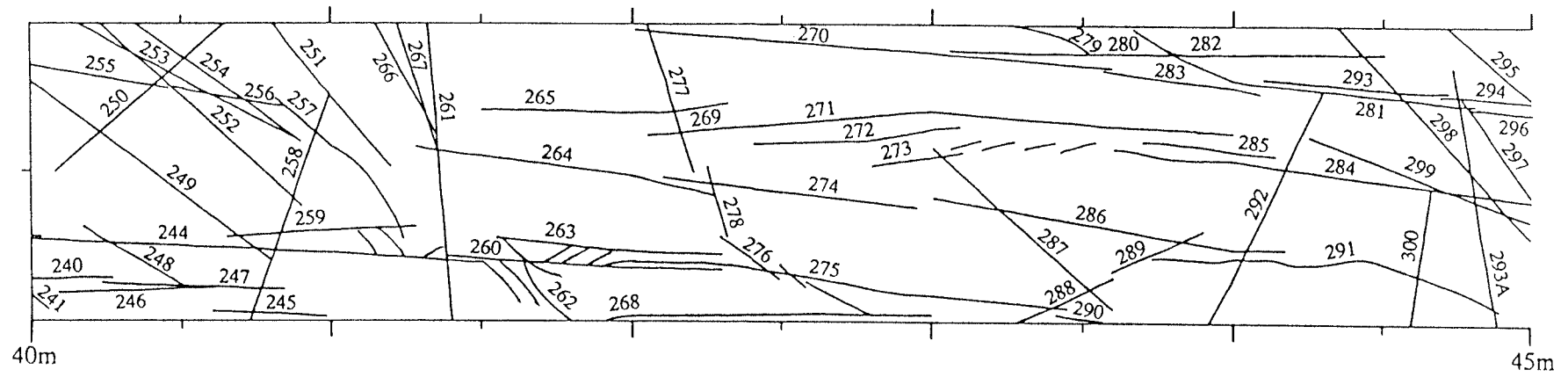


Fig.4 Fracture map of the cell area, Brändan area, Finnsjön site. Numbers of fractures refer to Table 1. Outcrop surface fractures are marked with circles.









Notation and abbreviation in Table 6

FRAC	number of mapped fracture, numbers as eg 32A are given to fractures which by mistake were incorrectly denoted in the field (double numbers)	INFILL	fracture infillings	NOTE	
ORIENT	eg NS0W/80SW is the strike and the dip. The strike is given as a deviation in orientation from the north. The dip is given as a deviation from the horizontal and with its dip direction noted. -/0 = horizontal fractures NS/90 = vertical north-south fractures EW/90 = vertical east-west fractures	PLAG	= plagioclase	T	tight, sealed
LENGTH	the total measured trace length is given in centimetres. A, B, C, and D represent those parts of the fracture which are situated outside the 1x1m cell. A=left side, B=upper side, C=right side and D=lower side (A=the 1m long NE-side of the 1x48m cell-area). Trace length inside the 1x1m cell-area is: LENGTH-(A+B+C+D) in centimeters	FSP	= feldspar	0	open
TERM	termination	MICA/MI	= mica	A,B,C,D	orientation of fractures outside the cell map against which mapped fractures terminates (see termination)
X;Y	the fracture terminates against fractures X and Y	QZ	= quartz	EN ECHELON	descriptive term of fracture configuration (stepped fracture)
0;Y	blind termination at one end and against fracture Y at the other	BI	= biotite	STEPPED SLAY/-ED	see en echelon descriptive term of fracture configuration (cf horse-tail structure)
-;Y	the termination of the fracture is not exposed at one of its ends and against fracture Y at the other.	AMPH	= amphibolite	DEXTRAL	right lateral displacement
		RUST	= iron oxy/-hydroxides	LEFT LAT	left lateral displacement
		DARK/DA	= dark coloured infillings, mafic minerals	ANASTOM	anastomosing fracture configuration, descriptive term of a network of fractures
		LIGHT	= light coloured infillings, presumably prehnite	EXFOLIATION	here often due to fire
		WHITE	= white infillings, presumably prehnite	OUTCROP SURFACE	fractures forming the morphology of the outcrop
		PINK	= presumably hematite stained prehnite		
		RED	= hematite stained infillings		
		?	= information missing		
		WALL ROCK	wallrock character		
		COLOR	colour		
		ALTERED	NO=no effects in the country rock/wallrock noted change in mineralogy, in this paper it denotes a mineral assemblage of quartz+acid plagioclase+sheet silicates. The rock is harder than the unaffected granodiorite and it is more resistive to weathering		
		WEATH	weathering, decay of the rock, mosly due to chemical action of water		
		PINK to RED	hydrothermal alteration		
		DUCTILE	ductile deformation in the wallrock		
		?	information missing		
		WIDTH	total width across the fracture in centimetres		

Table 6. Detailed fracture mapping, cell-area, Brändan area, Finnsjön.

FRAC	ORIENT	LENGTH	A	B	C	D	TERM	WIDTH	INFILL	WALLROCK	NOTE
		cm	cm	cm	cm	cm		mm		COLOR	cm
	1 N50W/82SW	84				4	3;9	<.1	?	NO	T
	2 N30E/77NW	45	8				3;0	<.1	0	NO	T
	3 N60E/70SE	>1206	>590		>500		-;-	1	?	NO	O,VERT+HOR EXP
	4 N60E/80NW	140			50		B;0	.1	?	NO	T?,B=N80E/85SE
	5 N30W/90	400		360			3;-	5	?	NO	O,LOCAL>10MMWIDE
	6 N70W/90	75		17			3;5	<.1	?	NO	T
	7 N72E/90	47					0;0	<.1	?	NO	T
	8										EXFOLIATION
	9 N30E/85SE	90				40	0;0	.1	?	NO	T
	10 N70W/85S	42					3;9	<.1	?	NO	T
	11 N30E/85NW	24					0;0	<.1	?	NO	T
	12 N35E/85NW	25			15		3;0	<.1	?	NO	T
	13 N23E/90	20					0;0	<.1	?	NO	T
	14 N24E/70SE	48			33		3;0	<.1	?	NO	T
	15 N70E/90	28					0;0	<.1	?	NO	T
	16 N70W/20NE	>60					1;9	?	?	NO	?
	17 N70E/90	120				30	19;0	<.1	?	NO	T,EN ECHLON
	18 N80E/90	167			60		19;0	.1	?	FAINT RUS	0.5 O,HAIR LINE
	19 N55W/90	140		63			0;3	<.1	?	NO	O?,SPLAY
	20 N55W/90	245				237	0;14	.1	?	NO	O
	21 N72W/60NE	>1000		>600	>460	>300	-;-	2	PLAG,MICA	NO	T,REACTIVATED
	22 N70E/90	>500					0;-	.1	?	NO	T
	23 N70E/90	114		74	19		0;24	.1	PINK PALE PINK	NO	.5 T
	24 N60W/72NE	320				240	0;0	<.2	?	NO	O
	25 N50E/90	260				210	21;0	.1	LIGHT	NO	T
	26 N65E/90	130				60	0;32	<.1	PALE PINK	NO	T
	27 N70E/90	87		52			0;0	<.1	?	NO	T
	28 N32W/40SW	>115				>35	23;-	<.1	?	NO	T?
	29 N25W/85NE	390		345			24;0	>10	0	ALTERED	O,REACTIVATED SHEAR
	30 N15W/65SW	350			325		0;0	.1	?	NO	T
	31 N70E/90	70			46		29;0	.1	?	NO	T
	32 N60W/80W	38					0;0	<.1	?	NO	T
32A	N70E/90	270				200	0;0	.1	?	NO	T
	33 N50W/20SW										?,OUTCROP SURFACE
	34 N65W/80NE	>230				>165	0;-	.2	?	NO	?,COMPOSITE FRACTURE

147	N40E/-	250		208		0;149	.2	?	ALTERED	8	T
148	N47E/-	160		66		0;145	.1	?	ALTERED	3	T
149	N60E/85SE	646		567		0;0	.3	PALE BROW	RED	.5	T
150	N65E/90	285	165	26		0;-	.2	?	RED	.5	T
151	N50E/-	>70		>26		0;-	.1	LIGHT	ALTERED	2.5	T
152	N45W/85NE	>340	>50		>150	-;-	1.5	DARK	NO		T
153	N65E/90	170	30	75		0;0	.1	PINKISH	NO		T
154	N36E/90					?	?	?	?		?, OUTCROP SURFACE
155	N54W/60SW					?	?	?	?		?, OUTCROP SURFACE
156	N05W/70W					?	?	?	?		?, OUTCROP SURFACE
157	N50W/75SW	88			36	0;-	?	?	NO		?, OUTCROP FRACTURE
158	N65W/72W	95			51	D;149	5	?	NO		O, D=N55W/80NE
159	N60E/90	29				158;157	.1	?	NO		O?
160	N60E/90	30				158;157	.1	?	WEATH	1.0	O, SEVERAL MINOR FRACTURES
161	N35E/90	170	12	58		170;153	.1	LIGHT	ALTERATIO	1.0	T
162	N40E/86SE	180		55		167;153	.1	LIGHT	ALTERED	4	T
163	N40E/85SE	197		82		153;166	.1	LIGHT	ALTERED	3	T
164	N40E/85SE	123		23		0;0	.3	LIGHT	ALTERED		T
165											MISSING NUMBER
166	N57W/80W	80				167;0	?	?	WEATH		?, OUTCROP SURFACE
167	N60E/90	130			60	-;B	.1	?	RED	2	T, B=N60E/90
168	N75E/85SE	45				0;167	.1	RUST	RED		T
169	N60W/80S	25				0;0	?	?	NO		?, OUTCROP SURFACE
170	N39E/80SE	270		165		0;0	.2	LIGHT	RED/ALTER	3.5;8	T
171	N45W/80W	75				0;162	.1	?	NO		?
172	N65E/90	240		90	44	0;C	.2	RUSTBROWN	NO		O
173	N35E/-	70		28		0;0	<.1	LIGHT	WEATH	1	T
174	N64E/90	>550	5	>440		0;-	.1	?	RUST		O
175	N40W/14SW	>150				?	?	?	?		?, OUTCROP SURFACE
176	N43W/65SW	265			180	-;174	1	?	NO		O
177	N65W/72NE	56				-:172	?	?	NO		?, OUTCROP SURFACE
178	N65E/80SE	530		335	140	B;0	1	QZ, FSP, MI	ALTERED	2	T, LEFT LAT
179	N38E/80SE	333		310		0;0	.5	LIGHT	ALTERED	7	T
180	N50E/14SE	150				?	?	?	?		?, OUTCROP SURFACE
181	N36W/90	>500				-;-	?	?	?		?, OUTCROP FRACTURE
182	N60E/75SE	124		75	33	0;C	.2	?	REDDISH	5	T, C=N32E/90
183	N60E/80SE	120		25	26	0;C	.1	?	REDDISH	2.5	T, C=N32E/90
184	N30E/90	30				0;0	<.1	?	NO		T

261	N50W/85SW	>600	375	125	-;-	5	?	PART	RED		O,AT INTERSECT
262	N85W/65NW	57		27	0;260	.2		PINKISH	RED	1.5	T
263	N37E/90	77	28		0;0	1.5		WHITE	RED	20	T
264	N48E/60SE	117	37		0;0	.1		?	RED	2	T
265	N33E/85SE	46			0;0	.1		?	RED	2	T
266	N77W/70SW	75	35		0;261	.1		?	RED	.5	T
267	N74W/80SW	350	303		-;261	.5		WHITE	RED	.5	O
268	N40E/90	187		137	0;0	.2		WHITE	RED	3.5	T
269	N30E/90	43	8		0;265	.2		?	RED	2	T
270	N39E/90	174	9		0;0	.3		?	RED	6	T
271	N37E/85SE	95		65	0;0	.2		WHITE	RED	3.5	T
272	N40E/85SE	68		5	0;0	.3		?	RED	4	T
273	N25E/-	31		4	0;0	.3		?	RED	4	T
274	N43E/-	85		11	0;0	.2		?	NO		T
275	N50E/90	160	10		0;0	.2		WHITE	RED	3	T
276	N75E/90	34		47	0;0	2		WHITE	RED	3	T
277	N65W/90	60			0;0	<.1		?	NO		T
278	N70W/86SW	33	13		0;0	<.1		?	NO		T
279	N45E/90	150	93		275;0	<.1		?	NO		T
280	N40E/90	78			280;0	.1		?	NO		T
281	N46E/90	149	67		0;0	.2		WHITE	RED	7	T
282	N41E/90	87		66	0;0	.5		?	RED	10	O
283	N50E/85W	60		9	0;0	1		WHITE	RED	8	T
284	N47E/90	104		60	0;0	1		WHITE	RED	>15	T
285	N43E/80SE	57		63	0;0	.2		WHITE	RED	3	T
286	N50E/55SE	130	13		0;0	.2		RED	RED	3	T
287	EW/85N	70		16	0;0	.3		WHITE	RED	3	T
288	N11E/70E	70			0;0	.1		?	RED	1.5	
289	N20E/55SE	35		41	0;D	.2		?	NO		T,D=N42E/90
290	N50E/90	200			0;0	.1		?	NO		T
291	N53E/90	32		180	0;0	2		WHITE	RED	8	T
292	N30W/45SW	192		18	0;0	?		?	?		?,OUTCROP SURFACE
293	N38E/90	68		72	110	283;D	.9	WHITE	RED	3.5	T,D=N40E/90
293A	N55W/90	>120			>30	0;-	1.5	?	NO	3	?
294	N43E/90	60		26		0;0	2	LIGHT	RED	3	O
295	N80E/-	>900	65	>800		0;-	2.5	EP	RED	3	T
296	N45E/90	46		21		0;0	1	?	RED	3	O
297	N77W/90	150		105		281;C	2	?	RED	12	O,C=N77W/90

298	N85E/90	190		65	35	B;297	2	?	RED	3	?,B=N45E/90
299	N65E/85NW	110			30	0;0	3	?	RED	3	O
300	N35W/60SW	70			21	284;290	.1	?	RED	.7	T
301	N40E/90	146			40	0;C	.3	WHITE	RED	1.5	T,C=N35E/-
302	N35E/90	49			9	0;0	.1	?	RED	.5	T
303	N47E/90	290			216	0;294	3.5	WHITE	RED	9	T
304	N50E/90	90			14	0;0	1	?	RED	3	T
305	N40E/85SE	384			305	0;306	2	WHITE	RED	8	T
306	N82E/90	54			54	0;0	.5	?	RED	3	?
307	N48E/85SE	57			11	0;0	?	?	RED		?
308	N50E/90	47				0;297	.1	?	NO		T
309	N59E/-	35				0;303	.2	?	NO		?
310	N50E/-	63				0;305	.2	RED	RED	1	?,EN ECHELON
311	N60E/85NW	112			17	0;0	.1	PINKISH	NO		T
312	N50E/-	50				0;307	.1	?	NO		T
313	N33E/70NW	28				0;0	.1	?	NO		T
314	N40W/35SW	>60		>20		0;-	.2	?	RED	1	T
315	N55E/90	33	22			0;303	.3	?	NO		T
316	N70E/70SE	>550		150	>380	0;-	1.5	EP	RED	10	O
317	N70E/70SE	>550		150	>380	0;-	5.5	QZ, FSP, DA	NO		T
318	N60E/-	110			22	0;303	2	QZ, FSP	NO		T, LEFT LATERAL
319	N85W/90	42				0;0	.2	?	NO		T
320	N65W/90	130				0;0	.1	?	NO		T
321	N50W/15NE	105				D;305	.4	?	NO		O, EXFOLIATION, D=N45E/-
322	N73E/-	41			22	0;305	.1	?	NO		T

Scan-line mapping:The scan-line starts at the southwestern end of the cell-area. The scan-line is 40m long and it is oriented in N70E, Fig. 2. The 24m point of the scan-line is the same as 1000N/807E of the local grid (cf SKB TR86-05). Fractures longer than 2dm are noted. The scan-line survey is summerized in Table 7.

Notations and abbreviation in Table 7

FRAC number of fracture
 INTERSEC location of intersection, given in metres
 from the starting point of the scan-line,
 0m in NE and 40m in SW
 INFILL/WIDTH and TYPE, WALLROCK/COLOR and WIDTH, and
 NOTE see above, Table 6.

Table 7. Detailed fracture mapping, scan-line, Brändan area, Finnsjön.

FRAC	INTERSECTORIENT	INFILL WIDTH	TYPE	WALLROCK COLOR WIDTH	NOTE
1	1.20	N35E/58NW			T
2	1.40	N45W/90		RED	T
3	1.74	N45E/90			1 O
4	2.80	N45E/90	10 QZ;FSP		
5	2.90	N85E/20S			T
6	3.05	N25E/20NW			?,UNDULATING
7	3.45	N10W/72SW			
8	3.60	N54E/60SE		RED	T
9	5.00	N80E/90	EP	RED	T
10	5.90	N43E/90		RED	
11	6.05	N58W/78SW			O
12	6.30	N28W/20SW			
13	7.32	N45E/90		RED	
14	7.87	N58W/90			
15	8.00	N60W/85SW			
16	8.05	N50E/90	WHITE		T
17	8.30	N42E/90			
18	8.78	N57W/90			
19	9.00	N18W/30SW		RED	
20	9.70	HOR			
21	9.90	N74W/67SW			
22	10.15	N30W/20SW			
23	11.70	N65E/90	2 WHITE		T
24	12.42	N55W/75SW			
25	13.00	N76W/10NE			OUTCROP SURFACE
26	13.80	N45W/20SW			
27	14.40	N62W/90			
28	14.85	N37E/90		RED	
29	15.10	N47E/90		RED	
30	15.50	HOR			OUTCROP SURFACE
31	15.90	N50E/90		RED	
32	16.40	N60W/90			
33	16.87	N10W/90			
34	17.22	N30E/90		RED	
35	17.40	N28W/-			
36	17.45	N25W/14SW			OUTCROP SURFACE

List of SKB reports

Annual Reports

1977-78

TR 121

KBS Technical Reports 1 – 120

Summaries

Stockholm, May 1979

1979

TR 79-28

The KBS Annual Report 1979

KBS Technical Reports 79-01 – 79-27

Summaries

Stockholm, March 1980

1980

TR 80-26

The KBS Annual Report 1980

KBS Technical Reports 80-01 – 80-25

Summaries

Stockholm, March 1981

1981

TR 81-17

The KBS Annual Report 1981

KBS Technical Reports 81-01 – 81-16

Summaries

Stockholm, April 1982

1982

TR 82-28

The KBS Annual Report 1982

KBS Technical Reports 82-01 – 82-27

Summaries

Stockholm, July 1983

1983

TR 83-77

The KBS Annual Report 1983

KBS Technical Reports 83-01 – 83-76

Summaries

Stockholm, June 1984

1984

TR 85-01

Annual Research and Development Report 1984

Including Summaries of Technical Reports Issued during 1984. (Technical Reports 84-01 – 84-19)

Stockholm, June 1985

1985

TR 85-20

Annual Research and Development Report 1985

Including Summaries of Technical Reports Issued during 1985. (Technical Reports 85-01 – 85-19)

Stockholm, May 1986

1986

TR 86-31

SKB Annual Report 1986

Including Summaries of Technical Reports Issued during 1986

Stockholm, May 1987

1987

TR 87-33

SKB Annual Report 1987

Including Summaries of Technical Reports Issued during 1987

Stockholm, May 1988

1988

TR 88-32

SKB Annual Report 1988

Including Summaries of Technical Reports Issued during 1988

Stockholm, May 1989

1989

TR 89-40

SKB Annual Report 1989

Including Summaries of Technical Reports Issued during 1989

Stockholm, May 1990

Technical Reports

List of SKB Technical Reports 1991

TR 91-01

Description of geological data in SKB's database GEOTAB

Version 2

Stefan Sehlstedt, Tomas Stark

SGAB, Luleå

January 1991

TR 91-02

Description of geophysical data in SKB database GEOTAB

Version 2

Stefan Sehlstedt

SGAB, Luleå

January 1991

TR 91-03

1. The application of PIE techniques to the study of the corrosion of spent oxide fuel in deep-rock ground waters

2. Spent fuel degradation

R S Forsyth

Studsvik Nuclear

January 1991

TR 91-04

Plutonium solubilities

I Puigdomènech¹, J Bruno²

¹Environmental Services, Studsvik Nuclear,
Nyköping, Sweden

²MBT Tecnología Ambiental, CENT, Cerdanyola,
Spain

February 1991

TR 91-05

**Description of tracer data in the SKB
database GEOTAB**

SGAB, Luleå

April, 1991

TR 91-06

**Description of background data in the SKB
database GEOTAB**

Version 2

Ebbe Eriksson, Stefan Sehlstedt

SGAB, Luleå

March 1991

TR 91-07

**Description of hydrogeological data in the
SKB's database GEOTAB**

Version 2

Margareta Gerlach¹, Bengt Gentschein²

¹SGAB, Luleå

²SGAB, Uppsala

April 1991

TR 91-08

**Overview of geologic and geohydrologic
conditions at the Finnsjön site and its
surroundings**

Kaj Ahlbom¹, Sven Tirén²

¹Conterra AB

²Sveriges Geologiska AB

January 1991

TR 91-09

**Long term sampling and measuring
program. Joint report for 1987, 1988 and
1989. Within the project: Fallout studies in
the Gideå and Finnsjö areas after the
Chernobyl accident in 1986**

Thomas Ittner

SGAB, Uppsala

December 1990

TR 91-10

**Sealing of rock joints by induced calcite
precipitation. A case study from Bergeforsen
hydro power plant**

Eva Hakami¹, Anders Ekstav², Ulf Qvarfort²

¹Vattenfall HydroPower AB

²Golder Geosystem AB

January 1991

TR 91-11

**Impact from the disturbed zone on nuclide
migration – a radioactive waste repository
study**

Akke Bengtsson¹, Bertil Grundfelt¹,

Anders Markström¹, Anders Rasmuson²

¹KEMAKTA Konsult AB

²Chalmers Institute of Technology

January 1991

TR 91-12

**Numerical groundwater flow calculations at
the Finnsjön site**

Björn Lindbom, Anders Boghammar,

Hans Lindberg, Jan Bjelkås

KEMAKTA Consultants Co, Stockholm

February 1991

TR 91-13

**Discrete fracture modelling of the Finnsjön
rock mass**

Phase 1 feasibility study

J E Geier, C-L Axelsson

Golder Geosystem AB, Uppsala

March 1991

TR 91-14

Channel widths

Kai Palmqvist, Marianne Lindström

BERGAB-Berggeologiska Undersökningar AB

February 1991

TR 91-15

**Uraninite alteration in an oxidizing
environment and its relevance to the
disposal of spent nuclear fuel**

Robert Finch, Rodney Ewing

Department of Geology, University of New Mexico

December 1990

TR 91-16

**Porosity, sorption and diffusivity data
compiled for the SKB 91 study**

Fredrik Brandberg, Kristina Skagius

Kemakta Consultants Co, Stockholm

April 1991

TR 91-17

Seismically deformed sediments in the Lansjärv area, Northern Sweden

Robert Lagerbäck
May 1991

TR 91-18

Numerical inversion of Laplace transforms using integration and convergence acceleration

Sven-Åke Gustafson
Rogaland University, Stavanger, Norway
May 1991

TR 91-19

NEAR21 - A near field radionuclide migration code for use with the PROPER package

Sven Norman¹, Nils Kjellbert²
¹Starprog AB
²SKB AB
April 1991

TR 91-20

Äspö Hard Rock Laboratory. Overview of the investigations 1986-1990

R Stanfors, M Erlström, I Markström
June 1991

TR 91-21

Äspö Hard Rock Laboratory. Field investigation methodology and instruments used in the pre-investigation phase, 1986-1990

K-E Almén, O Zellman
June 1991

TR 91-22

Äspö Hard Rock Laboratory. Evaluation and conceptual modelling based on the pre-investigations 1986-1990

P Wikberg, G Gustafson, I Rhén, R Stanfors
June 1991

TR 91-23

Äspö Hard Rock Laboratory. Predictions prior to excavation and the process of their validation

Gunnar Gustafson, Magnus Liedholm, Ingvar Rhén, Roy Stanfors, Peter Wikberg
June 1991

TR 91-24

Hydrogeological conditions in the Finnsjön area. Compilation of data and conceptual model

Jan-Erik Andersson, Rune Nordqvist, Göran Nyberg, John Smellie, Sven Tirén
February 1991